# Identification, delivery, and characterisation of wheat rust pathogen effector proteins

Cassandra Pritney Jensen

A thesis submitted to the University of East Anglia for the degree of Doctor of Philosophy

November 2020

# Abstract

Yellow rust of wheat, caused by the obligate biotrophic fungal pathogen *Puccinia striiformis* f. sp. *tritici* (*Pst*), is a devastating disease that poses a serious threat to global food security. Despite the losses caused by this pathogen, the infection process on the host species is poorly understood. This is largely due to the recalcitrance of this fungus to experimental manipulation. To date, there is no method for genetically transforming *Pst*, nor can this fungus be cultured under experimental conditions. Secreted virulence factors called effectors are a major component of pathogenicity on the wheat host. Further, some of these factors (deemed avirulence factors) can be recognised by certain host proteins, triggering an immune response. Therefore, it is critical to identify and functionally characterise these effectors to better understand the infection process on wheat host species. In this thesis, I use comparative genomics of spontaneous gain of virulence mutants to identify candidate avirulence effectors recognized by the specific host resistance protein YR2. Further, I explore different heterologous expression systems for the delivery of rust effectors in the native wheat host for subsequent characterisation. I show two previously described delivery systems involving the bacterial type III secretion system are unsuitable for screening avirulence properties of candidate rust effectors in wheat. I also develop a novel heterologous expression system using the *Magnaporthe oryzae* (*Triticum* pathotype, MoT), a different wheat infecting fungus that is experimentally tractable. This system is able to detect avirulence phenotypes of rust effectors only when sufficient mRNA levels of the transgene are produced. I obtained a single transformant which has multiple copies of the transgene that met this requirement. Using Nanopore sequencing technology I discovered this multi copy insertion occurs in a repeat rich region of the *M. oryzae* genome. Further, using CRISPR/Cas9 mediated targeted insertion, I explore different regions of the genome that may be suitable for optimal transgene expression. The results in this thesis therefore provide useful insight into the identification and functional characterisation of rust effectors in the native wheat host.

# Acknowledgements

*Wormhole Alien (doesn't understand linear time): You value your ignorance of what is to come?*

*Commander Sisko: That may be the most important thing to understand about humans. It is the unknown that defines our existence. We are constantly searching, not just for answers to our questions, but for new questions. We are explorers. We explore our lives day by day, and we explore the galaxy, trying to expand the boundaries of our knowledge. And that is why I am here. Not to conquer you with weapons, or with ideas. But to coexist… and learn.*

- *Star Trek, Deep Space 9. Emissary (1993).*

*The following is dedicated to the value of my ignorance.*

Firstly, I would like to thank the John Innes Foundation Rotation PhD program for allowing me to study among the most brilliant people I've ever met. Thank you to Diane Saunders for welcoming me into your lab and for reshaping my views of what good mentorship looks like. Thank you to Sophien Kamoun and Mark Banfield for being excellent committee members and for offering valuable advice. Thanks to Paul Nicholson for listening.

These past four years, more than the PhD itself, was about friendship. Thank you to Pilar, Vanessa, Nicola (Cook), Becky, Ashley, and Francesca for showing me what support and strength looks like. Thanks to Guru for help with molecular biology and how to navigate difficult situations. Thanks to Elizabeth for your kindness. A special thank you to Vincent Were for selflessly showing me leaf sheath assays. Thanks to all Saunders Lab members past and present who have made coming into work an absolute pleasure.

A special thanks to Aisling, Alex, and my godson Richard. Thank you for opening your lovely home to me during thesis writing and providing emotional support. Thanks to Millie for WFH Thursdays, and being my goth sister friend through all these years. Thanks to Nicola (Capstaff) and Cat for your unwavering support (even when I'm being a nightmare). Loving people is about seeing all the positive things in this world through them. Thanks to all my friends for showing me these things. Because of you all, I get to be a better person.

Most of all, thank you to my family. Mom and dad, this thesis, and all I do in life, is because of you. You sacrificed so much for my education. Look at where we are now.

# Table of Contents

# List of Figures

# List of Tables

# Abbreviations

| | |
|---|---|
| aa | Amino acid |
| AFLP | Amplified Fragment Length Polymorphism |
| APR | Adult Plant resistance |
| AVR | Avirulence protein |
| BAR | Bialaphos resistance |
| BF | Bright Field |
| BIC | Biotrophic Interfacial Complex |
| BLAST | Basic local alignment search tool |
| BSMV | Barley Stripe Mosaic Virus |
| CBD | Chaperone Binding Domain |
| CDS | coding sequence |
| CFU | Colony Forming Unit |
| Co-IP | Co-immunoprecipitation |
| CRISPR | Cluster Regularly Interspaced Short Palindromic Repeats |
| CTAB | hexadecyltrimethylammoniun bromide |
| DNA | Deoxyribonucleic Acid |
| DPI | Days Post Inoculation |
| DSB | Double Stranded Break |
| EGFP | Enhanced Green Fluorescent Protein |
| EMS | Ethyl methanesulfonate |
| ER | Endoplasmic Reticulum |
| ETI | Effector Triggered Immunity |
| ETS | Effector Triggered Susceptibility |
| GFP | Green Fluorescent Protein |
| GUS | β-glucuronidase |
| HDR | Homology Directed Repair |
| HIGS | Host Induced Gene Silencing |
| HPI | Hours Post Inoculation |
| HR | Hypersensitive response |
| IH | Invasive Hyphae |
| LRR | Leucine Rich Repeat |
| MCS | Multiple Cloning Site |
| MITE | Miniature inverted-repeat transposable element |
| NGS | Next Generation Sequencing |
| NHEJ | Non Homologous End Joining |
| NLR | Nucleotide binding leucine rich repeat |
| NLS | Nuclear Localisation Signal |
| OD | Optical Density |
| ORF | Open Reading Frame |
| PAM | Protospacer adjacent motif |
| PAMP | Pathogen associated molecular patterns |

| | |
|---|---|
| PCR | Polymerase chain reaction |
| pEDV | Effector Detector Vector |
| *Pgt* | *Puccinia graminis* f. sp. *tritici* |
| PM | Plasma Membrane |
| PRR | Pattern Recognition Receptor |
| *Pst* | *Puccinia striiformis* f. sp. *tritici* |
| PTI | Pattern Triggered Immunity |
| RAPD | Random amplification of polymorphic DNA |
| RFLP | Restriction fragment length polymorphism |
| RFP | Red fluorescent protein |
| RISC | RNA-induced silencing complex |
| RNA | Ribonucleic acid |
| RNP | Ribonucleoprotein |
| ROS | Reactive Oxygen Species |
| RT-PCR | Reverse transcription PCR |
| RT-qPCR | Quantitative reverse transcription PCR |
| SCR | Small Cysteine Rich |
| sgRNA | Small guide RNA |
| SNP | Single Nucleotide Polymorphism |
| SP | Signal Peptide |
| SSP | Small Secreted Protein |
| TF | Transcription Factor |
| TPM | Transcripts Per Million |
| VIGS | Virus Induced Gene Silencing |
| VOX | Viral Overexpression |
| WT | Wild Type |
| YR | Yellow Rust |

# Chapter 1 General Introduction

## 1.1 Wheat is an important staple crop

Since humankind domesticated wheat around 10,000 years ago, our civilisation has never been the same (Eckardt, 2010). The transition towards an agrarian society has increased our dependence on cereal crops, increasing the prevalence of these foods in human diets. In extant times, demand for wheat is forecast at 758 million tonnes for 2019/2020 (FAO, 2019). As a result, wheat is grown across more land area globally than any other crop (FAO, 2019).

Due to worldwide consumption, wheat plays an important role in human nutrition (Curtis *et al.*, 2002). Wheat grain consumption provides 20 % of the total calories consumed globally and over 25 % of total protein intake. This translates to more protein consumed globally from wheat than all types of meat combined (FAO, 2017). Cereals including wheat are also a significant source of micronutrients, providing 44 % and 25 % of daily iron and zinc intake respectively in the UK (Shewry and Hey, 2015).

With the ever-growing world population and rising demand for wheat, production must increase approximately 60 % by 2050 (Wheat-CRP, 2014). Reaching this goal is threatened by multiple factors, including limitations in arable land, climate change, drought, and crop diseases caused by pathogens (Oerke and Dehne, 2004). Specifically, pre-harvest pests account for a 35 % loss in crop yields globally (Popp and Hantos, 2013). For wheat in particular, pests and pathogens are responsible for approximately 21 % yield loss globally (Savary *et al.*, 2019). Therefore, improving wheat yield through control of pests and pathogens is essential for meeting global demand.

## 1.2 Wheat rust fungi threaten global food security

Fungal plant pathogens belonging to the order Pucciniales — known as the rust fungi — pose a significant threat to increased crop production (Voegele *et al.*, 2009). These rust fungi are obligate biotrophs, meaning they require a living plant host to complete their life cycle (Lorrain *et al.*, 2019). In the process, these fungi cause devastating disease on their hosts, which include cereals and legumes such as wheat, barley, bean, and soybean (Agrios, 2005). Within the Pucciniales, three species have been found to predominantly infect wheat: *Puccinia graminis* f. sp. *tritici* (*Pgt,* stem rust), *Puccinia triticina* (*Pt,* leaf rust), and *Puccinia striiformis* f. sp. *tritici* (*Pst,* yellow rust) (McIntosh *et al.*, 1995). Wheat rusts have plagued agriculture since

the domestication of cereal crops and continue to cause serious crop losses (McIntosh *et al.*, 1995).

### 1.2.1 *Puccinia striiformis* f. sp. *tritici* (*Pst*)

My research particularly focused on *Puccinia striiformis* f. sp. *tritici* (*Pst*) which causes the disease yellow rust of wheat. The asexual spores are highly adapted to wheat; however, infection can be seen on certain wild grasses, barley, and rye cultivars (Chen *et al.*, 2014). Throughout history, this fungus has afflicted agriculture, with the disease first described in Europe in 1777 (Eriksson & Henning, 1896). In recent years, *Pst* has become notorious for being the most damaging rust species to the production of wheat, with 88 % of global wheat production susceptible to yellow rust (Wellings 2011; Beddow *et al.*, 2015). Beddow *et al.* (2015) utilized long term crop loss data to model annual global losses to yellow rust, and concluded that 979 million American dollars, or 5.47 million tonnes of wheat are lost each year to this pathogen. To prevent these devastating losses, there needs to be a better understanding of the *Pst* infection process on its wheat host.

### 1.2.2 *Pst* asexual infection on wheat: host penetration and haustorium formation

Infection on the wheat host begins when a dikaryotic (N+N) asexual urediniospore lands on the host plant. After three hours post inoculation the urediniospore germinates and produces a germ tube (Moldenhauer *et al.*, 2006). This germ tube eventually enters the plant via a stoma and subsequently differentiates into the substomatal vesicle (Chen *et al.*, 2014). Other rust fungi produce a spherical appresorium at the stoma, however, this is rarely observed for *Pst* (Moldenhauer *et al.*, 2006). From the substomatal vesicle, infection hyphae are formed which grow intercellularly until a mesophyll cell is contacted. A haustorial mother cell is then formed, penetrating the plant cell wall, and subsequently invaginating the host plasma membrane (Mares, 1979). Specialised feeding structures called haustoria emerge, staying in close proximity with the host cytoplasm, but remain separated by the extra-haustorial matrix (EHMx) and the extra-haustorial membrane (EHM), thus producing a dynamic host-pathogen interface (Chen *et al.*, 2014; Hovmøller *et al.*, 2011). Through the haustoria, *Pst* is able to receive nutrients from the plant host, facilitating further colonisation (Voegele and Mendgen, 2011). Around 12-14 days after initial infection, sporulation occurs, whereby new urediniospores are produced and break through the surface of the wheat leaf. Under favourable conditions, these urediniospores may infect new wheat leaves, starting the asexual cycle anew (Chen *et al.*, 2014). A summary of this process can be found in **Figure 1-1.**

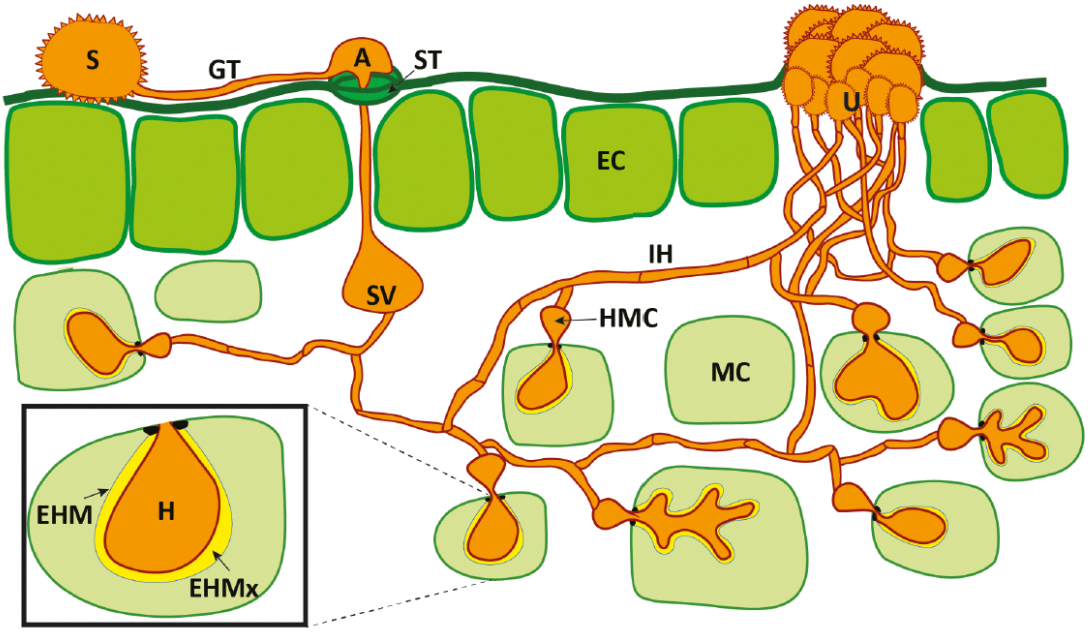


**Figure 1-1 Representation of the asexual cycle of *Puccinia* spp. on wheat.** Infection occurs when the dikaryotic urediniospore (S) lands on the leaf surface and eventually moves intercellularly through invasive hyphae (IH). The haustorium (H) forms once a mesophyll cell is contacted. The cycle is completed within 10–11 days, when thousands of new urediniospores (U) erupt through the leaf epidermis. GT, Germ tube; A, Appresorium; ST, Stoma; SV, Substomatal vesicle; HMC, Haustorial mother cell; EC, Epidermal cell; MC, Mesophyll cell; EHM, Extrahaustorial membrane; EHMx, Extrahaustorial matrix. This figure was published in Garnica *et al.* (2014) and is reused with permission under the Creative Commons Attribution License.

### 1.2.3 *Pst* Life cycle – sexual recombination produces genetic diversity

The above infection process on the wheat host only represents a small portion of the full *Pst* life cycle. *Pst*, like all cereal infecting rust fungi, have an incredibly complex macrocyclic life cycle (Aime *et al.*, 2017). The macrocyclic rusts are those that produce five spore stages sequentially throughout their life cycle. *Pst* is also heteroecious, meaning two unrelated plants are required to complete the life cycle (Lorrain *et al.*, 2019). The sexual cycle is beautifully described in Chen & Kang (2017), and briefly summarized in the following section. From the asexual uredinia, elongated telia are produced underneath the epidermis at the end of the wheat growing season in early autumn. Telia contain two separate cells whereby N+N nuclei fuse (karyogamy) to produce diploid teliospores. Each of the two cells of the telia germinate into the promycelium (also known as metabasidium) as meiosis occurs. The haploid (N) nuclei move into the promycelium-producing basidiospores. Basidiospores are dispersed by wind or rain, travelling to the alternate host plant and establishing infection by germinating and subsequently differentiating into pycnia. Host plants where *Pst* can complete their sexual cycle include *Berberis* spp. (ex. *B. chinensis, B. holstii*, *B. koreana*, *B. vulgaris*) and *Mahonia* spp. (*Mahonia aquifolium*) (Mehmood et al. 2020). Receptive hyphae and haploid pycniospores are produced from a single mating type denoted as + or -. A pycniospore from one mating type will fuse with the receptive hyphae from the other mating type to start the fertilization process. Around 16-20 days after inoculation, and after fertilization has occurred, aecia are produced on the adaxial side of the alternate host. Each aecium contains many aecial cups with hundreds of dikaryotic aeciospores (Zhao *et al.*, 2013). These aeciospores can travel to a new wheat host, whereby infection produces urediniospores. The full *Pst* life cycle is summarised in **Figure 1-2**.

As fertilisation produces aeciospores that are genetically different through sexual recombination, this part of the life cycle can produce novel strains with different virulence profiles. For example, Hovmøller *et al.* (2016) detected three *Pst* races in the post 2011 population in Europe, called 'Warrior', 'Kranich', and 'Triticale aggressive', that had been introduced by long range spore dispersal. The 'Warrior' race in particular rose to high frequencies in many European countries in the first year it was detected, displaying a faster spread than previous exotic incursions of yellow rust. 'Warrior' displayed both increased aggressiveness and a novel virulence profile in comparison to existing isolates this race would eventually replace (Sørensen *et al.*, 2014). The 'Warrior' and 'Kranich' races were found to originate from the Himalayan region of Asia, which has previously been described as a concentrated region of sexually recombining populations (Ali *et al.*, 2014; Hovmøller *et al.*, 2016). These two races therefore show the impact that both sexual recombination and long-

distance spore dispersal have on displacing clonal populations in distant regions, subsequently causing overwhelming crop loss.

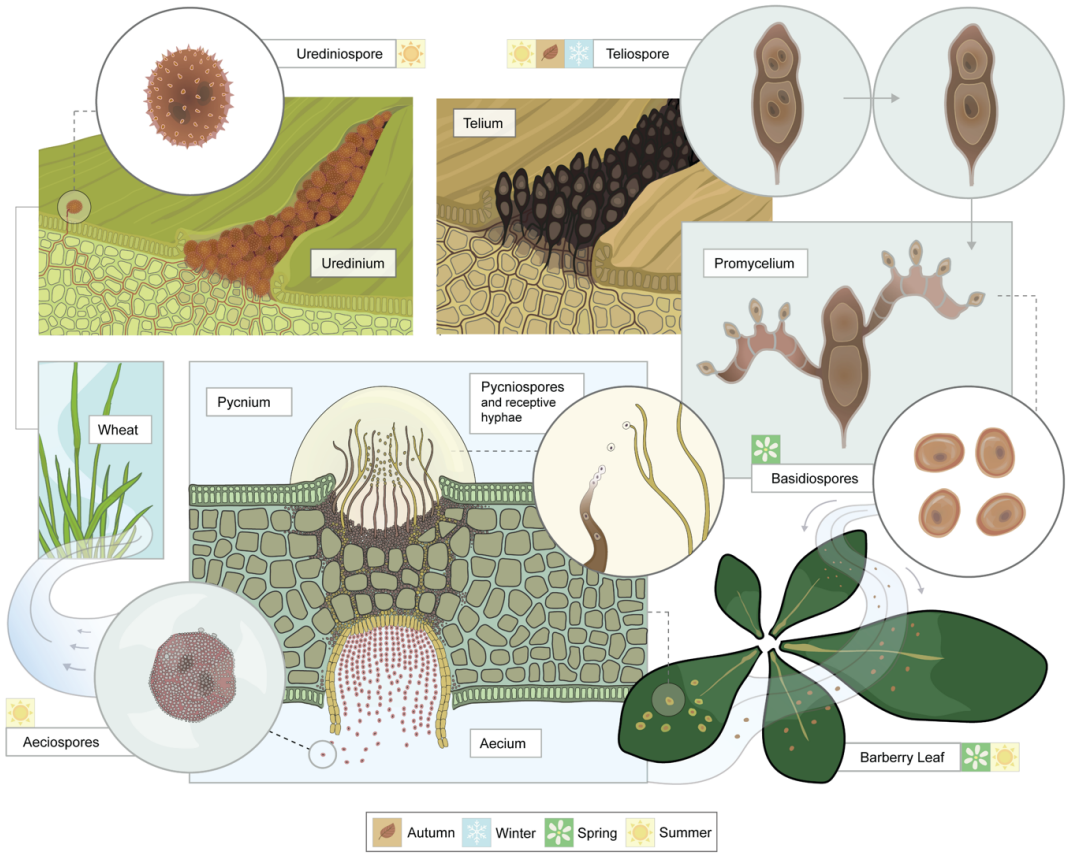


**Figure 1-2 Schematic representation of the *Pst* life cycle.** In the primary host, the fungus produces asexual urediniospores (N+N) and teliospores (2N) at the end of the growing season. Teliospores can infect the alternate host and sexually reproduce to generate genetically different aeciospores (N+N) which can infect the primary host. Figure from Bueno-Sancho *et al.* (2020) and reproduced here with their permission.

### 1.2.4 Strategies to combat rust pathogens

Currently, there are two main strategies to abrogate disease development in wheat caused by rust pathogens: 1) chemical control using fungicides, and 2) breeding for resistance in commercial wheat varieties. One of the main problems with relying on fungicides to curb disease is that chemical control can be quite costly. For example, fungicide application on wheat costs approximately 200 million dollars annually in Australia alone, with yellow rust being the major target (Oliver, 2014). Further, not only can pathogens develop resistance to fungicides, chemical control is seen as the less environmentally friendly option (Brethour and Weersink, 2001; Oliver, 2014). Therefore, a large focus has been put on breeding resistance genes into the wheat germplasm in attempt to keep rust infection under control (Ellis *et al.*, 2014). However, pathogens are capable of overcoming these resistances even within a few years after they have been deployed. Thus, it is imperative to uncover the genetic determinants of pathogenicity in order to develop more informed and robust breeding strategies.

## 1.3 Plant immunity: from two tiers to the new frontiers

The field of molecular plant microbe interactions (MPMI), often being abbreviated itself, is notoriously saturated with abbreviations representing key concepts. Some of these abbreviations persist in the MPMI canon despite recent revelations about the nebulous nature of these concepts. Like all areas of science, elegant models described previously can be further complicated by emerging views from the field.

For example, over a decade ago plant innate immunity was modelled as a two-tier defence system (Jones and Dangl, 2006). The first layer is known as pathogen-associated molecular pattern (PAMP)-triggered immunity, or PTI, which is initiated by receptors on the cell surface called pattern recognition receptors (PRRs). These PRRs initiate an immune response when conserved PAMPs such as chitin in fungi are detected (Win *et al.*, 2012). In response, pathogens can secrete effector proteins to manipulate the host and subvert PTI responses (Dodds and Rathjen, 2010). In host genotypes that contain the cognate resistance (*R*) gene, these effectors are recognized by plant intracellular receptors (Dangl *et al.*, 2013). These receptors have nucleotide binding leucine rich repeat domains and are thus called NLRs. This triggers the plants second line of plant defence, known as effector triggered immunity (ETI), which often leads to a hypersensitive cell death response (HR). This process is summarized in **Figure 1-3**.

However, recent studies suggest that PTI and ETI elicit similar and interacting pathways, and that perhaps there is no strict dichotomy between the two (Thomma *et al.*, 2011). Indeed, recent data from Ngou *et al.* (2020) suggest PTI is required for ETI, and that immune responses triggered by both types of immune receptors (cell surface vs. intracellular) mutually potentiate one another. Further, apoplastic effectors can be detected by cell surface receptors and trigger "PTI-like" responses, creating a tenuous definition for "effector triggered immunity" (Win *et al.*, 2012). Therefore, some scientists in the field call for a distinction between immunity triggered at the cell surface vs. immunity triggered by intracellular receptors instead of PTI vs. ETI. Although there is currently no consensus, some groups suggest surface-receptor-mediated immunity (SRMI) instead of PTI, and intracellular-receptor-mediated immunity (IRMI) instead of ETI (Ding *et al.*, 2019). For the purpose of this thesis, I will refer to PRR triggered immunity as PTI and immunity triggered by NLRs as ETI for simplicity.

This thesis is largely concerned with immune responses triggered by intracellular receptors that lead to a localised cell death. However, of course, to further complicate things, this type of immune response may not always produce cell death, but might only decrease pathogen proliferation (Jones and Dangl, 2006). When cell death does occur, it deprives biotrophic pathogens of critical nutrients, as they require living tissue to survive. Recent data suggests some NLRs can produce inflammasome-like structures called resistosomes (Wang *et al.*, 2019). These funnel shaped resistosomes translocate to the plasma membrane upon activation, likely causing cell death by forming toxin-like pores (Wang *et al.*, 2019).

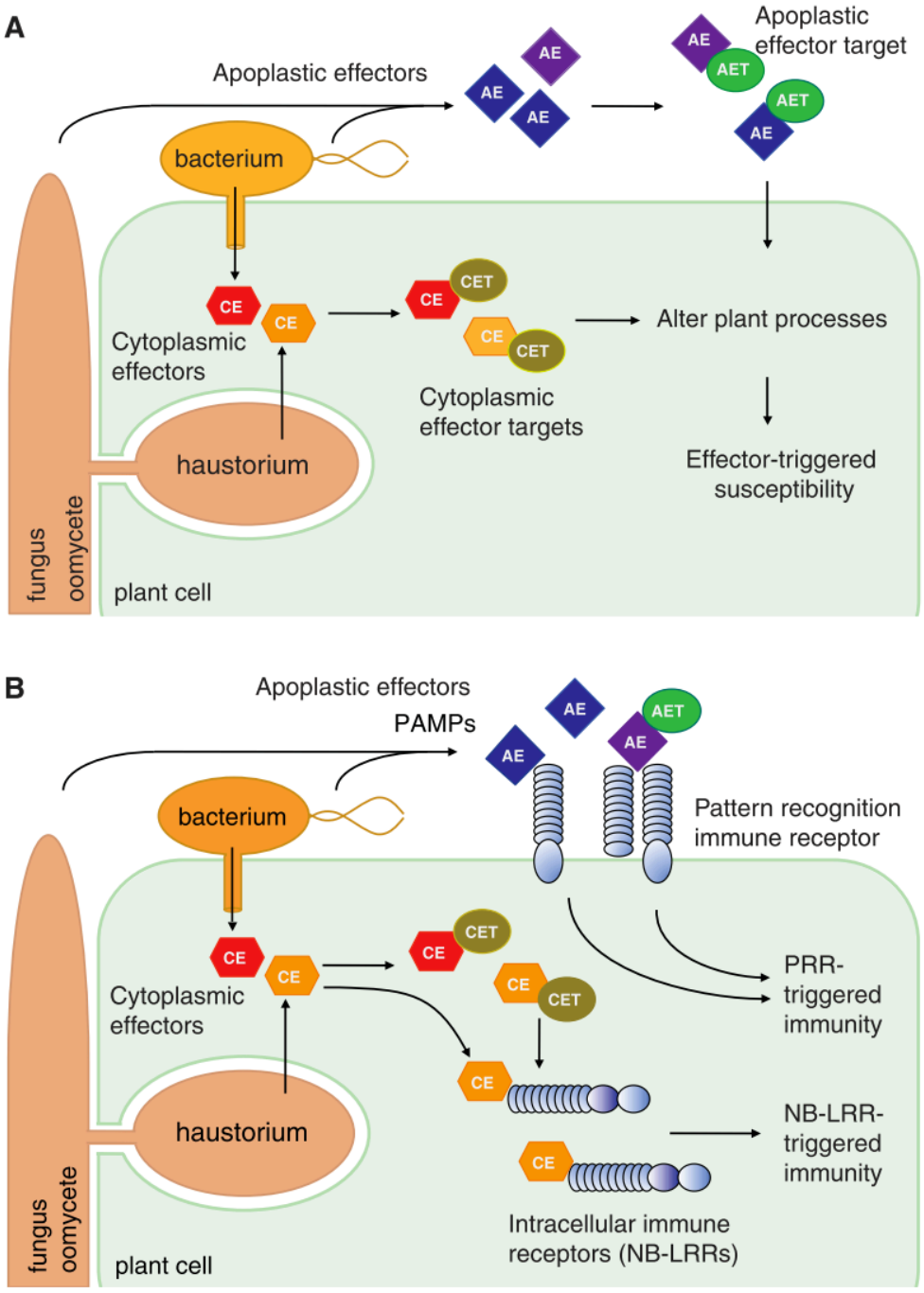


**Figure 1-3 Plant pathogen effectors and the plant immune system.** During a compatible infection, pathogens deliver apoplastic effectors (AE) or cytoplasmic effectors (CE). These effectors can target plant proteins in the apoplast (apoplastic effector target, AET) or cytoplasm (cytoplasmic effector target, CET). In susceptible genotypes (A), effector interactions with their target proteins can alter plant cell processes and suppress immune responses, leading to effector-triggered susceptibility (ETS). In resistant genotypes (B), pathogens are perceived by immune receptors that, in turn, stop pathogen growth. Cell surface pattern recognition receptors (PRRs) detect pathogen-associated molecular patterns (PAMPs), apoplastic effectors, and/or apoplastic effector–target interactions to initiate PRR-triggered immunity (PTI). Intracellular nucleotide-binding receptors (NB-LRR) induce NB-LRR-triggered immunity (ETI) on recognition of cytoplasmic effectors and/or cytoplasmic effectors–target interactions. This figure was published in Win *et al.* (2012) and is reused with permission from copyright holders under the Creative Commons Licence.

## 1.4 Resistance beyond NLRs

Other than NLR mediated resistance, plants can harbour what is called adult plant resistance (APR). Adult plant resistance is sometimes conferred by proteins involved in general plant physiology, for example Yr36, a chloroplast localized kinase that regulates the production of reactive oxygen species involved in immunity (Gou *et al.*, 2015). As suggested by its name, APR is generally effective in the adult stage of a plant whereas NLR mediated immunity is often conferred during the seedling stage as well (Ellis *et al.*, 2014). In terms of rust pathogens, infected wheat varieties with APR show signs of 'slow rusting,' in which spore production and disease development is delayed (Ellis *et al.*, 2014). It is important to note, however, that some NLR-mediated responses can also be weak, such as RPS4-mediated immunity triggered by AvrRps4 in *Arabidopsis thaliana* (Thomma *et al.*, 2011; Wirthmueller *et al.*, 2007). APR generally does not require elicitation by pathogen effectors in a gene-for-gene manner (Milne *et al.*, 2019; Ellis *et al.*, 2014). As such, APR resistance is thought to be 'durable' as a single mutation in an avirulent isolate is not sufficient to gain virulence to APR wheat varieties (Schwessinger, 2016). However, APR can still become less effective when genetically diverse isolates from distant populations replace local clonal isolates via long range spore dispersal (Sørensen *et al.*, 2014).

## 1.5 Rust effectors

### 1.5.1 Secretion through the haustoria: translocation across multiple membranes

The haustorium of fungi and oomycetes is a multi-faceted specialised structure that is used for both nutrient uptake and delivery of effectors into the host (Garnica *et al.*, 2014). In order to reach the host cytoplasm, effectors must first pass through the fungal cell wall into the extrahaustorial matrix, then pass through another membrane called the extrahaustorial membrane **(Figure 1-4).** Infection hyphae within the apoplast of the plant may also secrete effector proteins. These effectors must exit the fungal hyphae, enter the apoplast, and then pass through the plant cell wall and plasma membrane **(Figure 1-4).** Clearly, targeting effector proteins to the host cytoplasm is complicated due to the multiple membranes that need to be passed. The mechanism by which effectors translocate from the fungal haustoria into the host cytoplasm still remains poorly understood (Petre and Kamoun, 2014)

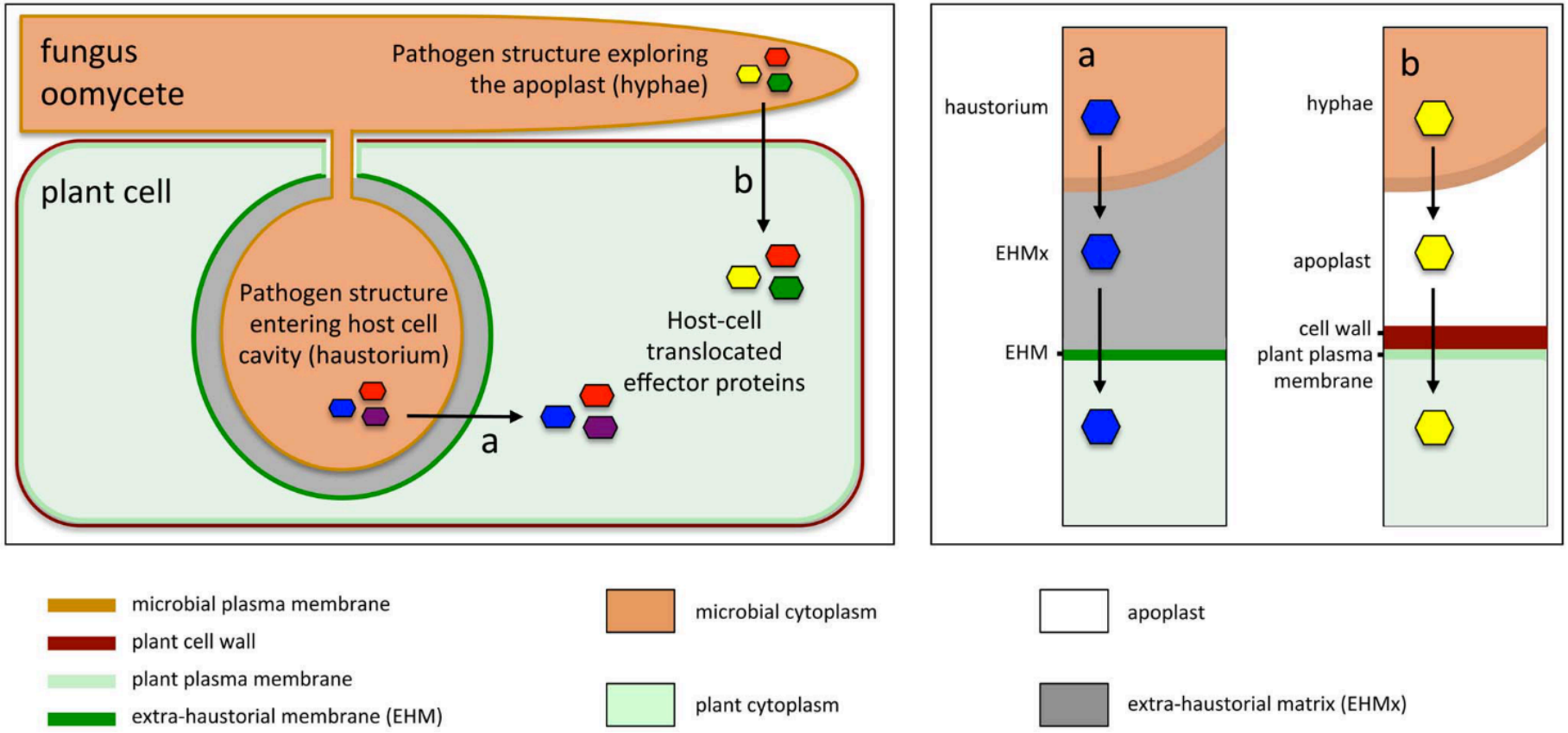


**Figure 1-4 Effectors must pass through multiple membranes before entering the host cytoplasm.** Left panel: Oomycete and fungal pathogens produce haustoria (a) and hyphae (b) that secrete effectors into host cell cytoplasm by unknown mechanisms. Right panel: Effectors secreted from haustoria (a) and hyphae (b) cross different biological membranes. EHMx, extrahaustorial matrix; EHM, Extrahaustorial membrane. This figure was published in Petre & Kamoun (2014) and is reused with permission from copyright holders under the Creative Commons License.

### 1.5.2 Rust effectors and virulence – manipulation of host processes

Very few effectors from the cereal rusts have been functionally characterised for roles in virulence, although a handful have been generally implicated in the suppression of host defence responses. For example, Cheng *et al.* (2017) discovered that the *Pst* effector PSTha5a23 can supress PTI-like responses induced by bacterial pathogens. Similarly, *Pst* effectors Pst_8713 and Pst_12806 were also shown to supress PTI mediated callose deposition in wheat (Zhao *et al.*, 2018; Xu *et al.*, 2019). *Pst* effectors can also supress ETI-like responses. For example, Ramachandran *et al.* (2017) delivered the *Pst* candidate effector Shr7 in wheat and noticed Shr7 can supress nonspecific cell death caused by *P. syringae* DC3000. Pst_12806 was also shown to supress HR in wheat caused by *P. syringae* DC3000 (Xu *et al.*, 2019).

Due to functional redundancy, silencing an effector may not lead to reduced virulence of the rust pathogen. For example, silencing *AvrL567* from flax rust does not show reduced growth on flax (Lawrence *et al.*, 2010). However, a decreased number of pustules was observed when the *PEC6* effector from *Pst* was silenced through host induced gene silencing (HIGS) (Liu *et al.*, 2016). This suggests a general role of PEC6 in supressing the wheat host immune response.

Examples of effector functions from other fungal plant pathogens suggest that these proteins have multiple modes of action to facilitate pathogen infection. One strategy is to avoid detection of the pathogen by the plant. A classic example of this is the Ecp6 effector of *Cladosporium fulvum* that can sequester chitin, preventing recognition by plant cell receptors at the plasma membrane (Jonge *et al.*, 2010). Another strategy is to interfere with host immune responses. For example, the apoplastic effector Pep1 from *Ustilago maydis* inhibits the plant peroxidase POX12 that produces reactive oxygen species (ROS), key molecules in plant defence (Hemetsberger *et al.*, 2012). Other effectors may interact with host proteins to redirect them away from production of host defence molecules. For example, the *U. maydis* effector Cmu1 diverts precursors of salicylic acid (SA) towards the production of aromatic amino acids (Djamei *et al.*, 2011). Since SA is a key hormone in plant defence, its reduction leads to increased *U. maydis* virulence. These strategies are summarised in the cartoon depicted in **Figure 1-5.**

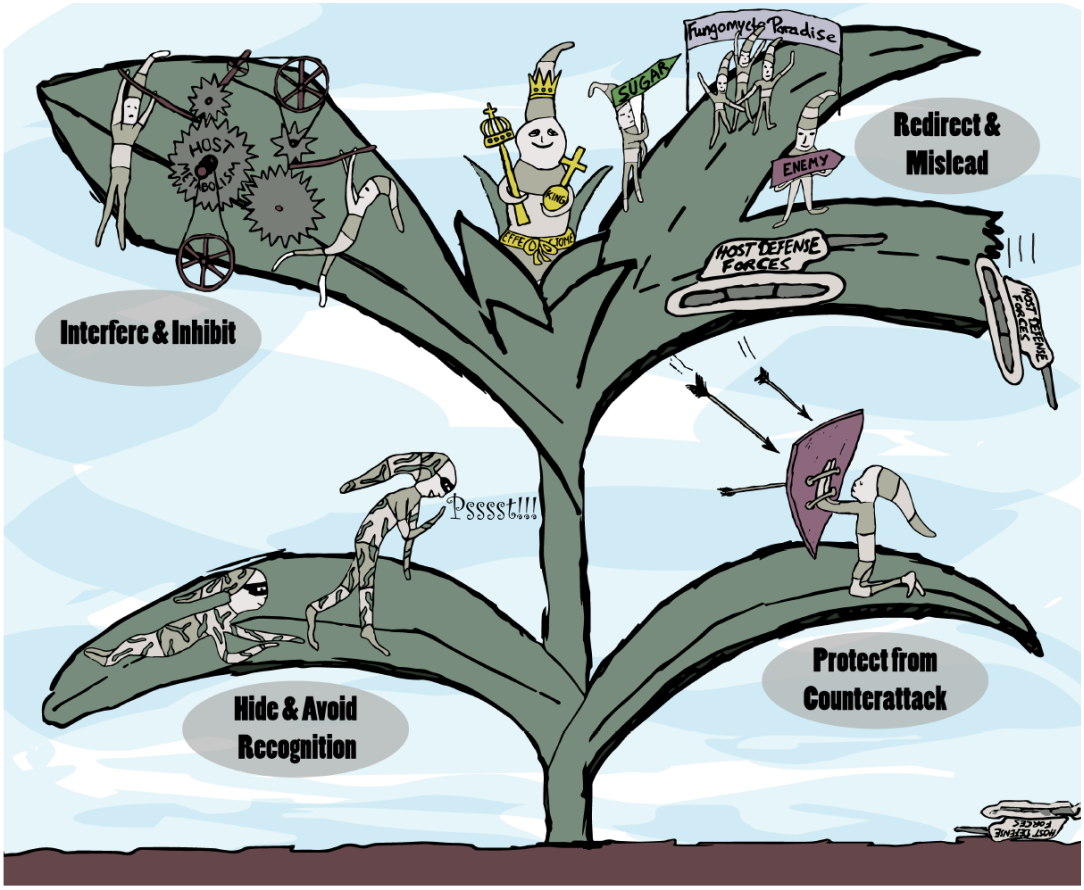


**Figure 1-5 Pathogen strategies for successful host invasion.** Fungi utilise their effector complement, or effectorome (illustrated as the king of the plant), to benefit pathogen proliferation. Some effectors can be used to block fungal recognition by the plant (bottom left). Others can protect fungi from the plant defence system (bottom right). Further, some effectors can interfere with plant host metabolism to dampen plant immune responses (top left). Additionally, fungi can use nutrients or other helpful components by redirecting them towards the pathogen and away from the plant (top right).This figure was published in Uhse & Djamei, (2018) and is reused with permission from copyright holders under the Creative Commons License.

### 1.5.3 Rust effectors and avirulence – tripping the wire

The pioneering work done on AvrL567 and AvrM from flax rust has established these AVR*s* as models for effector recognition by immune receptors. Both effectors are delivered into the host plant cytoplasm and are recognized by specific immune receptors via a direct interaction (Catanzariti *et al.*, 2006; Dodds *et al.*, 2004). Dodds *et al.* (2006) found 12 sequence variants of *AvrL567* from six rust strains. The six AvrL567 variants that were shown to be avirulent *in planta* were co-expressed in a yeast two-hybrid system to test their interaction specificity to the associated R proteins L5, L6, and L7. The AvrL567 variants A, B, F, J, and L are recognized by both L5 and L6, whereas AvrL567-D is L6 specific. The variants of AvrL567 found to be virulent *in planta* did not associate with either L6 or L7 in yeast. Similarly, Catanzariti *et al.* (2010) found avirulent variants of AvrM directly interact with the associated M resistance protein in a yeast two-hybrid assay. These results suggest recognition is based on a direct R-AVR protein interaction, and the authors suggest recognition by direct interaction may be overcome through sequence diversification, as seen in *AvrL567* and *AvrM,* rather than loss of function (Catanzariti *et al.*, 2010; Dodds *et al.*, 2006).

Both *AvrM* and *AvrL567* are also characterized by high levels of polymorphism as a result of diversifying selection. For example, there are 35 polymorphic positions in the 12 sequence variants of *AvrL567*, even though this gene encodes a protein of only 127 amino acids in length. Similarly, *AvrM* variants have 14 polymorphic positions including deletions, showing elevated sequence variation in comparison to the flanking sequence (Catanzariti *et al.*, 2006). It is often suggested that highly polymorphic effector genes are the result of an evolutionary arms race between these effectors and their interacting receptors. Indeed, structural analysis of AvrL567 variants A and D revealed polymorphisms in residues that interact with the associated R protein (Wang *et al.*, 2007).

In terms of the cereal rusts, only two avirulence effectors have been confirmed. Like *AvrM* and *AvrL567* from flax rust, the avirulence effector *AvrSr50* from *Pgt* is also polymorphic, with multiple alleles characterised from different isolates, and directly interacts with its cognate R protein (Chen *et al.*, 2017). Direct interaction with Sr50 was also confirmed using a yeast two-hybrid system, along with cell death assays in both *N. tabacum* and *N. benthamiana.* Similarly, direct interaction of the *Pgt* effector AvrSr35 with Sr35 was determined through cell death assays in *N. benthamiana* and also bimolecular fluorescent complementation (BiFC). The *AvrSr35* locus is also highly polymorphic, with many virulent isolates having severe deletions and truncations from transposon insertions in the avirulent allele (Salcedo *et al.*,

2017). A table of cereal rust effectors from *Pst* and *Pgt* that have been functionally characterised (in both virulence and avirulence) are summarized in **Table 1-1**.

**Table 1-1** Functionally characterised effectors from *Pst* and *Pgt*.

| Effector/AVR proteins | Pathogen | Localisation | Cellular function | Reference |
|---|---|---|---|---|
| PEC6 | *Pst* | Nucleus and cytoplasm in wheat epidermal cells | Suppression of PTI | (C. Liu *et al.*, 2016) |
| PSTha5a23 | *Pst* | Cytoplasm of wheat protoplasts | Suppression of PTI | (Cheng *et al.*, 2017) |
| Pst_8713 | *Pst* | Cytoplasm and nucleus of wheat protoplasts | Suppression of PTI, ETI | (M. Zhao *et al.*, 2018) |
| Pst 12806 | *Pst* | Chloroplasts in *N. benthamiana* | Suppression of PTI | (Xu *et al.*, 2019) |
| Shr7 | *Pst* | Not known | Suppression of ETI | (Ramachandran *et al.*, 2017) |
| PST02549 | *Pst* | P-bodies in the cytoplasm of *N. benthamiana* | Not known. Likely alters host transcription. | (Petre *et al.*, 2016) |
| PstSCR1 | *Pst* | Apoplast of *N. benthamiana* | Triggers PTI in non-host *N. tobacco* | (Dagvadorj *et al.*, 2017) |
| AvrSr35 | *Pgt* | Cytoplasm of wheat cells, ER and cytoplasm of *N. benthamiana* | Not known (avirulence) | (Salcedo *et al.*, 2017) |
| AvrSr50 | *Pgt* | Cytoplasm of wheat cells | Not known (avirulence) | (Chen *et al.*, 2017) |
| PGTAUSPE-10-1 | *Pgt* | Not known | Not known (avirulence) | (Upadhyaya *et al.*, 2014) |

## 1.6 The search for effectors

Understanding effector biology has given scientists a better understanding of disease development, ultimately influencing strategies to keep agricultural pests in check. It is important to continue identifying and functionally characterising plant pathogen effectors not only to uncover the incredible fundamental biology of these organisms, but also to shape the discovery of resistance genes in cultivars used for breeding programs (Kanja and Hammond-Kosack 2020). The following section is an overview of different methods for identifying candidate effectors, and how these methods have evolved over time.

### 1.6.1 Positional cloning

Most of the ground-breaking work on rust effectors has come from studies on the flax rust fungus, *Melampsora lini*. Indeed, the first rust effectors identified came from studying the *M. lini* – flax pathosystem. In the absence of sophisticated *in silico* technology, these effectors, for example AvrL567, were identified using traditional map-based cloning combined with expressed sequence tag libraries from infected materials as probes (Dodds *et al.*, 2004). Map based cloning involves following a phenotype of interest in a breeding population and looking for linkage to established genomic markers. *AvrL567* was identified by crossing the flax rust strain H (L5, L6, L7 avirulent) with strain C (L5, L6, and L7 virulent) to produce the hybrid CH5 strain. This strain was selfed, producing an F2 mapping population (Dodds *et al.*, 2004). A subset of clones from a cDNA library enriched for transcripts present in flax leaves during infection with the avirulent H strain were used as probes. These cDNA clones were used as DNA probes to detect restriction fragment length polymorphisms (RFLPs) segregating in the flax rust mapping family. One cDNA probe called IU2F2 detected RFLPs that co-segregated with the *AvrL567* locus corresponding to the cognate associated resistance genes L5, L6, and L7 in flax. Clones of this locus were isolated and narrowed down to a single gene that caused HR when transiently expressed in flax lines containing L5, L6, or L7, confirming its identity as *AvrL567* (Dodds *et al.*, 2004).

The flax rust system has been studied in depth since the 1970's when Flor established the gene-for-gene hypothesis defining interplay between host resistance (*R*) and rust avirulence (*AVR*) genes (Flor 1971). Therefore, this system has had much more time for the development of good genetic stocks, and a well-characterized mapping population with families segregating for multiple *AVR* loci (Duplessis *et al.*, 2012). Unfortunately, in other systems lacking these components, map-based cloning remains quite labour-intensive and time-consuming (Stergiopoulos and de Wit 2009). For example, establishing a sexual population for *Pst* under experimental conditions on the barberry alternate host has proven to be extremely difficult. This is because isolates that have undergone long term asexual reproduction produce few teliospores which are required to initiate the sexual cycle (Rodriguez-Algaba *et al.,* 2014). Despite this, a segregating population has been established for *Pst.* The resulting linkage map, however, produced markers that could not fully resolve virulence loci associated with a particular resistance gene (Yuan *et al.*, 2018). Fortunately, advances in next generation sequencing over the past few years have paved the way for a new era in effector discovery.

### 1.6.2 Genome Mining

Over the past decade, over 20 genomes of rust fungi have been sequenced (Lorrain *et al.*, 2019). Recent advances in long-read sequence technology have assisted the improvement of large rust genome assemblies in which the dikaryotic nuclei are partially phased (Lorrain *et al.*, 2019). These studies have not only uncovered important information about rust genome architecture, but also the prediction of candidate effectors. High-throughput computational methods for mining candidate effectors from full genomes has proven to be a valuable resource (Duplessis *et al.*, 2012). Genomic studies of plant pathogens, including rust fungi, have produced a characteristic profile for candidate effectors (Petre *et al.*, 2014). The following section describes common features typically used to mine effector candidates in genome wide studies.

### 1.6.3 Signal peptides, translocation motifs, and transmembrane domains

As previously described, in order for effectors to target host components and modulate plant immunity, they must first be secreted from the fungal pathogen. Thus, a common first step in effector mining is identifying proteins which have signal peptides. Programs such as SignalP predict signal peptide cleavage sites in proteins with high accuracy using sophisticated analytical algorithms including artificial neural networks (Petersen *et al.*, 2011). Not all proteins with signal peptides are secreted outside of the fungus. Signal peptides may also contain hydrophobic segments, usually longer than those in secretory proteins, that target proteins to a membrane (Sonah *et al.*, 2016). Therefore, in order to delimit secreted proteins from transmembrane (TM) proteins, it is necessary to identify TM domains within the secretome. A commonly used program to identify transmembrane domains is TMHMM (transmembrane hidden markov model), which uses a hidden Markov model to predict TM proteins and has been used in many effector prediction pipelines (Cantu *et al.*, 2013; Saunders *et al.*, 2012).

In oomycetes, numerous conserved translocation motifs have been discovered. Perhaps the best studied of these motifs is the RXLR motif found in *Phytophthora spp.* and downy mildews (Giraldo and Valent 2013). It is suggested that the RXLR motif plays a role in effector endocytosis into host cells by binding extracellular phosphatidylinositol-3-phosphate (PI3P), however these results remain controversial (Petre and Kamoun, 2014; Kale *et al.*, 2010). Other translocation motifs in oomycetes include the crinkler, or CRN motif, the YXSL[RK] motif from *Pythium ultimum*, and CHXC motif from *Albugo* species, all of which have putative functions in translocation into the host (Giraldo and Valent 2013). In fungi, translocation

motifs are less well defined, and most fungal effectors do not have an assigned putative translocation motif based on bioinformatic analyses (Rafiqi *et al.*, 2012). One of the few examples of an identified translocation motif in fungi comes from the ToxA effector from the necrotrophic fungus *Pyrenophora tritici-repentis*. This effector contains the RGD motif which directly binds to wheat mesophyll cells, allowing toxin internalization and cell death of the host plant (Manning *et al.*, 2008). Further, in the flax rust effectors AvrM and AvrL567, deletion studies have revealed N-terminal domains that are important in host translocation (Ve *et al.*, 2013; Rafiqi *et al.*, 2010). However, these host uptake regions were not found to be conserved in other fungi (Giraldo and Valent, 2013). In general, clearly conserved cell entry motifs analogous to the RXLR motif in oomycetes have not been identified so far in fungi (Rafiqi *et al.*, 2012).

### 1.6.4 Small cysteine rich proteins

Effectors that remain in the apoplast, and some that pass through the apoplast and into the host cytoplasm, often contain multiple cysteine residues. These effectors are deemed small cysteine rich proteins, or SCRs (Stergiopoulos and de Wit, 2009). These cysteine residues are involved in disulfide bridge formation that likely contribute to protein stability in the protease rich environment of the plant apoplast. For example, Avr4 and Avr9, effectors from the tomato leaf mould pathogen *Cladosporium fulvum,* contain disulfide bonds between cysteine residues that are required for stability and activity (Van den Hooven *et al.*, 2001; Van den Burg *et al.*, 2003). For cytoplasmic effectors, disulfide-bridge formation may contribute to proper tertiary folding required for the protein to be taken up by the host (Stergiopoulos and de Wit, 2009).

### 1.6.5 Genomic location of effectors

Previous analyses of fungal and oomycete pathogen genomes have revealed the presence of expanded genomes partially due to transposon proliferation and repetitive elements (Raffaele and Kamoun, 2012). Rust fungi are no exception, with the poplar rust and stem rust genomes being comprised of nearly 50 % repeats and transposable elements (Duplessis *et al.*, 2014). Such unstable repeat rich regions are often enriched with effector genes (Raffaele and Kamoun, 2012).

For example, 49.3 % of *Phytophthora infestans* secreted proteins are located within repeat rich, gene sparse regions, despite the fact that secreted proteins represent only 22.1 % of total genes (Raffaele *et al.*, 2010). Further, analysis of the phytopathogenic ascomycete *Leptosphaeria*

*maculans* genome revealed AT-rich blocks that are gene poor and transposable element rich. These particular regions are enriched in genes likely to have a role in pathogenicity (Rouxel *et al.*, 2011). In these AT-rich blocks, 20 % of the genes encode small secreted proteins (SSPs), most of which have features indicative of effectors, whereas only 4.2 % of genes located in GC-rich blocks encode SSPs, most of which lack features of known effectors of *L. maculans* (Rouxel *et al.* 2011). Thus, many fungal and oomycete plant pathogens display what is known as a "two speed genome" whereby genes associated with virulence are located in hypervariable regions enriched in repeats.

These studies suggest genomic plasticity plays a large role in the development and diversification of virulence traits and effector repertoires (Raffaele and Kamoun, 2012).Thus, location within repeat regions of the genome can be used as a requirement to rank the likelihood of a fungal secreted protein being an effector.

### 1.6.6 Other features of previously described fungal effectors

Since only a few rust effectors have been characterized, no general features have been identified that may be used in the computational prediction of effectors from fungi in the Pucciniales. Despite this, rust secretomes have been mined for candidate effectors by searching for other features of known effectors from filamentous pathogens in general. In addition to possessing a signal peptide, multiple cysteine residues, and residing in repeat rich genomic regions, such features include the presence of internal repeats, *in planta*-induced expression, similarity to haustorial proteins, and the absence of conserved protein domains, except for those associated with pathogenicity. For example, Saunders *et al.* (2012) designed an *in silico* pipeline to identify the putative effector repertoire from the genomes of poplar leaf rust and wheat stem rust. Using the aforementioned criterion, Markov clustering and hierarchical clustering were used to rank protein families of these two rust pathogens for their likelihood of being effectors.

### 1.6.7 Limitations to genome mining for effectors

Effector mining pipelines, although incredibly useful, are limited to assumptions based on previously described effectors. Many effectors however, deviate from these "common" characteristics of previously identified effectors. The stem rust effector AvrSr35, for example, has a mature length of 578 amino acids, which negates the "small size" assumption (Salcedo *et al.*, 2017). Further, recent data from phased rust genomes including *Pst* suggest a "one speed" genome instead of the commonly described "two speed genome." Effector candidates in *Pst* were not enriched in particular regions in comparison to other genes (Schwessinger *et*

*al.*, 2017). Evolution of effectors in a one-speed genome are purported to evolve via copy number variation and heterozygosity at the effector locus (Frantzeskakis *et al.*, 2019).

In combination with general candidate effector mining, comparative genomics has emerged as a powerful tool for effector identification (Cantu *et al.*, 2013; Plissonneau *et al.*, 2017; Saunders *et al.*, 2012; Upadhyaya *et al.*, 2015; Wu *et al.*, 2015). This approach involves comparing the genomes of multiple sequenced isolates with distinct virulence profiles. Non-synonymous single nucleotide polymorphisms (SNPs), and other changes in protein coding genes between sequenced isolates may reveal effector genes required for (a)virulence on particular wheat lines and not others.

### 1.6.8 Integration of comparative genomics and transcriptomics

The strength of comparative genomics was demonstrated in a study by Cantu *et al.* (2013) which used this approach to identify five *Pst* effector candidates that were highly expressed in haustoria and polymorphic between two UK isolates that differ in virulence to only two wheat varieties (YrRob and YrSol). After genome sequencing of the isolates, non-synonymous SNPs were called, and RNAseq data was used to identify transcripts specifically enriched in haustoria. Candidate effectors were determined by a scoring system, which involved annotating and ranking proteins based on known effector features. One candidate effector from this analysis, PST130_05023, has four amino acid substitutions between four sequenced isolates (UK isolates: PST-87/7, PST-08/21, US isolates: PST-21, PST-43, PST-130). The one specific substitution between the two UK isolates may explain the differential virulence of these two isolates seen on YrRob and YrSol. This gene, along with the other four candidates, are now of high priority for functional validation as virulence/avirulence factors in the wheat varieties Robigus and Solstice.

Furthermore, following a field pathogenomics study of 2013 UK isolates of *Pst*, Hubbard *et al.* (2015) were able to identify polymorphic and differentially expressed effector candidates which could be linked to the differential virulence profiles of *Pst* 2013 field isolates (Hubbard *et al.*, 2015). Thirty-nine *Pst* field isolates collected in the UK from 2013 were sequenced and aligned to the PST-130 reference genome. These field isolates were separated into four distinct population clusters using multivariate discriminant analysis of principal components (DAPC), which correlated directly with the isolate's virulence profile. Putative effectors were first identified by finding proteins that exhibited sequence conservation within population clusters, but variation between clusters. Next, proteins that had detectable secretion signals,

displayed features typical of characterized effector proteins, and that were significantly down or up regulated in comparison to genes in other population clusters were identified. Among the most highly ranked *Pst* effector candidates from a previous study, 10 genes were found to be upregulated and 9 were found to be down regulated (Hubbard *et al.*, 2015).

## 1.7 Functional validation of candidate rust effectors

Although many effector candidates have been identified, functional characterisation of these candidates has lagged behind due to the experimental intractability of the cereal rusts. A few systems are available for delivering rust effectors into the wheat host for detecting avirulence, however, each one of these systems has its limitations. Highlighting how little we know about cereal rust effectors, zero avirulence effectors have been confirmed for the leaf rust or yellow rust pathogen, and only two have been recently confirmed for the stem rust pathogen.

### 1.7.1 *Agrobacterium* mediated transient expression in surrogate plant systems

One high-throughput method for assessing avirulence properties of effectors *in planta* is the *Agrobacterium*-mediated transient expression system. In dicot plants, this method is routinely used to characterize effectors in the native host, including confirmation of avirulence properties (Upadhyaya *et al.*, 2014). This high-throughput method of characterising fungal effectors in dicot plants has not been as successful in crop host plants (Prasad *et al.*, 2019). Recently, this method been optimized for use in barley plants, however, *Agrobacterium* mediated transient expression remains inefficient and poorly suited for other crop hosts such as wheat (Prasad *et al.*, 2019).

Avirulence properties of effectors from wheat pathogens, however, can be detected through transient expression in a surrogate plant system, namely *Nicotiana benthamiana* (Petre *et al.*, 2014). This is only useful if the associated *R* gene has already been cloned and can be co-expressed with the avirulence effector, leading to a hypersensitive response. This is how the only confirmed avirulence effectors from the cereal rusts, *AvrSr50* and *AvrSr35*, were functionally characterised (Chen *et al.*, 2017; Salcedo *et al.*, 2017). Surrogate plant systems, however, can be prone to false negatives. Indirect recognition of an AVR by an R protein may require a host specific protein that is lacking or too divergent in *N. benthamiana*. For example, no cell death is observed when *AVRa9* from *Blumeria graminis* f. sp. *hordei* is co-expressed in *N. benthamiana* with the cognate *R* gene, *Mla9* (Saur *et al.*, 2019). However, co-expression in the native barley host will induce cell death, suggesting host specific proteins are required for the elicitation of HR.

Like most heterologous expression systems, transient expression in *N. benthamiana* may require optimisation to achieve appropriate protein levels and stability of both AVR and R protein (Bourras *et al.*, 2015; Saur *et al.*, 2019a; Saur *et al.*, 2019b). For example, Saur *et al.* (2019a) were able to detect cell death caused by recognition of AVRA1 by the R protein MLA1 only after labour intensive optimisation. In this case, cell death only occurred when AVRA1 was stabilised by a C-terminal fusion. Due to the widespread success of this system, usually with little optimisation required, this limitation is perhaps not given proper consideration.

### 1.7.2 Viral overexpression

Heterologous expression of effectors can also be mediated by viral surrogates. The barley stripe mosaic virus (BSMV) in particular can be used to deliver heterologous effectors in cereal hosts including wheat (Lee *et al.*, 2012). One of the first examples of this includes viral overexpression (VOX) of the apoplastic effector ToxA from the necrotrophic fungal wheat pathogen *Pyrenophora tritici-repentis*. BSMV-mediated ToxA overexpression in wheat resulted in extensive necrosis, suggesting successful delivery of this toxin in wheat cells (Manning *et al.*, 2010). Like all methods, the BSMV expression system has its limitations. In particular, stable overexpression is limited to protein size due to the compact nature of the virus. The upper limit of stable expression is approximately 150 amino acids, limiting any expression of effectors larger in size (Bouton *et al.*, 2018). However, this method can be used to confirm avirulence phenotypes of small effectors in wheat indirectly. For example, BSMV-mediated overexpression of *AvrSr50* in wheat leaves containing the cognate *R* gene induced an immune response that decreased the systemic spread of the virus itself (Chen *et al.*, 2017). Therefore, a decrease in BSMV disease symptoms is used as a proxy for avirulence phenotypes (Kanja and Hammond-Kosack, 2020). To date, this is the only example of a cytoplasmic avirulence effector being delivered into wheat using the viral overexpression system.

Recently, the foxtail mosaic virus (FoMV) VOX method was shown to stably overexpress larger constructs (up to 600 amino acids) in cereals, mitigating the size limiting factors of BSMV (Bouton *et al.*, 2018). Although both BSMV and FoMV are incredibly useful tools for delivering effectors in wheat, both systems share limitations. For example, viral overexpression systems can only be used on plant accessions that will tolerate systemic viral replication (Saur *et al.*, 2019). Further, both viruses create disease symptoms which can confound cell death caused by an effector. (Hein *et al.*, 2005; Bouton *et al.*, 2018). Although disease symptoms

caused by FoMV are purportedly less severe than those caused by BSMV, it still can complicate interpretation of phenotypic readouts (Bouton *et al.*, 2018). Screening for avirulence is therefore not only limited to wheat accessions that carry the cognate *R* gene but also to those that allow viral replication without excessive disease symptoms.

### 1.7.3 Biolistic assays

Another approach to deliver effectors *in planta* is transient expression via particle bombardment/biolistic transformation. This system has been used in rice, whereby delivery of the *Avr-Pita* effector from *Magnaporthe oryzae* was co-delivered with a GUS reporter gene into seedlings with the corresponding *R* gene *Pi-ta*. Reduced GUS activity was only observed when *Avr-Pita* was delivered in rice leaves expressing the corresponding resistance gene *Pi-ta* (Jia *et al.*, 2000). In this case, the reduced expression of a reporter gene is used as an indicator of HR. More recently, this method has been optimized for use in wheat. The powdery mildew (*Blumeria graminis* f. sp. *tritici)* effector *AvrPm3*$^{a2/f2}$ was co-bombarded into wheat cells with the associated *R* gene *Pm3a* along with a GUS reporter gene (Bourras *et al.*, 2015). The decrease in GUS expression in co-bombarded cells indicated cell death and thus suggested AvrPm$^{3a2/f2}$ is an avirulence effector (Bourras *et al.*, 2015). However, due to the labour-intensive nature of particle bombardment, it may not be viable for high-throughput screening (Upadhyaya *et al.*, 2014). Further, not all cells in the targeted region are transformed in this method, resulting in individual transformed cells scattered among untransformed ones (Yin and Hulbert, 2011). Depending on the efficiency of transformation, a clear pattern in reporter activity levels may be lost.

### 1.7.4 Protoplast assays

Avirulence properties of effectors can also be detected in plant host protoplasts. In this method, protoplasts from lines containing associated *R* genes are co-transfected with a construct containing an effector and a construct containing a reporter gene. Similar to the biolistic method, a decrease in reporter gene signal suggests cell death. This method has been employed in many cereal hosts including barley and rice (Chen *et al.*, 2006; Lu *et al.*, 2016; Ribot *et al.*, 2013). Lu *et al.* (2016) transformed barley protoplasts containing *MLA-1* or *MLA13* with *AVRa1* and *AVRa13* from *Blumeria graminis* f. sp. *hordei* (*Bgt)* respectively. In this case, luciferase activity was quantified as a proxy for cell death. A significant reduction of luciferase signal was detected in a Mla1-AVRa1 and Mla13-AVRa13 specific manner. Similarly, *R/AVR* pairs can be co-expressed in wheat and barley protoplasts to confirm avirulence properties of an effector. *AvrSr50* and *Sr50* were overexpressed along with a

reporter construct in wheat protoplasts, resulting in decreased luciferase activity and ultimately suggesting cell death (Saur *et al.*, 2019).

Protoplast assays, although incredibly useful, are labour-intensive and are not suitable for screening multitudes of effectors. These assays can also vary in efficiency if the associated *R* gene is not cloned, as native expression levels of the *R* gene in protoplasts can vary depending on which wheat variety is used (Peter Dodds, personal communication). Therefore, both *Agrobacterium* and protoplast methods are limited by the number of cloned associated *NLR* genes, which is very limited particularly for *Pst* and *Pt* (**Table 1-2**). Other methods must be used for screening multiple avirulence effector candidates, especially if the associated *R* gene has not been cloned.

**Table 1-2** Cloned NLR genes for resistance against wheat rust pathogens

| NLR name | Resistance to (*Pst*, *Pgt*, or *Pt*) | Reference |
|---|---|---|
| Yr10 | *Pst* | (Liu *et al.*, 2014) |
| Yr5/YrSp | | (Marchal *et al.*, 2018) |
| Yr7 | | (Marchal *et al.*, 2018) |
| YrAS2388 | | (C. Zhang *et al.*, 2019) |
| Lr1 | *Pt* | (Cloutier *et al.*, 2007) |
| Lr10 | | (Feuillet *et al.*, 2003) |
| Lr21 | | (Huang *et al.*, 2003) |
| Lr22a | | (Thind *et al.*, 2017) |
| Sr50 | *Pgt* | (Mago *et al.*, 2015) |
| Sr33 | | (Periyannan *et al.*, 2013) |
| Sr35 | | (Saintenac *et al.*, 2013) |
| Sr22 | | (Steuernagel *et al.*, 2016) |
| Sr45 | | (Steuernagel *et al.*, 2016) |
| Sr13 | | (Zhang *et al.*, 2017) |
| Sr21 | | (Chen *et al.*, 2018) |
| Sr46 | | (Arora *et al.*, 2019) |
| SrTA1662 | | (Arora *et al.*, 2019) |
| Sr26 | | Zhang *et al.*, under review<br>(Zhang *et al.*, 2020) |
| Sr61 | | Zhang *et al.*, under review<br>(Zhang *et al.*, 2020) |

### 1.7.5 The bacterial T3SS

A high-throughput method for functionally characterising effectors in wheat using the bacterial type III secretion system (T3SS) has previously been described (Upadhyaya *et al.*, 2014). Certain bacteria deliver effectors directly into the host cytoplasm via a pilus that traverses the plant plasma membrane (Wagner *et al.*, 2018). The T3SS can be exploited to target candidate effectors towards the pilus and directly into the host (Casper-Lindley *et al.*, 2002). This method was successfully used for a single *Pgt* candidate effector, but for unknown

reasons has not extensively been used in cereals for detecting avirulence properties (Upadhyaya *et al.*, 2014). This system was developed in wheat before the discovery of any avirulent cereal rust effectors, and thereby remains untested with appropriate positive controls.

## 1.8 Introduction to the current study

As previously mentioned, many candidate effectors have been identified using comparative genomics, transcriptomics, and genome mining. Despite this, no effectors that are recognized by a particular resistance protein in wheat have been characterized for *Pst* to date. Unfortunately, reliable and robust methods for delivering and functionally characterizing candidate effectors of *Pst* in the native wheat host remains limited. I aimed to address these issues with the following specific objectives:

1) Identify effector candidates of *Pst* that are specifically recognized by the resistance protein YR2 using comparative genomics of spontaneous gain of virulence mutants.
2) Explore the bacterial T3SS for the delivery and characterisation of candidate rust effectors in wheat using an established stem rust AVR as a positive control.
3) Develop a novel heterologous expression system using an experimentally tractable fungal wheat pathogen for detecting rust effector avirulence phenotypes in the native wheat host.

# Chapter 2 Comparative genomics of spontaneous gain of virulence mutants reveal candidate *AvrYr2* effectors

## 2.1 Abstract

Currently, all candidate effectors of *Pst* are not associated with a single resistance protein in wheat. Here, I designed an *in silico* pipeline to mine effector candidates of *Pst* that specifically target the YR2 resistance protein. This pipeline is based on comparative genomics, a process that detects polymorphisms between *Pst* isolates that have the exact same virulence profile except for the ability to infect YR2 wheat. Further, the accuracy of this pipeline has been improved by exploiting recently generated highly contiguous reference genomes. This pipeline has produced three candidate effectors that are of high priority to functionally characterise experimentally.

## 2.2 Introduction

### 2.2.1 Comparative genomics from population samples: limitations

Since the release of the first *Pst* reference genome (Cantu *et al.*, 2011) scientists have discovered multiple candidate effectors of this pathogen using comparative genomics. This approach involves identifying polymorphisms within genes encoding secreted proteins that occur between isolates with differing virulence profiles. For example, Cantu *et al.* (2013) compared two isolates of similar origin that differ in virulence to only two different wheat varieties *YrRob* and *YrSol*. Focusing on genes that were polymorphic between these two isolates produced candidate effectors potentially recognized by the specific R proteins present in the different wheat varieties.

These polymorphic sites may be important for the 3D structure of the effector protein, which may affect binding to effector targets, and thus virulence on wheat. However, one challenge regarding this approach is not knowing which polymorphisms are associated with changes in virulence, rather than simply due to divergent evolutionary origins of the isolates. This can be a problem even in closely related isolates, as somatic mutations can accumulate in asexual populations over time (Seidl and Thomma, 2014). Further, comparing isolates with multiple differences in their virulence profile makes it difficult to associate polymorphisms with the ability to infect specific wheat varieties.

### 2.2.2 Spontaneous gain of virulence mutants: the ideal comparative genomics dataset

One way to mitigate this problem is to isolate a spontaneous gain of virulence mutant from an avirulent strain. Since the isolates share a common evolutionary background, any changes may be associated with a single resistance gene and are less likely to be a result of evolutionary divergence. Chen *et al.* (2017) used this method to identify one the first confirmed avirulence effectors from *Puccinia graminis* f. sp. *tritici* (*Pgt*), AvrSr50. By sequencing a spontaneous gain of virulence mutant to wheat harbouring the *Sr50* R gene, the authors were able to identify a 2.5Mbp loss of heterozygosity event in which an entire chromosomal arm from one haplotype replaced the other. Within this region, Chen *et al.* (2017) found 24 genes annotated as haustorially secreted proteins, one of which was confirmed as *AvrSr50*. Another way to obtain gain of virulence mutants is through large-scale induced mutagenesis. For example, gain of virulence mutants to Sr35 were induced by subjecting a *Pgt* isolate carrying *AvrSr35* to EMS mutagenesis (Salcedo *et al.*, 2017). By comparing the WT isolate to the gain of virulence mutants, the authors were able to find *AvrSr35*. To date, these are the only examples of functional validation of an avirulent candidate effector from the cereal rusts. Both have been identified via genome wide comparative genomics of gain of virulence mutants, uncovering the potential of this approach in identifying effectors from rust fungi.

### 2.2.3 Gain of virulence – Variation occurs in the absence of sex

Many different kinds of mutations can occur to produce a gain of virulence mutant during the asexual phase of a pathogen. Previously thought to be evolutionary dead ends, organisms in the asexual state have shown evolutionary adaptation in many different ways (Seidl and Thomma, 2014). A few of these mechanisms are summarised in **Figure 2-1**.

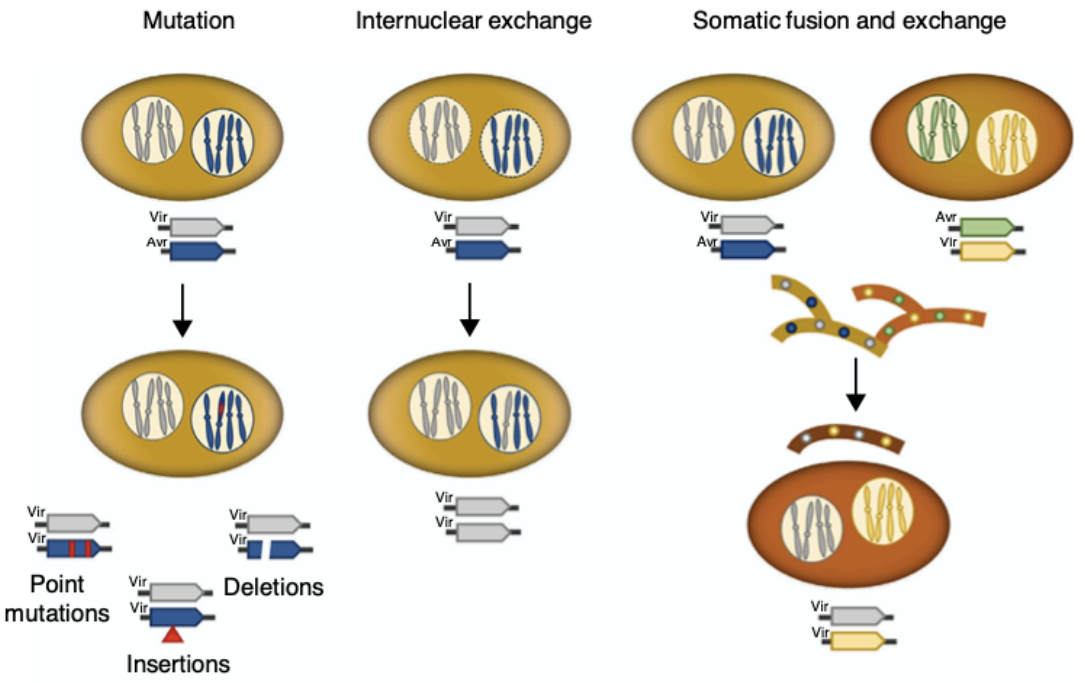


**Figure 2-1 Different ways rust fungi can lose avirulence during the asexual stage.** Left panel: single step point mutations, insertions, and deletions in an aviruelnt allele can lead to gain of virulence. Middle panel: avirulent alleles can be lost and replaced with the virulent allele from the other nuceli via internuclear exchange. Right panel: dikaryotic hyphae can fuse, exchange nuclei, and produce novel strains with new virulence profiles. This figure was published in Figueroa *et al*. (2020) and is reused with permission from copyright holders under license number 4950700637198.

#### 2.2.3.1 Mutations: point mutation, insertions, deletions

Clonal populations that exclusively reproduce asexually on wheat hosts are able to overcome resistance in a stepwise manner. Single amino acid changes in avirulence proteins (point mutations) can lead to newly virulent isolates due to evasion of recognition by the associated R protein (Ellis *et al.*, 2014; Wellings, 2011). This is exacerbated by the presence of monocultures of wheat varieties that lack diversity in resistance genes. This type of agricultural practice often results in high selection pressure of *Pst* to overcome the few resistance genes deployed in a wheat field at a given time (Schwessinger, 2016). Newly emerged pathotypes that appear virulent on previously resistant wheat varieties are often genetically related to pre-existing isolates, suggesting mutation as the cause of novel virulence (Hovmøller *et al.*, 2011).

For example, (Steele *et al.*, 2001) tested the hypothesis that modern pathotypes from Australia and New Zealand, each of which have assorted virulence profiles, originated from the first *Pst* isolate detected in Australia in 1979. Molecular variation in seven different pathotypes were detected via random amplified polymorphic DNA (RAPD) primers. Over 300 potentially polymorphic loci, no differences were detected between isolates. Due to the lack of genetic

diversity in modern Australian and New Zealand yellow rust isolates, the authors suggest that multiple virulences evolved in a stepwise manner from an original clonal lineage.

In addition to point mutations, insertions of transposable elements and non-repetitive DNA can disrupt avirulence genes leading to gain of virulence. For example, some virulence alleles of the *Pgt* effector *AvrSr35* contain multiple MITE (miniature inverted-repeat transposable element) insertions (Li *et al.*, 2019). Large DNA insertions can also disrupt avirulence alleles rendering them unrecognizable by the host. For example, sequencing *AvrSr50* from multiple *Pgt* isolates revealed the most common virulence allele has a large 26 kbp insertion disrupting the gene (Chen *et al.*, 2017). Other virulence alleles of *AvrSr50* were also gained through point mutations. Deletion events may also lead to gain of virulence. For example, the avirulent locus *AvrSr27* from *Pgt* contains two genes that have been deleted in various virulent isolates (Figueroa *et al.*, 2020). In summary, point mutations and small insertion/deletion variants (indels) provide genetic variation whereby virulence can be gained in the absence of sexual recombination (**Figure 2-1**, left panel).

#### 2.2.3.2 Internuclear exchange and somatic fusion

Another mechanism for gain of virulence is internuclear exchange (**Figure 2-1**, middle panel). The spontaneous gain of virulence mutant for *Sr50* mentioned previously arose through this type of mutation (Chen *et al.*, 2017). Chromosome 14 from the nuclei carrying the virulent allele was duplicated and subsequently replaced the homologous chromosome carrying the avirulent allele. Somatic fusion of asexual hyphae leading to nuclear exchange has recently been proposed as another mechanism whereby novel virulence can occur (**Figure 2-1**, right panel). For example, the *Pgt* Ug99 lineage shares an entire haplotype with the 21-0 race. The absence of recombination in this shared haplotype suggests Ug99 arose via a nuclear exchange event (Li *et al.*, 2019).

### 2.2.4 Introduction to the current study

Two gain of virulence mutants to YR2 were previously isolated from Sørensen *et al.* (2013), providing an ideal comparative genomics dataset to search for *AvrYr2*. One pair of isolates originate from the UK (W1 and M1) and the other from Denmark (W2 and M2) (**Table 2-1**). Each pair represent near isogenic lines in which one isolate has spontaneously gained virulence on YR2 wheat presumably through loss of a dominant avirulent allele by some unknown mechanism (**Figure 2-2**). Therefore, the mutants in this study represent recent spontaneous gain of virulence mutants from the same clonal lineage as the wild type. It is likely the WT

isolates are heterozygous for the *AvrYR2* allele, as avirulent alleles are often dominant. To confirm the mutant isolates were not introduced via exotic incursion, Sørensen *et al.* (2013) demonstrated the two mutants shared the same AFLP fingerprint and virulence profile to their respective wild type isolates, except for YR2 virulence. I predict using spontaneous gain of virulence mutants will decrease the amount of variation due to evolutionary divergence not associated with virulence. Furthermore, I predict that comparing isolates with only one difference in their virulence profiles will identify candidate effectors that exclusively target YR2 in wheat.

**Table 2-1** Virulence profiles of isolates and references used in this chapter

| Isolate designation | | | Virulence Phenotype[a] | | | | | | | | | | | | | | | | |
|---|---|---|---|---|---|---|---|---|---|---|---|---|---|---|---|---|---|---|---|
| ID | Genotype | Lineage | 1 | 2 | 3 | 4 | 5 | 6 | 7 | 8 | 9 | 10 | 15 | 17 | 25 | 27 | 32 | Sd | Sp |
| UK75/30 | Wildtype (W1) | 1 | - | - | - | - | - | - | - | - | - | - | - | - | 25 | - | 32 | Sd | Sp |
| Mut15/05 | Mutant (M1) | 1 | - | 2 | - | - | - | - | - | - | - | - | - | - | 25 | - | 32 | Sd | Sp |
| DK24/95 | Wildtype (W2) | 2 | - | - | 3 | 4 | - | 6 | - | - | - | - | - | - | 25 | - | 32 | Sd | - |
| Mut21/06 | Mutant (M2) | 2 | - | 2 | 3 | 4 | - | 6 | - | - | - | - | - | - | 25 | - | 32 | Sd | - |
| PST104E | Reference | - | - | 2 | 3 | 4 | - | - | - | - | - | - | - | - | 25 | - | - | Sd | - |
| 11281 | Reference | - | - | - | - | - | - | - | - | - | - | - | - | - | - | - | - | - | - |

[a] Names designate virulence corresponding to specific yellow rust resistance genes. -, avirulence; Sd, Strubes dickoff; Sp, Spalding prolific. Virulence profiles taken from (Li *et al.*, 2019; Hovmøller *et al.*, 2013; Wellings, 2007)

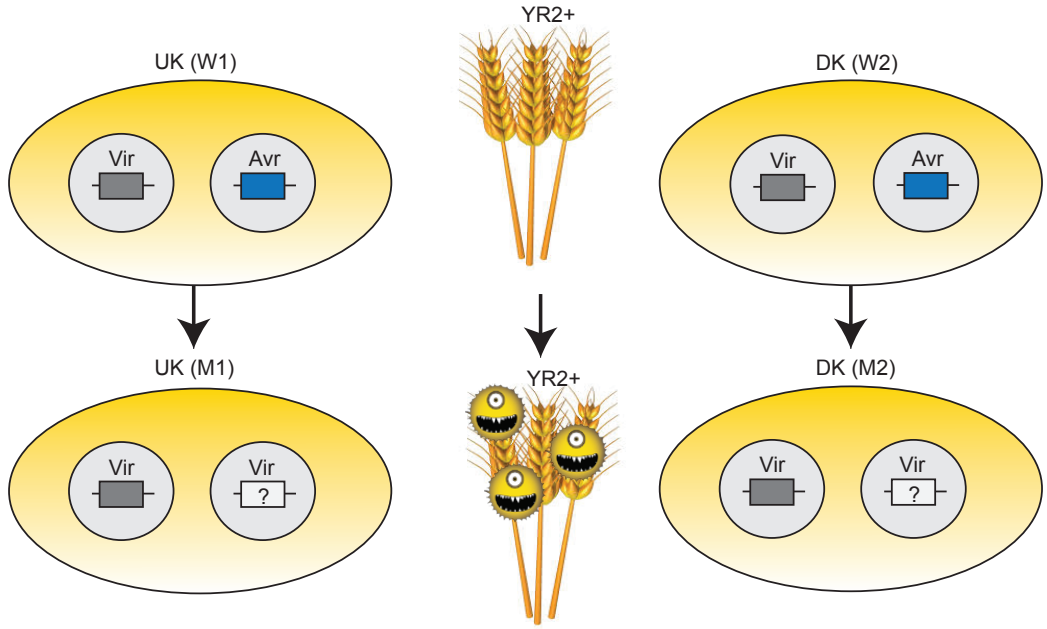


**Figure 2-2 Schematic of wildtype and mutant isolates used in this study.** Mut1 is a spontaneous gain of virulence mutant derived from W1 (originating from the UK), and M2 is a spontaneous gain of virulence mutant derived from W2 (originating from Denmark). In both W1 and W2, a change has occurred in the avirulent allele by some unknown mechanism to produce gain of virulence mutants.

### 2.2.5 Variant calling: the reference matters

In this study, I use reference-based variant calling to detect mutations that differ between the wildtype and mutant isolates. This method requires aligning short reads to a reference genome and identifying variants in comparison to that reference (Horner *et al.*, 2009). Previous *Pst* reference genomes have been sequenced solely using short read data, producing highly fragmented contigs (**Table 2-2**). This is largely due to the inability of short read sequences to resolve repetitive areas of the genome (Pfeifer, 2017). In these instances, genes encoding effector proteins can often map to incomplete or inaccurate areas of the reference. However, recent advances in long-read sequencing technology and assembly software has helped resolve repetitive regions, leading to more contiguous genomes (Sedlazeck *et al.*, 2018). These genomes are partially phased, meaning any sequences that diverge from the primary haplotype, or the primary contig, are separated into haplotigs. For example, the reference genome of isolate PST-104E137A- contains substantially fewer contigs in contrast to the widely used unphased reference of isolate PST-130 providing a much more contiguous reference for *Pst* (**Table 2-2**).

For the analysis in this chapter, I chose two separate reference genomes, both of which are partially phased. One reference, PST-104E, was chosen for belonging to the same NW European clonal lineage to the W1, W2, M1, and M2 isolates (Hovmøller and Justesen, 2007; Schwessinger *et al.*, 2018). This will likely decrease mismapping of phylogenetically divergent reads. This reference, however, is virulent on YR2 (**Table 2-1).** Therefore, there is a possibility this reference may not contain the *AvrYr2* sequence if the isolate lost avirulence due to deletion. Another possibility is that other mutations have rendered the avirulent allele a pseudogene, therefore not being annotated as a gene at all. Due to this reason, a second reference that is avirulent on YR2 was chosen, PST-11281. This isolate was sampled from wheatgrass (*Agropyron cristatum*) in the US, and is highly avirulent on many wheat cultivars, including YR2 (Xia *et al.*, 2019). This isolate, however, is likely phylogenetically divergent to the W1, W2, M1, and M2 isolates, increasing the chance of mismapping.

**Table 2-2** Publicly available reference genomes for *Pst* and their properties

| Isolate | No. Contigs[a] | Technology/phased | Total length (bp) | No. proteins predicted | Reference |
|---|---|---|---|---|---|
| PST-130 (unphased) | 29,178 | Short reads/not phased | 65Mb | 18,149 | (Cantu *et al.*, 2011) |
| PST-21 | 43,106 | Short reads/not phased | 73Mb | 20,653 | (Cantu *et al.*, 2013) |
| PST-43 | 49,784 | Short reads/not phased | 71 Mb | 21,036 | (Cantu *et al.*, 2013) |
| PST-87/7 | 55,502 | Short reads/not phased | 53 Mb | 20,688 | (Cantu *et al.*, 2013) |
| PST-08/21 | 50,898 | Short reads/not phased | 56 Mb | 20,875 | (Cantu *et al.*, 2013) |
| PST-78 | 17,295 | Short reads/not phased | 117.31 Mb | 19,542 | (Cuomo *et al.*, 2017) |
| CY32 | 12,833 | Fosmid to fosmid/not phased | 115 Mb | 25,288 | (Zheng *et al.*, 2013) |
| **PST-104E137A-** | P: 156 H: 475 | Long reads/partially phased | P: 83Mb H: 73Mb | P: 15,928 H: 14,321 | (Schwessinger *et al.*, 2018) |
| **PST-11281** | P: 381 H: 873 | Long reads/partially phased | P: 84.75Mb H: 60.09 Mb | P: 16,869 H: 12,145 | (Li *et al.*, 2019) |
| PST-130 (phased) | P: 151 H: 458 | Long reads/partially phased | P: 85.4Mb H: 65.9Mb | P: 17,881 H: 14,173 | (Vasquez-Gross *et al.*, 2020) |
| PST-DK0911 | P: 94 H: 1176 | Long reads/partially phased | P: 74Mb H: 52Mb | P: 15,070 H: 14,321 | (Schwessinger *et al.*, 2019) |
| 93-210 | 493 | Long reads/not phased | 84 Mb | 16,513 | (Xia *et al.*, 2018) |

[a]P, Primary contigs; H, Haplotigs

### 2.2.6 YR2

*YR2* is a seedling resistance gene that behaves in a gene-for-gene manner with *Pst* isolates avirulent on YR2 wheat (Calonnec *et al.*, 1997). Virulence to Yr2 became common in the 1970s which contributed to epidemics and crop losses during that time period (Wellings, 2011). Currently *YR2* is not cloned, however, the closest SSR marker determined is 5.6 cM from the *YR2* locus on chromosome 7B (Lin *et al.*, 2005). Although *YR2* is not cloned, avirulence to YR2 can be tested on Kalyansona, the differential wheat line for YR2.

## 2.3 Methods

### 2.3.1 Isolates and genomic data used in this study

DNA from the four isolates (W1, M1, W2, M2) used in this study were provided by Sørensen *et. al.* (2013). All genomic paired end sequence data from the four isolates were previously generated by the Saunders lab using Illumina Hiseq2500 sequencing. The reference genome PST-11281, including the secretome and proteome is publicly available at https://github.com/yuxiang-li/Puccinia_striiformis_genome_11_281. The PST-104E reference genome, including the proteome and secretome is also publicly available at https://github.com/BenjaminSchwessinger/Pst_104_E137_A-_genome.

### 2.3.2 Short read pre-processing

Illumina short reads were processed using Trimmomatic v0.33 (Bolger *et al.*, 2014) with the following parameters: "ILLUMINACLIP: TruSeq3-PE-2.fa:2: 30:10:2:true SLIDINGWINDOW:4:10 MINLEN:36". The ILLUMINACLIP parameter identified and eliminated Illumina adapters specified in the Truseq3 library. Using SLIDINGWINDOW:4:10, reads were scanned in a 4 bp window and trimmed when the average quality dropped below 10. The default parameter MINLEN:36 dropped reads below 36 bases long. After trimming, the quality of the reads was checked with FastQc v.0.11.7 (Andrews, 2010).

### 2.3.3 Alignment

Illumina reads were aligned to either the PST-11281 or PST-104E reference genome using BWA-MEM v.0.7.7 with default parameters (Li and Durbin, 2009). SAM files were sorted, PCR duplicates were removed, and read groups were added using Picard Tools (Broad Institute) v1.134 parameters SORT_ORDER=coordinate MarkDuplicates and AddOrReplaceReadGroups.

### 2.3.4 Variant Calling and Hard Filtering

Variant calling was performed with GATK v3.8.0 using HaplotypeCaller (Poplin *et al.* 2017). SNPs were filtered using GATK VariantFiltration with the default recommendations: "QD < 2.0 || FS > 60.0 || MQ < 40.0 || MQRankSum < -12.5 || ReadPosRankSum < -8.0". Indels were filtered using the following: "QD < 2.0 || FS > 200.0 || ReadPosRankSum < -20.0". Gene deletions were identified using HTSeq (Anders *et al.*, 2015) with parameters -count –-

type exon. Genes that had a coverage of less than 10 were considered a full gene deletion. Unmapped reads were *de novo* assembled using ABySS (Simpson *et al*., 2009).

### 2.3.5 Finding Candidates

Variants that were private to the mutant libraries in comparison to their respective WT library were obtained using bcftools v.1.9 with parameters "-p vcfcompare -n-1 -c all WTlib.vcf Mutlib.vcf". To find variants producing deleterious changes in genes coding for proteins, each .vcf file was run through SnpEff v 3.3a (Cingolani *et al*., 2012). The .vcf files were then filtered for those that produced deleterious changes associated with coding sequences. These genes were then filtered for those that are part of the reference secretome. Variants were confirmed manually by visual inspection of read mapping tracks in IGV v 2.8.12 (Robinson *et al*., 2011).

### 2.3.6 Identifying Candidate Properties

Protein domains of effector candidates were identified using InterProScan (Mitchell *et al*., 2019). Matching genes in other reference genomes were identified using BlastP. Expression data was identified using publicly available information (Cantu *et al*., 2013).

## 2.4 Results

### 2.4.1 Genome sequencing and alignment

To determine variants between the wild type and spontaneous gain of virulence mutants, I first aligned Illumina short read sequences to either the PST-104E or PST-11281 reference genome. Reads were aligned to the primary contigs and haplotigs separately. False positive variants due to mismapping at the alternate haplotype are equally likely for the wildtype and mutant isolate libraries. These common mutations will be eliminated later in the analysis (section 2.4.3). The coverage of each alignment ranges from approximately 25x for the M2 library to ~50x coverage in the W1 library (**Table 2-3**). The lower coverage in the mutated libraries is due to fewer QC passed reads provided for the analysis. Reads that did not map to either the primary contigs or haplotigs were *de novo* assembled. None of these contigs provided open reading frames containing a candidate *AvrYr2* effector.

**Table 2-3** Alignment statistics of each isolate to the two reference genomes

| Reference | Estimated Mean Coverage | Genotype | QC passed reads | % mapped | % properly paired | % singletons |
|---|---|---|---|---|---|---|
| PST-104E Pcontig | 45x | W1 | 57077856 | 68.7 | 63.08 | 2.66 |
| | 34x | M1 | 47230491 | 63.1 | 54.04 | 3.45 |
| | 39x | W2 | 54671133 | 62.39 | 54.76 | 3.35 |
| | 25x | M2 | 37594785 | 57.55 | 48.66 | 3.66 |
| PST-104E Hcontig | 48x | W1 | 57084239 | 64.21 | 58.22 | 2.77 |
| | 36x | M1 | 47236439 | 58.83 | 49.71 | 3.51 |
| | 41x | W2 | 54687237 | 57.90 | 50.01 | 3.41 |
| | 26x | M2 | 37594967 | 53.00 | 44.25 | 3.54 |
| PST-11281 Pcontig | 45x | W1 | 57120800 | 69.43 | 62.15 | 3.35 |
| | 34x | M1 | 47264894 | 64.16 | 53.28 | 4.26 |
| | 39x | W2 | 54712666 | 63.28 | 53.82 | 4.16 |
| | 25x | M2 | 37622932 | 58.54 | 47.89 | 4.47 |
| PST-11281 Hcontig | 53x | W1 | 57123365 | 59.75 | 51.92 | 3.5 |
| | 40x | M1 | 47274065 | 54.66 | 43.7 | 4.34 |
| | 46x | W2 | 54737822 | 53.98 | 44.36 | 4.09 |
| | 29x | M2 | 37617257 | 49.76 | 39.76 | 4.09 |

### 2.4.2 Variant Calling and Annotating

After aligning reads to the reference genome, variants were detected using GATK HaplotypeCaller (Poplin *et al.*, 2017). This software works by *de novo* assembling regions different from the reference, simultaneously identifying SNPs and indels. After variants were identified, SnpEff was used to annotate those variants and predict the outcome of these effects (ex. non-synonymous changes etc). Each library (W1, M1, W2, M2) had the same percentage of variant type when aligned to the same reference. For example, 34.77 % of variants called for each library were in the downstream region (5 kbp) of annotated genes when the PST-104E genome was used as a reference (**Figure 2-3**a). These numbers are quite similar when variant types are identified using PST-11281 as a reference. For example, all samples had 34.75 % of variants in the downstream region when using the PST-11281 reference genome (almost identical to the PST-104E reference) (**Figure 2-3**c). Of all the variant types that were predicted to be the most deleterious, the majority of them cause non-synonymous changes (**Figure 2-3**b, d).

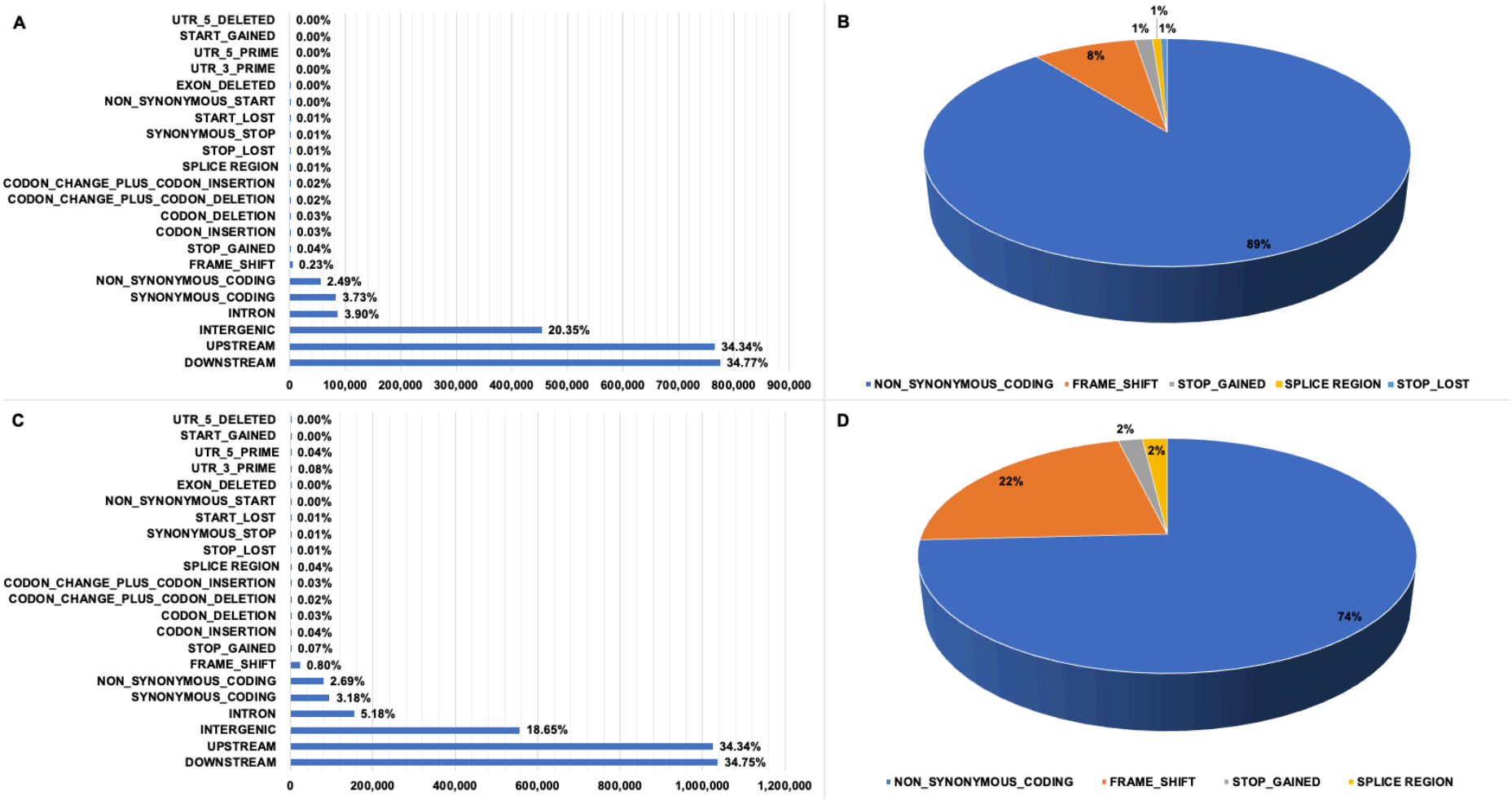


**Figure 2-3 Types and frequencies of variant effects.** A) The percentage of SNPs causing each type of effects when using the PST-104E and C) PST-11281 reference. B) The types and percentage of SNP effects causing predicted deleterious effects when using the PST-104E and d) PST-11281 reference.

### 2.4.3 Identifying candidates

After identifying all possible variants in each isolate library, I created a pipeline to search for variants associated with *AvrYr2* avirulence summarised in **Figure 2-4**. First, genes with variants common between the mutant isolate and their respective wild type progenitor were discarded. These variants are likely due to phylogenetic divergence between the isolates and the reference. These variants may also be a result of reads from one haplotype aligning to the other. These events are likely to occur in both wild type and mutant isolates, creating common false positives that can be removed. Next, genes with variants specific to the mutant isolate in comparison to their wild type progenitor were identified. Due to the possibility that PST-104E carries the same type of virulent allele that has arisen in the gain of virulence mutants, variants specific to the wild type isolate in comparison to their respective mutants were also identified. Following this step, genes with variants common in either both wild type isolates or both mutant isolates were identified. This gene list was further refined by selecting genes encoding secreted proteins. The alignment of the raw reads in these specific genes were examined manually in IGV. The majority of genes had variants called in one wild type, but variants in the associated mutant were on the borderline of being called. For example, an 80/20 SNP ratio may be called in the WT, but the mutant may have a ratio of 81/19 that does not get called. These genes were then removed from the candidate list.

After manual curation, I did not find any candidate genes with this pipeline. Due to the possibility that different genes have been mutated to produce the same gain of virulence phenotype, I repeated the pipeline, but did not require the variants to occur in the same genes of both UK and DK lineages. Using this method, I found three genes with variants in the M1 isolate in comparison the W1 isolate (**Table 2-4**). These genes were identified when using PST-11281 as the reference. Two variants caused a non-synonymous change in a gene encoding a secreted protein, and one variant caused a SNP in an intron. In all cases, the wild type had 100 % of all reads supporting a single nucleotide. The mutants however, had a strong SNP ratio near 50/50 suggesting one nucleus has mutated at this particular position (**Table 2-4**).

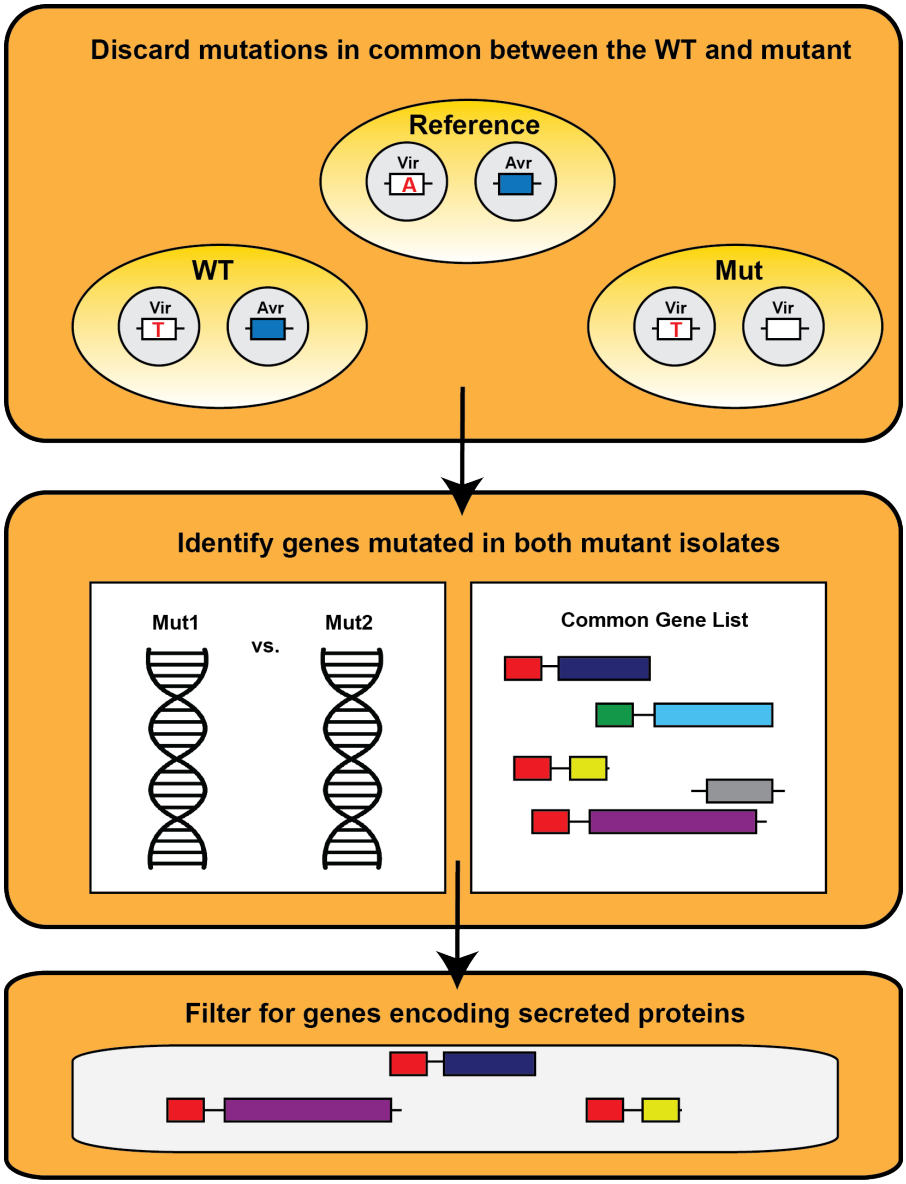


**Figure 2-4 *In silico* pipeline for mining *AvrYr2* candidates.** Each WT and mutant isolate were aligned to the reference genome. Mutations common in both the WT and mutant isolate (shown as T in this example) in comparison to the reference (shown as A in this example) were discarded. Next, genes with mutations in both mutant isolates were identified. Lastly, candidate genes were filtered for those that had predicted signal peptides.

**Table 2-4** Variants in candidate *AvrYr2* genes

| Gene Name | Length of protein (amino acids) | SNP location | W1 SNP RATO | M1 SNP RATIO | Type of change |
|---|---|---|---|---|---|
| PS_11-281_00009225 (P contig) | 1241 | Codon 801 | G: 100 | C/G: 45/55 | Non synonymous coding |
| PS_11_281_scaffold_712 (H contig) | 798 | Codon 773 | G:100 | C/G: 45/55 | Non synonymous coding |
| PS_11_281_scaffold_9696 (H contig) | 1591 | - | C:100 | C/T: 52/48 | SNP in intron |

### 2.4.4 Candidate properties

To further characterise the candidate effectors, I searched for conserved protein domains using InterProScan (Mitchell *et al.*, 2019). Candidates PS_11-281_00009225 and PS_11_281_scaffold_712 both contain zinc finger domains **(Table 2-5)**. These two proteins are likely allelic variants of one another, as they share 77.58 % pairwise identity when compared at the amino acid level. To identify expression data from these candidate genes, I first performed a BLAST search to find matching proteins in the PST-130 genome, as RNA-seq data is available for this isolate. Both PS_11-281_00009225 and PS_11_281_scaffold_712 have PST-130 matches that are highly expressed in haustoria **(Table 2-5)**. PS_11_281_scaffold_9696 seems to be more elusive, as no conserved protein domains were identified. Further, there is no RNA-seq data available for this candidate.

**Table 2-5** Properties of candidate *AvrYr2* effectors

| Gene Name | Closest match in PST-130 | Conserved protein domains | RNA-seq info (PST-130) |
|---|---|---|---|
| PS_11-281_00009225 | PST130_15095, PST130_15096 | Zinc finger, RING-type; Zinc finger, C3HC4 RING-type | Top 10% genes expressed in haustoria |
| PS_11_281_scaffold_712 | PST130_15096 | Zinc finger, C3HC4 RING-type | Top 10% genes expressed in haustoria |
| PS_11_281_scaffold_9696 | PST130_03978 | none | - |

## 2.5 Discussion

### 2.5.1 Properties of candidate effectors

#### 2.5.1.1 Zinc finger domains

In this analysis, two candidate effector genes (likely allelic variants or paralogs of one another) contain zinc finger domains. These domains are widely found in eukaryotes and are able to interact with DNA, RNA, and other proteins (Cassandri *et al.*, 2017). Many proteins with zinc finger domains are transcription factors that can directly interact with DNA. The flax rust gene *AvrP,* for example, encodes an effector with zinc finger like domains (Zhang *et al.*, 2018). Despite no predicted nuclear localisation signal, AvrP localises to the nucleus, suggesting a function in transcriptional regulation. Polymorphisms within the protein surface dictate gain or loss of recognition by the associated *R* gene *P*. It is possible candidates PS_11-281_00009225 and PS_11_281_scaffold_712 function in a similar way. It would be interesting to see if these proteins also localise to the nucleus despite not having a predicted nuclear localisation signal. Another possibility is that these candidates are positive regulators of another gene involved in gene for gene recognition with YR2 (elaborated in section 2.5.2).

#### 2.5.1.2 Variants located in introns

One effector candidate from this analysis, PS_11_281_scaffold_9696, has a variant residing in an intron. Although many variants within introns have a negligible effect, some can alter splicing of the transcript. For example, some introns contain splice enhancer or repressor sites (Cooper, 2010). It is possible this variant has altered splicing or other regulation properties of this gene, leading to the gain of virulence phenotype.

### 2.5.2 Variants found in one mutant but not the other? Mutations in different genes may lead to the same phenotype

In this analysis, I only discovered mutations between the W1 and M1 libraries that were not found when comparing W2 and M2. It is possible a mutation in a different gene has occurred in M2 that has led to the same phenotype of gain of virulence. One possibility is that avirulence to YR2 is encoded by two separate genes. For example, in *Phytophthora sojae*, avirulence on soybean plants carrying *Rps1b* is encoded by *Avr1b-1* and *Avr1b-2* (Shan *et al.*, 2004). *Avr1b-1* encodes for a small secreted protein that triggers *Rps1b* mediated immunity, whereas *Avr1b-2* is a trans acting gene that is a positive regulator of *Avr1b-1* transcription. Mutations in either gene can lead to gain of virulence on *Rps1b* plants. It is also possible a mutation could have occurred in one mutant, whereas an epigenetic change may have occurred in the other mutant.

### 2.5.3 Beyond mutation: epiallelic variation can cause gain of virulence

Another limitation to the current study is that epigenomic changes not detectable in the DNA sequence of an organism can cause gain of virulence. As only DNA sequence data was used in this analysis, the identification of potential epialleles would be missed. For example, Pais *et al.* (2018) discovered an effector gene, *Avrvnt1* of *P. infestans,* that is not expressed in a particular isolate despite a lack of polymorphisms in the coding sequence. This silencing lead to gain of virulence on potato isolates carrying the cognate *R* gene. Similarly, multiple *Phytophthora sojae* strains carrying the *Avr1c* gene gained virulence on soybean plants carrying *Rps1c* through silencing of *Avr1c* (Na *et al.*, 2014). It is hypothesized epigenetic control of transcription allows the pathogen to recycle effectors when the associate *R* gene is not deployed in the wheat population (Gijzen *et al.*, 2014). Therefore, obtaining RNA-seq data of the isolates used in the YR2 analysis would allow detection of any epiallelic variation between the wildtype and mutant that would be missed in the original analysis.

### 2.5.4 Issues with reference-based SNP calling

Comparative genomics has heavily relied on reference-based SNP calling to determine genomic differences between pathogen isolates. Generally, short reads are aligned to a reference sequence to detect SNPs, short insertions and deletions (Horner *et al.*, 2009). Although incredibly useful, reference-based SNP calling has many limitations. Any errors or misassembly in the reference may lead to erroneous or missing variants called in the dataset (Eschenbrenner *et al.*, 2020).

The two main reasons some *AvrYr2* candidates may have been missed in this chapter is A) incomplete annotation in the references utilised and B) using reference genomes that were not derived from the wild type isolates. Some reference genomes do not have complete annotations. For example, protein fragments from *Puccinia triticina* have been mapped to regions of the reference genome that have no annotations (Bakkeren and Szabo, 2020). Therefore, variant calling pipelines that search for variants in predicted secreted proteins may miss changes in unannotated genes. In this chapter, unannotated regions were not included in the analysis, suggesting *AvrYr2* candidates may have been overlooked due to a missing annotation in the reference genome.

Another serious issue pertaining to the discovery of avirulence alleles is that extensive genomic structural variation and accessory regions that are not found in the reference are rarely detected via reference-based SNP calling (Pfeifer, 2017). Missing information in the reference often

leads to off-target alignments. In *Pst*, this is particularly an issue as structural variations between clonal isolates can occur in spontaneous gain of virulence mutants (Chen *et al.*, 2017). Further, as avirulence alleles can be lost via large-scale rearrangements and deletions, reference genomes that contain the virulent allele of the gene in question will likely contain missing data. To mitigate this issue, further analysis using the WT strain as a reference should be performed as described in section 2.5.5.

Other issues pertaining to reference based SNP calling arise when short reads are aligned to repeat rich regions (Krusche *et al.*, 2019). Reads originating from repeat rich regions tend to map equally well to multiple places in the genome, leading to erroneous variant calls (Pfeifer, 2017) . This is particularly a problem with *Pst*, where up to half of the entire genome can contain repetitive sequences (Schwessinger *et al.*, 2018). A similar issue arises when individual isolates contain high genetic variability between them (Pfeifer, 2017). This can be a concern even in asexual lineages of plant pathogenic fungi, as isolates can diverge quickly in a stepwise manner to evade *R* gene recognition (Möller and Stukenbrock, 2017). Further, repeat content and transposable elements can be enriched in clonal lineages in comparison to sexual lineages — a hypothesized signature of asexual evolution over time (Schwessinger *et al.*, 2020; Ma *et al.*, 2010). Internuclear heterozygosity within an individual can also be incredibly high (Schwessinger *et al.*, 2018). This often leads to the mismapping of alternative alleles or paralogs.

In the human reference genome GRCh37, it is predicted that 5.5 % of the entire sequence is inaccessible to short read sequencing and mapping algorithms due to repeat rich regions, structural variations between haplotypes, and recent duplications (Tian *et al.*, 2018). These inaccessible regions are predicted to be associated with disease phenotypes. It is possible large regions of the *Pst* genome are also inaccessible to short read sequencing and mapping algorithms due to similar reasons. For example, generating a partially phased reference genome of two dikaryotic oat crown rust isolates revealed structural variation not only between nuclei of a single individual, but also between the different isolates (Miller *et al.*, 2018). Further, by comparing three partially phased *Pst* genomes produced with long read technology, Vasquez-Gross *et al.* (2020) determined structural changes affected more regions of the genome than SNPs alone. These large structural variations were not discovered until highly contiguous *de novo* assemblies were produced for these rust species.

Although all isolates analysed in this chapter belong to the same NW European clonal lineage as the PST-104E reference, due to all of the above issues, it is possible *AvrYr2* candidates have been missed (Schwessinger *et al.*, 2018; Sørensen *et al.*, 2013). Further, PST-104E is virulent on YR2 wheat, providing the possibility that the *AvrYr2* allele may be missing due to a large-scale deletion event. The following section describes alternatives to reference-based SNP calling that will likely uncover these candidates in future experiments. I hypothesize these alternatives will become widely achievable as second generation (highly scalable short read technology such as illumina sequencing) and third generation (technology currently under development, such as nanopore long read technology) sequencing becomes more affordable and accessible.

### 2.5.5 Searching for Avirulence: Generating a new reference genome

Issues with reference-based SNP calling can be overcome by *de novo* assembling the isolates being studied before variant calling (Eschenbrenner *et al.*, 2020, **Figure 2-5**). The *de novo* assembly stage can integrate reads from different sequence technologies to maximise accuracy of the assembly. Long read sequencing technology such as Nanopore sequencing can resolve repetitive regions, however, these methods suffer from high error rate (Sedlazeck *et al.*, 2018). This can be circumvented by correcting long sequencing data with short reads. Therefore, long read data ensures long scaffolds and high contiguity, whereas short reads provide high coverage and can correct errors from long reads (Antipov *et al.*, 2016). Therefore, the Yr2 analysis presented in this chapter would benefit from sequencing one or both wildtype isolates using long-read sequencing technology.

This method was successfully employed when Salcedo *et al.* (2017) discovered the avirulent allele of the *Pgt* effector *AvrSr35*. A parental isolate containing the avirulent allele was subjected to EMS mutagenesis, and 15 gain of virulence mutants were obtained. The parental isolate was sequenced using a combination of short and long read technology, providing an accurate reference. By mapping short read data from the 15 mutants to the new reference genome, the authors were able to find *AvrSr35*. This study highlights the power of gain of virulence mutants combined with the *de novo* assembly of the WT isolate in the discovery of rust avirulent alleles.

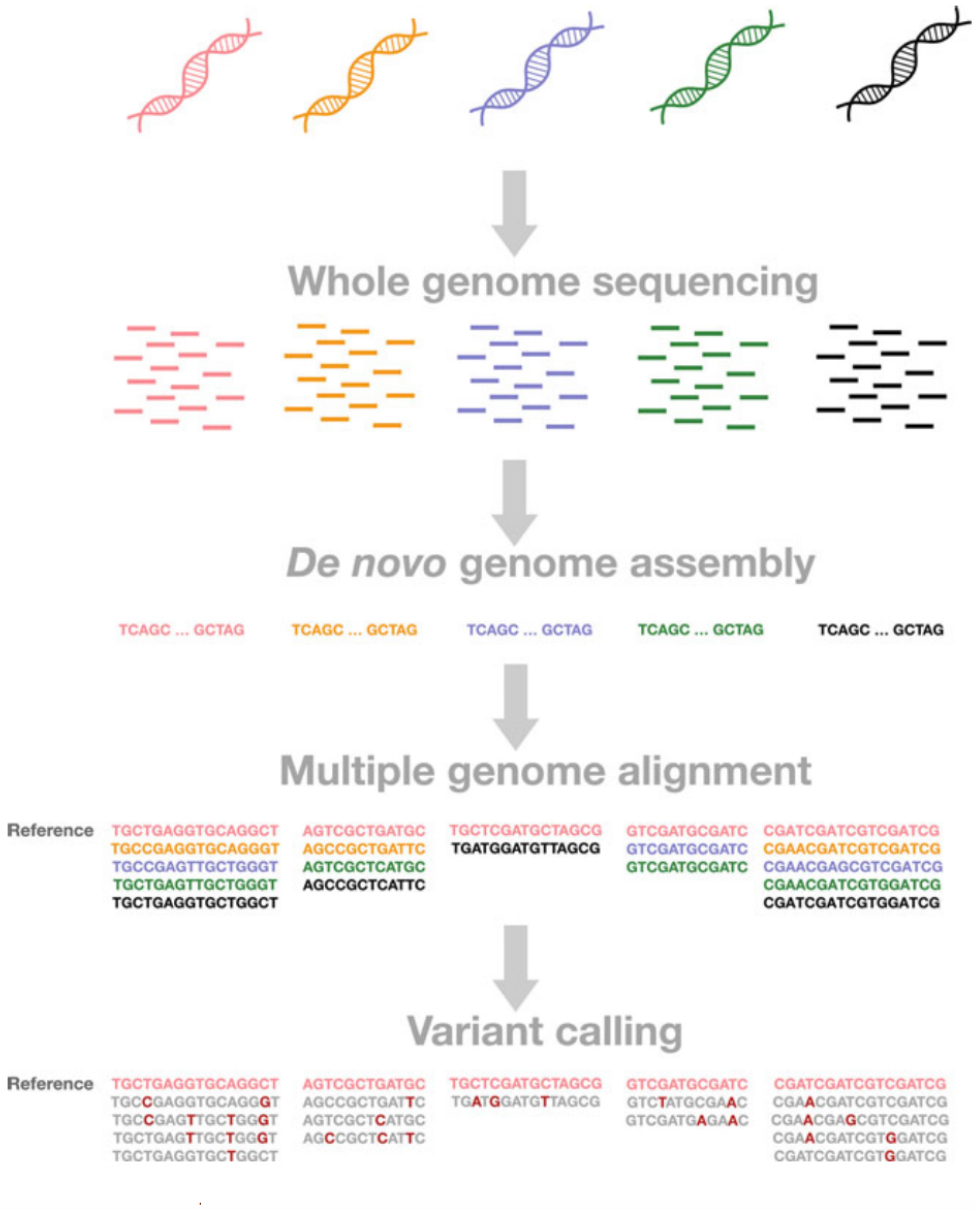


**Figure 2-5 A summary of variant calling using multiple genome alignment.** Genomes of multiple indivuduals are first *de novo* assembled using short and/or long read sequencing. These assemblies are then aligned to create a mltiple genome aligment. Variant positions are then called using appropriate programs. This figure was published in Eschenbrenner *et al.* (2020) and is reused with permission from copyright holders under the Creative Commons license.

### 2.5.6 Assembling a pan-genome for *Pst*

Currently there is no pan-genome assembled for *Pst*. A pan-genome is an assembly containing sequences found in multiple individuals of a species, along with genes found in only some individuals (Bayer *et al.*, 2020). Creating a pan-genome for *Pst* will be realised when more accurate *de novo* assembled genomes from isolates with different virulence profiles become available. One of the main drawbacks of the *AvrYr2* analysis described in this chapter is that the PST-104E reference may not contain the avirulent allele of *AvrYr2*. The avirulent allele in the reference could be lost via multiple mechanisms, including large-scale deletion. In this case *AvrYr2* derived reads would not properly map due to missing data in the reference.

The importance of creating a pan-genome can be demonstrated by the usefulness of the PGTAus-pan reference of *Pgt*. This reference genome contains an assembly from long read and short read sequences from an Australian founder isolate with the pathotype 21-0 (Upadhyaya *et al.*, 2015). Further, reads from four other isolates hypothesized to be founder races of clonal lineages currently in Australia were *de novo* assembled. Regions of these *de novo* assemblies not present in the 21-0 assembly were added to create PGTAus-pan. Sequencing the founder isolates of clonal lineages means deletions in extant isolates can be detected, as the lost sequences will likely be present in the founder isolates. This was particularly helpful in the *AvrSr50* analysis, whereby the wild type isolate containing the avirulent *AvrSr50* allele was derived from a pathotype included in the pan-genome (Chen *et al.*, 2017). Comparative genomics between a spontaneous gain of virulence mutant and this wild type isolate was successful, presumably because the reference contained the avirulent *AvrSr50* allele the authors were searching for.

### 2.5.7 Conclusion

In summary, three candidate genes have been identified in this analysis that are associated with virulence to YR2 wheat. These candidates are now of high priority to functionally characterise. Further analyses will include multiple genome alignment before variant calling instead of reference-based SNP calling (**Figure 2-5**). Further, obtaining RNA-seq data of each isolate would help identify epiallelic variation that may have been missed in this analysis.

# Chapter 3 Methods for molecular biology

## 3.1 PCR methods

### 3.1.1 Standard PCR

Standard PCR with DreamTaq polymerase (Fisher Scientific) was performed when accuracy was not required (ex. colony PCR). A single 25 µL reaction contained 2.5 µL 10X DreamTaq Buffer, 0.5 µL 10 mM dNTP, 0.5 µL 10 mM of each forward and reverse primer, 0.2 µL DreamTaq DNA polymerase (0.625 U total), 1 µL 10 pg - 1 µg template DNA, and nuclease-free water to a total volume of 25 µL. The PCR reactions were performed on a thermal cycler with conditions summarized in table **Table 3-1**. After cycling was finished, reactions were stored at 4 ˚C. Primer pair annealing temperatures were calculated using the ThermoFisher Tm calculator.

**Table 3-1** Standard PCR thermal profile

| Stage | Temperature C | Time | Number of Cycles |
|---|---|---|---|
| Initial denaturation | 95 ˚C | 3 minutes | 1x |
| Denaturation | 95 ˚C | 30 seconds | |
| Annealing | Variable | 30 seconds | 25 – 40x |
| Extension | 72 ˚C | 1 minute per kb | |
| Final extension | 72 ˚C | 5 minutes | 1x |

### 3.1.2 Colony PCR

Colony PCR for genotyping was performed using standard PCR conditions described in section **3.1.1** with the following modifications. Instead of 1 µL template DNA, a small amount of bacteria from positive colonies were transferred to the PCR reaction mix using a pipette tip. The PCR reaction was then mixed by pipetting up and down.

### 3.1.3 Hi-fidelity PCR

Hi-fidelity PCR using the Phusion polymerase (New England Biolabs) was used when sequence accuracy and blunt end PCR products were needed. A single 25 µL contained 0.2 µM dNTPs, 0.5 µM of each forward and reverse primer, 1x HF buffer, 3 % DMSO and 0.4 units of Phusion® polymerase, DNA template < 250 ng. The PCR reactions were performed on a thermal cycler with conditions summarized in **Table 3-2**. After cycling was finished, reactions were stored at 4 ˚C. Primer pair annealing temperatures were calculated using the ThermoFisher Tm calculator.

**Table 3-2** PCR thermal profile for Phusion high-fidelity polymerase

| Stage | Temperature ˚C | Time | Number of Cycles |
|---|---|---|---|
| Initial denaturation | 98 ˚C | 30 seconds | 1x |
| Denaturation | 98 ˚C | 10 seconds | |
| Annealing | Variable | 30 seconds | 25 – 35x |
| Extension | 72 ˚C | 30 seconds per kb | |
| Final extension | 72 ˚C | 5 minutes | 1x |

### 3.1.4 Agarose gel electrophoresis

For all PCR protocols, DNA fragments were separated by electrophoresis in a 1 % agarose gel. Agarose was dissolved in 1x Tris- borate-EDTA (TBE) buffer and 0.5X GelRed® (Biotium) was added before solidification. DNA samples were prepared by adding 1x purple loading dye (NEB) before loading into wells of the gel along with a 0.1-10 kb DNA molecular marker (New England Biolabs). Electrophoresis was performed at ~ 100V until DNA bands were sufficiently separated. Gels were imaged using Azure c200 Gel Imaging Workstation (Azure Biosystems) by exposing the gel to UV light.

## 3.2 DNA purification methods and sequence verification

### 3.2.1 Purification of PCR products

DNA bands obtained from **3.1.4** that were required for sequencing or cloning were visualised on a long wavelength UV transilluminator. The desired fragments were excised using a razor blade and placed in 2 mL Eppendorf tubes. DNA was purified using QIAquick Gel Extraction Kit (Qiagen) following the manufacturer's instructions. PCR products that were directly purified without gel separation were purified using the QIAquick PCR Purification Kit (Qiagen).

### 3.2.2 Plasmid purification by miniprep

Positive colonies obtained from section **3.1.2** were used to inoculate 10 mL Luria Broth (LB) overnight cultures with appropriate antibiotic (working concentrations in **Appendix 1**). *E. coli* cultures were grown at 37 ˚C with shaking overnight. Depending on the amount of DNA required, plasmids from overnight cultures were obtained using the QIAprep spin miniprep or midiprep kit (Qiagen) following the manufacturers protocol.

### 3.2.3 DNA sequence verification

DNA concentration of purified PCR products or plasmids from sections **3.2.1** and **3.2.2** were measured on a nanodrop spectrophotometer (ThermoFisher Scientific). The DNA, along with sequencing primers., were sent to Genewiz (Brooks Life Sciences) for Sanger sequencing. The sequences were analysed using the Geneious Prime software v 2020.2.4.

## 3.3 Cloning

### 3.3.1 Gateway cloning

Blunt end DNA fragments were produced using Hi-fidelity PCR described in section **3.1.3.** Primers were designed to insert a CACC overhang at the 5' end of the PCR product. Purified PCR product (described in section **3.2**) was ligated into the pENTR-D-TOPO (Invitrogen) entry vector using the manufacturer's instructions. Ligation reactions were transformed into *E. coli* (section**)** and DNA from positive colonies were PCR amplified (**3.1.2**) followed by sequencing (**3.2.3**).

DNA from the entry vector was cloned into a Gateway compatible vector using the LR clonase II reaction (Thermo Fisher) following the manufacturers protocol. Ligation reactions were transformed into *E. coli* (section **3.3.4)** and DNA from positive colonies were PCR amplified (**3.1.2**) followed by sequencing (**3.2.3**).

### 3.3.2 Traditional "cut and paste" cloning

The DNA fragments of interest (inserts) were released from a primary vector or purified PCR product (obtained from section **3.2.1**) using appropriate restriction enzymes (NEB). The secondary (or destination) vector was also pre-digested with appropriate restriction enzymes creating compatible ends. All restriction enzymes used in this thesis were compatible with CutSmart Buffer (NEB). Reactions contained 1 µg DNA, 1x CutSmart Buffer, 1.0 µL (20 unites) enzyme, and water to 50 µL. Reactions were incubated at 37 ˚C for 1 hour, followed by heat inactivation at 65 ˚C for 20 minutes before DNA fragments were size separated using gel electrophoresis (**3.1.4**). The appropriate fragments were purified from the gel (**3.2.1**) and ligated together using T4 DNA ligase (NEB).

Ligation reactions contained 2 µL 10X T4 Ligase buffer, 50 ng Vector DNA, Insert DNA (calculated using a molar ratio of 1:3 vector to insert), water to 20 µL, and 1 µL T4 DNA ligase. Ligation reactions were then incubated at 16 ˚C overnight and terminated at 65 ˚C for

10 minutes. 1-5 µL of the ligation reaction was transformed into *E. coli* using the method described in **3.3.4**. DNA from positive colonies were PCR amplified (**3.1.2**) followed by sequencing (**3.2.3**).

### 3.3.3 Golden Gate cloning

The Golden Gate assembly enables a single-step digestion and ligation "diglig" assembly of multiple components into a destination vector. This method uses type II restriction enzymes *BsaI* and *BpiI* which cut outside of the recognition sequence, allowing the production of custom overhangs. Compatible 4 bp overhangs at the junction of each module were designed following the plant Golden Gate standards (Patron *et al.*, 2015).

New level zero modules were cloned into the PUAP1 universal acceptor (Patron *et al.*, 2015) by PCR amplifying target DNA using primers designed as described in Patron *et al.* (2015). Sequences with existing *Bsa*I and *Bpi*I sites were first domesticated as described in section **3.3.3.1**. PCR products were purified as described in section **3.2.1**. Each diglig reaction contained 200 ng of the PUAP1 plasmid, a 2:1 molecular ratio of insert:acceptor, 1.5 µL T4 Ligase Buffer (NEB), 1.5 µL 10x Bovine Serum Abumin (BSA), 200 units T4 DNA ligase (NEB), 5 units of *Bpi*I (ThermoFisher). The reactions were incubated on a thermal cycler with conditions described in **Table 3-3**.

Level 1 expression vectors were cloned by ligating multiple level zero components into a level 1 backbone. Each diglig reaction contained 200 ng of the acceptor plasmid, each level zero vector at a 2:1 molecular ratio of insert:acceptor, 1.5 µL T4 Ligase Buffer (NEB), 1.5 µL 10x Bovine Serum Abumin (BSA), 200 units T4 DNA ligase (NEB), 5 units of *BsaI* (ThermoFisher). The reactions were incubated on a thermal cycler with conditions described in **Table 3-3**.

*E. coli* was transformed with 1-5 µL of the ligation reaction using the method described in **3.3.4.** DNA from positive colonies were PCR amplified (**3.1.2**) followed by sequencing (**3.2.3**).

**Table 3-3**Thermal cycling conditions for "Diglig" reactions

| Temperature ˚C | Time | Number of Cycles |
|---|---|---|
| 37 ˚C | 20s | 1 X |
| 37 ˚C<br>16 ˚C | 3 minutes<br>4 minutes | 26 X |
| 50 ˚C | 5 minutes | 1 X |
| 80 ˚C | 5 minutes | 1 X |
| 16 ˚C | hold | hold |

#### 3.3.3.1 Domesticating DNA for Golden Gate: Q5 Site Directed mutagenesis

Both *Bsa*I and *Bpi*I sites were removed from sequences using a Q5 site directed mutagenesis kit (NEB) following the manufacturers protocol. Single nucleotide synonymous changes were introduced to remove *Bsa*I and *Bpi*I recognition sites while retaining the amino acid sequence. Primers were designed using the NEBaseChanger software (http://nebasechanger.neb.com/). 5 µL of the KLD reaction was transformed into *E. coli* using the method described in **3.3.4.** DNA from positive colonies were PCR amplified (**3.1.2**) followed by sequencing (**3.2.3**).

### 3.3.4 *E. coli* transformation by heat shock

*E. coli* was transformed with vectors obtained from cloning methods described in sections 3.3.1, 3.3.2, 3.3.3. For routine cloning, vectors were transformed into the DH5α (ThermoFisher Scientific) strain. Approximately 100 ng of the plasmid of interest were incubated with 50 µL of commercial cells for 30 minutes on ice. The plasmid was then transformed by heat shock at 42 ˚C for 45 seconds and kept on ice for 2 minutes. Transformed cells were incubated for at least 1 hour at 37 ˚C in 700 µL of SOC medium.

Vectors that were difficult to clone were transformed into One Shot TOP10 cells (ThermoFisher Scientific). Approximately 100 ng of the plasmid of interest or 1-5 µL of a ligation reaction was pipetted into a vial of competent cells and incubated on ice for 30 minutes. The plasmid was transformed into the cells via heat shock by placing the cells in a 42 ˚C heat bath for 30 seconds. The cells were then cooled in ice for at least 2 minutes. Pre-warmed SOC medium (250 µL) was added to the cells, which were then shaken for at least 1 hour at 37 ˚C.

After the 1 hour incubation step, each transformation mixture (20-200 µL) was spread over LB-Agar plates containing the appropriate antibiotic selection. Plates were incubated at 37 ˚C overnight and single colonies were selected and grown in liquid LB media with antibiotic at 37 ˚C overnight with continuous shaking at 200 rpm. The presence of DNA of interest was confirmed using colony PCR (**3.1.2).** This was subsequently confirmed via Sanger sequencing as described in section **3.2.3**. Overnight bacteria culture from confirmed positive colonies were stored in 40 % glycerol at -80 ˚C.

# Chapter 4 Utilising the bacterial type III secretion system for the delivery of rust effectors in wheat

## 4.1 Abstract

Many candidate effectors have been predicted for the wheat rusts, however, very few have been functionally characterised in the native host. In particular, only two rust effectors conferring avirulent phenotypes have been confirmed in wheat, including *AvrSr50* and *AvrSr35* from stem rust. This is likely due to the lack of available systems for high-throughput screening of effector function in wheat. In this chapter I tested two previously described methods for suitability in screening avirulence phenotypes of biotrophic fungal effectors in wheat. This included: (i) utilising the *Pseudomonas fluorescens* effector to host analyser (EtHAn) system described in Upadhyaya *et al*. (2014) and ii) the *Burkholderia glumae* delivery system described in Sharma *et al*. (2013). Using two previously described avirulence effectors from fungal pathogens of wheat, I showed the EtHAn system was unable to elicit *R* gene dependent HR. Further, I showed the wild type *B. glumae* strain tested is not suitable for screening avirulence phenotypes, as the wild type strain elicits nonhost cell death in multiple wheat accessions tested. Further, I describe a novel bacterial delivery system using the phytopathogenic bacteria *Burkholderia cepacia* that proliferates in wheat but does not naturally cause nonhost cell death. This system is also incapable of causing *R* gene dependent HR on wheat when expressing *AvrSr50* or *AvrRmg8*. Previously published bacterial delivery systems for fungal effectors in wheat were developed before the emergence of any confirmed avirulence effectors for the wheat rusts. The results in this chapter therefore reveal critical information for designing experiments involving the bacterial T3SS as a delivery system in wheat, especially when screening for avirulence phenotypes of the wheat rusts.

## 4.2 Introduction

### 4.2.1 A high-throughput system is needed to test candidate effectors of the cereal rusts in wheat

Recent developments in genomics and bioinformatics have prompted a radiation in effector prediction for the wheat rusts (Duplessis *et al*., 2011; Kiran *et al*., 2017; Garnica *et al*., 2013; Cantu *et al*., 2013; Upadhyaya *et al*., 2015; Saunders *et al*., 2012). High-throughput methods for delivering rust effectors in wheat are therefore required to screen through large numbers of candidates. Although *Agrobacterium* mediated transient expression is a useful high-throughput method for characterising rust effectors in dicot host plants, these assays have not yet been successful in wheat (Catanzariti *et al*., 2006; Dodds *et al*., 2004; Upadhyaya *et al*., 2014). Effectors from the wheat rusts can be confirmed by *Agrobacterium* mediated transient

expression in *Nicotiana benthamiana,* only if both the *AVR* and *R* gene are cloned and co-expressed together, leading to a hypersensitive response. This is how the only confirmed avirulence effectors from the cereal rusts, *AvrSr50* and *AvrSr35*, were functionally characterised (Salcedo *et al.*, 2017; Chen *et al.*, 2017). This method is restricted by the number of cloned associated *R* genes, which is very limited particularly for *Pst* (Klymiuk *et al.*, 2018). Therefore, an alternative method must be used for screening multiple avirulence effector candidates, especially if the associated *R* gene has not been cloned.

Other existing methods for effector delivery in wheat such as particle bombardment and protoplast transformation have proven to be incredibly laborious and time consuming (Upadhyaya *et al.*, 2014). Functionally characterising the large repertoire of candidate rust effectors in the native wheat host thus poses an arduous and challenging task. Alternatively, utilizing the type III secretion system (T3SS) of bacteria to deliver fungal candidate effectors *in planta* remains an incredibly attractive method for high-throughput functional analysis of effectors in the host cytoplasm. This is because bacteria can be easily cultured and transformed across a short time scale under experimental conditions. Thus, a bacterial delivery system is valuable for studying candidate effectors of genetically intractable organisms like the wheat rusts.

### 4.2.2 Introduction to the bacterial T3SS: a useful surrogate system for functionally characterising fungal effectors

Previously, bacterial delivery systems have been developed by harnessing the T3SS of gram-negative bacteria. Both pathogenic and symbiotic bacteria utilise the T3SS to deliver effectors directly into the host cytoplasm. This allows establishment of a close relationship with different types of eukaryotic hosts, including plants (Grant *et al.*, 2006). Phytopathogenic bacteria use the T3SS to deliver a range of effectors into their host plants to manipulate the environment in favour of disease development. This includes dampening host defences, which facilitates pathogen propagation and survival (Grant *et al.*, 2006; Chang *et al.*, 2014). Bacteria deliver type III effectors through a membrane-embedded nanomachine that spans the bacterial inner membrane and outer membrane, the plant cell wall, and the plant plasma membrane (**Figure 4-1,** Büttner and He, 2009). A key component of this nanomachine is a needle like structure called the pilus that acts as a channel for translocation of effectors into the host (Tang *et* al., 2006). The pilus is 2-3 nm in diameter, suggesting translocated proteins must be at least partially unfolded as they enter the host (Chang *et al.*, 2014).

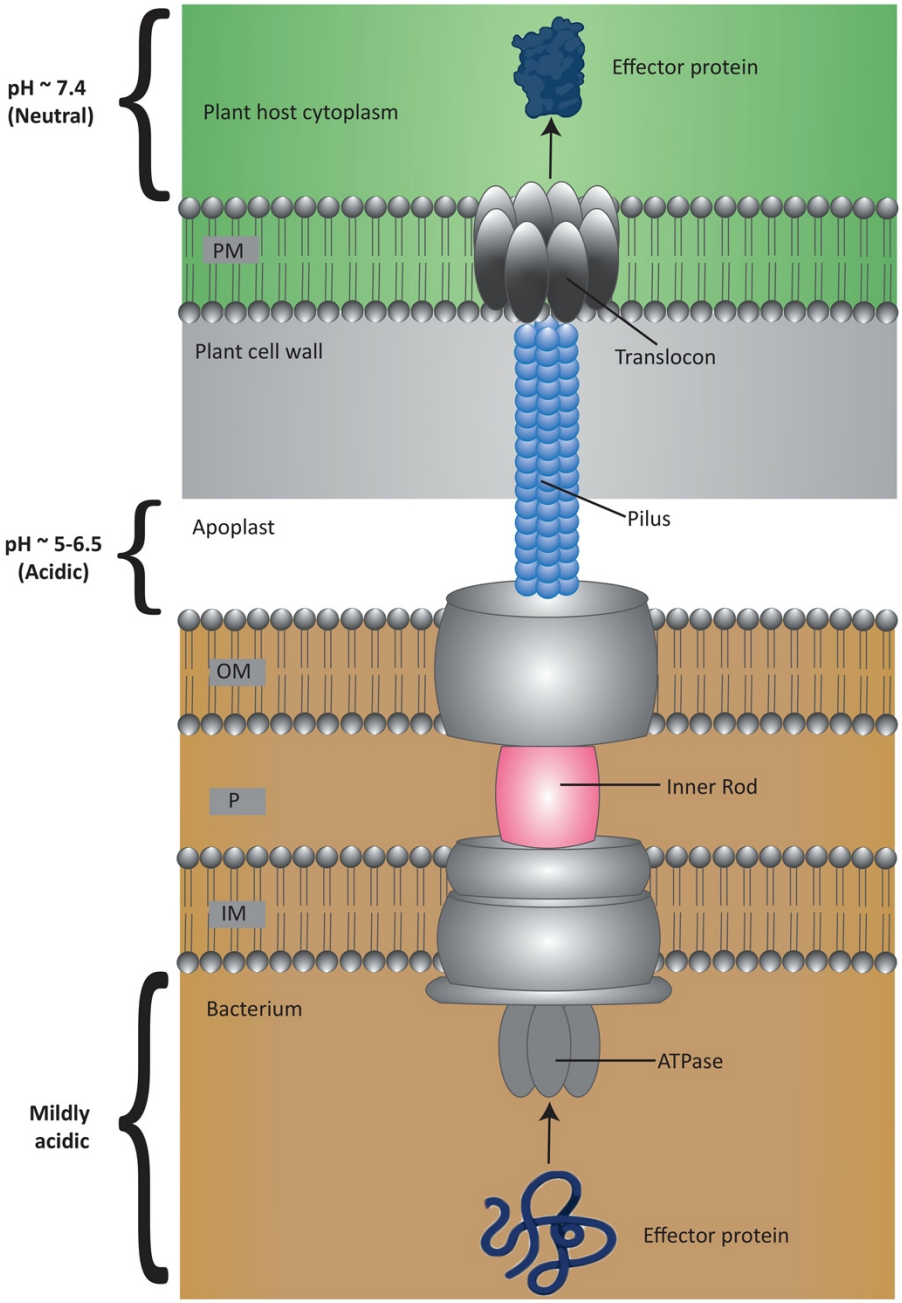


**Figure 4-1 Schematic representation of the T3SS of plant pathogenic bacteria**. The basal body of the T3SS spans the bacterial inner membrane (IM), the periplasm (P), the bacterial outer membrane (OM). The pilus crosses the plant apoplast, and plant cell wall. Translocon proteins embedded in the host plasma membrane (PM) form a pore for transporting proteins into the host cytoplasm. Partially unfolded effector proteins in the acidic bacterial cytoplasm enter the T3SS via an ATPase. Effectors fold into a functional confirmation in the neutral pH of the host plant cytoplasm. Redrawn from Louhou *et al.* (2013) with permission from copyright holders under the Creative Commons License.

The building blocks of the T3SS, including the pilus, are encoded by hypersensitive response and pathogenicity (*hrp*) genes (Büttner and He, 2009). Mutating these genes leads to disruption of disease development, and the inability of bacteria to elicit cell death on nonhost plants. The *hrp* genes are only induced when bacteria are infiltrated into plants or are incubated in media that mimics the apoplast (acidic, low osmolarity, and nutritionally poor) (Tang *et al.,* 2006). The expression of *hrp* genes is also coordinated and hierarchal (Lohou *et al*., 2013). Expression starts with genes expressing subunits closer to the base of the T3SS, followed by the pilus subunits, translocon proteins, and finally effector proteins (Puhar and Sansonetti, 2014).

These effector proteins are targeted to the T3SS via a non-cleavable N-terminal secretion signal 20-30 amino acids in length (Büttner and He, 2009; Chang *et al.,* 2014). Although these signals share no similarity in amino acid sequence, they do share amino acid composition. The N-terminal sequence is enriched in polar amino acids, is amphipathic, and has few charged hydrophobic amino acids (Arnold *et al*., 2009; Samudrala *et al.,* 2009). Due to these characteristics, the N-terminus is likely flexible and unfolded, which is necessary for passage through the narrow pilus of the T3SS (Büttner and He, 2009). N-terminal secretion signals of the T3SS are not usually cleaved, however, some effectors are processed into shorter peptides *in planta.* For example, AvrRps4 from *Pseudomonas syringae* pv. *pisi* is cleaved *in planta* between amino acids G133 and G134 (**Figure 4-2a**, Sohn *et al*., 2009). This cleavage is required for full virulence activity in *Arabidopsis* plants (Sohn *et al*., 2009). Similarly, AvrRpt2 from *Pseudomonas syringae* pv. *tomato* strain DC3000 is N-terminally processed in *Arabidopsis* host plants. (Mudgett and Staskawicz, 1999). The C-terminal AvrRpt2 then cleaves the host protein RIN4, which subsequently activates RPS2-mediated disease resistance. (Grant *et al*., 2006).

In addition to N-terminal processing, some type III effectors are post-translationally modified *in planta*. For example, the *P. syringae* effector AvrRpm1 is myristoylated and palmitoylated at its N terminus (Nimchuk *et al*., 2000). These are fatty acid modifications necessary for targeting AvrRpm1 to the plasma membrane, where it hyper phosphorylates host protein RIN4. This in turn leads to RPM1 mediated defence responses. (Grant *et al*., 2006). Post translational modification at the N terminus of bacterial type III effectors is therefore crucial for proper localisation.

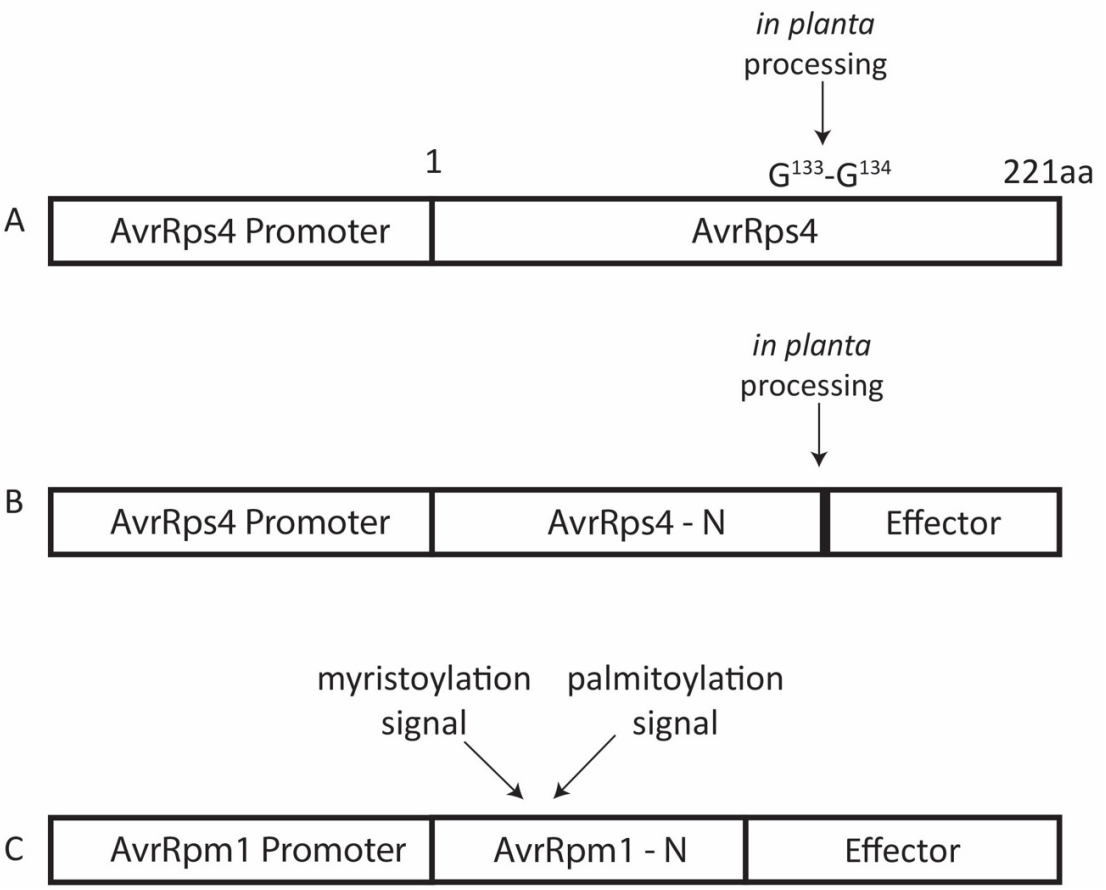


**Figure 4-2 Representations of expression constructs in pEDV vectors.** A) Representation of the bacterial effector Avr***Rps4***, including its *in planta* cleavage site between G133-134. B) Representation of the *AvrRps4* pEDV. This vector contains the N-terminal secretion signal of *AvrRps4*, including the *in-planta* processing site. Candidate effectors can be cloned into the C terminus in frame with the *AvrRps4* secretion signal. C) Representation of the *AvrRpm1* pEDV. This vector contains the N-terminal secretion signal of the bacterial effector *AvrRpm1*. This secretion signal contains the myristoylation and palmitoylation motifs that target AvrRpm1 to the plant plasma membrane. Candidate effectors can be cloned into the C terminus in frame with the *AvrRpm1* secretion signal.

In summary, bacteria have evolved an elegant mechanism to deliver effector proteins directly into the host cytoplasm using a T3SS. Previous studies on bacterial effectors have delimited minimal N-terminal amino acid sequences required for targeting effectors to this secretion pathway. Scientists have been able to exploit this information to heterologously express and deliver non-bacterial effectors into the host cytoplasm.

### 4.2.3 The T3SS can be harnessed to study non-bacterial effectors

One of the first studies to heterologously express non-bacterial effectors using the T3SS was described by Sohn *et al.* (2007). The authors delivered *Hyaloperonospora parasitica* effector proteins ATR1 and ATR13 into *Arabidopsis* leaves by utilising the T3SS of *Pseudomonas syringae pv. tomato DC3000.* This was achieved by cloning the effectors in frame with the N-terminal region of *AvrRps4*, which includes an *in planta* processing site, leading to free oomycete protein in the host cytoplasm. The cloning vector including the *AvrRps4* promoter and *AvrRps4* N-terminal secretion signal was thus deemed the "effector detector vector" (pEDV; **Figure 4-2b**). *Pseudomonas syringae* pv. *tomato* DC3000 expressing *ATR1* and *ATR13* effectors fused to the secretion signal of *AvrRps4* were able to elicit *R* gene (*RPS4*) dependent cell death. Rentel *et al.* (2008) were able to develop a similar system using the promoter and N terminus of *AvrRpm1* (**Figure 4-2c**).

Unfortunately, the *Pseudomonas syringae* pv. *tomato* DC3000 strain utilized in these studies is not compatible for use in monocot hosts. Yin & Hulbert (2011) noticed the wild type DC3000 strain caused strong cell death on all wheat lines tested. Thus, this strain is not compatible for effector delivery in wheat, as cell death would mask any phenotype caused by an avirulence effector. A DC3000 derivate called CUCPB5500, which has 18 effectors deleted, still caused cell death, although less in magnitude (Yin and Hulbert, 2011). Another strain, called the Effector-to-Host Analyzer (EtHAn), did not cause any noticeable cell death phenotypes on all wheat lines tested, suggesting this strain is compatible for effector delivery in wheat (Yin and Hulbert, 2011).

### 4.2.4 The T3SS of the EtHAn strain can be harnessed to deliver fungal effectors in wheat

The EtHAn strain, a modified version of the non-pathogenic soil bacterium *Pseudomonas fluorescens* Pf0-1, does not elicit cell death because it lacks any virulence factors required for growth *in planta*. However, it has the *hrp* genes stably integrated into its genome, meaning it can assemble the T3SS (Thomas *et al.*, 2009). The EtHAn strain expressing *AvrRpm1* or *AvrRpt2* was able to elicit HR when infiltrated in *Arabidopsis* plants with the cognate R

proteins, RPM1 and RPS2 respectively (Thomas *et al.*, 2009). This confirms the T3SS of EtHAn is fully functional *in planta*. Further, the EtHAn strain expressing *AvrRpm1* or *AvrRpt2* is able to induce $H_2O_2$ production when infiltrated into wheat, suggesting this system is also compatible for effector delivery in cereals (Yin and Hulbert, 2011).

To demonstrate rust effectors can be delivered in wheat using the T3SS, Upadhyaya *et al.* (2014) utilised the EtHAn system in combination with the pEDV. The authors showed that although the EtHAn strain does not proliferate inside wheat leaves over time, it still delivers detectable levels of protein *in planta.* On the other hand, a known pathogenic bacteria of wheat, *Xanthomonas translucens,* clearly multiplied over time in the apoplast. The authors also noted that the amount of protein delivered inside wheat leaves correlated with growth *in planta* over time. Unfortunately, wild type *X. translucens* also elicited nonhost cell death on wheat, deeming it unsuitable for screening avirulence phenotypes of effectors. Therefore, despite delivering comparatively less protein *in planta,* the pEDV EtHAn system was utilized for screening avirulence phenotypes of candidate rust effectors in wheat. Upadhyaya *et al.* (2014) subsequently cloned candidate rust effectors from *Puccinia graminis* f. sp. *tritici* (*Pgt)* into a pEDV vector carrying the *AvrRpm1* promoter, and modified *AvrRpm1* signal peptide. This signal peptide has mutations in the myristoylation and palmitoylation motifs, preventing trafficking of the protein to the plant plasma membrane. Using this system, a candidate effector PGTAUSPE-10-1 was delivered into wheat lines carrying different stem rust resistance genes. Clear HR was detected on wheat line W3534 (*Sr22*+), suggesting this candidate effector is *AvrSr22*. These data suggest the EtHAn system can deliver proteins into wheat leaves and can subsequently be used for screening avirulence phenotypes of candidate rust effectors.

### 4.2.5 The T3SS of *Burkholderia glumae* can be harnessed to deliver fungal effectors in wheat

A study by (Sharma *et al.*, 2013) similarly sought to develop a high-throughput system to deliver effectors into monocot plants using the bacterial T3SS. Two known genes encoding cytoplasmic AVR proteins from the rice pathogen *Magnaporthe oryzae*, *Avr-Pik* and *Avr-Pii,* were cloned into a pEDV vector with the type III secretion signal from *AvrRps4*. Subsequently, *Burkholderia glumae* (a bacterial crop pathogen) was transformed with the pEDV-Avr-Pik-NLS or pEDV-Avr-Pii-NLS constructs. Translocation of fluorescently tagged effectors were determined via microscopy after inoculation of *Burkholderia glumae* strains carrying Avr-Pik-NLS or Avr-Pii-NLS on wheat leaf sheaths. At 3 DPI, clear

fluorescent signals could be detected in the nuclei of leaf sheaths, suggesting the *B. glumae* pEDV system is also effective in delivering effector proteins in wheat.

Although bacterial delivery remains a promising option for screening avirulence phenotypes in wheat, there have previously been no confirmed wheat rust *AVRs* that could be utilised as appropriate positive controls for testing these systems. To date, the avirulence phenotype of PGTAUSPE-10-1 has not been followed up for further confirmation in wheat. Recently, the first *AVR* effectors from stem rust, *AvrSr50* and *AvrSr35,* have been confirmed via *Agrobacterium* mediated transient co-expression in *N. benthamiana* with the corresponding *R* genes *Sr50* and *Sr35* respectively (Chen *et al*., 2017; Salcedo *et al*., 2017). In this chapter, I used the T3SS of both EtHAn and *B. glumae* to deliver the positive control *AvrSr50* into plants containing to cognate *R* gene. Further, I used *AvrRmg8* — a previously characterised avirulence effector from the hemibiotrophic fungal pathogen *Magnaporthe oryzae* (*Triticum* pathotype) — as a second positive control for testing these delivery systems in detecting avirulence phenotypes in wheat (Anh et al. 2018).

## 4.3 Methods

### 4.3.1 Plant materials used in this study

Differential wheat lines for *AvrSr50* (Gabo and Gabo + *SR50*) were kindly provided by Peter Dodds (CSIRO, Canberra, ACT, Australia). The diverse set of wheat accessions shown in **Figure 4-5** was provided by the JIC seed store (Norwich, UK). S-615 (*Rmg8*+) wheat was provided by Sophien Kamoun (TSL, Norwich, UK).

### 4.3.2 Bacterial strains used in this study

All bacterial strains used in this study are listed in **Appendix 2**. *Burkholderia glumae* strains used in this study (106619, 301682, 302544, 302744, 302925, 302928) from Sharma *et al.* (2013) were originally obtained from NIAS (National Institute of Agrobiological Sciences) (Tsukuba, Ibaraki, Japan). *Burkholderia cepacia* strain ATCC 24516 and *Pseudomonas syringae pv. lapsa* strain ATCC10859 were obtained from the American Type Culture Collection (Manassas, Virginia). *Pseudomonas fluorescens* EtHAn was obtained from CSIRO (Canberra, ACT, Australia).

### 4.3.3 Preparation of bacterial inoculum under normal conditions

Frozen glycerol stocks stored at -80 °C of *Burkholderia* and *Pseudomonas* strains were streaked onto Kings B (KB) and LB agar respectively with appropriate antibiotic (**Appendix 1**). Plates

were incubated for 36 h at 29 °C to obtain a confluent lawn. A loopful of culture was added to 50 mL liquid KB or LB media with appropriate antibiotic in a 250 mL flask and was incubated at 29 °C with shaking (200 rpm) for 24 h. Cultures were cooled on ice, transferred to a 50 mL Falcon tube, and centrifuged at 5000 x g at 4 °C for 10 minutes. Cultures were re-suspended in 10 mM $MgCl_2$ to the appropriate $OD_{600}$ (0.001 – 5.0).

### 4.3.4 Preparation of bacterial inoculum under T3SS pre-induction conditions

Bacteria were prepared under T3SS pre-induction conditions as described in Upadhyaya *et al.* (2014). Glycerol stocks of *Pseudomonas fluorescens* EtHAn or *Burkholderia cepacia* were plated on LB agar or KB agar plates with appropriate antibiotics (**Appendix 1**) at 28 ˚C for 36 h. A loopful of the cultures were inoculated into 5 mL LB or KB. Cultures were incubated overnight at 28 ˚C with shaking (200 rpm). Overnight cultures were added to 50 mL LB or KB with antibiotics and incubated at 29 ˚C with shaking (200 rpm) until an $OD_{600}$ >0.8 was reached (4-6 h). Cultures were then cooled on ice, transferred to a 50 mL Falcon tube, and centrifuged at 5000 x g at 4 ˚C for 10 minutes. Cultures were resuspended twice in 25 mL cold 10 mM $MgSO_4$. Cell pellets were resuspended in a minimal medium (50 mM potassium phosphate buffer, 7.6 mM $[NH_4]_2SO_4$, 1.7 mM $MgCl_2$, and 1.7 mM NaCl; pH 5.7 to 5.8) with appropriate antibiotics and 10 mM fructose to an $OD_{600}$ of 0.8. Resuspended cultures were incubated at 20 ˚C overnight with shaking (200 rpm). Cells were chilled and harvested by centrifuging at 5000 x g for 10 minutes at 4 ˚C and resuspended in 10 mM $MgCl_2$ to the appropriate $OD_{600}$ for infiltration.

### 4.3.5 Infiltration of bacterial inoculum into wheat leaves

Bacterial suspensions in 10 mM $MgCl_2$ were pressure infiltrated into the adaxial side of the second leaf of 2-3-week-old wheat plants. Each bacterial suspension was infiltrated in 2-3 spots until a 1 $cm^2$ region was soaked with inoculum. Infiltrated plants were kept in a closed box with water overnight then transferred to a glasshouse. Induction of HR-like symptoms were assessed up to 14 DPI.

### 4.3.6 Colony forming unit assay

*Pseudomonas fluorescens* EtHAn was grown on LB agar plates with 10 µg/mL tetracycline, and *B. cepacia* was grown on KB agar plates with 50 µg/mL gentamycin. Plates were incubated at 28 °C for 36-48 h. Bacteria were harvested from the plates and resuspended in 50 mL 10 mM $MgCl_2$. Bacterial suspensions were transferred to a 50 mL Falcon, centrifuged at 5000 x g at 4 °C for 10 mins. The supernatant was discarded, and bacteria were resuspended in 10 mM

$MgCl_2$ to a final $OD_{600}$ of 0.001. Bacteria were infiltrated on the adaxial side of the second leaf of three-week-old Gabo wheat plants with a 1 mL needleless syringe. The infiltration buffer ($MgCl_2$) was also infiltrated into leaves as a negative control. Four leaf discs were harvested for each sample at every time point using a 4 mm diameter cork borer (Sigma Aldrich), resulting in a total area of 0.5 $cm^2$ leaf tissue collected. For each condition, leaf samples were collected from six different infiltrations, resulting in six biological replicates. Leaf samples were placed in a 1.5 mL microcentrifuge tube with 500 µL 10 mM $MgCl_2$ and a single 2 mm tungsten bead. Leaf tissues were subsequently disrupted using a Tissuelyser (Qiagen) set at 30 Hz for 30 s. Bacteria were diluted in a tenfold dilution series up to $10^{-7}$. A total of 10 µL from each dilution were dropped on selective KB or LB medium agar plates, which were then incubated at 28 °C for 36-48 h. The number of colonies (CFU per drop) were counted, and results were plotted on a line graph using ggplot2 in R (Wickham, 2009). Each point represents the average of six biological replicates, with error bars representing the standard error of the mean. Significant differences in CFU counts between *P. fluorescens* EtHAn and *B. cepacia* was calculated at each time point using a two tailed t- test assuming equal or unequal variance, depending on F-test values. Normalized distribution of data was checked using the Shapiro-Wilk test. P-values are indicated as ns (non-significant), $P > 0.05$; *, $P < 0.05$; **, $P < 0.01$; ***, $P < 0.001$.

### 4.3.7 Plasmid constructions

#### 4.3.7.1 *AvrSr50* in pEDV

The *AvrSr50* and *AvrRmg8* control genes were cloned into the pNR526-G2AC3A **(Appendix 4)** destination vector using Gateway cloning according to the manufacturer's instructions (Invitrogen) as described in section **3.3.1**. The coding sequence of *AvrSr50* virulent and avirulent alleles were kindly provided by Peter Dodds (CSIRO, Canberra, ACT, Australia). The sequence was subsequently synthesized into a puC57 vector by GenScript (Piscataway, NJ, USA). The avirulent allele of *AvrSr50* was amplified via PCR using primers AvrSr50-TOPOF and Sr50-TOPOR. The virulent *avrSr50* allele was amplified via PCR using primers avrSr50-TOPOF and Sr50-TOPOR **(Appendix 2).** The *AvrRmg8* coding sequence (without the native signal peptide) was PCR amplified from wheat blast isolate BTJP4-1 genomic DNA, using primers AvrRmg8TOPF and AvrRmg8R (**Appendix 3)** as described in **3.1.3**. Strain BTJP4-1 was kindly provided by Sophien Kamoun (TSL, Norwich, UK). Blunt-end fragments were produced using the proofreading Phusion high fidelity DNA polymerase (Thermo scientific) and ligated into the pENTR/D-TOPO entry vector (Invitrogen) as described in **3.3.1**. Blunt-end fragments were produced using the proofreading Phusion high

fidelity DNA polymerase (Thermo Scientific) as described in section **3.1.3**. Genes were amplified without the predicted signal peptide and cloned into the pENTR/D- TOPO entry vector via TA cloning (Invitrogen). Inserts from the entry vector were introduced into the GATEWAY destination vector pNR526-G2AC3A via LR recombination using Gateway LR Clonase II enzyme mix (Thermo Fisher) as described in **3.3.1**. All plasmids were sequenced and confirmed via analysis using Geneious software (Biomatters Ltd.).

#### 4.3.7.2 Trimethoprim in pEDV

*Burkholderia cepacia* strain ATCC 25416 is naturally resistant to many antibiotics, including gentamycin (selection in the pEDV vector pNR526-G2AC3A). Strain ATCC 25416, however, is susceptible to the trimethoprim antibiotic. To insert a trimethoprim resistance cassette into pNR526-G2AC3A, I PCR amplified the trimethoprim resistance gene (TpR) from plasmid pTKDP-dhfr (Addgene) using primers dhfr-BsrD1-F and dhfr-BsrD1-R **(Appendix 2)** as described in section **3.1.3.** The PCR product was digested with *BsrD*I, and the pNR526-G2AC3A vector backbone was digested with *Bcg*I (New England Biolabs) as described in section **3.3.2**. The digestion reactions were size separated on a gel, bands were excised, purified, and ligated to produce pNR526-G2AC3A-Tpr **(Appendix 4)** as described in section **3.3.2.**

#### 4.3.7.3 *AvrSr50, AvrRmg8* in trimethoprim pEDV

*AvrSr50* and *AvrRmg8* in the pENTR/D-TOPO entry vector generated in 4.3.7.1 were transferred to the destination vector PNR526-G2AC3A-Tpr via LR recombination using Gateway LR Clonase II enzyme mix (Thermo Fisher) as described in **3.3.1.**

### 4.3.8 Bacterial transformation

#### 4.3.8.1 Electroporation

Wild type *Burkholderia glumae* and *Pseudomonas fluorescens* EtHAn were made electro-competent using previously described methods (Saitoh & Terauchi, 2013; Choi *et al*., 2006). Frozen glycerol stock of either *B. glumae* or *P. fluorescens* were inoculated onto KB agar plates and incubated at 28 °C for 2-3 days in the dark. A fresh colony was transferred to 5 mL LB in a 15 mL tube and incubated at 28 °C for 16 h with shaking at 200 rpm. Cultures were transferred to 1 mL aliquots and centrifuged at 3500 x g at 4 °C for 5 min. The pellet was then resuspended in 1 mL filter sterilized 300 mM sucrose. Cultures were centrifuged again at 3500 x g at 4 °C for 5 min. The supernatant was discarded, and the pellet was resuspended

in 200 µL 300 mM sucrose solution and divided into 100 µL aliquots. Cells were used immediately for the transformation step. Vectors were transformed into *Burkholderia glumae* and *P. fluorescens* EtHAn competent cells using electroporation, following conditions described in Saitoh & Terauchi (2013) and Choi *et al.* (2006) respectively. One microgram of plasmid was added to 100 µL electrocompetent cells, and the mixture was added to an electroporation cuvette (0.1 cm electrode gap). The cells were electroporated using a Gene Pulser (BioRad) set at 25 µF, 1.8 kV, and 200 ohms. Cells were resuspended in 1 mL LB and transferred to 1.5 mL tubes. The tubes were incubated on a shaker set at 200 rpm and 28 °C for 2 h. Cells were plated on KB agar with appropriate antibiotic and incubated at 28 °C for 2-3 days. Positive colonies were detected via colony PCR as described in **3.1.2.**

#### 4.3.8.2 Triparental mating

*B. cepacia* cannot be transformed via electroporation or heat shock methods, however, it can be transformed via triparental mating. Glycerol stocks of *E. coli* helper strain pKR2013 **(Appendix 4)**, donor strain (*E.coli* with TpR pEDV vector), and acceptor strain (*B. cepacia*) were streaked onto LB (*E.coli*) or KB (*B. cepacia*) agar plates with appropriate antibiotic. *E. coli* plates were incubated at 37 °C overnight, and *B. cepacia* plates were incubated at 28 °C for 36-48 h. Overnight liquid cultures were inoculated from streaked plates with appropriate antibiotic. From these overnight cultures, 1 mL was centrifuged at 3 minutes at 3000 rpm. Each strain was resuspended in 1 mL LB and centrifuged again for 3000 rpm for 3 minutes. Each strain was then resuspended in 200 µL LB. In a single tube, 100 µL *B. cepacia*, 20 µL of the helper plasmid, and 20 µL of the donor plasmid were mixed together. This mating mixture was then plated on a KB agar plate for 24 h in a 28 ˚C cabinet without antibiotic. Cells on the plate were resuspended in 1 mL KB, diluted 1:10, 1:100, and 1:1000. Each dilution was plated on KB agar plates supplemented with gentamycin (50 µg/mL) and trimethoprim (100 µg/mL). Plates were incubated for 48 h at 28 ˚C. Positive colonies were confirmed via colony PCR as described in **3.1.2.**

### 4.3.9 Dendrogram analysis of common wheat varieties

The dendrogram of common wheat varieties was previously generated by Pilar Corredor-Moreno (Saunders Lab, JIC). Publicly available single nucleotide polymorphism (SNP) data from 103 wheat varieties was sourced from the Breeders' 35K Axiom® array which is an open collection of over 35,000 SNPs used to differentiate a wide range of wheat common accessions (Wilkinson *et al.* 2012). Plink 1.9 --distance square function (www.cog-

genomics.org/plink/1.9/) (Chang *et al.*, 2015) was used on this SNP data to build a distance matrix. A total of 34,516 variants were filtered to build the matrix. The R package 'Ape' (Paradis *et al.*, 2004) was used to create a dendrogram using a hierarchical clustering approach.

## 4.4 Results

### 4.4.1 The *Pseudomonas fluorescens* EtHAn system expressing *AvrSr50* or *AvrRmg8* is unable to elicit *R* gene dependent HR in wheat

The pEDV EtHAn system was developed before any avirulence effectors of the cereal rusts (or any biotrophic/hemibiotrophic pathogen of wheat) were confirmed. This has recently changed, as *AvrSr50* and *AvrSr35* have been characterised and confirmed as avirulence effectors of stem rust (Chen *et al.*, 2017; Salcedo *et al.*, 2017). To show the pEDV EtHAn system is suitable for detecting avirulence phenotypes of rust effectors, I used one of the first confirmed avirulence effectors from stem rust, *AvrSr50*, as an appropriate positive control (Chen *et al.* 2017). *AvrRmg8* from the hemibiotrophic fungal pathogen *Magnaporthe oryzae* pathotype *Tritici* (MoT) was also chosen as a positive control (Wang *et al.*, 2018). The avirulent allele of *AvrSr50* and *AvrRmg8* were cloned into a vector containing the *AvrRpm1* promoter and modified *AvrRpm1* signal peptide. This modified pEDV vector, called pEDV G2AC3A **(Appendix 4),** has the myristoylation and palmitoylation signals removed from the signal peptide to prevent localization to the plasma membrane. Bacteria were infiltrated at an $OD_{600}$ of 2.0 into wheat lines differential for *Sr50* and *Rmg8*, and phenotypes were observed over a seven-day period (**Figure 4-3A**). Infiltration buffer ($MgCl_2$), wild type EtHAn strain, and EtHAn expressing the virulent *avrSr50* allele did not elicit HR on any wheat variety as expected (**Figure 4-3B-C**). However, EtHAn expressing *AvrSr50* or *AvrRmg8* also did not elicit HR in an *R* gene dependent manner (**Figure 4-3B-C**). Cell death from an incompatible reaction usually occurs at 72 hours post infiltration (HPI), with clear water soaking lesions visible prior to HR (Upadhyaya *et al.*, 2014). In this case, no visible water soaking lesions or cell death phenotypes developed over the course of 7 days post inoculation (DPI). These data suggest the pEDV EtHAn system is not suitable for detecting the avirulence phenotypes of the AvrSr50 or AvrRmg8 effectors in the native wheat host.

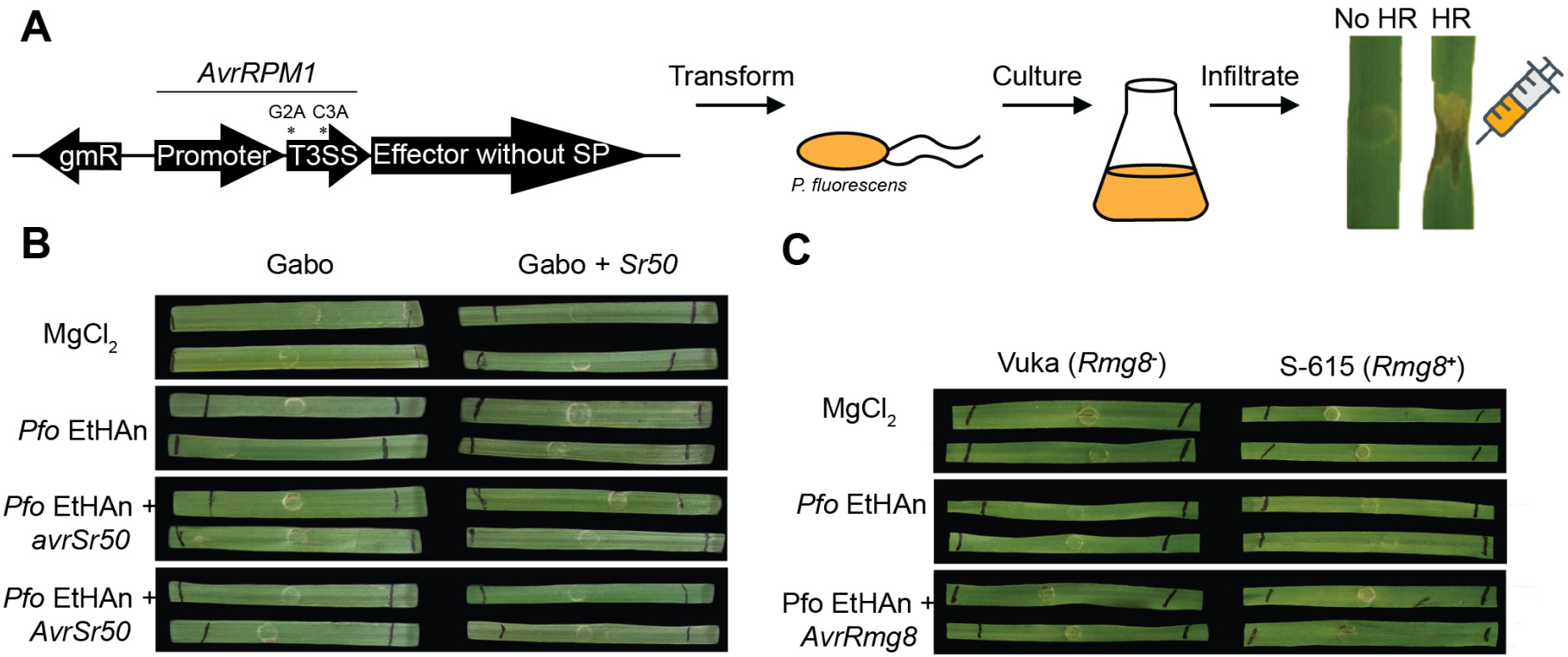


***Figure 4-3 Pseudomonas fluorescens* EtHAn expressing *AvrSr50* or *AvrRmg8* does not elicit *R* gene dependent HR in wheat.** A) Schematic diagram of the EtHAn delivery system. A modified version of the pEDV (pNR526-G2AC3A) was transformed into *P. fluorescens* EtHAn. The promoter and T3SS of the vector originate from *AvrRPM1* from *P. syringae.* Stars indicate alanine substitutions at the G2 and C3 residues previously shown to prevent localisation to the plasma membrane. Positive transformants were cultured and subsequently infiltrated into the appropriate wheat lines. gmR, Gentamycin resistance. B) *P. fluorescens* EtHAn expressing *AvrSr50* on *Sr50*+ plants and **C,** *AvrRmg8* on *Rmg8*+ plants do not elicit HR. Bacterial strains were infiltrated at an $OD_{600}$ of 2.0. Photographs were taken 7 days post-inoculation. Representative photographs from three independent biological replicates are shown. All replicates displayed the same phenotype.

### 4.4.2 Wild type *Burkholderia glumae* strain 106619 elicits strong HR on all wheat accessions tested

Similar to the pEDV EtHAn system, Sharma *et al.* (2013) were able to deliver fungal effectors into wheat cells using the bacterial T3SS. Specifically, the authors were able to deliver two *Magnaporthe* effectors in wheat using *Burkholderia glumae*. I tested the *B. glumae* pEDV system (Sharma *et al.*, 2013) for suitability in detecting avirulence properties of rust effectors. To this aim, I transformed *B. glumae* with a pEDV vector containing *AvrSr50* or *AvrRmg8* and subsequently infiltrated wheat lines differential for *Sr50* and *Rmg8*. However, I noticed *B. glumae* caused HR-like cell death on wheat lines lacking the associated *R* gene. At an $OD_{600}$ of 0.5 and 0.1, wild type *B. glumae* elicited strong cell death on all differential wheat lines tested **(Figure 4-4).** In order to check whether these phenotypes are specific to these four wheat lines, *B. glumae* was infiltrated into leaves of multiple wheat accessions from different phylogenetic clades indicated in **Figure 4-5A.** Similar to the lines differential for *AvrSr50* and *AvrRmg8*, all other varieties tested showed signs of cell death 1-2 days post infiltration at an $OD_{600}$ of 0.5 and 0.1 (**Figure 4-5B)**. Due to the ability of wild type *B. glumae* to elicit cell death on so many genetically diverse wheat accessions, this would limit the ability to screen rust effectors in lines naturally containing corresponding resistance genes. Hence, the *B. glumae* pEDV system would not be an ideal system for high-throughput screening of multiple rust effectors for detecting avirulence properties.

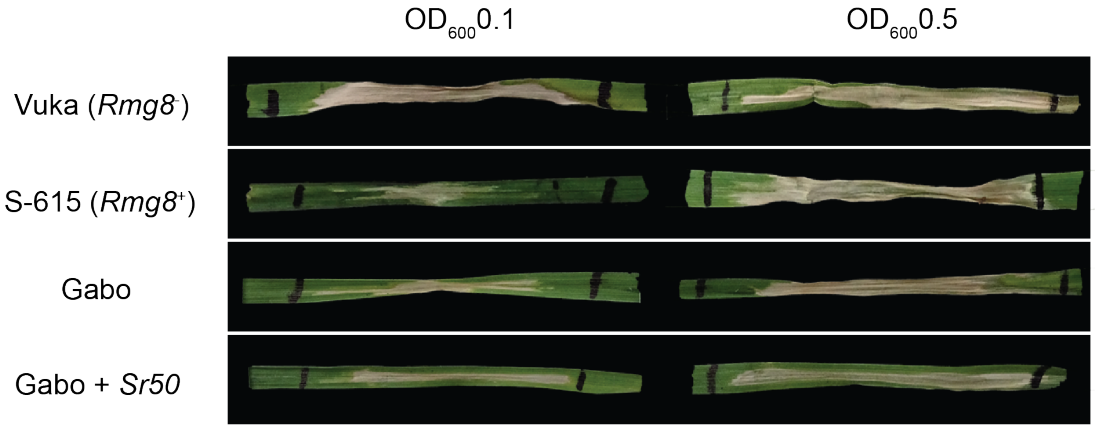


**Figure 4-4 Wild type *Burkholderia glumae* strain 106619 elicits HR on wheat lines differential for *Sr50* and *Rmg8*.** Photographs were taken 2 days post-inoculation. Representative lesions from three different inoculations are shown.

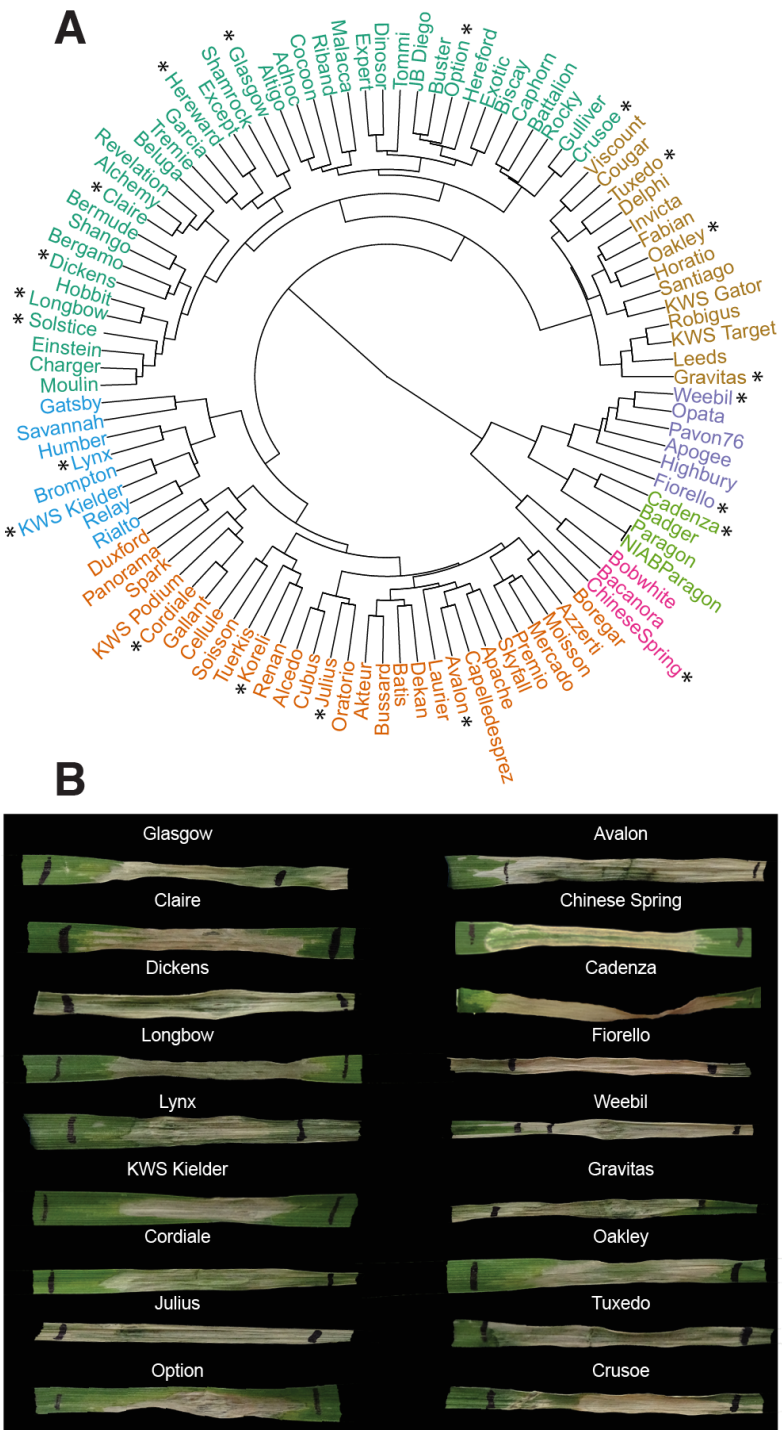


**Figure 4-5 *Burkholderia glumae* strain 106619 elicits cell death across a set of genetically diverse wheat lines.** A) Dendrogram showing the relationship between 103 commercial wheat accessions. Accessions chosen to test HR induced by *B. glumae* are denoted by an asterisk. The dendrogram was constructed using data from 34,516 single nucleotide polymorphism (SNP) positions from 103 wheat varieties and a hierarchical clustering approach. Colours represent seven distinct clades identified. B) All 18 wheat varieties infiltrated with *B. glumae* strain 106619 displayed cell death. Bacteria were infiltrated at an $OD_{600}$ of 0.5 and photographs taken 7 days post-infiltration. Representative lesions from three separate infiltrations are shown. All biological replicates displayed a cell death phenotype.

### 4.4.3 *Burkholderia cepacia* is the only wild type bacterial strain tested that may be suitable for development as a high-throughput screening system of rust effectors in wheat

Bacteria that would be suitable for effector delivery would need to be pathogenic on wheat (express a T3SS and proliferate *in planta*), but also must not elicit cell death under natural conditions. To identify other bacterial strains that may be suitable for development as a high-throughput screening system I tested other cereal infecting bacteria that were likely to be virulent (and thus replicated *in planta*) for non-specific cell death on wheat. First, I investigated five other *B. glumae* strains named 301682, 302544, 302744, 302925, and 302928 **(Appendix 2)** as these strains were originally tested by Sharma *et al.* (2013) for varying levels of pathogenicity on cereals. Some of these strains were more virulent than strain 106619, which was used for microscopy studies in the paper. Additionally, we tested a strain of *P. syringae* (*Pseudomonas syringa* pv. *lapsa*) known to be pathogenic on wheat. Lastly, we tested *Burkholderia cepacia*; a species that is pathogenic on both humans and plants. *B. cepacia* was the only strain that did not cause cell death on wheat variety Vuka when tested at two different optical densities **(Figure 4-6).** Clear cell death phenotypes appeared 48 h after infiltration for all other strains. Wild type *B. cepacia* also did not elicit cell death when infiltrated into wheat lines differential for *Sr50* and *Rmg8* at an $OD_{600}$ of 0.5 and 0.1 (**Figure 4-7A).** These data suggest *B. cepacia* may act as a suitable strain for delivering effectors in wheat using the pEDV vector as *B. cepacia* did not induce HR in the varieties tested.

The next step was to confirm that *B. cepacia* was also able to proliferate *in planta*. I hypothesize pEDV EtHAn expressing *AvrSr50* or *AvrRmg8* is unable to cause *R* gene dependent HR due to poor proliferation of the bacteria *in planta* (Upadhyaya *et al.*, 2014). This may lead to low levels of avirulence effector protein delivered in wheat, resulting in a lack of HR. To determine if *B. cepacia* was able to proliferate at higher levels *in planta* than EtHAn, I performed a colony forming unit (CFU) assay over time on infiltrated wheat leaves. The amount of colony forming units per $cm^2$ of infiltrated wheat was determined over four days. On day four, the number of EtHAn bacteria remained similar to time point zero, supporting previous observations by Upadhyaya *et al.* (2014) **(Figure 4-7B).** In contrast, the CFU count of *B. cepacia* increased by two log fold in comparison to time point zero **(Figure 4-7B).** These data suggest replication of *B. cepacia in planta* may lead to enough protein production/delivery of avirulence effectors in wheat to elicit HR. In combination with the inability to cause cell death on its own, this would indicate *B. cepacia* may potentially be suitable for screening avirulence phenotypes of candidate rust effectors in wheat.

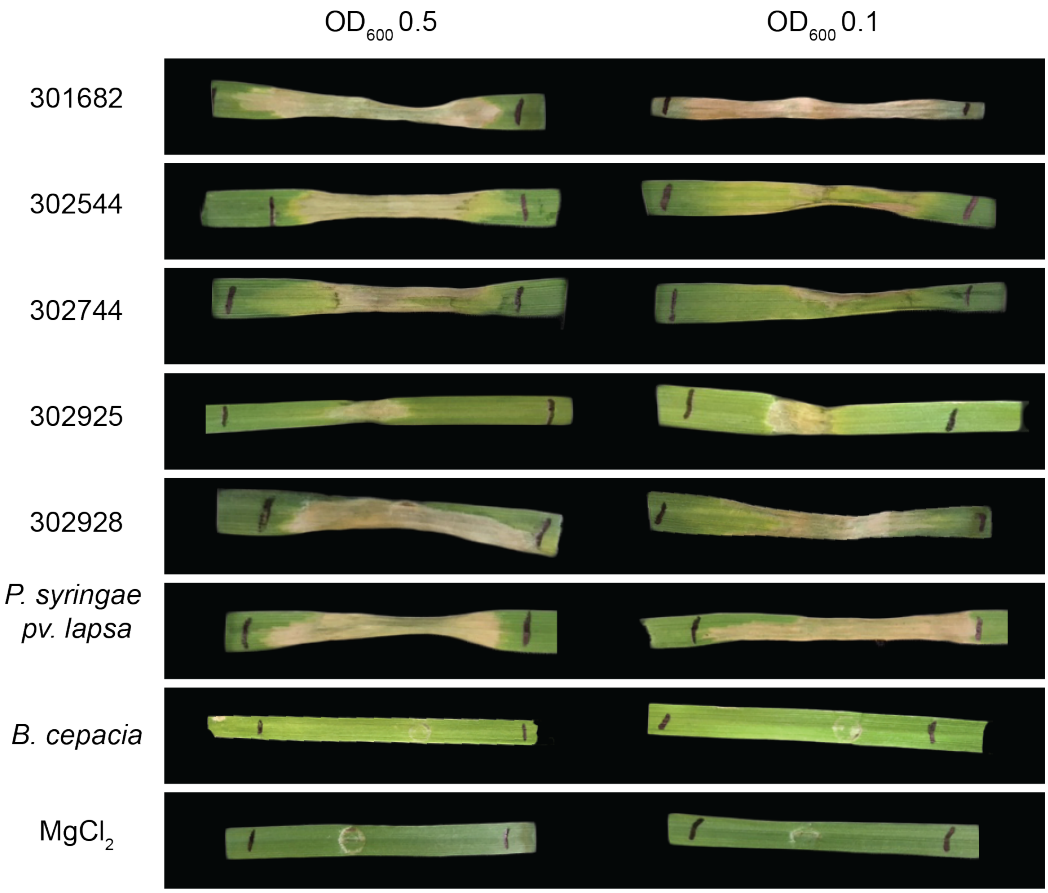


**Figure 4-6 All wild type phytopathogenic bacterial strains tested elicit cell death on wheat except *Burkholderia cepacia* strain ATCC 25416.** Strains 301682, 302544, 30277, 203925, and 302928 are *Burkholderia glumae* strains from Sharma *et al.* (2013). Bacteria were infiltrated on Vuka leaves at two different optical densities. Images were taken at 7 DPI. Representative lesions from at least three different inoculations are shown.

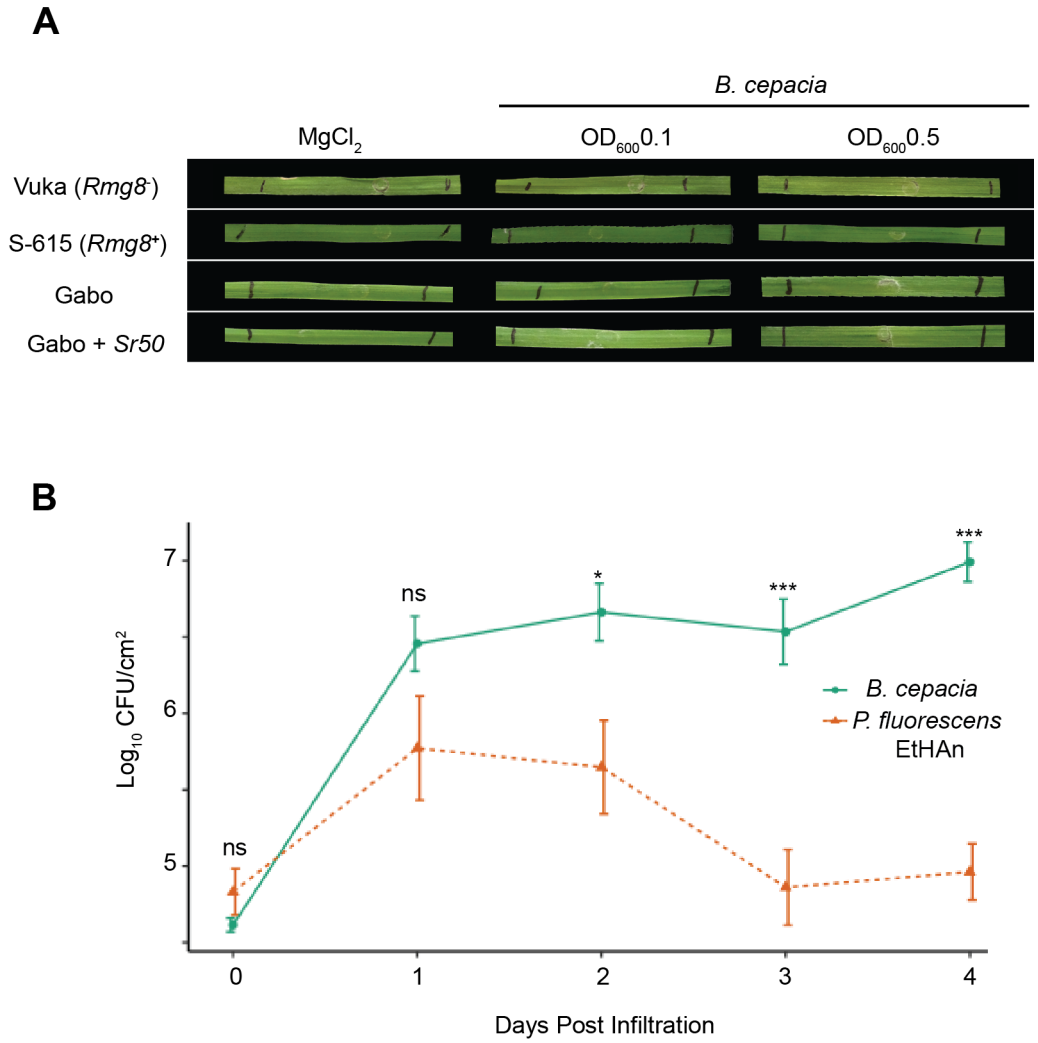


**Figure 4-7 *Burkholderia cepacia* did not exhibit cell death when infiltrated into wheat varieties differential for *Sr50* and *Rmg8* and proliferated *in planta*.** A) *B. cepacia* strain ATCC25416 does not elicit HR on the wheat varieties differential for *Sr50* and *Rmg8* when infiltrated at an $OD_{600}$ of 0.1 or 0.5. Representative photos from three independent biological replicates are shown and photographs were taken 7 days post-infiltration (DPI). All biological replicates displayed the same phenotype. B) *B. cepacia* strain ATCC25416 proliferates *in planta* over time, whereas the number of colony forming units (CFU) per $cm^2$ of leaf area for *P. fluorescens* EtHAn remained constant. Both strains were independently infiltrated into three-week-old Gabo wheat leaves at an $OD_{600}$ of 0.001 suspended in $MgCl_2$. Bacteria in the leaves were quantified at 0-4 dpi. Each point represents the average of six biological replicates, with error bars representing the standard error of the mean. Significant differences in CFU counts between *P. fluorescens* EtHAn and *B. cepacia* was calculated at each time point using a two tailed t- test assuming equal or unequal variance, depending on F-test values. Normalized distribution of data was checked using the Shapiro-Wilk test. P-values are indicated as ns (non-significant), $P > 0.05$; *, $P < 0.05$; **, $P < 0.01$; ***, $P < 0.001$.

### 4.4.4 *Burkholderia cepacia* expressing *AvrSr50* or *AvrRmg8* under the pEDV vector does not elicit HR in an R dependent manner

To test if the *B. cepacia* pEDV system was suitable for detecting avirulence properties of effectors in wheat, I transformed this strain with either *AvrSr50* or *AvrRmg8*. When selecting for transformants containing the original pNR526 G2AC3A vector **(Appendix 4)** I noticed many colonies grew on selective media, none of which had the vector. I hypothesized the wild type *B. cepacia* strain may be naturally resistant to the selective antibiotic (gentamycin). Indeed, when I incubated *B. cepacia* on plates with commonly used antibiotics (including gentamycin), a confluent lawn of bacteria grew. There were reports *B. cepacia* is also resistant to multiple antibiotics in a clinical environment, where it can infect immuno-compromised individuals with cystic fibrosis (Avgeri *et al*. 2009). Trimethoprim is one of the only antibiotics effective for treating clinical cases of *B. cepacia* infection, so I decided to evaluate whether it could also inhibit growth of the plant infecting *B. cepacia* strain used in this chapter (Avgeri *et al*., 2009). Indeed, our *B. cepacia* strain was unable to grow on plates supplemented with trimethoprim, confirming it is susceptible to this antibiotic. Thus, I inserted a trimethoprim resistance gene into the bacterial T3SS vector (pEDV). However, it was also discovered *B. cepacia* is recalcitrant to transformation by heat shock and electroporation methods. I therefore successfully developed a transformation protocol involving triparental mating, in which a helper *E.coli* strain could be used to facilitate the transfer of the pEDV vector into the acceptor strain (*B. cepacia*) as described in section 4.3.8.2.

Once we were able to transform *B. cepacia* with *AvrSr50* or *AvrRmg8*, bacteria were infiltrated into wheat lines differential for *Sr50* or *Rmg8* respectively. Infiltrations were performed at two optical densities ($OD_{600}$ 0.5 and 2.0) and cell death phenotypes monitored over a seven-day period. During this time, there was no evidence of a *R* gene dependent HR phenotype for *B. cepacia* expressing *AvrSr50* or *AvrRmg8* **(Figure 4-8A,B).** At the higher $OD_{600}$ of 2.0, *B. cepacia* elicited a non-specific chlorotic phenotype on Vuka and S-615, which is likely the result of native *B. cepacia* elicitors being expressed to sufficient levels to elicit a chlorotic response **(Figure 4-8B).**

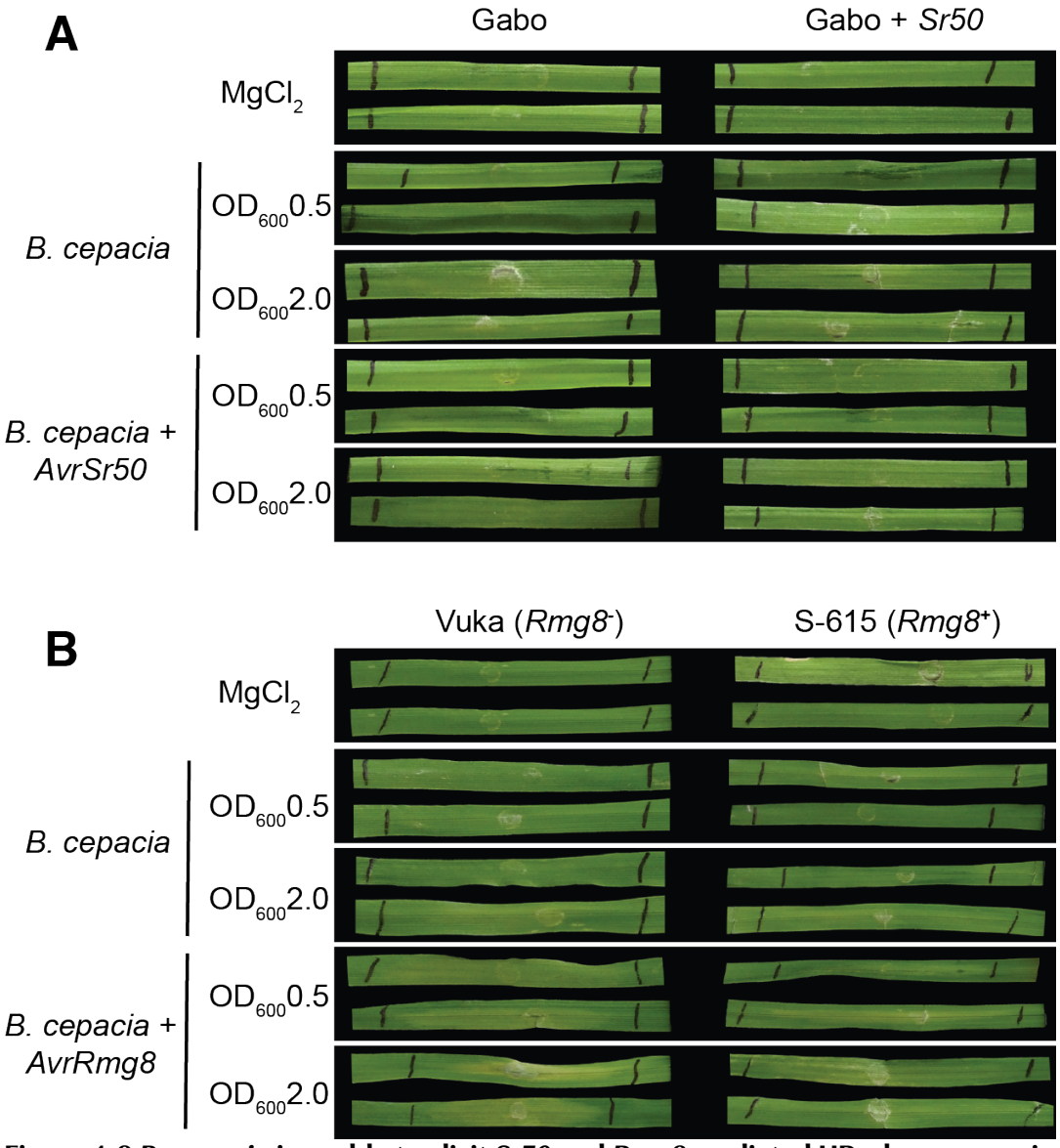


**Figure 4-8 *B. cepacia* is unable to elicit *Sr50* and *Rmg8* mediated HR when expressing the corresponding avirulence effectors.** *B. cepacia* expressing *AvrSr50* was unable to induce HR on *Sr50*+ plants (**A**) or when expressing *AvrRmg8* on *Rmg8*+ plants (**B**). Infiltrations were performed at an $OD_{600}$ of 0.5 and 2.0. Representative leaves from at least three independent biological replicates are shown. All biological replicates displayed the same phenotype. Pictures were taken 7days post-infiltration.

### 4.4.5 EtHAn and *B. cepacia* expressing *AvrSr50* or *AvrRmg8* under the pEDV vector does not elicit HR in an *R* gene dependent manner using T3SS inducing buffer.

It has been shown that the delivery of proteins via the T3SS of *Pseudomonas spp.* can be enhanced by growing bacteria in culture media that mimics the apoplast (Huynh *et al.*, 1989; Rahme *et al.*, 1992; Stauber *et al.*, 2012). This buffer pre-induces the T3SS, leading to an increase in T3SS protein delivery (Stauber *et al.*, 2012). For example, Upadhyaya *et al.* (2014) were able to detect increased levels of Cya (calmodulin-dependent andenylate cyclase domain A) protein delivery into wheat after pre-inducing the T3SS. To test if pre-induction of the T3SS could lead to *R* gene dependent cell death, pEDV EtHAn expressing *AvrSr50* or *AvrRmg8* was cultured in apoplast mimicking media prior to infiltration (Upadhyaya *et al.*, 2014). Pre-induced cultures were re-suspended in $MgCl_2$ and infiltrated into wheat lines differential for *Sr50* or *Rmg8*. Some cell death can be observed at 14 days post infiltration; however, they were not *R* gene dependent (**Figure 4-9A,B).** For example, wild type EtHAn seemed to elicit clear cell death on *Sr50*- wheat leaves when infiltrated at $OD_{600}$ 2.0. This illustrates that pre-induction of *P. fluorescens* EtHAn through growth in minimal media may activate indiscriminate necrosis in wheat that could then be problematic when using *P. fluorescens* EtHAn as a protein delivery system in wheat and in particular when screening for HR induction.

We also tested if pre-induction of *B. cepacia* expressing *AvrSr50* or *AvrRmg8* could elicit *R* gene dependent cell death. Following infiltration, leaves were observed over a 7-day period. No evidence of *R*-gene dependent HR phenotypes for *B. cepacia* strains expressing *AvrSr50* or *AvrRmg8* following potential pre-induction were seen **(Figure 4-10A,B).** However, similar to *P. fluorescens* EtHAn, *B. cepacia* elicited cell death on a few leaves in an indiscriminate manner that was not linked to AVR and R protein combinations.

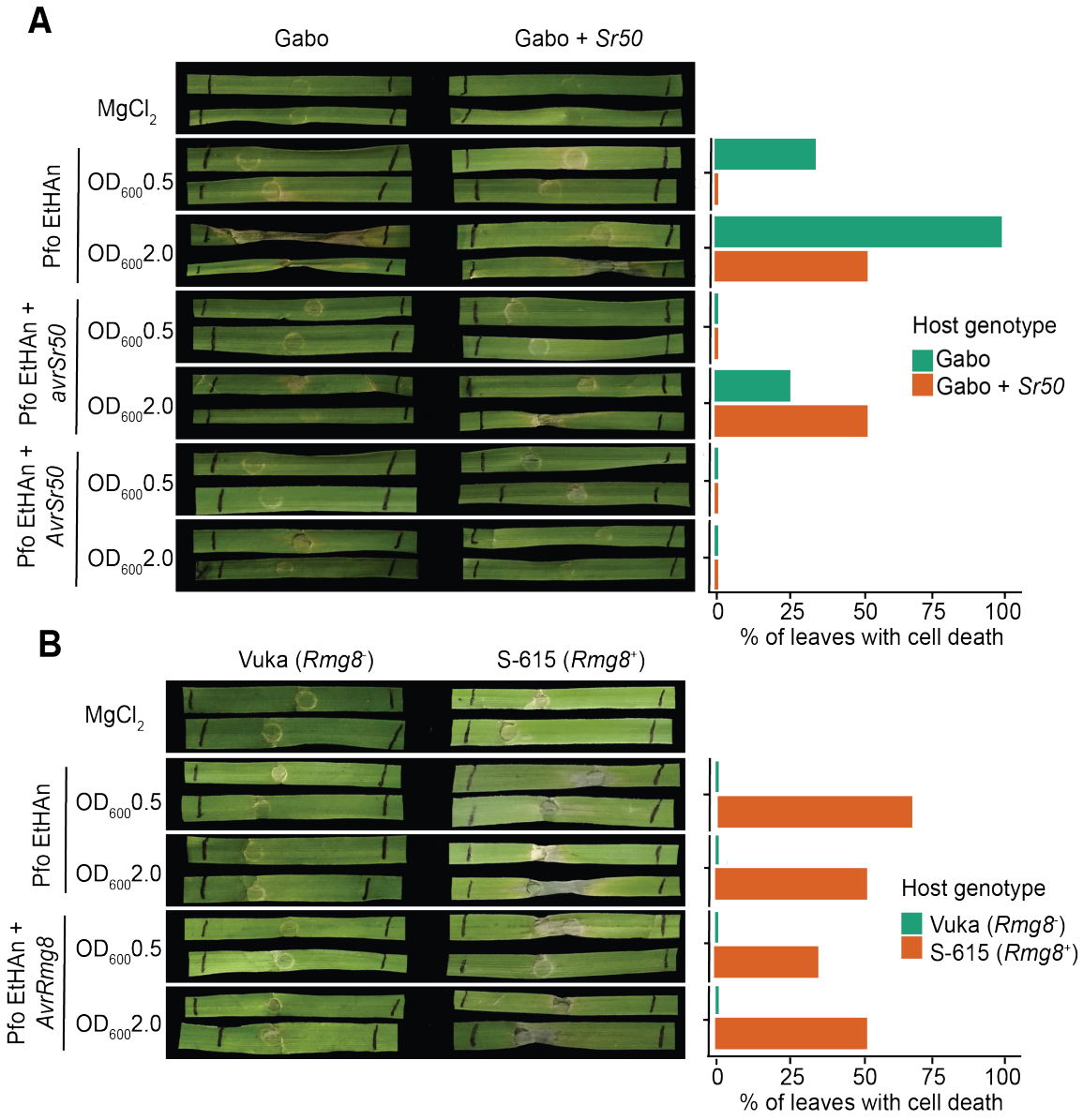


**Figure 4-9 *P. fluorescens* EtHAn grown in a T3SS pre-inducing media is unable to elicit *R* gene dependent HR**. When pre-induced in media mimicking the apoplast, EtHAn was unable to induce HR in an R dependent manner when **A,** expressing *AvrSr50* on *Sr50*+ plants, and **B,** expressing *AvrRmg8* on *Rmg8*+ plants. Infiltrations were performed at an $OD_{600}$ of 0.5 and 2.0. Representative leaves from at least three independent biological replicates are shown. Pictures were taken 7 days post-infiltration. Not all biological replicates displayed the same phenotype. A bar graph including percentage of leaves showing a cell death phenotype is shown in the right-hand panel.

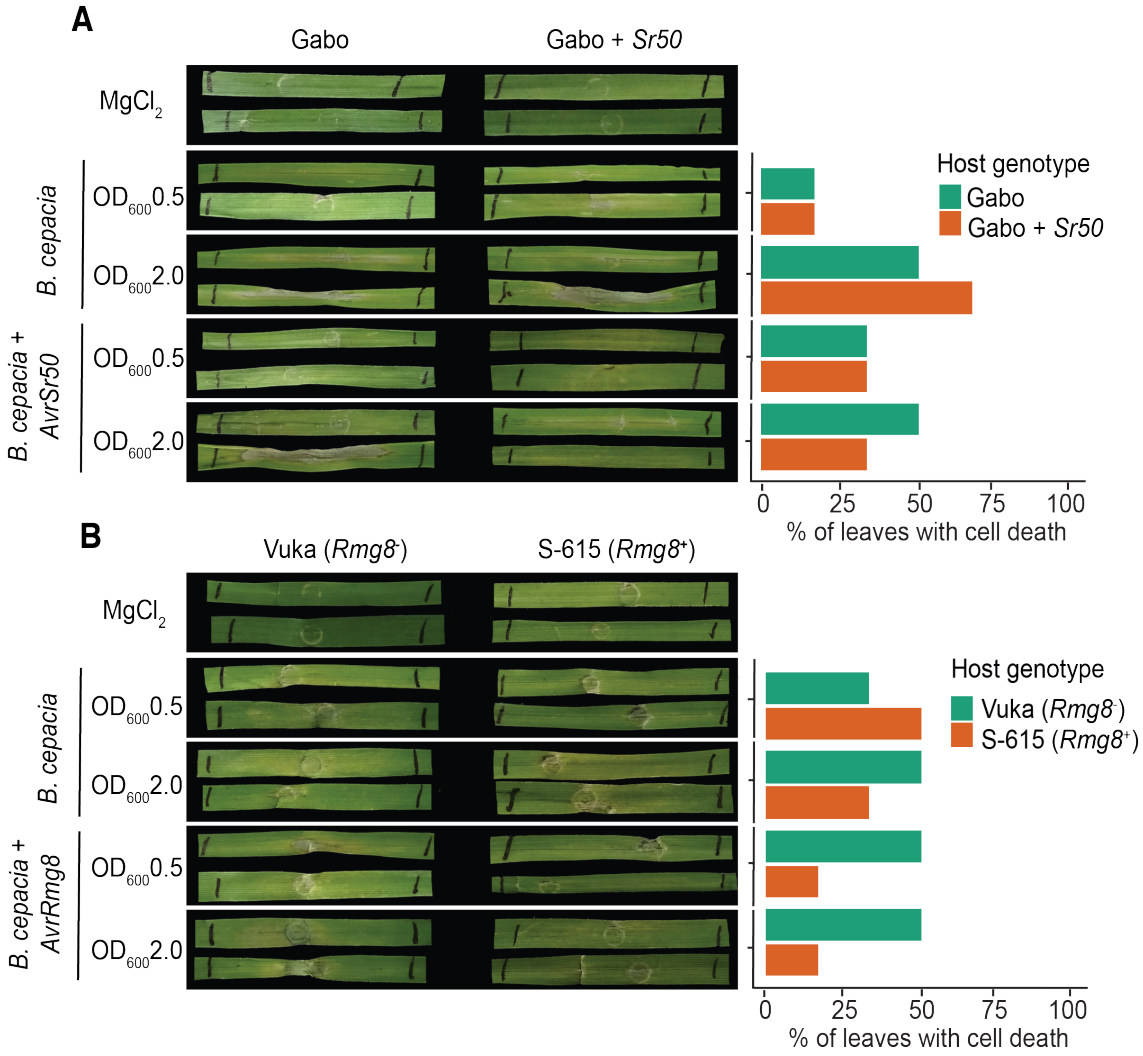


**Figure 4-10 *B. cepacia* grown in a T3SS pre-inducing media is unable to elicit *R* gene dependent HR**. When pre-induced in media mimicking the apoplast, *B. cepacia* was unable to induce HR in an R dependent manner when **A,** expressing *AvrSr50* on *Sr50*+ plants, and **B,** expressing *AvrRmg8* on *Rmg8*+ plants. Infiltrations were performed at an $OD_{600}$ of 0.5 and 2.0. Representative leaves from at least three independent biological replicates are shown. Pictures were taken 7 days post-infiltration. Not all biological replicates displayed the same phenotype. A bar graph including percentage of leaves showing a cell death phenotype is shown in the right-hand panel.

## 4.5 Discussion

### 4.5.1 EtHAn appears unsuitable for screening candidate avirulence effectors in wheat

Using two previously characterised avirulence effectors of biotrophic/hemibiotrophic fungal pathogens of wheat, I showed that pEDV EtHAn does not elicit *R* gene dependent HR (**Figure 4-3**). Similarly, this system failed to elicit an immune response in Barley lines containing the cognate *R* gene when delivering *AVRa1* or *AVRa13* from *Blumeria graminis* f. sp. *hordei* (*Bgh*) (Lu *et al.*, 2016; Saur *et al.*, 2019). To date, this system has only been successful for identifying avirulence properties of fungal effectors in cereals once (Upadhyaya *et al.*, 2014).

One possibility is that EtHAn is delivering low levels of protein into wheat cells. Indeed, Upadhyaya *et al.* (2014) found EtHAn delivered less protein *in planta* in comparison to the known pathogenic bacteria of wheat, *Xanthomonas translucens*. To demonstrate how much protein was being delivered *in planta*, the authors transformed both EtHAn and *X. translucens* with a pEDV vector containing a calmodulin-dependent adenylate cyclase (*Cya*) from *Bordetella pertussis*. The Cya protein domain is inactive in prokaryotes but becomes active and produces cAMP in eukaryotes in the presence of calmodulin. When both strains were infiltrated into wheat leaves, *X. translucens* gave a significantly higher cAMP signal. This suggests that EtHAn is delivering low levels of protein *in planta,* especially in comparison to *X. translucens*.

Despite low levels of protein delivery in wheat, Upadhyaya *et al.* (2014) were able to use the pEDV EtHAn system to discover a candidate avirulent *Pgt* effector (PGTAUSPE-10-1) that caused HR on *Sr22*+ wheat. However, to date this candidate *AVR* gene has not been subsequently confirmed as a true avirulence protein. One possibility is that the cell death caused by PGTAUSPE-10-1 may not be related to the *R* gene locus containing *Sr22* in wheat line W3534. The wheat lines used to screen avirulence activity were not near isogenic, suggesting cell death could potentially be caused by other loci unrelated to *R* genes. It is also conceivable that this system could work for another *R/AVR* pair that requires a lower threshold of AVR detection to elicit HR.

Future work will include confirmation of fungal effector translocation into wheat cells. Although previous studies have shown EtHAn can deliver a Cya domain into wheat, it has not been shown this system can deliver a fungal effector tagged with the Cya domain. Confirmation of translocation could also be achieved by tagging a fluorescent protein to a

fungal effector, however, fluorescent proteins often clog the narrow pilus of the T3SS (Galán, 2009). In summary, these future experiments would help uncover whether or not heterologous fungal protein is actually being translocated into wheat cells using this system.

### 4.5.2 *B. glumae* and *B. cepacia* are unsuitable for screening candidate avirulence effectors in wheat using the pEDV vector

Similar to the pEDV EtHAn system, Sharma *et al.* (2013) were able to successfully deliver fungal effectors in wheat using the T3SS of *Burkholderia glumae*. Effectors from *Magnaporthe oryzae* fused with a nuclear localisation signal and fluorescent tag were clearly seen in the nucleus 3 DPI using confocal microscopy, despite previous reports that fluorescent tags usually clog the pilus (Galán, 2009). However, when I infiltrated the same wild type *B. glumae* strain into multiple wheat accessions, nonhost cell death appeared within 48 hours post inoculation (**Figure 4-5**). It is possible Sharma *et al.* (2013) did not see cell death during their confocal microscopy experiments due to the method of inoculation. Sharma *et al.* (2013) immersed leaf sheaths or cut leaves in bacterial inoculum ($OD_{600}$ 0.75), whereas I infiltrated bacteria directly into the apoplast of wheat seedlings. Indeed, HR like cell death was not detected in rice leaf sheaths when an avirulence effector was delivered in plants with the cognate *R* gene using the *B. glumae* pEDV system (Hiromasa Saitoh, personal communication). However, when *B. glumae* was infiltrated into cereal leaves, Sharma *et al.* (2013) were also able to see non-specific cell death (Hiromasa Saitoh, personal communication). Therefore, this system may be used to deliver effectors of cereal phytopathogens in wheat for microscopy studies. However, the data presented in this chapter suggests it cannot be used to screen avirulence phenotypes of candidate effectors in wheat.

I hypothesize it is possible the T3SS can be used to screen avirulence phenotypes of candidate effectors in wheat under three conditions. One, the bacteria must not cause non-host cell death on its own. Secondly, the bacteria must deliver sufficient protein to elicit HR. Third, the effector must not require eukaryotic specific post-translation modifications that cannot be conferred by bacteria. I discovered a phytopathogenic bacteria, *B. cepacia*, that may fulfill at least the first two requirements. Specifically, *B. cepacia* did not cause nonhost cell death under normal infiltration conditions **(Figure 4-6Figure *4-7*).** *B. cepacia* also proliferated to higher levels than EtHAn in wheat, suggesting it may deliver more protein *in planta* (**Figure 4-7**). However, it was not able to elicit *R* gene dependent HR when expressing *AvrSr50* or *AvrRmg8* in the pEDV vector (**Figure 4-8**). I hypothesize *B. cepacia* is still not delivering enough protein to elicit *R* gene dependent HR.

### 4.5.3 Pre-inducing the T3SS of EtHAn or *B. cepacia* elicits non-specific cell death

I hypothesized that pre-inducing the T3SS may increase protein delivery by EtHAn or *B. cepacia*. However, growing these bacteria in pre-inducing media prior to infiltration led to nonspecific cell death in wheat **(Figure 4-9, Figure 4-10).** It is possible EtHAn contains unknown elicitors that only cause cell death when protein delivery reaches a certain threshold. These unknown elicitors may lie in the hrp/hrc region from *P. syringae pv. syringae 61* (Psy61) that was incorporated into the *Pf0-1* progenitor isolate of EtHAn (Thomas *et al.*, 2009). A similar nonhost response was reported for *P. fluorescens* EtHAn in tomato and tobacco. However, the *Pf0-1* progenitor isolate which lacks the hrp/hrc region did not elicit nonhost cell death, suggesting EtHAn may contain elicitors in this region (Thomas *et al.*, 2009). Similarly, O'Neill et al. (2018) found EtHAn induced more callose deposition than *Pf0-1* when infiltrated in *N. benthamiana* suggesting the hrp/hrc region integrated into EtHAn can elicit an immune response.

I found that the nonhost defence response caused by pre-induced EtHAn occurred more frequently in certain host genotypes, suggesting that wheat varieties may differ in response to these elicitors. For example, the S-615 variety was particularly prone to non-specific cell death caused by pre-induced EtHAn **(Figure 4-9B)**. Similarly, when the T3SS of *B. cepacia* is pre-induced, it starts to elicit non-specific cell death. It is likely inducing the T3SS increases protein delivery by *B. cepacia.* However, the non-specific cell death suggests *B. cepacia* carries its own virulence factors that elicits non-host cell death when enough protein is delivered. Knowing that pre-induction can induce non-specific cell death will guide future use of this system for protein delivery in wheat.

### 4.5.4 EtHAn is suitable for delivering effectors and assessing avirulence phenotypes in other plant systems than wheat

Although pEDV EtHAn could not be used to elicit *R* gene dependent HR with the effectors tested in this chapter, it has been successfully used for this purpose in other plant systems. For example, pEDV EtHAn mediated delivery of the flax rust effector AvrM elicited strong HR in transgenic tobacco carrying the cognate *R* gene (Upadhyaya *et al.*, 2014). Furthermore, many bacterial effectors expressed by pEDV EtHAn have shown to elicit *R* gene dependent HR in *Arabidopsis* (Thomas *et al.*, 2009). Similar to wheat, EtHAn does not proliferate over time inside *Arabidopsis* leaves (Thomas *et al.*, 2009). However, the ability of EtHAn to elicit HR when expressing avirulence effectors in *Arabidopsis* suggests the threshold to elicit cell

death may be lower in *Arabidopsis* than in wheat. It is also possible the T3SS of EtHAn may be more active in these other plant species than in wheat. Phytopathogenic bacteria only express effector proteins and T3SS machinery when particular chemical signals from a potential plant host are perceived (Anderson *et al.*, 2014). These signals may be different across plant species, leading to differential recognition and thus induction of the T3SS. While the EtHAn system can be used to assess avirulence of effectors in other plant species, it clearly must be further modified for usage in wheat.

### 4.5.5 EtHAn is suitable for detecting virulence phenotypes in wheat, but not avirulence

The EtHAn system has not yet been used to confirm avirulence properties of effectors, however, it has been used multiple times to investigate virulence phenotypes of candidate rust effectors in wheat. Although EtHAn itself does not cause cell death or chlorosis in wheat, it does elicit PTI responses in wheat, including callose deposition. Cheng *et al.* (2017) delivered a candidate *Pst* effector, PSTha5a23, using the pEDV EtHAn system and noticed decreased callose deposition in comparison to infection with EtHAn alone. These data suggest expression of the candidate effector could be supressing PTI associated callose deposition in wheat. Using the same method, candidate *Pst* effectors Pst_8713 and Pst_12806 were also shown to supress PTI mediated callose deposition in wheat (Zhao *et al.*, 2018; Xu *et al.*, 2019). The EtHAn delivery system, therefore, can be used successfully to elucidate function of heterologous rust effectors in terms of PTI suppression.

Delivery of candidate effectors in wheat using pEDV EtHAn can also be used to show suppression of ETI. Ramachandran *et al.* (2017) delivered *Pst* candidate effector Shr7 in wheat using pEDV EtHAn and subsequently infiltrated the area with *P. syringae* DC3000. The region infiltrated with Shr7 showed reduced HR in comparison to leaves infiltrated with *P. syringae* DC3000 on its own. These data suggest Shr7 can supress nonspecific cell death caused by *P. syringae* DC3000. Using the same method, Pst_12806 was shown to supress HR in wheat caused by *P. syringae* DC3000 (Xu *et al.*, 2019). It is possible the threshold for eliciting HR is generally much higher in wheat in comparison to the threshold needed to induce virulence phenotypes, such as suppression of PTI and ETI. This may explain why the pEDV EtHAn system is so effective for characterising virulence phenotypes of rust effectors, but not avirulence phenotypes.

### 4.5.6 Chimeric effectors may not be recognized by the bacterial T3SS, or may not function properly in the plant cytoplasm

In addition to insufficient levels of protein being delivered, the EtHAn and *Burkholderia* systems may be producing aberrant chimeric protein products that could evade immune signalling normally induced by a wild type effector. Delivery systems mediated by the T3SS require chimeric proteins with a bacterial N-terminal secretion signal and C-terminal effector protein. These N-terminal peptides that target proteins to the T3SS are not normally cleaved, unless the effector contains an *in-planta* processing site. These chimeric proteins may not efficiently enter the host cytoplasm for many reasons. Firstly, the chimeric protein may take on a confirmation that cannot pass through the narrow pilus of the T3SS. Many bacterial effectors have evolved folding kinetics that favour a disordered state in the mildly acidic bacterial cytoplasm, leading to a partially unfolded conformation needed for passage through the pilus (Dawson *et al.*, 2009). These proteins are also highly stable in the neutral host cytoplasm, leading to a conformation needed for proper functioning **(Figure 4-1**, Dawson *et al.*, 2009). For example, *AvrPto*, an effector from the bacteria *P. syringae*, has an intrinsic pH sensor to control folding dynamics across pH gradients (Dawson *et al.*, 2009). In the neutral pH of the host cytoplasm, *AvrPto* is stable and in a functional conformation. As the pH is lowered to the acidic conditions of the bacterial cytoplasm, a conserved residue called H87 is ionized. This ionization leads to protein instability, and ultimately the loss of a folded confirmation. This confirmation subsequently allows passage through the narrow pilus. However, effectors from other organisms, including rust fungi, may not have evolved the same folding kinetics. Therefore, it is possible chimeric proteins may clog the narrow pilus. This phenomenon has been demonstrated in the bacterial human pathogen *Yersinia enterocolitica.* Effectors were fused to stably folded protein domains, which subsequently blocked the T3SS (Lee and Schneewind, 2002; Feldman *et al.*, 2002). When these domains were destabilised by a chaperone or by mutations, the chimeric proteins no longer blocked the pilus and were secreted. Ultimately, heterologous expression of rust effectors may similarly produce protein products with stably folded domains, precluding secretion through the pilus.

Disruption of secretion though the pilus may also be affected by lack of chaperone binding domains in chimeric rust effectors targeted to the T3SS. Many bacterial effectors that do not have special folding kinetics have evolved close relationships with chaperone proteins. Chaperone proteins bind directly to their cognate effectors via a chaperone binding domain (CBD) and unfold them for passage through the pilus (Lohou *et al.*, 2013; Feldman and Cornelis, 2003). Chaperone proteins are often small (15-20 kDa), and have an alpha helix at

the C-terminus (Lohou *et al.*, 2013). Although small, chaperone proteins perform many roles. Firstly, they can guide unfolded effectors for ATP-dependent entry into the T3SS (Akeda and Galán, 2005). As the normal folding conditions for effectors are within the host cytoplasm, chaperones can also prevent degradation inside the unfavourable environment of the bacterial cell (Lohou *et al.*, 2013). For example, the ShcM chaperone is required for the secretion and the translocation of the HopM1 effector from *P. syringae* pv. *tomato* into the plant host. ShcM directly binds to HopM1 via a chaperone binding domain, subsequently protecting it from degradation by Lon proteases inside the bacterial cytoplasm (Losada and Hutcheson, 2005). Effectors from other organisms would not have the same chaperone binding domains as bacterial effectors. Therefore, a chimeric protein with a C-terminal rust effector may be subject to degradation, or improper unfolding for passage through the pilus.

In addition to obstruction of passage through the T3SS pilus, chimeric effectors may disrupt proper localisation. Targeting effectors to the correct subcellular compartment *in planta* is also influenced by the T3SS N-terminal secretion signal. For example, effectors that function near the host plasma membrane may benefit from an *AvrRpm1* signal peptide that contains myristoylation and palmitoylation signals. These signals are known to target *AvrRpm1* to the plant plasma membrane, and subsequently augments its avirulence activity (Nimchuk *et al.*, 2000). Similarly, effectors that function in the cytoplasm would require, for example, an *AvrRps4* secretion signal that targets proteins to the nucleus and cytoplasm (Sohn *et al.*, 2012). Indeed, a cytoplasmic effector from the oomycete *Hyaloperonospora arabidopsidis*, ATR1, is only able to induce HR in *Arabidopsis* plants carrying the cognate *R* gene when fused to the *AvrRps4* signal peptide, but not the *AvrRpm1* signal peptide (Goritschnig *et al.*, 2012). Alternatively, ATR1 may only function/fold properly as a free protein without an N-terminal peptide. This would occur with an *AvrRps4* signal peptide which has a cleavage site, and not an *AvrRpm1* signal peptide. However, not all AvrRpm1 protein is targeted to the plant plasma membrane (Guttman and Greenberg, 2001). Therefore, in cases where the *AvrRps4* secretion signal impedes folding of chimeric effectors, the *AvrRpm1* signal peptide may be appropriate for targeting cytoplasmic effectors to the right location. This may explain why, for example, oomycete effector ATR39-1 only triggers an *R* gene dependent HR when expressed as a fusion to the *AvrRpm1* signal peptide, and not *AvrRps4* (Goritschnig *et al.*, 2012). Clearly, whether or not chimeric effectors will properly fold and function *in planta* must be assessed on a case-by-case basis.

This is further demonstrated by experiments where the N-terminal secretion signal between effectors of phylogenetically distant species of bacteria have been swapped (Puhar and Sansonetti, 2014). For example, the secretion signal from the bacterial plant pathogen *Dickeya dadantii* can be used to translocate effectors from *Pseudomonas syringae* and *Yersinia* when heterologously expressed in *E. coli* (Puhar and Sansonetti, 2014). Mechanisms of recognition and targeting of bacterial effectors to the T3SS may be conserved between distantly related species. In conclusion, the folding kinetics of a chimeric effector will depend on the compatibility between the N-terminal secretion signal and C-terminal effector domain.

### 4.5.7 General considerations and caveats for using the bacterial T3SS for assessing avirulence phenotypes in wheat

Protein delivery mediated by the bacterial T3SS may work if the N-terminal and C-terminal domains retain the functional confirmation for proper targeting and localisation *in planta*. It is also possible current bacterial delivery systems could work for detecting avirulence phenotypes if other *R/AVR* pairs are used that require a lower threshold for causing cell death. Further, expression of the same *R* gene can differ between wheat accessions and transgenic lines. It is possible a reaction may be seen only on certain accessions that have a particularly high expression of the *R* gene being studied. Therefore, I do not discourage the use of the bacterial T3SS for delivery and characterisation of fungal effectors *in planta*. However, if these systems are to be used in the future, one must keep in mind false negatives are likely to occur.

The bacterial T3SS may be used to functionally characterise fungal effectors on a case-by-case basis, however, it should not be used to conclusively screen effectors for avirulence phenotypes on its own. The data presented in this chapter suggest current methods using the T3SS for delivering rust effectors in wheat are not reliable or consistent for detecting avirulence phenotypes. This is likely due to insufficient protein being delivered to reach the threshold required to elicit HR. Theoretically, a reliable system could be developed if certain criteria are met. Firstly, the bacteria must not elicit HR on its own. Secondly, the bacteria must deliver enough effector protein to elicit HR. Finally, chimeric proteins must be folded and targeted correctly to the T3SS. Meeting all of these criteria is conceivably possible, and the data presented in this chapter provide critical information for the development of a consistent delivery system mediated by the T3SS.

## 4.6 Conclusion

In this chapter, I investigated whether two previously published methods for delivering fungal effectors in wheat using the bacterial T3SS are suitable for detecting avirulence phenotypes of fungal effectors (Upadhyaya *et al.*, 2014; Sharma *et al.*, 2013). Using *AvrSr50* and *AvrRmg8* as positive controls, I showed that *P. fluorescens* EtHAn cannot elicit *R* gene dependent HR in wheat. Further, I show the T3SS of *B. glumae* strain 106619 used in Sharma *et al.* (2013) is not suitable for avirulence screening of candidate effectors, as the wild type strain elicits HR on multiple wheat accessions tested. I tested another phytopathogenic bacteria, *Burkholderia cepacia*, for suitability in delivering fungal effectors in wheat for the purpose of detecting avirulence. Although *B. cepacia* proliferates in wheat and does not cause HR on its own, it was not able to elicit *R* dependent HR. When grown in T3SS inducing media, *B. cepacia* and EtHAn elicit non-specific cell death, likely conferred by native virulence factors. It is theoretically possible to use the T3SS of bacteria to identify and characterise fungal effectors in wheat, however, multiple caveats must be kept in mind when planning experiments. This is especially pertinent, as the previously described caveats are not mentioned in current reviews that mention the T3SS for functionally characterising fungal effectors in wheat (Prasad *et al.*, 2019; Lorrain *et al.*, 2019).

# Chapter 5 Utilising *Magnaporthe oryzae* (*Triticum* pathotype) for the heterologous expression of rust effectors in wheat

## 5.1 Abstract

Characterisation of effectors from filamentous plant pathogens in cereal hosts not only requires the development of high-throughput functional assays, but also the concomitant use of low-medium throughput techniques for confirmation. A largely unexplored low-medium throughput avenue for delivering rust effectors in wheat includes heterologous expression in a different fungus that is experimentally tractable. To this aim, I chose the wheat (*Triticum*) infecting pathotype of *Magnaporthe oryzae* (MoT). In this chapter I characterized one *M. oryzae* transformant that is able to cause a *Sr50* dependent hypersensitive response (HR) in wheat when expressing *AvrSr50*. This particular transformant has a wheat blast cytoplasmic effector promoter and signal peptide upstream of the *AvrSr50* coding sequence and 40 copies of this construct in its genome. Expression studies indicated this transformant expresses more *AvrSr50* transcript than other transformants with a lower copy number. Whole genome sequencing using Nanopore technology revealed the entire donor DNA plasmid was tandemly inserted 40 times into a genomic region with structural variation between the wheat blast and rice blast reference genome. This region is also highly enriched in transposable elements and predicted *M. oryzae* effector proteins. Further, I investigated whether insertion location may be important for the expression of *AvrSr50* by utilising CRISPR/Cas9 genome editing. Finally, I explore the utility of an *M. oryzae* delivery system for visualising rust effector proteins in wheat using confocal microscopy. The findings presented in this chapter provide the foundations for the subsequent optimisation of an *M. oryzae* mediated delivery system of rust effectors in wheat, particularly for the purpose of detecting avirulence phenotypes.

## 5.2 Introduction

An ideal surrogate fungal species for the heterologous expression and delivery of effectors in wheat would have the following characteristics:

a) Naturally infect many wheat genotypes
b) Experimentally tractable (can be cultured and transformed in the laboratory)
c) A model organism with a plethora of genomic resources
d) For the purpose of detecting avirulence phenotypes of cytoplasmic effectors in wheat, the fungus should be a biotroph or a hemi-biotroph

*M. oryzae* is an ascomycete fungus that can infect multiple grasses, including economically important cereal crops such as rice, wheat, barley, and millet (Talbot, 2003). The *M. oryzae*

*Triticum* pathotype (MoT) that causes wheat blast disease fulfils all the above requirements as an ideal species for the heterologous expression and delivery of effectors in its native wheat host. Although other fungi do meet some of these requirements, the resources available are not quite as developed as those for *M. oryzae*. The following section will introduce *M. oryzae* in the context of the above characteristics.

### 5.2.1 *Magnaporthe oryzae* causes devastating disease on many plant species including wheat

The most studied *M. oryzae* pathotype is the rice infecting strain that causes rice blast. The rice blast fungus can infect many parts of the plant, including the leaves, stems, nodes, and panicles (Wilson and Talbot, 2009). This particular disease destroys enough rice to feed 60 million people per year, causing a major threat to global food security (Pennisi, 2010). This is highlighted by the fact rice provides 19 % of a person's average daily calories consumed worldwide, with numbers rising to 30 % in Asia alone (Elert, 2014). Over the past few years, there have been incredible advances in understanding the cell biology of infection of this fungus (Yan and Talbot, 2016). This is likely due to the high impact this fungus has on worldwide agriculture and its amenability to experimental manipulation (Ebbole, 2007).

The *M. oryzae Triticum* pathotype (MoT, or wheat blast) is a genetically distinct pathotype that poses a severe threat to global wheat production (Ceresini *et al.*, 2018). This pathotype is capable of infecting all above ground parts of the wheat plant (Cruz and Valent 2017). *M. oryzae* infection on wheat was first reported in Brazil in 1985, and soon spread to neighbouring wheat-producing countries in South America (Igarashi *et al.*, 1986, Cruz & Valent, 2017). Losses in these regions range from low to 100 %, with higher losses associated with El Niño weather conditions (continuous rains followed by high humidity) (Kohli *et al.*, 2018). Recently, wheat blast has garnered significant attention due to the 2016 outbreak in Bangladesh (Callaway, 2016). Farmers were found burning infected fields in attempt to control the disease, which had ultimately spread to approximately 15,000 hectares (Callaway, 2016). This outbreak also represented the first occurrence of the disease in Asia, which was likely caused by strains originating from South America (Islam *et al.*, 2016). Recently, MoT has also been confirmed for the first time on wheat growing in Africa (Tembo *et al.*, 2020). MoT strains not only infect different wheat cultivars as evidenced through multiple disease epidemics, but it can also infect triticale, barley, durum wheat, oat, and some weed species (Urashima and Kato, 1993; Islam *et al.*, 2020). The potential for wheat blast to spread to other

wheat growing regions continues to fuel further research involving the molecular mechanisms of infection (Islam *et al*. 2020).

### 5.2.2 *M. oryzae* is an experimentally tractable model organism

Perhaps one of the most attractive features for studying *M. oryzae* is its amenability to experimental procedures (Ebbole, 2007; Wilson and Talbot, 2009). For one, this fungus can be cultured under experimental conditions outside of living host tissue (Valent *et al.,* 1991). Secondly, there are well-established protocols for genetically transforming *M. oryzae* that are relatively straightforward to perform, including protoplast and *Agrobacterium* mediated transformation (Talbot, 2003). During transformation, DNA enters the genome randomly with an efficiency of about 40 transformants per microgram using the protoplast method (Talbot, 2003).

In *M. oryzae*, DNA enters the genome primarily through the non-homologous end-joining (NHEJ) pathway for repairing double stranded breaks (DSBs). Therefore, targeted gene replacement via homologous recombination occurs at low frequencies; from 1 – 25 % success rate depending on the locus (Krappmann, 2007). Knocking out components of the NHEJ pathway (known as Ku70 or K780 mutants), however, can increase homology directed repair (HDR), and therefore targeted gene replacement (Villalba *et al*., 2008). Recently, Foster *et al*. (2018) developed a method for CRISPR (clustered regularly interspaced short palindromic repeat)-Cas9 (CRISPR-associated nuclease 9) mediated genome engineering in *M. oryzae* that increases the frequency of DSB's occurring in a gene of choice. In the CRISPR/Cas9 system, the Cas9 endonuclease is targeted to a specific genomic sequence of interest by a single guide RNA (sgRNA) via Watson-Crick base-pairing (**Figure 5-1**, Ding *et al*., 2016). A protospacer-adjacent motif (PAM) with the sequence of 5' NGG 3' is required immediately downstream of the targeted DNA for recognition by Cas9 (Sternberg *et al*., 2014). The Cas9 endonuclease creates a DSB at the recognition locus. The subsequent repair of the induced DSB allows genome engineering based on either NHEJ or HDR (Dicarlo *et al*., 2013). The NHEJ pathway is error prone and usually introduces an insertion or deletion at the break site (Ding *et al*., 2016). If a donor DNA with flanking regions homologous to the genomic break site is provided, the DSB can be repaired via HDR using the donor DNA as a template (Dicarlo *et al*., 2013). The donor DNA is then integrated into the genome at the DSB site.

CRISPR/Cas9 components can either be expressed *in vivo* within the organism of interest via plasmid delivery or can be delivered as a pre-complexed ribonucleoprotein (RNP) (Cho *et al*.,

2013). In the first scenario, a plasmid carrying the Cas9 coding sequence and sgRNA sequence are transformed into the cell, in which both elements are transcribed *in vivo* (**Figure 5-2A).** The Cas9 and sgRNA then complex within the cell before genome editing. In the second approach, purified nuclear-localised Cas9 protein and *in vitro* synthesized sgRNA are pre-complexed into an RNP (**Figure 5-2B)**. After transfection the RNP constructs are cleared from the cell, whereas plasmid mediated delivery continuously transcribes CRISPR/Cas9 components within the cell (Gearing, 2016). As stable expression of Cas9 is toxic to *M. oryzae*, the RNP delivery method remains more efficient (Foster *et al.*, 2018). In summary, many methods to genetically manipulate *M. oryzae* exist, including targeted insertion of a gene of interest. The experimental tractability of this organism and the many tools available for genetic manipulation makes *M. oryzae* an ideal surrogate for heterologous expression of candidate effectors.

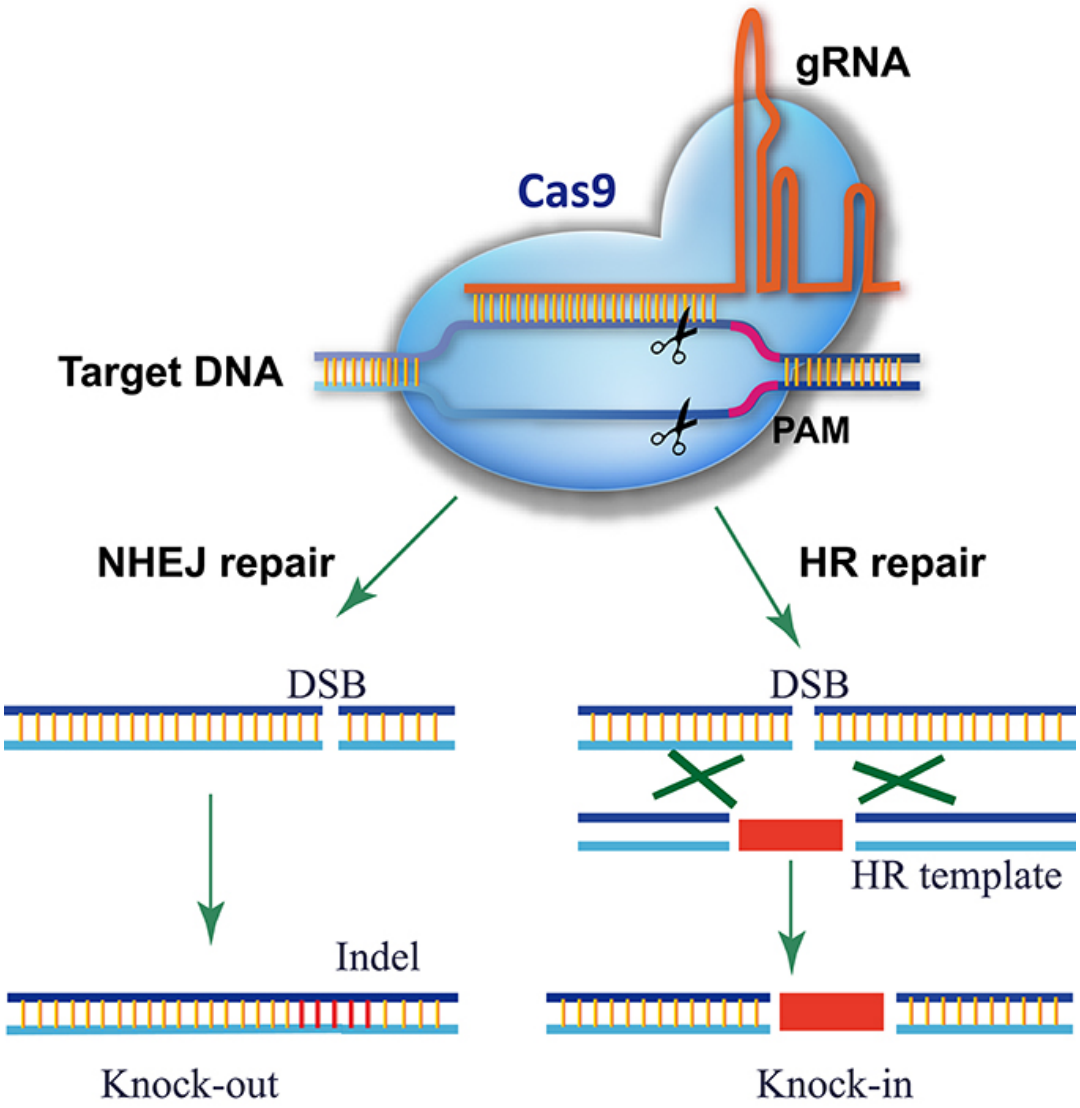


**Figure 5-1 Schematic illustration of Cas9/gRNA genome editing.** The Cas9 protein (in blue) is directed to a DNA target by a gRNA through base pairing. The recognition site is upstream of the PAM (NGG) sequence. The Cas9/gRNA complex introduces a double stranded break which is repaired by either NHEJ or HDR. The NHEJ pathway will introduce an indel for knockout experiments. Kock-in experiments occur via HDR when a donor template is present with homologous sequences flanking the transgene. This image was first published in Ding *et al.* (2016) and is reused here with permission under the Creative Commons Attribution Licence.

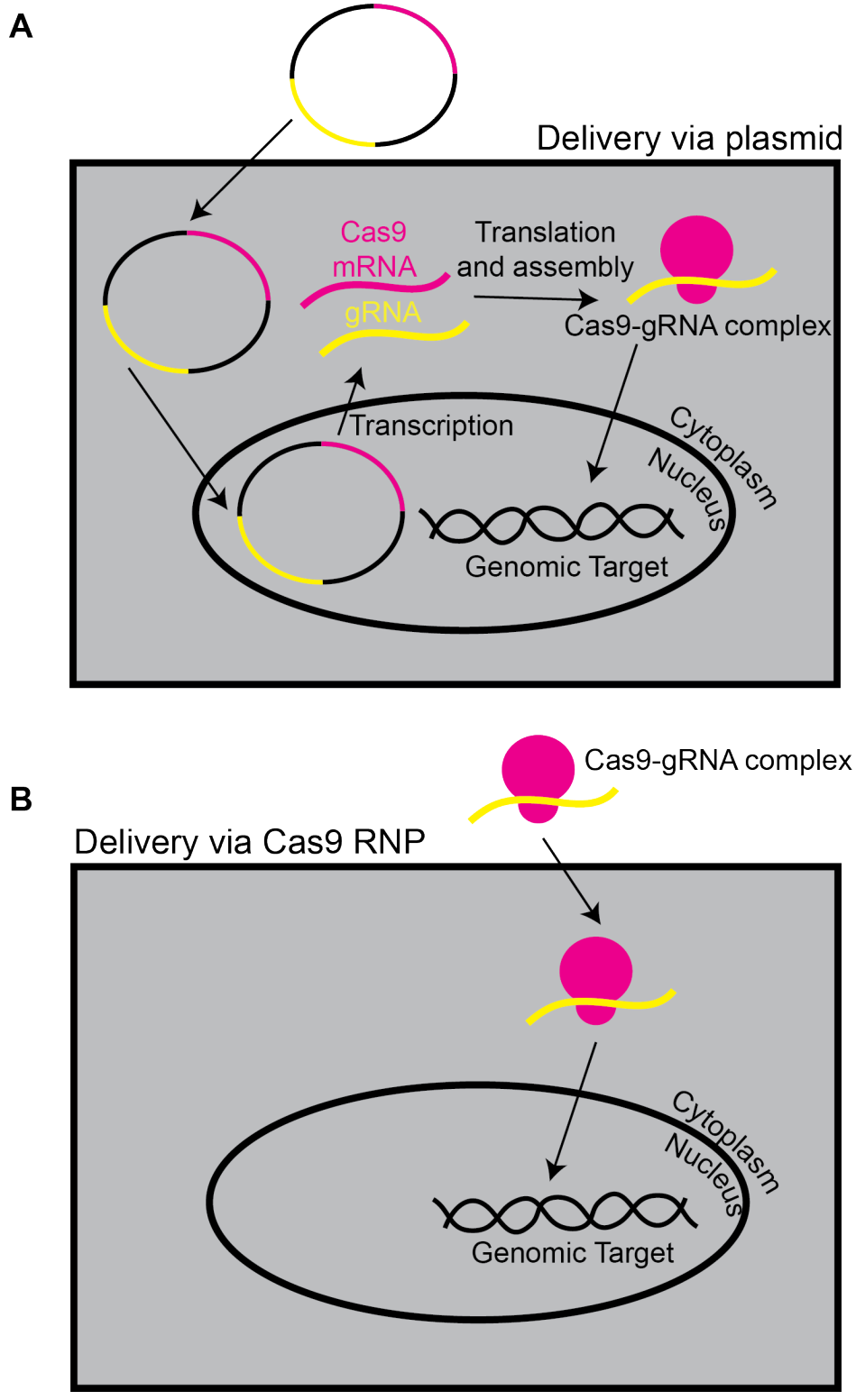


**Figure 5-2 Plasmid vs. RNP mediated Cas9/gRNA delivery.** A) Plasmid based delivery of Cas9/gRNA complexes require transcription and translation of both elements inside the target cells. B) Cas9 RNPs are delivered into cells as pre-assembled Cas9/gRNA complexes ready to interact with the target DNA. Modified from Gearing (2016).

### 5.2.3 *M. oryzae* has many genomic resources

The *M. oryzae* genome was the first fungal plant pathogen genome to be sequenced (Dean *et al.*, 2005). Since then, due to advances in whole genome and next generation sequencing (NGS) technology, over 50 *M. oryzae* whole genome assemblies have been successfully generated (Bao *et al.*, 2017; Wu *et al.*, 2015; Xue *et al.*, 2012; Zhang *et al.,* 2016; Dean *et al.*, 2005). One of the most recent genome assemblies to be added to the list is a wheat blast reference genome of the MoT strain B71 (Peng *et al.*, 2019). In addition to effector discovery, these resources have provided insight into the contribution of genomic plasticity to host adaptation, specificity, and host range (Bao *et al.*, 2017; Ebbole, 2007).

#### 5.2.3.1 Genomic resources have contributed to the identification of many avirulence genes

Map-based cloning, comparative genomics, and transcriptome studies have led to the cloning of multiple avirulence effectors (at least 12) responsible for varying virulence phenotypes between different isolates (Mosquera *et al.*, 2009; Fernandez and Orth, 2018; Wu *et al.*, 2015). One of the first avirulence effectors cloned, and perhaps one of the most well studied, is a host specificity determinant called *PWL2*. *M. oryzae* isolates harbouring this gene are no longer able to infect weeping lovegrass (Sweigard *et al.*, 1995). Although its role in infection is currently unknown, *PWL2* is expressed highly during infection and is present in many field isolates (Sweigard *et al.*, 1995; Mosquera *et al.*, 2009). Another cloned effector with implications in host specificity is *PWT3* (Ceresini *et al.*, 2018). The role of avirulence gene *PWT3* has been implicated in the emergence of wheat blast in Brazil. The authors posit wheat blast emerged from a *Lolium* infecting isolate that had undergone a host shift (Inoue *et al.*, 2017). The *Lolium* derived isolates carrying the Ao avirulence allele at the *PWT3* locus were able to infect a widely planted wheat cultivar lacking the associated *R* gene *rwt3.* Isolates emerged with mutations at the *PWT3* locus, which ultimately led to the wheat blast epidemic in South America (Inoue *et al.*, 2017; Ceresini *et al.*, 2018).

Genomic and transcriptomic resources from wheat infecting isolates have also led to the cloning of avirulence gene *AvrRmg8* which is present in strains associated with the recent outbreak in Bangladesh (Wang *et al.*, 2018; Anh *et al.*, 2018). Seedling assays have shown isolates carrying *AvrRmg8* are unable to infect wheat cultivar S-615 which harbours *Rmg8* (Wang *et al.*, 2018). These data provide encouraging results for deployment of resistant wheat varieties in Bangladesh (Islam *et al.*, 2020).

#### 5.2.3.2 Genomic plasticity

Not only have multiple effector genes been cloned, but fundamental concepts have emerged about how genomic plasticity may contribute to the evolution of these genes. Many filamentous fungi, including *M. oryzae*, have a 'two-speed genome' which contain gene sparse, repeat rich regions that evolve more rapidly than the rest of the genome (Raffaele and Kamoun, 2012). These regions enriched in effector genes are thought to serve as a 'cradle' for adaptive evolution (Dong *et al.,* 2015). A classic example of this concept is demonstrated by the multiple translocations of the avirulence gene *Avr-Pita* (Chuma *et al*., 2011). This gene was initially found in a repeat rich subtelomeric region and has been found to translocate to other retro-transposon rich regions of the genome. The authors suggest frequent loss, recovery, and translocation of *Avr-Pita* represents adaptation towards the deployment of the associated resistance gene *Pita* (Chuma *et al*., 2011).

Long read sequencing technologies such as PacBio and Nanopore provide additional resolution to whole-genome assemblies in comparison to short reads generated from NGS platforms, especially in regions enriched in effectors (Faino *et al*., 2016). New long read sequence technology can therefore allow the evaluation of repetitive elements and their involvement in the evolution of virulence. For example, Bao *et al*. (2017) constructed whole genome assemblies of *M. oryzae* field isolates using PacBio sequencing and were able to detect large-scale chromosomal rearrangements potentially induced by transposable elements. In summary, the plethora of genomic studies and resources from *M. oryzae* provide criticial information on effector biology that will no doubt be useful when harnessing this fungus for the heterologous expression of effectors from other fungi.

### 5.2.4 *M. oryzae* is a hemibiotroph that secretes effectors into the cytoplasm using signal peptides

Heterologous expression of effectors in *M. oryzae* for delivery into the wheat host will not only require knowledge about genome biology, but it will also require advances in cell biology for the proper targeting of effectors to their correct domains. The following section introduces the cell biology of *M. oryzae* infection, including effector secretion during early time points of infection in host plants.

#### 5.2.4.1 *Magnaporthe oryzae* life cycle

Most knowledge of the *M. oryzae* life cycle is provided by studies involving rice infecting pathotypes which is summarized in **Figure 5-3** (Wilson and Talbot, 2009). *M. oryzae* infection

begins when a three-celled asexual spore called a conidium lands on a rice leaf. The conidium subsequently germinates into a germ tube that eventually differentiates into the appresorium (Talbot, 2003). The appresorium is a critical structure for entry into rice cells, producing enough turgor pressure to force a penetration peg through the plant cuticle and into the epidermis (De Jong *et al*., 1997). The fungus then produces invasive hyphae (IH) that are always surrounded by invaginated rice plasma membrane (Wilson and Talbot, 2009). During this prolonged biotrophic phase, IH move cell to cell via plasmodesmata (Kankanala *et al.,* 2007). Through these hyphae, the fungus is able to secrete effectors that manipulate host biology in favour of disease progression (Valent & Khang, 2010). Simultaneously, IH are specialized feeding structures that uptake nutrients derived from living plant cells. As *M. oryzae* is a hemibiotroph, it subsequently enters a necrotrophic phase whereby nutrition is derived from dead or dying rice tissue (Wilson and Talbot, 2009). Disease lesions begin to appear 72 to 96 hours after initial infection (Wilson and Talbot, 2009) with symptoms appearing as early as 48 hours post infection (HPI) for wheat blast (Ceresini *et al*., 2018). Sporulation then occurs under conditions of high humidity. These spores are then able to spread to adjacent plants by wind or dewdrop splash, renewing the cycle (Talbot, 2003).

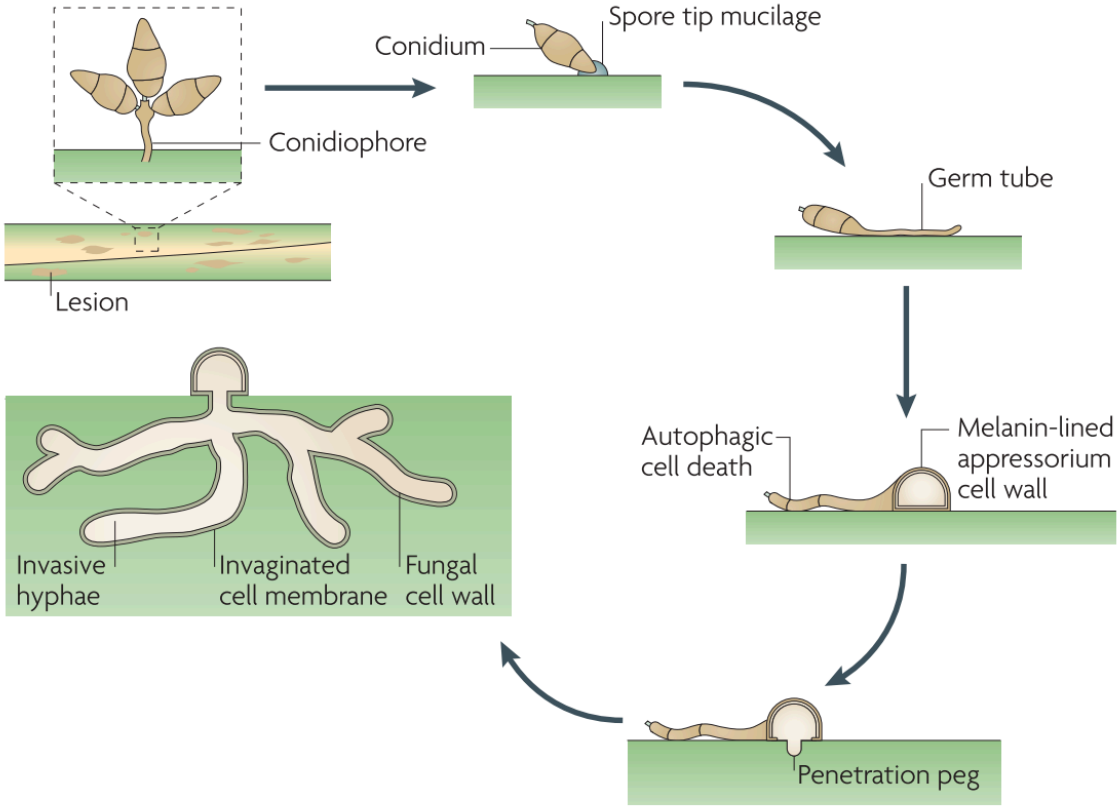


**Figure 5-3 *Magnaporthe oryzae* life cycle.** The infection cycle starts when a three celled spore called a conidium adheres to the plant cell surface through secretion of an adhesive. As the spore tip mucilage holds the conidium in place, a germ tube emerges which eventually differentiates into an appresorium. The conidium undergoes autophagic cell death, while the appresorium produces substantial turgor through melanisation. This produces a downward force in which the penetration peg enters the host cell through the epidermis. During the biotrophic phase, the plasma membrane becomes invaginated around invasive hyphae. For rice infecting strains, disease symptoms can occur 72 -96 hours after infection. Sporulation occurs under conditions of high humidity. New conidia can transfer to nearby plants through dewdrop splash. This image was first published in Wilson and Talbot (2009) and is reused with permission from copyright holders under the license number 4951350146260.

#### 5.2.4.2 Intracellular invasive growth and effector secretion of *M. oryzae*

The early stages of invasive growth of the blast fungus are summarized in **Figure 5-4**. **Figure 5-4A** shows the differentiation of the penetration peg into the primary invasive hyphae (IH). Further, this diagram illustrates the IH are surrounded by the plant derived extra invasive hyphal membrane (EIHM) during its biotrophic phase (Fernandez and Orth, 2018). **Figure 5-4B** shows a structure called the biotrophic interfacial complex (BIC) that begins to develop at the tip of primary IH (Khang *et al.*, 2010). It has been shown that cytoplasmic effector proteins preferentially accumulate at the BIC before passing through the EIHM and into the plant host cytoplasm (Khang *et al.*, 2010). It was later shown that the BIC lies outside of the fungal plasma membrane and is essentially a plant-derived interface (Giraldo *et al.*, 2013). Further, secretion of effectors via the BIC occurs through a Golgi independent, non-conventional pathway involving exocysts (Giraldo *et al.*, 2013). Apoplastic effectors, on the other hand, do not accumulate in the BIC but are secreted via the conventional endoplasmic reticulum (ER)-Golgi pathway and disperse evenly into the EIHM compartment (Giraldo *et al.*, 2013; Khang *et al.*, 2010). It is now clear that targeting proteins to these two distinct secretion systems is dependent on specific N-terminal signal peptides. Fluorescent proteins fused to a cytoplasmic effector signal peptide and promoter accumulate at the BIC and are subsequently translocated into the host cell (Khang *et al.*, 2010). Conversely, fluorescent proteins fused to an apoplastic effector promoter and signal peptide were found in the apoplastic space outlining invasive hypha (Khang *et al.*, 2010).

The discovery of N-terminal signal peptides that target proteins inside the cytoplasm is pertinent information for developing a heterologous expression system for delivering effectors inside the host cytoplasm. Hypothetically, known N-terminal signal peptides of cytoplasmic effectors could be tagged onto a protein of interest for internalisation into the host cytoplasm. Other experimentally tractable fungi have the capability of targeting proteinaceous effectors into the host cytoplasm, however, these mechanisms of internalisation are not easily transferred to any protein of interest. The effector SnToxA from the necrotrophic fungal wheat pathogen *Parastagonospora nodorum*, for example, is internalized into the host cytoplasm where it interacts with *Tsn1* resulting in cell death (Liu *et al.*, 2006). The internalisation of this effector is dependent on an RGD motif present in residues 136-143 (Manning *et al.*, 2008). Therefore, a cleavable N-terminal secretion signal would be preferable to attaching an RGD motif to a protein of interest, as such a motif may alter effector folding/function.

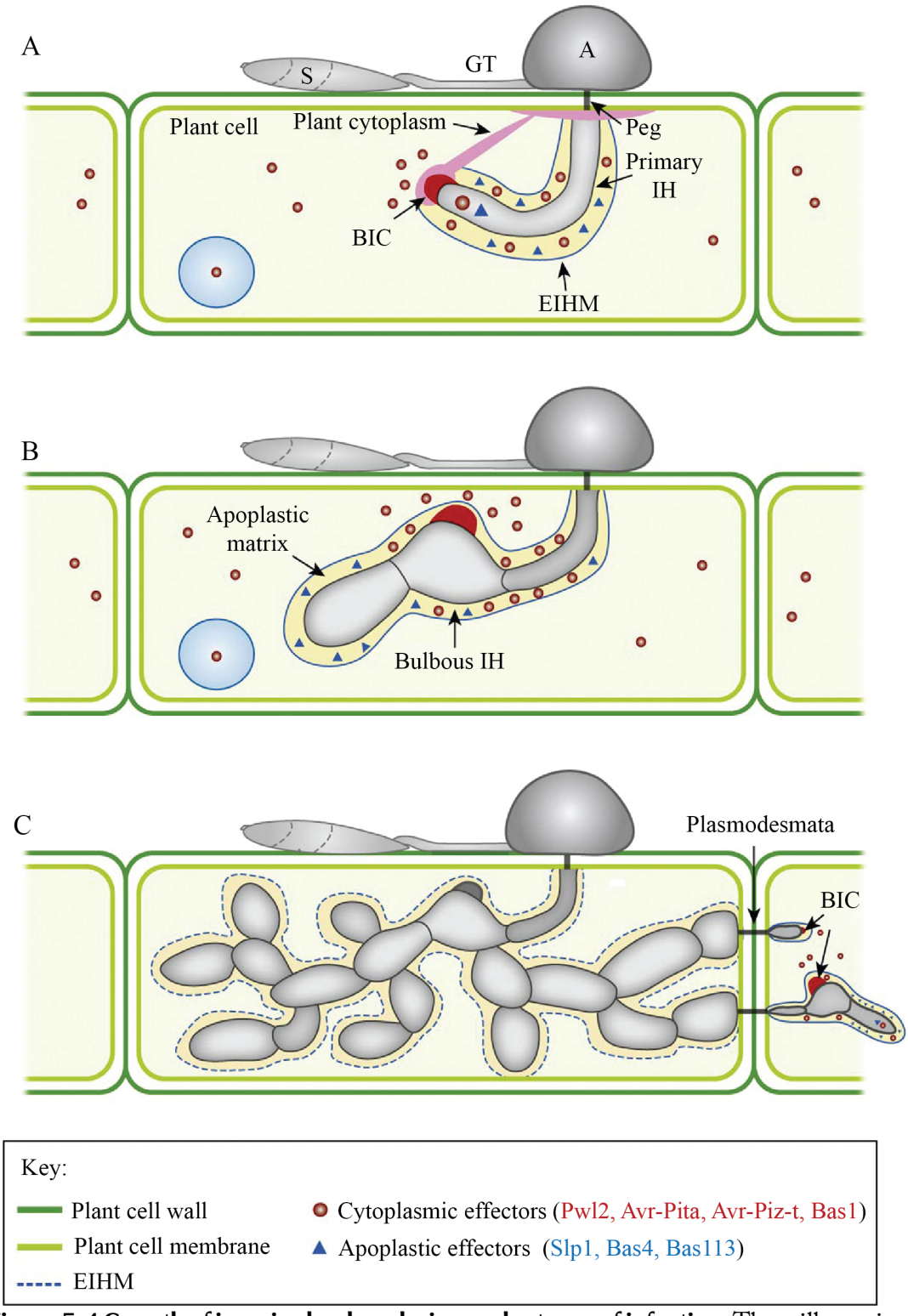


**Figure 5-4 Growth of invasive hyphae during early stages of infection.** These illustrations are based on rice infecting isolates 22-40 h post inoculation inside rice cells. A) The BIC initially develops at the tip of the first invasive hyphae. B) The BIC then localizes that the subapical region of the first bulbous IH. C) As the hyphae moves between plasmodesmata, new BICs are formed in the IH tip in adjacent cells. S, spores; GT, germ tube; A, appressorium; N, nucleus; BIC, biotrophic interfacial complex; IH, invasive hyphae; EIHM, extrainvasive hyphal membrane. This image was first published in Fernandez & Orth (2018) and is reused with permission from copyright holders under the license number 4951350438782.

### 5.2.5 Host pathogen interfaces of haustoria and non-haustoria forming fungi: commonalities and differences

Expressing rust effectors inside an *M. oryzae* surrogate will not only require knowledge of invasive hyphae, however, it will also require an understanding of the secretion systems employed by the rust species of interest. Biotrophic and hemibiotrophic pathogenic fungi utilize either invasive hyphae or haustoria as a site for effector secretion and nutrient uptake from the plant (Gan *et al.*, 2010). To compare and contrast these two different strategies, I will focus on the haustoria forming biotrophic rusts, and the invasive hyphae forming hemibiotrophic blast fungus *M. oryzae*. The first noticeable difference between these fungi is the method of growth from cell to cell once invasion inside the plant tissue occurs. *Magnaporthe* invasive hyphae are intracellular, and move from one cell to the next via plasmodesmata (Giraldo and Valent, 2013). By contrast, rust invasive hyphae are always extracellular and move within the apoplast, only entering host cells via specialized feeding structures called haustoria (Garnica *et al.*, 2014).

Despite these differences, the invasive hyphae and haustoria perform similar functions. They are both at the intimate host-pathogen interface where nutrients are taken up by the fungi and effector proteins are secreted into the plant. Both structures are always surrounded by a plant-derived structure called the extra haustorial membrane (EHM), or extra invasive hyphal membrane (EIHM) for rust fungi or *M. oryzae* respectively (**Figure 5-5**, Gan *et al.*, 2010). Both the EHM and EIHM keep the intracellular fungal structures separated from the host cytoplasm. Furthermore, in both scenarios, cytoplasmic effectors must pass through multiple membranes before reaching the host cytoplasm. In the case of haustoria, fungal effectors must pass through the haustorial membrane, the haustorial cell wall, the extrahaustorial matrix, and finally the extrahaustorial membrane (**Figure 5-5A**, Gan *et al.*, 2004). The exact mechanisms involved in this process remain poorly understood. For *M. oryzae*, cytoplasmic effectors must similarly pass through the fungal plasma membrane and cell wall of the invasive hyphae (**Figure 5-5B**, Gan *et al.*, 2010). Next, effectors pass through the EIHM and into the plant host cytoplasm. As described in the previous section, this is mediated by preferential accumulation at the biotrophic interfacial complex, and subsequent secretion through a Golgi independent exocyst pathway (Khang *et al.*, 2010; Giraldo *et al.*, 2013). Whether or not haustoria forming fungi employ a similar strategy for secretion into the host cytoplasm remains unknown.

In summary, the *M. oryzae Triticum* pathotype is a promising surrogate fungus for the secretion of heterologous rust effectors into the wheat cytoplasm. Although wheat blast and

rust fungi are phylogenetically distant (Ascomycete vs. Basidiomycete respectively), both fungi produce similar intracellular structures for the secretion of effectors into the host cytoplasm. Further, many N-terminal signal peptides of *M. oryzae* cytoplasmic effectors are known which may be used for targeting heterologous effectors to the BIC and thus the host cytoplasm. In this chapter, I utilise the many genomic and experimental resources available for *M. oryzae* to develop a heterologous expression system for delivering rust effectors in wheat.

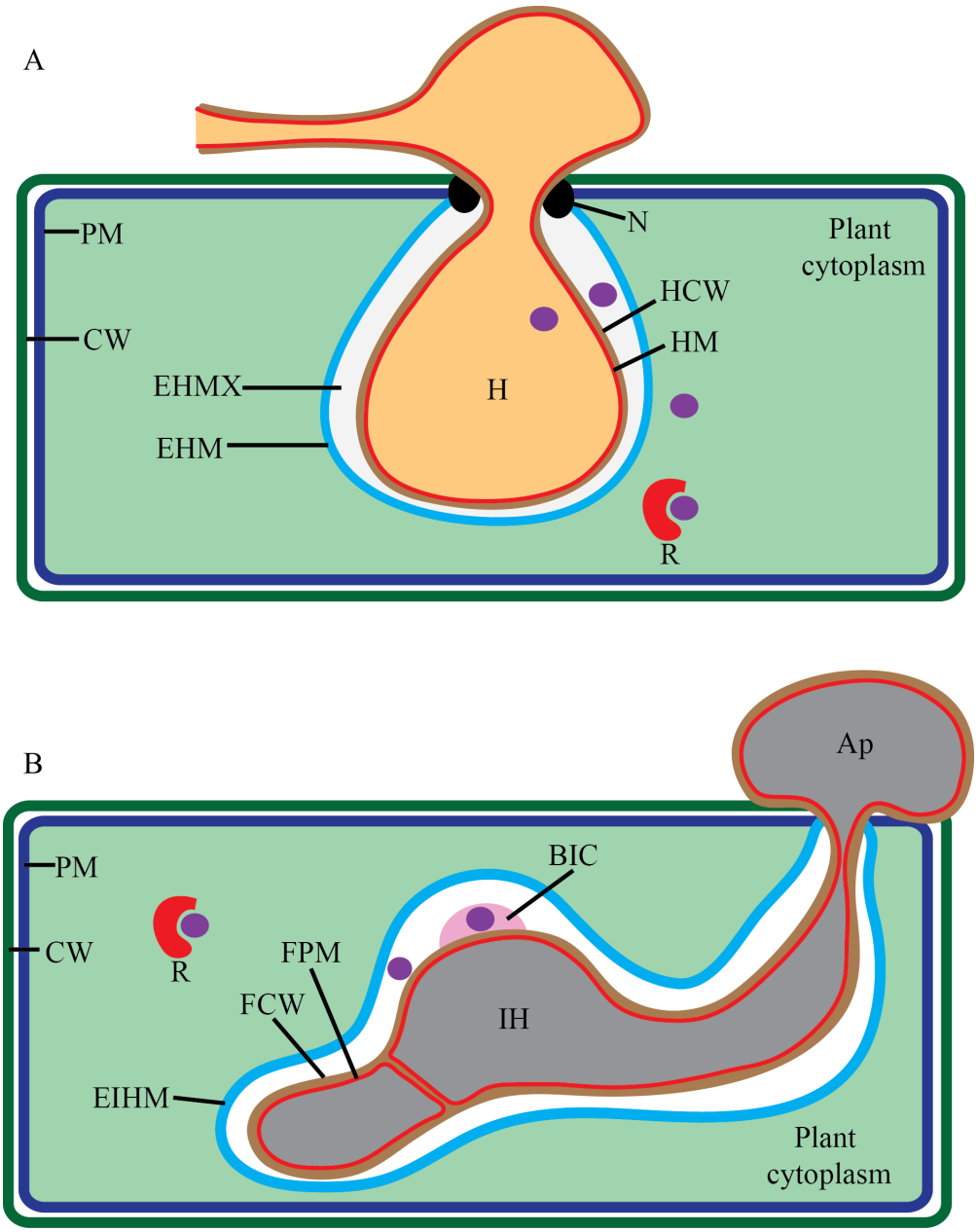


**Figure 5-5 Host pathogen interfaces of fungi producing invasive hyphae vs. haustoria** A) Haustoria forming fungi, such as the cereal rusts, secrete effectors (purple) to the extrahaustorial matrix (EHMX); a discrete compartment sealed off from the rest of the apoplast via a neckband (N). Effectors cross the extrahaustorial membrane (EHM), a membrane derived from the host plasma membrane that invaginates around the haustorium, into the host cytoplasm, where they may interact with target proteins or the cognate host R protein. B) Non haustoria forming fungi, such as *Magnaporthe oryzae*, grow within host cells via invasive hyphae (IH), which are surrounded by the host plasma membrane-derived extra-invasive hyphal membrane (EIHM). Cytoplasmic effectors are secreted into the biotrophic interfacial complex (BIC), which may mediate effector entry across the EIHM into the host cell. PM, plant plasma membrane; CW, plant cell wall; HM, haustorial membrane; HCW, haustorial cell wall; Ap, appressorium; FPM, fungal plasma membrane; FCW, fungal cell wall. Adapted from Gan *et al.* (2010).

## 5.3 Methods

### 5.3.1 *Magnaporthe* strains and wheat lines used in this study

Wheat blast isolate BTJP4-1 and wheat line S-615 were provided by Sophien Kamoun, The Sainsbury Laboratory, Norwich, UK (Islam *et al.*, 2016). Wheat blast isolate PY06047 was provided by Nicholas Talbot, The Sainsbury Laboratory, Norwich, UK. *AvrSr50* differential wheat lines (Gabo, Gabo + *Sr50*) were provided by Peter Dodds, CSIRO, Canberra, ACT, Australia (Chen *et al.*, 2017). A list of fungal strains and transformants used in this thesis is provided in **Appendix 6**.

### 5.3.2 AvrRmg8 protein alignment

Previously published *AvrRmg8* sequences from wheat blast isolates BR48, BR5, and BR116.5 were obtained from Wang *et al.* (2018). Genomic DNA was isolated from PY06047 and BTJP4-1 following the protocol described in **5.3.5**. The *AvrRmg8* sequence was PCR amplified from DNA of these isolates using primers AvrRmg8F and AvrRmg8R (**Appendix 7**) as described in **3.1.3.** The PCR product was purified and sent for Sanger sequencing as described in **3.2.3.** Amino acid alignments were performed using Geneious Prime 2020.2 (Biomatters Ltd.).

### 5.3.3 Fungal growth, maintenance and storage

*Magnaporthe* strains were grown through filter paper discs (3 mm, Whatman International) and desiccated for long term storage at -20 ˚C. For routine growth, desiccated discs were grown on complete media (CM) agar (For 1 L combine 10 g D-glucose, 2 g peptone, 1 g yeast extract, 1 g casamino acids, 6 g $NaNO_3$, 0.52 g KCl, 0.52 g $MgSO_47HOH$, 1.5 g $KH_2PO_4$, 1 mL trace elements (in 100 ml add 2.2 g $ZnS0_47HOH$, 1.1 g $H_3BO_3$, 0.5 g $MnCl_24HOH$, 0.5 g $FeSO_47HOH$, 0.17 g $CoCl_26HOH$, 0.16 mg $CuSO_45HOH$, 0.15 mg $Na_2MoO_42HOH$, 5 g $Na_4EDTA$), 1 mL vitamin solution (in 100 ml add 0.01 g biotin, 0.01 g pyridoxine, 0.01 g thiamine, 0.01 g riboflavin, 0.01 g PABA (p-aminobenzoic acid) and 0.01 nicotinic acid), adjusted to pH 6.5 with NaOH, and 15 grams of agar for solid media) at 24 ˚C in a controlled growth room set at 12 h light/ 12 h dark cycle.

### 5.3.4 Magnaporthe transformation

Wild type PY06047 or BTJP4-1 strains were transformed following the protoplast method adapted from Talbot *et al.* (1993). Wild type strains were grown on CM agar for approximately one week. Young mycelium from the edge of a colony was cut and blended in

150 mL liquid CM. Blended liquid cultures were incubated for 48 h at 25 ˚C with shaking at 125 rpm. Mycelia was then harvested by filtering through miracloth (Merck). The mycelium was then transferred into a sterile Falcon tube (Corning) with 40 mL OM buffer (1.2 M $MgSO_4 \cdot 7H_20$, 10 mM $NaPO_4$, 5 % (w/v) Glucanex (Novo Industries, Copenhagen), pH 5.4 using 1 M $Na_2HPO_4$). The Falcons were then placed in a shaking incubator for 3 hours at 75 rpm and 30 ˚C. The OM and fungal mixture were then carefully transferred to fill half a sterile Oakridge tube (Nalgene) and overlaid with equal parts cold ST buffer (0.6 M sorbitol, 0.1 M Tris HCL pH 7.0). The Oakridge tubes were centrifuged for 15 minutes at 4085 x g and 4 ˚C in a HB-6 swinging bucket rotor (Thermo Fisher Scientific). Protoplasts were recovered at the OM/ST hazy interface using a pipette and transferred to a new sterile Oakridge tube. The protoplasts were washed by filling the tubes with cold STC buffer (1.2 M sorbitol, 10 mM Tris HCL pH 7.5, 10 mM $CaCl_2$). Protoplasts were pelleted by centrifugation at 1470 x g at 4 ˚C for 10 minutes, and the supernatant discarded. The wash step was repeated twice by filling tubes with 10 mL cold STC followed by centrifugation at 1470 x g at 4 ˚C. Protoplasts were resuspended in STC buffer and aliquoted in 150 mL volumes at a concentration of $10^7$/mL and mixed with 2-6 µg of DNA. The protoplasts were incubated with DNA at room temperature for 20 minutes. After the incubation step, 1 mL of PTC buffer (60 % (w/v) PEG 4000, 10 mM Tris-HCL pH 7.5, 10 mM $CaCl_2$) was added to each 150 mL aliquot and gently mixed by pipetting up and down. The PTC mixture was incubated at room temperature for 15 minutes then added to 150 mL molten (45 ˚C) BDCM bottom agar (0.8 M sucrose, 1.7 g $L^{-1}$ yeast nitrogen base without amino acids and Ammonium sulphate, 2 g $L^{-1}$ Ammonium nitrate, 1 g $L^{-1}$ asparagine, 10 g $L^{-1}$ glucose, pH 6.0 with $Na_2HPO_4$ 1 M, 1 % agar). Bottom agar was then split between 5-6 sterile petri dishes and incubated for 16-48 h in the dark at 24 ˚C. The plates were then overlaid with BDCM top agar (1.7 g $L^{-1}$ yeast nitrogen base, 2 g $L^{-1}$ Ammonium nitrate, 1 g $L^{-1}$ asparagine, 10 g $L^{-1}$ glucose, 1% agar) with either Glufosinate ammonium (Basta) or Chlorimuron ethyl (Sulfonylurea) selection at a concentration of 600 µg/mL. Transformants were then subcultured onto new CM agar plates containing 300 µg/mL Basta or Sulfonylurea. For genotyping, fungi were grown on cellophane discs, and DNA was extracted following 5.3.5. Successful transformation was determined by PCR amplification of insert DNA as described in section 3.1.1 .

### 5.3.5 Fungal CTAB DNA extraction for genotyping and Nanopore sequencing

DNA extractions were performed with the help of Phoebe Davey, Francesca Minter, and Andrey Korolev (Saunders lab). Using a mortar and pestle, fungal cellophane discs were

ground in liquid nitrogen into a fine powder and transferred into a 1.5 mL Eppendorf tube with 500 µL CTAB buffer (2 % (w/v) Hexadecyltrimethylammonium Bromide (CTAB), 100 mM Tris base, 10 mM Ethylenediaminetraacetic acid (EDTA) and 0.7 M NaCl. Samples were incubated at 60 °C for 30 minutes with occasional shaking. An equal volume of chloroform isoamyl alcohol (24:1) was added to the tubes and shaken for 20 minutes. The tubes were then centrifuged at 13 000 rpm for 10 minutes. The top aqueous phase was transferred to a new Eppendorf with 500 uL CIA and shaken for 5 minutes. The tubes were again centrifuged at 13 000 rpm for 10 minutes. The top aqueous phase was transferred to a new Eppendorf tube with an equal volume of phenol chloroform isoamyl alcohol 125:24:1. Tubes were shaken until the solution turned cloudy and then centrifuged at 13 000 rpm for 5 minutes. The top aqueous phase was transferred to a new Eppendorf tube with 1 mL ice cold Isopropanol (Propan-2-ol), mixed, and then incubated at -20 °C for a minimum of 20 minutes. The DNA was pelleted by centrifugation at 15 000 x g for 10 minutes. The supernatant was then decanted, and the tubes were left open to dry the pellet. The pellet was resuspended in 500 uL sterile water, 0.1 volume 3 M NaOAc, and 1 mL ice cold 100 % ethanol. The tubes were then incubated at -20 °C for 10 minutes and centrifuged at 15 000 x g for 20 minutes. The supernatant was decanted, and the pellet was washed with 400 uL ice cold 70 % ethanol. This was followed by a final centrifugation step at 15 000 x g for 5 minutes. The supernatant was decanted, and the pellet dried in a speed vacuum desiccator. The DNA pellet was resuspended in 25 – 50 µL in sterile water and stored at -20 °C.

### 5.3.6 *Magnaporthe* infection assays

Conidia from 1-2-week-old cultures grown on CM agar were resuspended using a sterile glass spreader and sterile water. The conidial suspension was filtered through miracloth (Merck) and spores were counted on a haemocytometer. The conidial suspension was then diluted to a concentration to $1x10^5$ spores/mL in 0.25 % (v/v) tween gelatine. Detached leaves were placed in petri dishes containing 1 % water agar. Spot inoculation was performed by placing 5 µL droplets of conidial suspension on detached leaves and wicking away droplets after 24 h. Spray inoculation was performed using an artist's paintbrush and placing leaves in high humidity in the dark for 24 h. For both inoculation methods, leaves were placed in a growth chamber set at the same conditions for growing inoculum (section 5.3.3). Infection phenotypes were assessed at 4-5 days post inoculation (DPI). Lesion lengths were measured in Image J and statistical differences between lesions were performed using a student's T test (***: $p < 0.005$, **: $p < 0.01$, *: $p < 0.05$; 2-tailed t-test).

### 5.3.7 Cloning vectors for Magnaporthe transformations

All vectors cloned for standard *Magnaporthe* protoplast transformations (using the NHEJ pathway) are listed in (**Appendix 5**). All primers used for cloning are listed in **Appendix 7**. To clone pPWL2:AvrRmg8, the avirulent allele of *AvrRmg8* was amplified by PCR from BTJP4-1 genomic DNA using primers AvrRmg8_BamH1F and AvrRmg8_EcoRV_R as described in **3.1.1.** Both PCR product and vector backbone pCB-Ppwl2-mcherry-stop (**Figure 5-6,** Saitoh *et al.*, 2012) were digested with the restriction enzymes *Bam*HI and *Eco*RV according to the manufacturers protocol (New England Biolabs) as described in **3.3.2.** The digested backbone was treated with alkaline phosphatase (Roche) to prevent self-re-ligation. The PCR product and digested backbone were ligated to produce pPWL2:AvrRmg8 as described in **3.3.2.**

To clone pPWL2:AvrSr50, the avirulent allele of *AvrSr50* was PCR amplified as described in **3.1.1** using from a vector containing the *AvrSr50* coding sequence provided by Peter Dodds (CSIRO, Canberra, ACT, Australia). *Bam*HI and *Eco*RV sites were introduced at the 5' and 3' ends respectively of the full coding sequence via PCR amplification using primers sr50-BamHIF and Sr50-EcoRV-R. The PCR product of *AvrSr50* and vector backbone pCB-Ppwl2-mcherry-stop were digested with *Bam*HI and *Eco*RV according to the manufacturers protocol (New England Biolabs) as described in **3.3.2**. Mcherry from pCB-Ppwl2-mcherry-stop was replaced with an *AvrSr50* insert via ligation using a T4 DNA ligase (New England Biolabs) to produce Ppwl2:AvrSr50 as described in **3.3.2**.

To produce pRp27-AvrSr50, pPWT3-AvrSr50, and pTrpc-AvrSr50, promoters p*RP27* and p*PWT3* from wheat blast (*Magnaporthe oryzae*) and p*TrpC* from *Aspergillus nidulans* were PCR amplified from wheat blast genomic DNA (strain PY06047) and vector pBHt2G-RFP (Addgene) respectively as described in section **3.1.1**. *Not*I and *Xba*I restriction sites were introduced at the 5' and 3' ends of these promoters respectively using primer pairs pRP27-Not1F and pRP27-Xba1R, pPWT3-Not1F and pPWT3-Xba1R, and pTrpc-Not1F and pTrpc-Xba1. The PCR product and pCB-*Ppwl2-AvrSr50* backbone were digested, purified and ligated to produce pRp27:AvrSr50, pTrpc:AvrSr50, and pPWT3:AvrSr50 as described in section **3.3.2.**

To produce vectors pRP27:PWT3SP:AvrSr50, pPWT3:PWT3SP:AvrSr50, and pTrpc:PWT3SP:AvrSr50 the *AvrSr50* signal peptide was replaced with the wheat blast signal peptide from *PWT3* using PCR 'sowing by overlap extension' of PY06047 genomic DNA.

Primers PWT3SP-BAMHI-F and PWT3SP-OverlapAvr-R were used to amplify the *PWT3* signal peptide, with a 3' region overlapping with the *AvrSr50* coding region (not including the signal peptide). PCR cycling conditions were as described in **3.1.1** with the modification of a 1 s extension time. The *AvrSr50* coding sequence (not including the signal peptide) was amplified using primers AvrSr50-OverlapPWT3SP-F and AvrSr50-HindIII-R, introducing a 5' overlap region with the *PWT3* signal peptide. A final overlap extension PCR was performed using the above two PCR products as DNA template, with the addition of the terminal primers PWT3SP-BAMHI-F and AvrSr50-HindIII-R. This PCR product was purified and digested with *Bam*HI and *Hind*III, along with the backbone vectors pRp27:AvrSr50, pTrpC:AvrSr50, and pPWT3:AvrSr50 as described in **3.3.2** . Digested PCR products and backbone vectors were ligated using T4 DNA ligase (NEB) to produce pRP27:PWT3SP:AvrSr50, pPWT3:PWT3SP:AvrSr50, and pTrpc:PWT3SP:AvrSr50 as described in **3.3.2**.

To produce pPWL2:PWT3SP:AvrSr50 both vectors pCB-Ppwl2-mcherry-stop and pPWT3:PWT3SP:AvrSr50 were digested with the restriction enzymes *Not1*HF and *Xba*1 (New England Biolabs) as described in **3.3.2**. DNA fragments from digested vectors were size separated on a 1 % agarose gel. The PWL2 promoter band and PWT3SP *AvrSr50* backbone (without the PWT3 promoter) were excised from the gel and ligated using T4 DNA ligase (New England Biolabs) to produce pPWL:PWT3SP:AvrSr50 as described in **3.3.2**.

All subsequent cloning was performed using the Golden Gate method as described in section **3.3.3** as Golden Gate domesticated *Magnaporthe* protoplast transformation compatible vectors became available (Pennington *et al*., 2017). To produce pPWT3:PWT3SP:AvrPm3$^{a2/f2}$ new level zero components were cloned for the pPWT3 promoter, PWT3 signal peptide, and *AvrPm3*$^{a2/f2}$ coding sequence (without the native signal peptide). Primers pPWT3_GGF and pPWT3_GGR, and PWT3SP_GGR and PWT3SP_GGR were used to PCR amplify level zero inserts from vector pPWT3:PWT3SP:AvrSr50. PCR products were purified and inserted into the universal level zero vector acceptor PUAP1 (Weber *et al*. 2011) as described in section **3.3.3**. Primers AvrPm3a_GGF and AvrPm3a_GGR were used to PCR amplify the *AvrPm3*$^{a2/f2}$ coding sequence from a vector provided by Corrine Arnold (Brown lab, JIC) and the PCR product ligated into PUAP1. The transcription terminator SCD1 from pCB-Ppwl2-mcherry-stop was PCR amplified using primers 3SCD1T_GGF and 3SCD1T_GGR. The PCR product

was purified and ligated into PUAP1. Level 0 constructs were integrated into the pcb-1532B level 1 vector acceptor (Pennington *et al.*, 2017) using methods described in **3.3.3**.

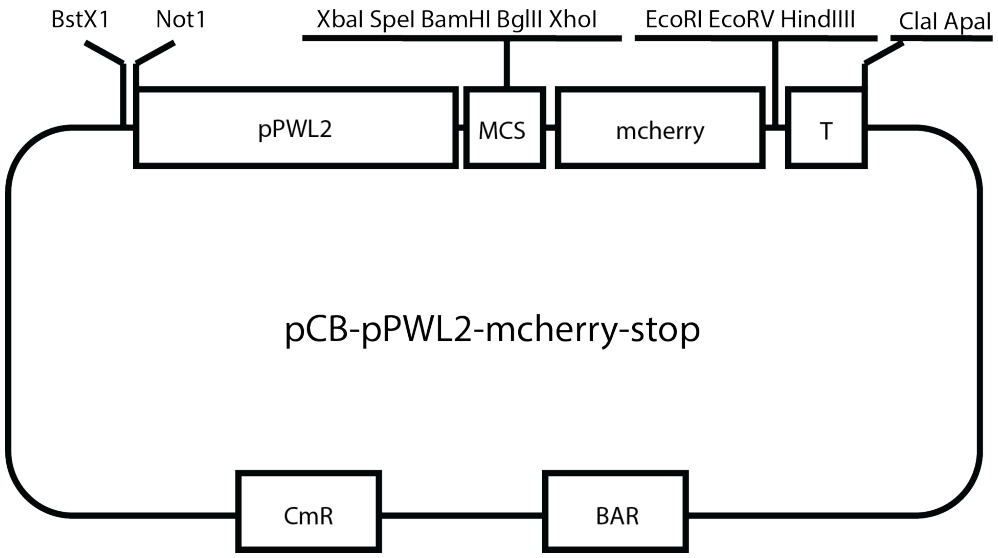


**Figure 5-6. Vector map of pCB-pPWL2-mcherry-stop.** pPWL2, the promoter from the *M. oryzae* cytoplasmic effector PWL2; MCS, multiple cloning site; T, SCD1 terminator; Cmr, chloramphenicol resistance; BAR, bialaphos resistance.

### 5.3.8 Copy number analysis

Copy number analysis of transgenes was performed by iDNA genetics (Norwich, Norfolk, UK) using a TaqMan real-time PCR assay, using a probe against the *BAR* (Bialaphos resistance) gene (the fungal selection gene contained in *Magnaporthe* expression constructs).

### 5.3.9 Relative expression using RT-PCR

Three-week-old Gabo wheat plants (*Sr50-)* were spray inoculated with $1x10^5$ conidia/mL from the WT strain (PY06047), a single copy pPWT3:PWT3SP:AvrSr50 transformant (PS-7), two double copy transformants (PS-10, PS-22), and the 40 copy transformant (PS-2). Total RNA was extracted from leaves 3 DPI using the RNeasy Plant Mini Kit (Qiagen). RNA was subsequently treated with TURBO DNase (Life technologies) to remove genomic DNA. The concentration of DNase-treated RNA was measured on the Qubit Fluorometer (Life Technologies). Using 2 µg of each sample, cDNA was synthesized using Superscript II Reverse Transcriptase (Life Technologies) with a mixture of oligo (dT) and random hexamer primers. The expression of *AvrSr50* and the *M. oryzae* actin gene (*Mo-actin*) were confirmed via PCR using primers and conditions indicated in **Appendix 8.**

### 5.3.10 RNA extraction for RNA-seq and RNA-seq analysis

RNA extracted from section **1.3.9** was sent for RNA-seq with the help of Clare Lewis (Saunders Lab). Good quality RNA (RNA Integrity Number (RIN) > 7) was sent for library preparation and sequencing to GENEWIZ (UK). Sequencing was carried out on the Illumina HiSeq 2500 platform (150 bp, paired end reads). RNA-seq paired end reads were trimmed and filtered using Trimmomatic version 0.39 (Bolger, Lohse, and Usadel, 2014). Transcript abundances (TPM values; transcript per million) were quantified from filtered paired-end reads using Kallisto v 0.46 (Bray *et al.*, 2016). The transcriptome from wheat blast reference genome (B71ref1), along with the *AvrSr50* transcript, was used for TPM calculations.

### 5.3.11 RT-qPCR

The second leaf from three-week-old Gabo plants were spray inoculated with transformants PS-7 (single copy *AvrSr50*) and PS-2 (40 copy *AvrSr50*) in a detached leaf assay as described in section **5.3.6.** Leaves were collected at 1 – 5 DPI and flash frozen in liquid nitrogen. Total RNA was extracted from leaves using the RNeasy Plant Mini Kit (Qiagen). RNA was subsequently treated with TURBO DNase (Life Technologies) to remove genomic DNA. The concentration of DNase-treated RNA was measured on the Qubit Fluorometer (Life technologies). Using 3 ug of each sample, cDNA was synthesized using Superscript II Reverse Transcriptase (Life technologies) with a mixture of oligo (dT) and random hexamer primers. Primers for RT-qPCR were designed following a set of standard criteria (Udvardi, Czechowski, and Scheible 2008): (i) Primer Tm = 60 ± 1 ˚C; (ii) Primer length: 18 to 25 bases; (iii) GC content between 40 and 60 %; (iv) Short PCR product (between 60 and 150 bp). Primers used to amplify the *M. oryzae* actin control and *AvrSr50* are listed in **Appendix 9**.

RT-qPCR was performed using LightCycler 480 SYBR Green I Master Mix (Roche) in 384-well plates with each primer at a final concentration of 0.25 μM and 0.05 μL of cDNA in a 10 μL reaction. The RT-qPCR program used consisted of a preincubation at 95 ˚C for 5 minutes; followed by 45 amplification cycles of 95 ˚C for 10 seconds, 60 ˚C for 15 seconds, and 72 ˚C for 30 seconds and a final melt-curve step cooling to 65 ˚C and then heating to 97 ˚C with five reads per 1 ˚C as the temperature increased. Melt curves were examined to contain a single PCR product. Crossing thresholds were calculated using the second derivative method provided in the LightCycler 480 SW 1.5 software (Roche).

Primer efficiencies were calculated for each primer pair using a serial dilution of cDNA (1, 1:2, 1:4, 1:8, 1:16, 1:32). The Cp (Crossing point) value for each cDNA concentration was plotted against the logarithm of the cDNA concentration to build a standard curve. The amplification factor was calculated (Schmittgen and Livak 2008) by the following equation using the slope of the standard curve. Good primer efficiency was considered when the amplification factor is ~2.

$$Amplification\ factor = 10^{-\frac{1}{slope}}$$

To measure gene expression using RT-qPCR, three technical replicates were used per reaction. The mean Cp of *AvrSr50*, or the target gene (T) in experiment (TE) and control (TC) samples was obtained. The mean Cp values were also obtained for the control housekeeping gene *M. oryzae* Actin (H) in the experiment (HE) and control samples (HC). I calculated the difference between TE and HE (TE-HE) and TC and HC (TC-HC) to obtain ΔCp values for the experiment (ΔCTE) and control (ΔCTC) conditions, respectively. ΔΔCp was calculated by finding the difference between ΔCTE and ΔCTC. Fold change was calculated as $2^{-\Delta\Delta Cp}$.

### 5.3.12 Nanopore sequencing, assembly of the PS-2 genome, and genome coverage analysis

Assistance with Nanopore library preparation was provided by Nicola Cook (Saunders Lab). DNA from PS-2 was extracted using a CTAB/phenol chloroform protocol described in section **5.3.5**. The length of DNA fragments after extraction was determined using the Femto Pulse System (Agilent). Purity of genomic DNA was determined using a Nanodrop, and concentration was determined using a Qubit Fluorometer (Invitrogen). After passing quality control, 4 µg of DNA was used for library construction following the 1D genomic DNA by ligation kit (SQK-LSK109) from Oxford Nanopore (Oxford Nanopore Technologies). The sample was sequenced on a MinION sequencer using flow cells FLO-MIN106D R9 (Oxford Nanopore Technologies) following the manufacturer's instructions. Base calling and demultiplexing was performed using Albacore v.2.3.3 (Oxford Nanopore Technologies). Reads were *de novo* assembled into contigs using Canu v1.8 (Koren *et al.* 2017). To find the insertion region, the *AvrSr50* donor vector was used as a query in a BLAST search against the contigs produced by Canu. Raw nanopore reads were first aligned to all contigs using minimap2 version 2.7 (Li, 2018). To determine contig coverage, samtools coverage (version 1.10) was used with default parameters (Li *et al.* 2009). To determine the coverage of the

tandem insertion, samtools coverage was used with the following parameters: -r tig00000018:3376081-3474584 raw_reads_aligned_sorted.sam.gz

### 5.3.13 Whole genome assembly alignments for collinearity analyses

The PS-2 contigs were aligned to wheat blast reference (B71ref1) and the rice blast reference (70-15) genome using the NUCmer utility of the MUMmer3 software (Kurtz *et al.* 2004). The coordinate output file was filtered for sequence alignments >10kb in length, with >70% similarity (delta-filter options -l 10000 -i 70). The MUMmerplot utility was used to generate a dot plot for visualization (with options -l and –color). The colour scale was adjusted to display similarity between 80 % and 100 %.

### 5.3.14 De-novo transcriptome Assembly

RNA-seq reads from transformant PS-2 generated from section **5.3.10** were *de novo* assembled using Trinity v2.11.0 (Grabherr *et al.* 2011). The *de novo* assembled transcripts were used as a database for a BLAST search using the *AvrSr50* coding sequence as a query.

### 5.3.15 Discovery of Effectors in PY06047

I obtained sequences from previously described *M. oryzae* effectors described in Yoshida *et al.* (2016). I performed a BLAST search on the PY06047 Nanopore reference to find presence/absence polymorphisms for these avirulence genes. For avirulence genes present in the genome, I obtained TPM expression values from the RNA-seq analysis from section 5.3.10.

### 5.3.16 Cloning donor DNA for CRISPR/Cas9 targeted insertion of *AvrSr50*

Donor DNA vectors for targeted insertion of *AvrSr50* are listed in **Appendix 10**. All primers described in this section are listed in
**Appendix** 7. All vectors were cloned using the Golden Gate method as described in section **3.3.3**. Donor DNAs consisted of the pPWT3:PWT3SP:AvrSr50 construct with homologous regions to the insertion site flanking the 5' and 3' ends. Homologous regions were cloned to start at either side of the predicted cut site (around 3 bp upstream of the selected PAM sequence described in section **5.3.17**) and were extended until a *Bpi*I or *Bsa*I site was detected with a limit of 800 bp. For targeted insertion to MGG_04257, two new level zero vectors corresponding to the 5' and 3' homology regions were cloned into the universal acceptor plasmid PUAP1 (Weber *et al.* 2011). Using primers 5'04257_GGF and 5'04257_GGR, and

3'04257_GGF and 3'04257_GGR, 5' and 3' homology regions were PCR amplified from PY06047 genomic DNA. Similarly, primers 5'Pib_GGF and 5'Pib_GGR, and 3'Pib_GGF and 3'Pib_GGR were used to PCR amplify 5' and 3' homologous regions from PY06047 genomic DNA. Using primers 5'Rmg8_GGF and 5'Rmg8_GGR, and 3'Rmg8_GGF and 3'Rmg8_GGR, the 5' and 3' homology regions of *AvrRmg8* were PCR amplified from BTJP4-1 genomic DNA. The same level zero construct described in **5.3.7** containing PWT3SP was used to clone all donor DNAs. Level zero constructs containing the p*PWT3* promoter and *SCD1* terminator were cloned by PCR amplifying vector pPWT3:AvrSr50 using the following primer pairs: pPWT3_TGAC_GGF and pPWT3_GGR, and SCD1T_GGF and SCD1T_TACT_GGR. The PCR products were purified and ligated into the universal Golden Gate level zero acceptor PUAP1 as described in section **3.3.3**. The *AvrSr50* coding sequence was first domesticated to remove *Bsa*I and *Bpi*I sites as described in section **3.3.3.1** using primers AvrSr50_Q5_F and AvrSr50_Q5_R. For insertion into the PUAP1 vector (Weber *et al.* 2011), *AvrSr50* was first PCR amplified using primers AvrSr50_GGF and AvrSr50_GGR. All level zero constructs were assembled together into a level 1 acceptor listed in **Appendix 10**. using the method described in section **3.3.3**.

### 5.3.17 RNP mediated CRISPR/Cas9 targeted insertion of *AvrSr50*

Targeted insertion of pPWT3:PWT3SP:AvrSr50 to *AvrPib*, MGG_04257, and *AvrRmg8* in *Magnaporthe oryzae* isolates PY06047 and BTJP4-1 was performed using repair of CRISPR/Cas9 induced DSBs by HDR as described in Foster *et al.* (2018). sgRNAs were designed using Geneious prime 20202.2 and are listed in **Appendix 11**. CRISPR sites with the highest activity score as calculated by Doench *et al.* (2014) and with the highest specificity score (no off-targets) were chosen. sgRNAs were synthesized using the EnGen sgRNA synthesis kit (NEB) using the manufacturer's instructions. Immediately after synthesis, sgRNAs were purified using a T2040 RNA clean-up kit (NEB). sgRNAs were then complexed with 6 µg purified Cas9 (NEB) at a 1:1 molar ratio for 10 minutes at room temperature. Normal protoplast transformations were performed as described in **5.3.4.** During the DNA incubation step, the appropriate donor DNA (2 µg in 6 µL) with homologous regions flanking the insert was added along with pre-complexed Cas9/sgRNA (4 µL).

### 5.3.18 Cloning and *Magnaporthe* transformations for microscopy

The BAS4:GFP (*BAR* selection) vector was provided by Vincent Were (Talbot lab, TSL). The pPWT3:PWT3SP:AvrSr50:mcherryNLS vector was constructed using four separate level zero components. The first three level zero components: p*PWT3*, *PWT3*SP, and *AvrSr50*

are described in section 5.3.16. The mcherryNLS level zero construct was cloned from the pcb-pPWL2-mcherryNLS vector (Saitoh *et al.*, 2012) using primers mcherry_GGF and NLSstop_GGR. All level zero components were assembled into the level 1 acceptor vector pcb1532-S as described in section **3.3.3**.

### 5.3.19 Leaf Sheath Inoculations for Microscopy

Leaf sheath inoculations were performed with the help of Vincent Were (Talbot lab, TSL). To observe the localisation of *AvrSr50* in invasive hyphae, leaf sheaths from Gabo wheat were inoculated with 4 mL of a suspension at 5 x $10^4$ of conidia $mL^{-1}$ in 0.2 % (w/v) gelatine using a syringe as described in (Kankanala *et al.,* Valent 2007). The inoculated leaf sheaths were incubated at 24 °C for at least 27 h before dissecting a thin layer of the inner leaf sheath using a blade and mounted on a glass slide for microscopy.

### 5.3.20 Confocal Microscopy

Confocal microscopy was performed with the help of Vincent Were (Talbot lab, TSL). Laser Confocal microscopy imaging was carried out using a Leica, TCS SP8 motorised inverted laser confocal microscope at 63x objective with oil immersion. Lasers were set as follows: for GFP and RFP tagged proteins excitation was set at 488 and 561 nm laser diodes and the emitted fluorescence detected using 495-550 and 570-620 nm, respectively.

## 5.4 Results

### 5.4.1 A wheat blast strain carrying the *AvrRmg8* allele can be used as a positive control for HR induction in infection assays

To use *M.* oryzae as a surrogate system for detecting HR induced by avirulent rust effectors, I first sought to find a positive control for cell death in leaf infection assays. To this aim, I decided to use a MoT strain carrying the avirulent allele of *AvrRmg8*, which is recognized by the *R* gene *Rmg8* present in S-615 wheat (Anh *et al.*, 2018). I selected the Brazilian isolate PY06047 for use due to its aggressive virulence and ability to conidiate well under laboratory conditions. To check if this MoT strain carries an avirulent allele of *AvrRmg8*, the gene was PCR amplified and the amino acid sequence aligned to three previously described alleles; type eI, eII, and eII', which are all avirulent on S-615 wheat (Wang *et al.*, 2018). However, the PY06047 isolate had an uncharacterised allele which I termed eII" (**Figure 5-7A**). This allele is identical to eII, except for one amino acid substitution C3R. To check if the PY06047 $AvrRmg8^{C3R}$ eII variant was avirulent on S-615 wheat, I inoculated this strain on detached leaves using spray and spot inoculation, along with a Bangladeshi strain BTJP4-1 which

carries the avirulent eI type allele (confirmed using PCR amplification and sequencing in this thesis).

Clear localized HR can be seen on S-615 plants when inoculated with BTJP4-1 using both inoculation methods (**Figure 5-7B**). This was quantified by measuring lesion lengths, which were significantly smaller on S-615 leaves than Vuka (*Rmg8-*) (**Figure 5-7**C). *Rmg8-* control plants (Vuka) are clearly susceptible to both BTJP4-1, and Brazilian isolate PY06047. S-615 plants were also susceptible to PY06047 using the spray inoculation method. However, spot inoculation experiments with PY06047 infecting S-615 resulted in slightly smaller lesions in comparison to infection on Vuka plants (**Figure 5-7C)**. This may be explained by genetic variation between Vuka and S-615 that is not associated with *Rmg8* (they are not near isogenic lines). An alternative explanation may be that the eII" allele of PY06047 is only partially virulent. Due to the visually obvious avirulence phenotype of isolate BTJP4-1 on S-615 wheat, I decided to use this strain as a positive control for the induction of HR. This positive control was used in all subsequent infection assays described in this thesis.

A

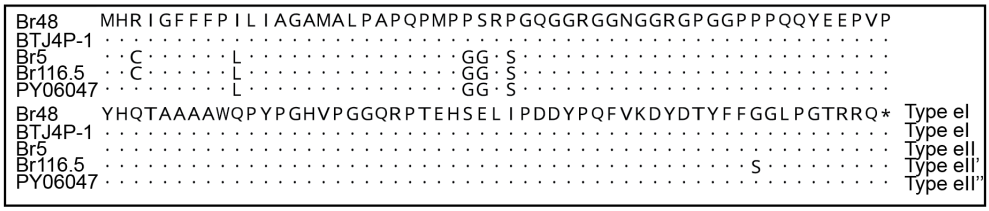


B

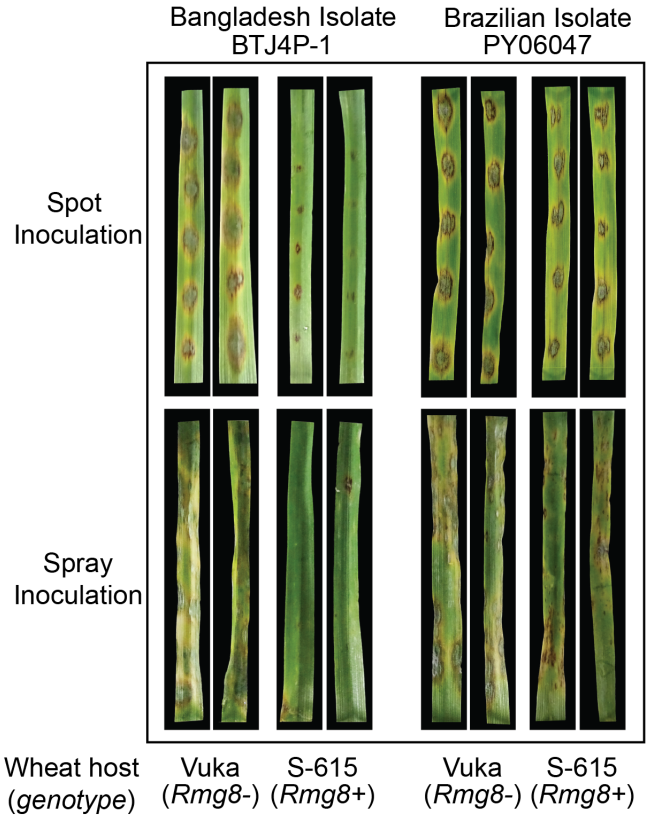


C

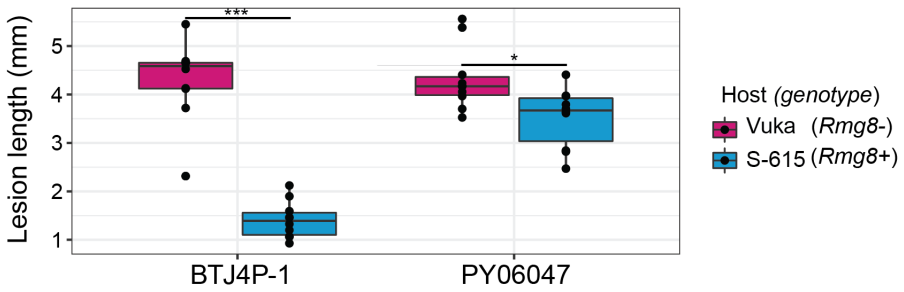


**Figure 5-7 Wheat blast isolate BTJP4-1 carrying *AvrRmg8* can be used as a positive control for HR in infection assays.** A) Amino acid alignment between known AvrRmg8 alleles and the novel allele found in isolate PY06047. B) The second leaf of 14-day old wheat seedings were inoculated with conidium using spray or spot inoculation methods. Images from representative leaves were taken 4 DPI C) Lesion lengths on 2-3 wheat leaves from each host genotype were measured at 4 DPI. Asterisks denote statistically significant differences (***: $p < 0.001$, **: $p < 0.01$, *: $p < 0.05$; 2-tailed t-test).

### 5.4.2 Transformants expressing the *AvrRmg8* control gene under the *PWL2* promoter are able to elicit R dependent HR

Previous studies have shown the *PWL2* effector is highly expressed in *M. oryzae* during infection on rice leaves and can be visualised in the BIC when fused to fluorescent markers (Mosquera *et al*. 2009; Khang *et al*. 2010; Saitoh *et al*. 2012). Therefore, I initially chose this promoter to express rust effector proteins in MoT. To this aim, I obtained vector pPWL2:mcherry (**Figure 5-6**) from Saitoh *et al*. (2012). As a positive control to see if the vector was functional in MoT, I cloned the avirulence coding sequence of *AvrRmg8* (from isolate BTJP4-1, including the native *AvrRmg8* signal peptide) into the pPWL2:mcherry backbone, and removed the fluorescent tag to produce pPWL2:AvrRmg8 (**Figure 5-8**A). This construct was then transformed into strain PY06047. Three separate transformants were obtained which were subsequently spot inoculated onto *Rmg8*+ and *Rmg8*- plants. Out of three transformants, two were able to elicit *Rmg8* dependent HR (**Figure 5-8**B). The lesion lengths from these two transformants, PWLRmg-1 and PWLRmg-5 were significantly smaller on *Rmg8*+ wheat than *Rmg8*- wheat (**Figure 5-8C)**. These data confirm the vector obtained from Saitoh *et al*. (2012) is functional and can be used in a wheat blast isolate to express avirulence genes.

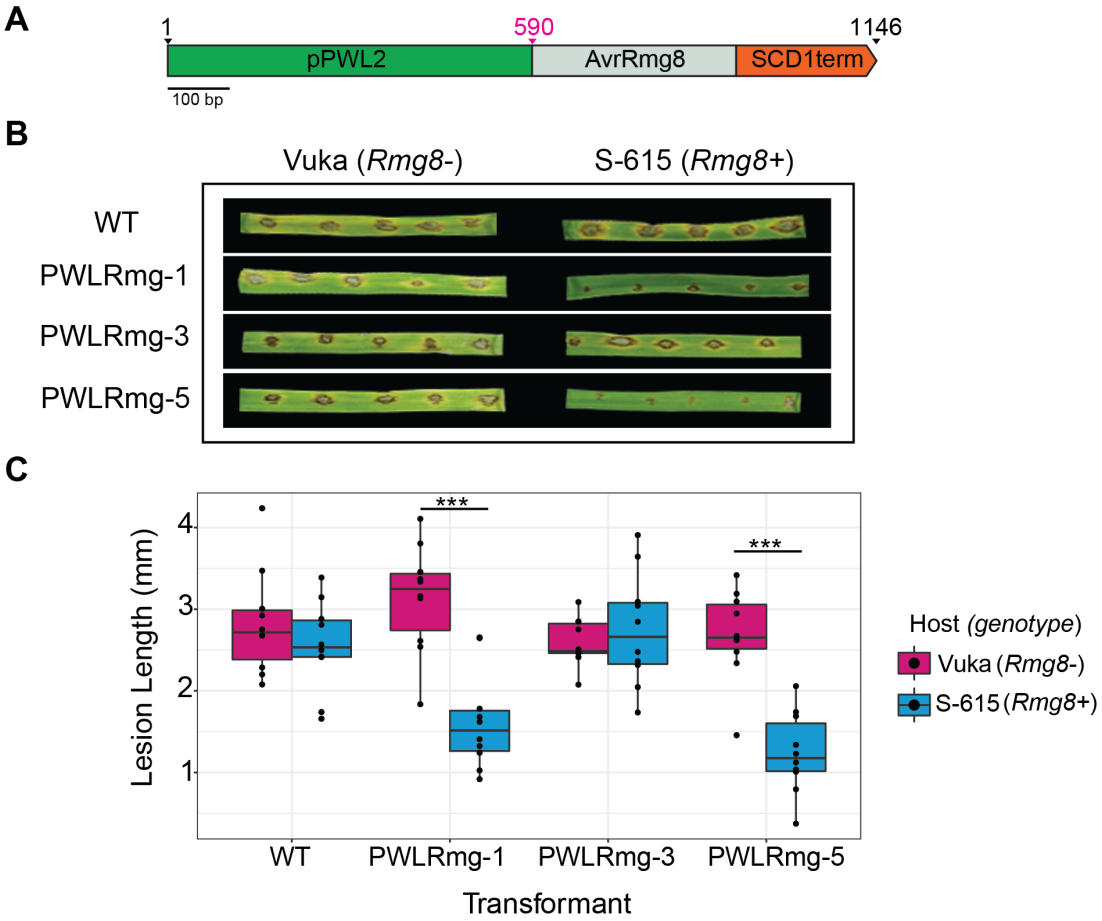


**Figure 5-8 The *PWL2* promoter can be used to express sufficient levels of *AvrRmg8* to induce *R* dependent HR.** A) Representation of the p*PWL2* donor DNA construct containing the *AvrRmg8* coding sequence. The start and end of the gene construct is denoted by black arrows. The start of the *AvrRmg8* coding sequence is denoted by the pink arrow. The scale bar shows 100 bp. B) The second leaf of 14-day old wheat seedings were inoculated with conidium from three separate transformants (PWLRmg1,3,5) using the spot inoculation method. Images from representative leaves were taken at 4 DPI C) Lesion lengths on 2-3 wheat leaves of each host genotype were measured at 4 DPI. Asterisks denote statistically significant differences (***: $p < 0.001$, **: $p < 0.01$, *: $p < 0.05$; 2-tailed t-test).

### 5.4.3 Transformants with the *PWL2* promoter driving expression of *AvrSr50* are unable to elicit *R* dependent HR

To express rust effectors in wheat blast, I decided to continue using *AvrSr50* as a rust effector positive control for detecting avirulence phenotypes (Chen, 2017). First, I cloned *AvrSr50* into the pPWL2:mcherry vector (**Figure 5-6**) removing the mCherry tag. It is currently unknown whether rust cytoplasmic effector signal peptides are functional in *M. oryzae* for targeting effectors into the host cytoplasm. Therefore, I decided to clone *AvrSr50* into the pPWL2 vector with (**Figure 5-9A**) and without (**Figure 5-9C**) the native rust effector signal peptide. Previous studies have shown *M. oryzae* cytoplasmic effector signal peptides are sufficient for targeting fluorescent proteins into the BIC and the host cytoplasm (Khang *et al.* 2010). Therefore, I chose the signal peptide from the *PWT3* effector (*PWT3*SP) that is found in wheat blast isolates (**Figure 5-9C**). Three separate transformants were obtained for each construct and were spot inoculated onto *Sr50*+ and *Sr50*- plants (**Figure 5-9A,C**). Transformants with either construct did not produce lesion lengths significantly different between *Sr50*+ or *Sr50*- leaves (**Figure 5-9B, D**). Although p*PWL2* has been previously described as a strong promoter during infection on rice plants, these data suggest a stronger, constitutive promoter may be required to drive *AvrSr50* expression to levels required for HR. Further, it is possible the MoT strains require the use of promoters more commonly found in wheat infecting isolates. To date *PWL2* has only been identified in the mini-chromosome of few wheat blast infecting isolates (Peng *et al.*, 2019). Although MoT strains are considered the same species as those strains infecting rice, they are genetically distinct and do not infect rice plants (and vice versa) (Yoshida *et al.*, 2016). In summary, the data presented in this section suggests a different promoter and/or signal peptide combination may be more suitable for expressing *AvrSr50* in wheat blast.

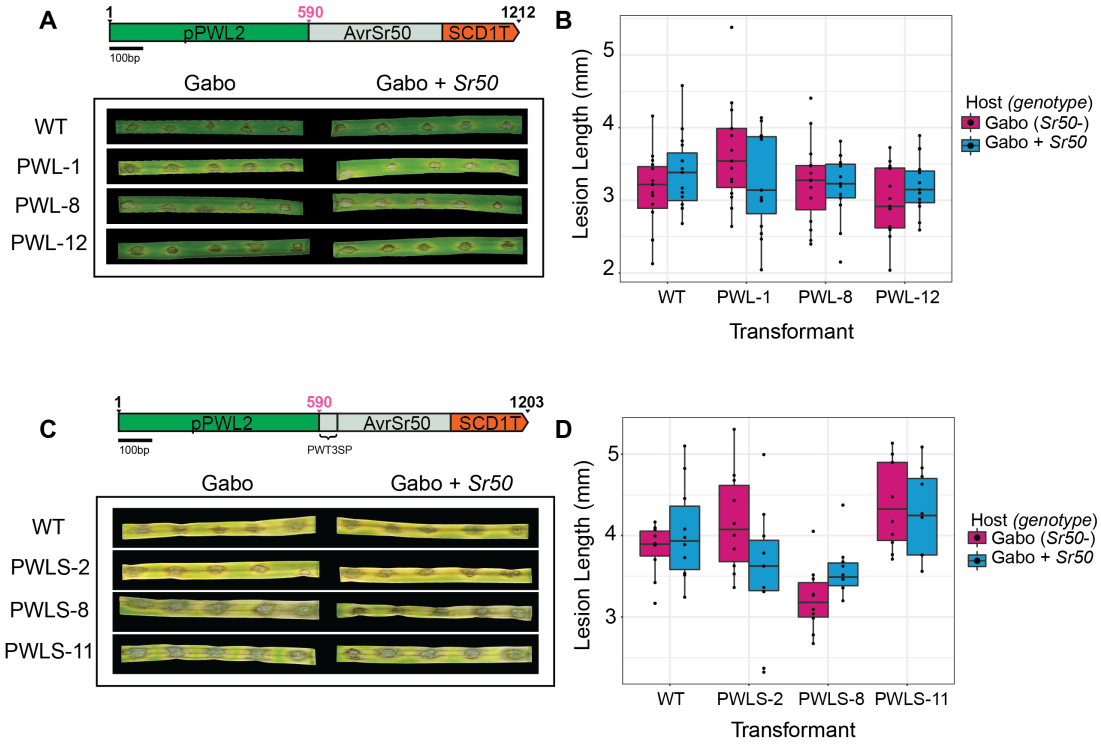


**Figure 5-9 Transformants expressing *AvrSr50* under the *PWL2* promoter are unable to elicit R dependent HR.** A,C) Conidia from transformants containing the pPWL2:AvrSr50 and pPWL2:PWT3SP:AvrSr50 construct were inoculated on the second leaf of 14-day old wheat seedings using the spot inoculation method. Images from representative leaves were taken at 4 DPI. The start and end of the transgene constructs are shown with black arrows. The start of the coding sequence is denoted by a pink arrow. The scale shows 100bp. The native signal peptide is used unless otherwise stated. B,D) Lesion lengths on 2-3 wheat leaves of each host genotype were measured at 4 DPI. Lesions were measured from each transformant shown in 'A,C' respectively.

### 5.4.4 Transformants with a wheat blast or constitutive promoter are unable to elicit R dependent HR when used in combination with the native *AvrSr50* signal peptide

To test the possibility of using a wheat blast effector promoter for expressing *AvrSr50*, I chose to use the promoter of the effector PWT3. This effector has previously been described and is found in many wheat blast isolates (Inoue *et al.* 2017). MoT isolates with the intact Ao avirulence allele cannot infect wheat with the associated *R* gene *Rwt3*. Isolates with the B type allele, or the Ao type allele with disruptions in the coding sequence are able to infect both *Rwt3*+ and *Rwt3*- plants. Due to the sequence availability of this effector, I was able to successfully clone the *PWT3* promoter from the PY06047 isolate used for transformations in this thesis. First, I replaced the p*PWL2* promoter from the pPWL2:AvrSr50 vector with the p*PWT3* sequence from PY06047 to produce pPWT3:AvrSr50 **(Figure 5-10A).** None of the individual transformants obtained with this construct showed signs of R dependent HR **(Figure 5-10A);** All lesion lengths on *Sr50*+ leaves were not significantly different than those on *Sr50*- leaves **(Figure 5-10B).**

It is possible a stronger, constitutive promoter is required for the expression of *AvrSr50*, or the native *AvrSr50* signal peptide is not functional in *M. oryzae.* To address the first possibility, I chose two constitutive fungal promoters known to be functional in filamentous fungi. The first promoter, the *M.* oryzae ribosomal protein 27 (*RP27*), is a common promoter used for the constitutive expression of proteins including effectors (Jones *et al.*, 2017; Khang *et al.*, 2010; Shipman *et al.*, 2017). An *M. oryzae* transformant with the *P27* promoter and *Avr-Pita1* signal peptide driving EGFP expression presented BIC fluorescence at 27 HPI (Khang *et al.* 2010). These previous studies suggest the P27 promoter may be a suitable constitutive promoter for expressing *AvrSr50* in MoT. The second promoter chosen was the *TrpC* constitutive promoter from *Aspergillus nidulans*. This promoter is widely used to express selection genes in multiple fungal species, including *M. oryzae* (Carroll, Sweigard, and Valent 1994). First, I PCR amplified the *RP27* promoter from PY04027 genomic DNA and the TrpC promoter from the pBHt2G-RFP (Addgene) vector. Next, I replaced the p*PWL2* promoter from pPWL2:AvrSr50 with either constitutive promoter to produce pRP27:AvrSr50 **(Figure 5-10C)** and pTrpc:AvrSr50 **(Figure 5-10E).** Two separate transformants containing either construct were obtained and spot inoculated onto *Sr50*+ and *Sr50*- leaves (**Figure 5-10C, Figure 5-*10*E)**. Disease lesions from transformants with either constitutive promoter were not significantly different on leaves with the corresponding *R* gene (**Figure 5-10D, Figure 5-*10*F)**. In summary, neither a wheat blast effector promoter nor a constitutive fungal promoter is effective for expressing *AvrSr50* when the native rust signal peptide is used.

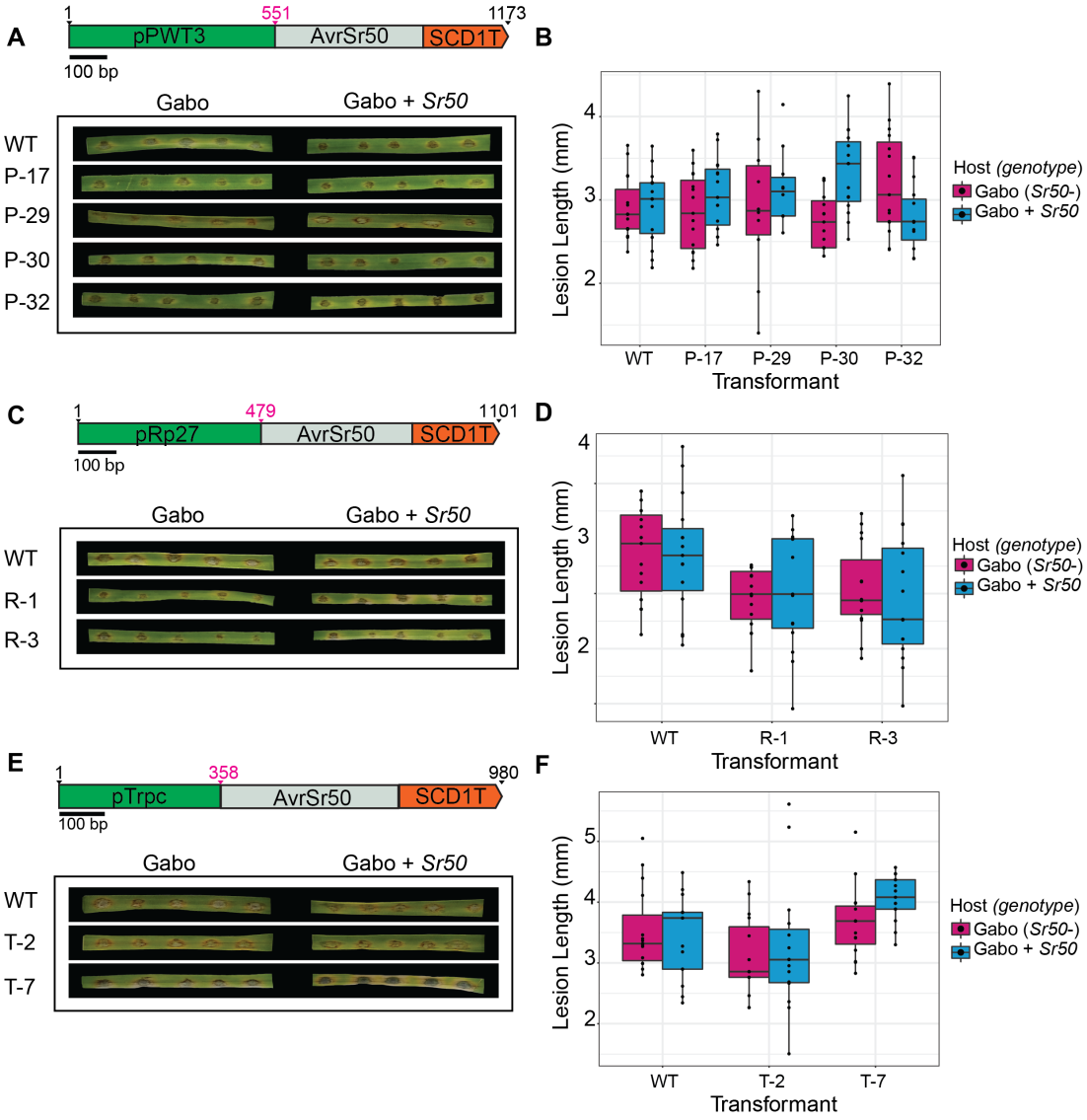


**Figure 5-10 Transformants containing a constitutive fungal promoter or a wheat blast cytoplasmic effector promoter in combination with the *AvrSr50* native signal peptide are unable to elicit *R* dependent HR.** Conidia from transformants containing the A) pPWT3:AvrSr50 C) pRP27:AvrSr50, and E) pTrpc:AvrSr50 constructs were inoculated on the second leaf of 14-day old wheat seedings using the spot inoculation method. Black arrows above transgene models indicate the start and end of the construct. The start of the coding sequence is denoted by a pink arrow. The scale shows 100 bp. The native *AvrSr50* signal peptide is used in all constructs. Images from representative leaves were taken at 4 DPI. B,D,F) Lesion lengths on 2-3 wheat leaves of each host genotype were measured at 4 DPI. Lesions were measured from each transformant shown in 'A,C,E' respectively.

### 5.4.5 A single transformant expressing *AvrSr50* with a wheat blast signal peptide is able to elicit *R* dependent HR

Due to the possibility that *M. oryzae* could require a species-specific signal peptide for targeting effectors to the BIC and thus the host cytoplasm, I decided to replace the native *AvrSr50* signal peptide with a wheat blast cytoplasmic effector signal peptide (*PWT3*SP). The PWT3SP:AvrSr50 construct was then cloned into a vector with the promoters from the previous section (p*PWT3*, p*RP27*, and p*Trpc*). Transformants with constitutive promoters (**Figure 5-11C, E**) were unable to produce disease lesions significantly different on *Sr50*+ leaves in comparison to *Sr50*- leaves (**Figure 5-11D, F).** A single transformant with the PWT3:PWT3SP combination (PS-2) displayed signs of HR on *Sr50*+ leaves (**Figure 5-11A**). Disease lesions from this transformant were significantly smaller on *Sr50*+ leaves in comparison to *Sr50*- leaves (**Figure 5-11A).** All other transformants with this same expression construct did not display *R* dependent HR (**Figure 5-11A,B).** To confirm the PS-2 HR phenotype, I repeated infection assays three times using both spot and spray inoculations. A representative of these infection assays are shown in **Figure 5-12A**. Transformant PS-2 consistently showed a cell death phenotype in an *Sr50* dependent manner, with disease lesions significantly smaller on *Sr50*+ leaves (**Figure 5-12B)**. These assays confirm the PS-2 transformant, which has a wheat blast cytoplasmic effector promoter and signal peptide, is able to elicit *R* dependant HR when expressing *AvrSr50*.

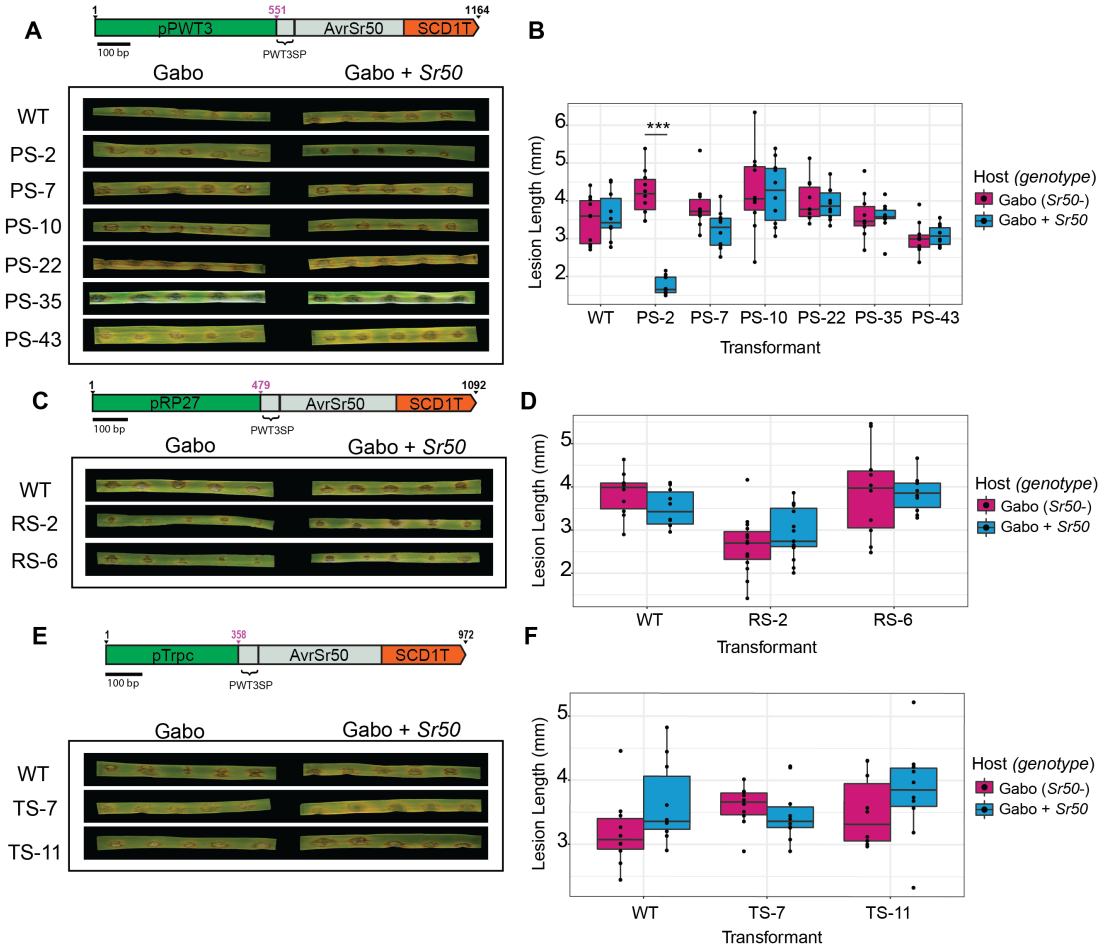


**Figure 5-11 A single transformant with the *PWT3* promoter and signal peptide is able to elicit *R* dependent HR. All other transformants containing the *PWT3*SP did not show this phenotype.** Conidia from transformants containing the A) pPWT3:AvrSr50 C) pRP27:AvrSr50, and E) pTrpc:AvrSr50 constructs were inoculated on the second leaf of 14-day old wheat seedings using the spot inoculation method. Images from representative leaves were taken at 4 DPI. B,D,F) Lesion lengths on 2-3 wheat leaves of each host genotype were measured at 4 DPI. Black arrows above transgene models indicate the start and end of the construct. The start of the coding sequence is denoted by a pink arrow. The scale shows 100 bp. The *PWT3* signal peptide is used in all constructs. Lesions were measured from each transformant shown in 'A,C,E' respectively. Asterisks denote statistically significant differences (***: $p < 0.001$, **: $p < 0.01$, *: $p < 0.05$; 2-tailed t-test).

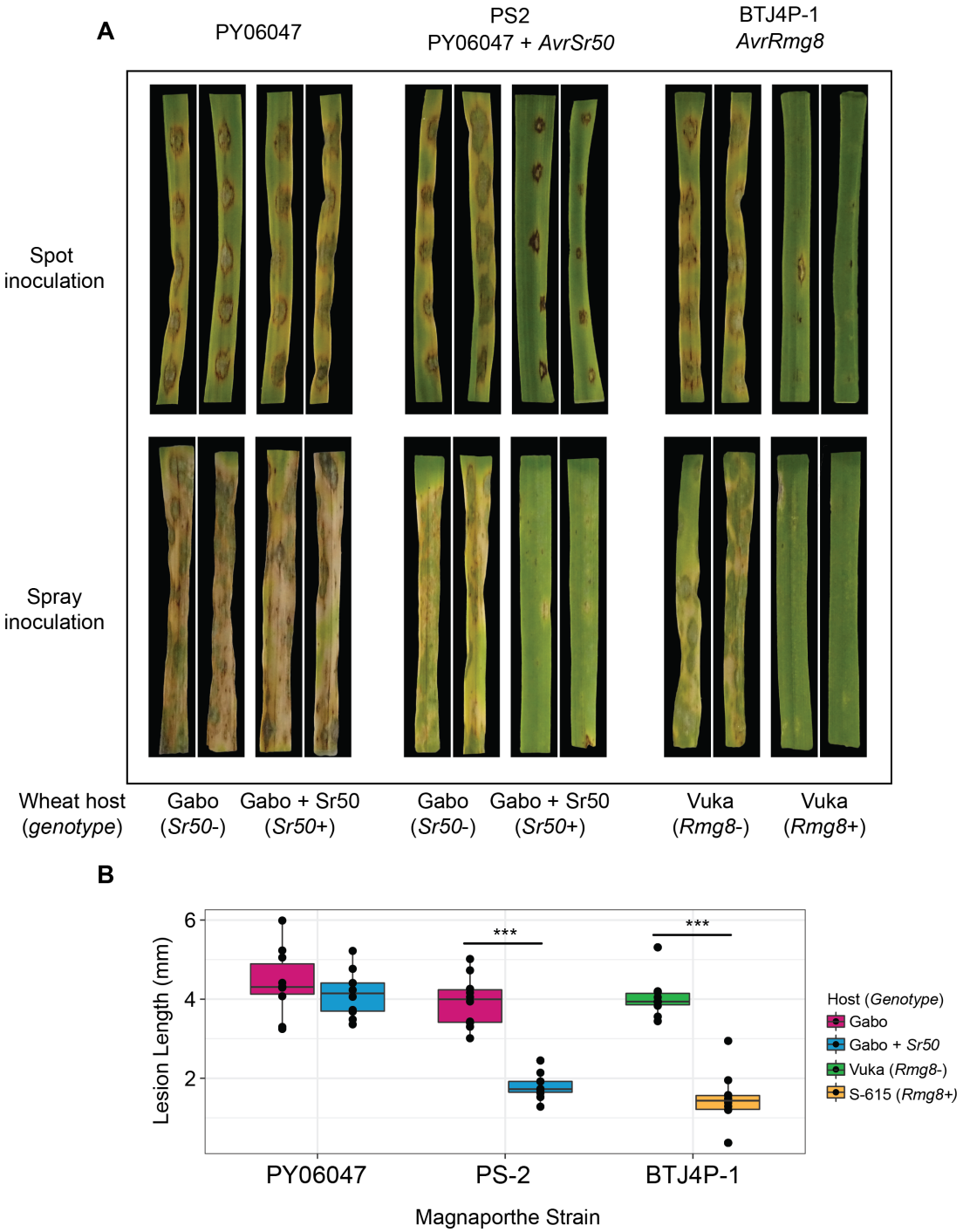


**Figure 5-12 Transformant PS-2 elicits *Sr50* dependent HR.** A) Transformant PS-2 was inoculated on the second leaf of 14-day old wheat seedings using the spray and spot inoculation methods. Untransformed PY06047 was used as a negative control, and BTJP4-1 was used as a positive control for an HR phenotype on wheat. Images from representative leaves were taken at 4 DPI. B) Lesion lengths on 2-3 wheat leaves of each host genotype were measured at 4 DPI. Lesions were measured from each *M. oryzae* isolate indicated. Asterisks denote statistically significant differences (***: $p < 0.001$, **: $p < 0.01$, *: $p < 0.05$; 2-tailed t-test).

### 5.4.6 Transformant PS-2 has more copies of *AvrSr50* than all other transformants

The other eight transformants with the same construct as PS-2 did not display *Sr50* dependent HR (**Figure 5-11**A). During protoplast transformation, it is common to obtain copy number variants (Jeenes *et al.*, 1991). Multiple transgene copies can sometimes induce silencing leading to lower levels of mRNA (Su *et al.*, 2012). On the other hand, if the multiple copies are not silenced, additive effects of each gene can increase overall levels of mRNA. To determine if copy number variation is contributing to the PS-2 HR phenotype, I analysed all confirmed transformants for copy number variation. Genomic DNA was sent to IDNA genetics (Norwich, UK), and copy number was determined using a TaqMan real-time PCR assay using a probe against the resistance gene in the donor vector (BAR). Using this analysis, it was determined transformant PS-2 had 40 copies of *AvrSr50*, while all other transformants with the same expression construct had 1-3 copies (**Table 5-1**).

### 5.4.7 Expression data suggests *AvrSr50* expression is increased in PS-2 in comparison to other transformants

Multiple copies of the pPWT3:PWT3SP:AvrSr50 transgene may lead to increased *AvrSr50* mRNA levels. To determine if the PS-2 transformant was expressing *AvrSr50* to higher levels than other transformants, I conducted semi-quantitative RT-PCR experiments followed by RNA-seq. First, I extracted RNA from tissue infected with transformants PS-7 (1 copy), PS-10 (2 copies), PS-22 (2 copies), PS-2 (40 copies), and the WT strain. Tissue was collected from 1-3 DPI. I was only able to obtain visible bands for *AvrSr50* from tissue collected at 3 DPI (**Figure 5-13**). RT-PCR data from PS-2 infected leaves of replicates one and two showed a brighter band than other transformants with 1-2 copies of the same construct (**Figure 5-13**). This suggests PS-2 could have higher *AvrSr50* expression levels than other transformants. However, in replicate 3, the *AvrSr50* expression band was not brighter than the one shown for PS-22 (which has two copies of the same construct). Differing levels of overall infection on the leaves collected at this time point (3 DPI) could explain this. Further, each biological replicate was performed on separate days with separate inoculum. Different infections may progress differently if not performed with the exact same conditions. Therefore, the variation in strength of the PS-2 band may be explained by variation in infection progression.

RNA from the RT-PCR experiment was subsequently sent for RNA-seq. Transcripts per million (TPM) values of *AvrSr50* were calculated for transformants PS-7, PS-22, and PS-2 (**Figure 5-14A).** Transformant PS-2 showed increased expression in comparison to transformants with less copies, however, the increase was not significant. This may be explained by the variation between biological replicates also seen with the RT-PCR data.

Nonetheless, the increased expression of the PS-2 transformant suggests increased copies of *AvrSr50* is associated with increased levels of mRNA. Figure 5-14B shows TPM values for a control gene (subunit of the exocyst complex - MGG_01760) which does not significantly vary between transformants.

**Table 5-1** Transgene copy number of MoT transformants.

| Construct Name | Transformant Name | *R* gene dependent HR | Copy Number[1] |
|---|---|---|---|
| pPWL2:AvrRmg8 | PWLRmg-1 | Y | 1 |
| | PWLRmg-3 | N | 1 |
| | PWLRmg-5 | Y | 1 |
| pPWL2:AvrSr50 | PWL-1 | N | 2 |
| | PWL-2 | N | 3 |
| | PWL-5 | N | 2 |
| | PWL-8 | N | 1 |
| | PWL-12 | N | 1 |
| pPWT3:AvrSr50 | P-17 | N | 1 |
| | P-29 | N | 1 |
| | P-30 | N | 1 |
| | P-32 | N | 1 |
| pRP27:AvrSr50 | R-1 | N | 3 |
| | R-3 | N | 2 |
| pTrpc:AvrSr50 | T-2 | N | 3 |
| | T-7 | N | 1 |
| pPWL2:PWT3SP:AvrSR50 | PWLS-2 | N | 1 |
| | PWLS-8 | N | 21 |
| | PWLS-11 | N | 1 |
| pPWT3:PWT3SP:AvrSr50 | PS-2 | Y | 40 |
| | PS-7 | N | 1 |
| | PS-10 | N | 2 |
| | PS-22 | N | 2 |
| | PS-35 | N | 3 |
| | PS-41 | N | 1 |
| | PS-42 | N | 1 |
| | PS-43 | N | 1 |
| | PS-44 | N | 1 |
| pRP27:PWT3SP:AvrSr50 | RS-2 | N | 1 |
| | RS-6 | N | 4 |
| pTrpc:PWT3SP:AvrSr50 | TS-7 | N | 2 |
| | TS-11 | N | 1 |

[1]Copy number analysis was performed by IDNA genetics (Norwich, UK).

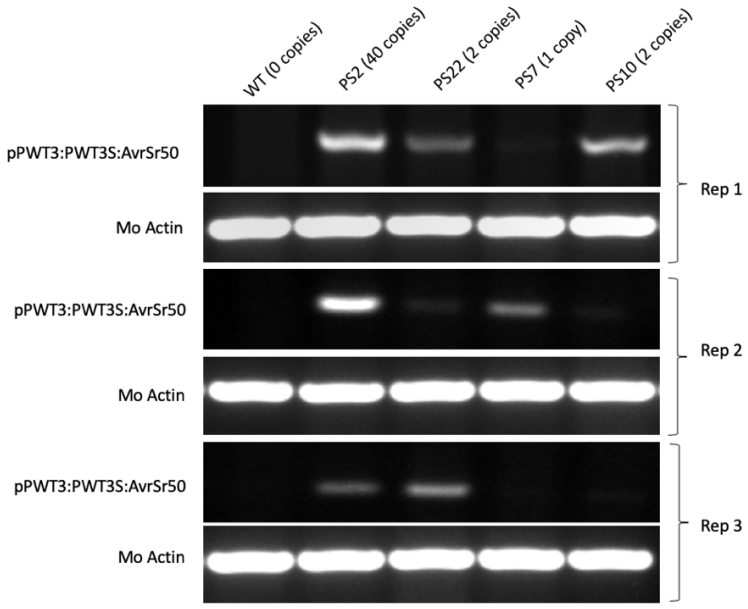


**Figure 5-13 Semi-quantitative RT-PCR shows transformant PS-2 is expressing AvrSr50 at 3DPI.** M. oryzae actin is used as a positive control. Transformants PS-2, PS-22, PS-7, PS-10, and the WT strain were infected on whole Gabo (*Sr50-*) plants and leaves were collected 3 DPI. Three biological replicates were sampled. Each biological replicate was taken from infections set up on different days with inoculum set up from different plates.

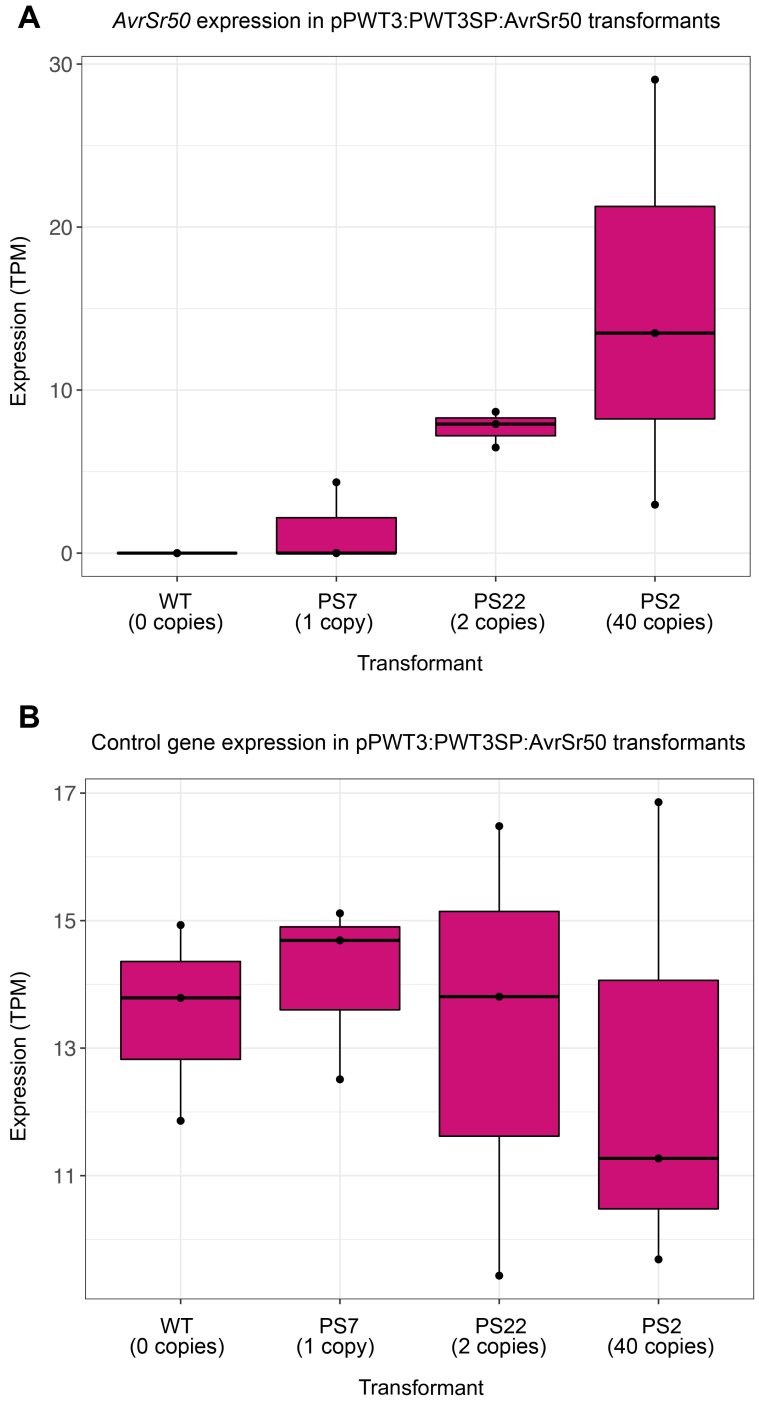


**Figure 5-14 RNA-seq data from tissue collected 3DPI suggest PS2 expresses more *AvrSr50* than other transformants with the same expression construct.** A) *AvrSr50* expression of transformants PS-7, PS-22, PS-2, and the untransformed WT strain. B) Control gene (subunit of the exocyst complex, MGG_01760) expression of *Magnaporthe* transformants. Isolates were infected on whole Gabo (*Sr50-*) plants and the second leaf was collected 3 DPI. Each data point represents a single biological replicate. Each biological replicate was taken from infections set up on different days with inoculum set up from different plates. Expression data is expressed as TPM (transcripts per million), calculated using Kallisto, version 0.46.0.

### 5.4.8 An RT-qPCR time course confirms *AvrSr50* expression is significantly increased in PS-2 in comparison to other transformants at 2DPI

To validate the RNA-seq data and to determine the expression profile of the PS-2 transformant over time I performed RT-qPCR with infected tissue collected from 1-5 DPI (**Figure 5-15**). Expression was calculated relative to *AvrSr50* expression of the single copy transformant (PS-7) at 1 DPI. The PS-2 transformant showed higher relative expression of *AvrSr50* than PS-7 at each day post infection. At 2 DPI, PS-2 expression of *AvrSr50* reached its peak at 10-15 x significantly higher expression than PS-7. Together the expression analysis illustrated that PS-2 expressed more *AvrSr50* transcript than other transformants carrying the same construct with a lower copy number.

### *5.4.9* Whole genome sequencing and de novo assembly of PS-2 shows a large tandem insertion of *AvrSr50*

#### 5.4.9.1 Nanopore sequencing and assembly

It is also unknown if the 40 copies of *AvrSr50* in PS-2 have inserted into multiple independent places within the genome or as a tandem insertion. Another possibility is that one of these 40 copies has inserted near a particularly strong promoter and is the main driving force of *AvrSr50* expression in comparison to the other copies. Knowing the position of the *AvrSr50* copies within the PS-2 genome is therefore pertinent for developing an informed strategy in replicating the phenotype of this transformant. To determine the location of the 40 *AvrSr50* copies, I sequenced the whole genome of PS-2 using Nanopore technology due to the possibility of a tandem insertion that could be resolved by Nanopore sequencing. The PS-2 sequencing run produced N50 read lengths and total base counts comparable to those of wheat blast isolates sequenced by Win *et al.* (2019) using similar methods (**Table 5-2**). For the PS-2 sequencing run, I obtained 6.3 Gbp total base counts, which translates to approximately 153 x coverage for a 41 Mb genome. The PS-2 sequenced reads were assembled into 21 contigs using the Canu (v1.7) software (Koren *et al.*, 2017). The genome assembly statistics for PS-2 are comparable to the best assemblies generated from Win *et al.* (2019) (**Table 5-3**). Taken together, these data suggest enough reads have been generated during the sequencing run to generate an assembly with good coverage.

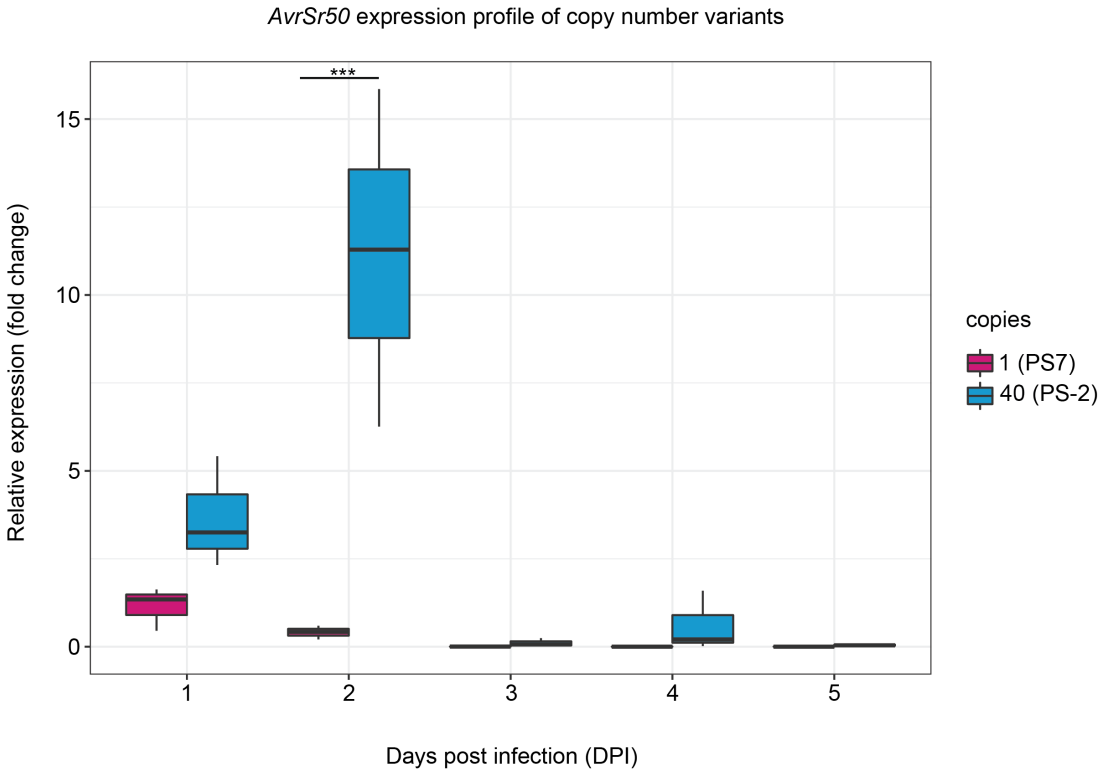


**Figure 5-15 PS-2 *AvrSr50* relative expression peaks at 2DPI.** *AvrSr50* relative expression measured using RT-qPCR from wheat infected with PS-7 (single copy) and PS-2 (40 copies) transformants. The second leaf from 14-day old Gabo (Sr50-) wheat seedlings were infected with inoculum from each transformant. Three separate leaves were sampled from days 1-5 post infection. Expression is shown as the fold change relative to the average of PS7 infected leaves at 1 DPI. Asterisks denote statistically significant differences (***: $p < 0.001$, **: $p < 0.01$, *: $p < 0.05$; 2-tailed t-test).

**Table 5-2** Summary statistics of Nanopore sequencing runs

| Wheat blast isolate | Number of Reads | Base Count (Gbp) | Read N50 (bp) | Reference |
|---|---|---|---|---|
| PS-2 | 577, 392 | 6.3 | 24,624 | This study |
| BTJP4-1 | 464,107 | 3.1 | 9,437 | Win *et al.* (2019) |
| BTMP13-1 | 181,812 | 1.4 | 25,365 | Win *et al.* (2019) |
| BTGP1-b | 158,055 | 1.3 | 11,213 | Win *et al.* (2019) |
| BTGP6-f | 284,212 | 1.9 | 9,448 | Win *et al.* (2019) |
| BR32 | 655,377 | 5.5 | 11,021 | Win *et al.* (2019) |

**Table 5-3** Summary statistics of genome assemblies from Nanopore sequencing reads

| Wheat blast isolate | Number of Contigs | Assembly Length (bp) | NG50 (bp) | Max length (bp) | Mean Length (bp) | Min length (bp) |
|---|---|---|---|---|---|---|
| PS-2 | 21 | 42,866,477 | 6,394,504 | 7,937,122 | 2,041,260 | 44,244 |
| BTJP4-1 | 59 | 44,506,712 | 4,344,896 | 7,174,201 | 754,351 | 13,054 |
| BTMP13-1 | 16 | 43,978,087 | 6,037,509 | 10,783,101 | 2,748,630 | 7,390 |
| BTGP1-b | 74 | 44,406,102 | 2,814,025 | 6,505,875 | 600,082 | 5,533 |
| BTGP6-f | 57 | 44,234,333 | 3,705,381 | 6,048,575 | 776,041 | 8,312 |
| BR32 | 21 | 41,471,325 | 5,047,693 | 11,366,628 | 1,974,825 | 18,099 |

#### 5.4.9.2 High levels of co-linearity between the contigs of PS-2 and the wheat blast reference chromosomes (B71)

Quality assessment of the PS-2 assembly was determined by aligning the PS-2 contigs with the wheat blast reference genome B71ref1 (Peng *et al.*, 2019), and the rice blast reference genome 70-15 (Dean *et al.*, 2005). These alignments suggested significant co-linearity between PS-2 and B7ref1 chromosomes (**Figure 5-16**). Additionally, the overall sequence identity between the two isolates was near 98 %, as indicated by the orange coloured line of the dot plot (**Figure 5-16**). Overall co-linearity was also observed when PS-2 contigs were aligned with the chromosome quality reference genome of rice blast isolate 70-15 (MG8) (**Figure 5-17**). Further, the seven largest PS-2 contigs align very closely with the seven chromosomes of both the rice blast and wheat blast reference genomes, suggesting a near chromosome level PS-2 assembly. These results suggest acceptable quality of the PS-2 assembly generated in this chapter.

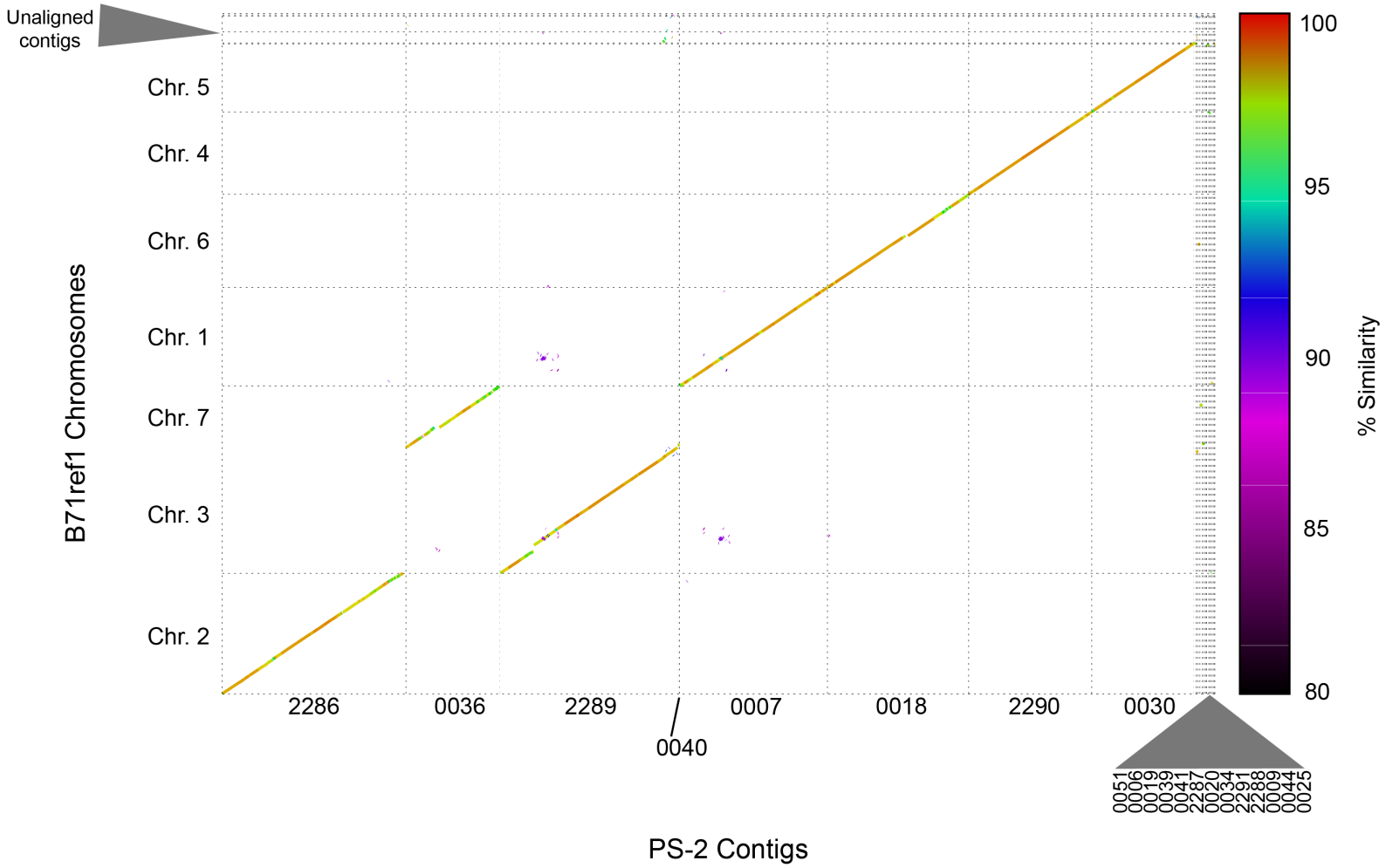


**Figure 5-16 The PS-2 genome assembly is overall colinear with wheat blast reference genome.** Co-linearity dot plot of alignments between PS-2 contigs and B71ref1 chromosomes. The orange coloured line indicates sequence similarity of ~98 % across the genomes.

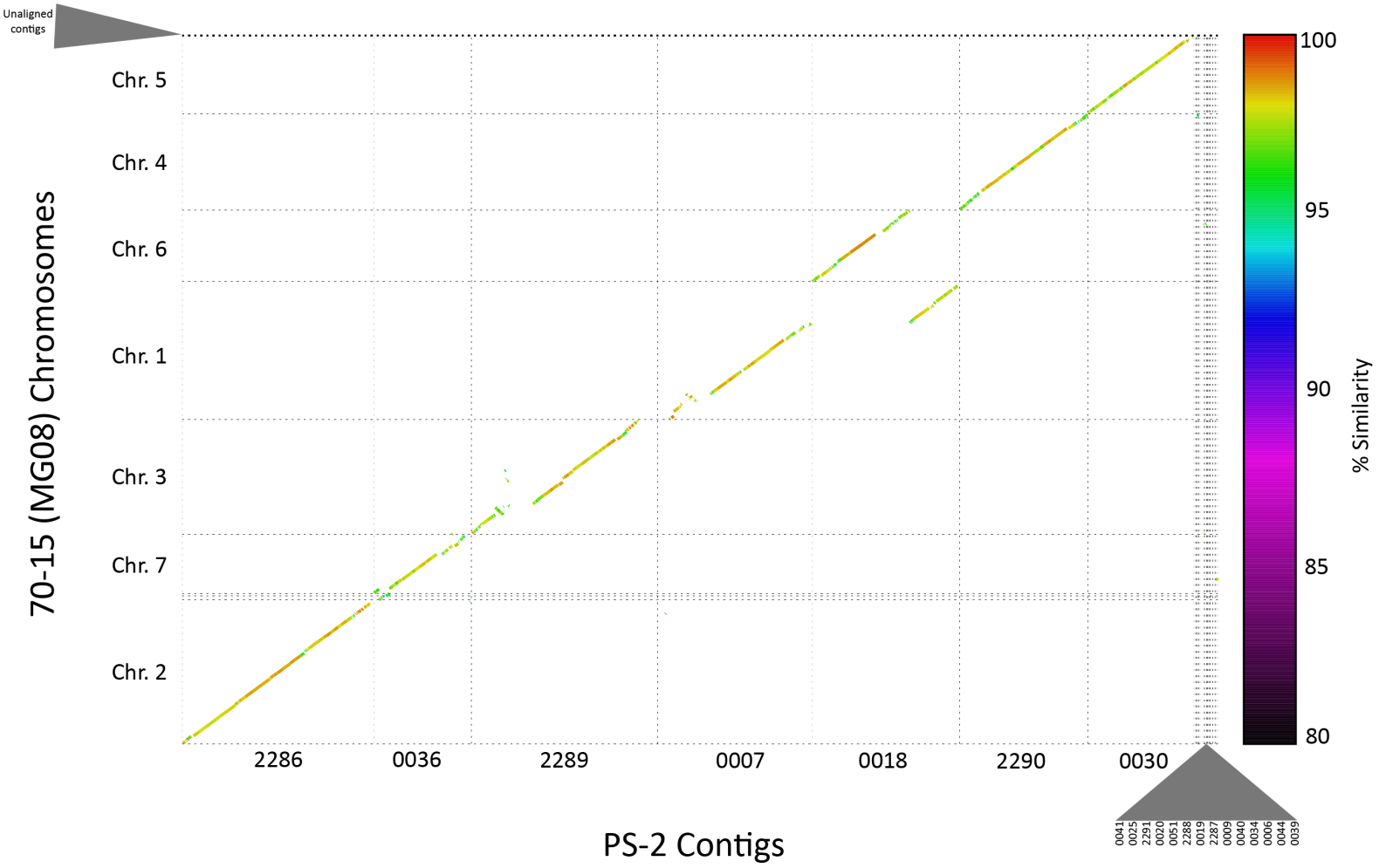


**Figure 5-17 The PS-2 genome assembly is overall colinear with the rice blast reference genome.** Co-linearity dot plot of alignments between PS-2 contigs and 70-15 chromosomes. The orange coloured line indicates sequence similarity of ~95 % across the genomes

#### 5.4.9.3 The PS-2 tandem insertion is located on contig 0018 of the PS-2 assembly near a region of structural variation

Using a BLAST search, I was able to locate a single tandem insertion of *AvrSr50* within contig 0018 of the PS-2 assembly. There is no evidence of insertion events anywhere else in the PS-2 assembly, suggesting all copies may have inserted into a single place within the genome. The tandem insertion included the entire donor vector concatenated multiple times with a total length of 98,512 bp (**Figure 5-18**). Contig 0018 contained 17 copies of *AvrSr50,* which is less than the 40 copies determined using TaqMan real-time PCR. However, due to the repetitive nature of the sequence, it is possible there were more copies than the assembly software could resolve. Indeed, many of the unassembled contigs are saturated end to end with a tandem sequence of pPWT3:PWT3SP:AvrSr50. To determine if the assembly software could resolve the tandem insertion, raw nanopore reads were aligned to the 0018 contig using the minimap aligner (Li, 2018). Visual analysis of the alignment was performed using the Geneious Prime software version 2020.2 (Biomatters Ltd). No single reads were found spanning the entire tandem insertion, suggesting the software could not resolve all copies of *AvrSr50*. Further, the read coverage from this alignment was determined using the samtools coverage utility (Li *et al.,* 2009). The coverage of contig 0018 is 139x, whereas the interval containing the tandem insertion has a coverage of 226x. These data suggest the copies of *AvrSr50* in contig 0018 only show around half of all copies in the tandem insertion. Therefore, the true copy number of the tandem insertion was not fully resolved using de-novo assembly but can be estimated at around 40 copies. For simplicity, the rest of this thesis will continue to refer to the tandem insertion as having 40 copies.

Upstream of the 40-copy insertion, the entire 0018 contig aligns with chromosome 6 of the rice blast reference genome, as determined by a BLAST search (**Figure 5-18**). Curiously, immediately downstream of the insertion site there are 10,000 base pairs of *E.coli* chromosomal DNA. It is likely the vector donor concatenated along with part of the *E.coli* chromosome before inserting into the *Magnaporthe* genome. Interestingly, only 13,000 bp downstream of the insertion site is contiguous with chromosome 6 of the rice blast reference genome. Co-linearity plots suggest large regions of contig 0018 downstream of the insertion site align with chromosome 1 of the rice blast reference genome (***Figure 5-17***). Further, alignments with B7ref1 chromosomes suggest contig 0018 is completely co-linear with B7ref1 chromosome 6 (***Figure 5-16***). This suggests the region downstream of the insertion site is not an error in the PS-2 assembly, but merely represents a large structural variation between the

wheat blast and the rice blast reference genome. These findings correspond with reports from Peng *et al.* (2019) in which two megabases of chromosome 1 from MG8 is found on chromosome 6 of wheat blast reference genome (B71Ref1). This same chromosomal re-arrangement was found in a rice infecting isolate in which mobile elements were found at the centre of the break point, suggesting TE elements in the role of genomic plasticity of this region (Bao *et al.* 2017).

The insertion event was found disrupting gene MGG_04257 which is located on chromosome 6 of the rice blast reference genome. In a dual RNA-seq analysis of infected rice tissue at 24 hours post infection, MGG_04257 was found upregulated 219-fold (Kawahara *et al.*, 2012). The authors also note MGG_04257 has a signal peptide and is predicted to be a secretory lipase (Kawahara *et al.*, 2012). It is possible that this gene codes for an effector protein, as extracellular fungal lipases are known to have a function in plant cell wall degradation and inhibition of callose deposition during early stages of infection (Blumke *et al.*, 2014). Additionally, two other neighbouring genes (MGG_04258 and MGG_04259) also have predicted signal peptides. Therefore, this particular location may be enriched in effectors and thus highly upregulated and transcriptionally active during early time points of infection. It is plausible then, that both copy number and insertion location may contribute to the likely required levels of transcription required for *Sr50* dependent HR.

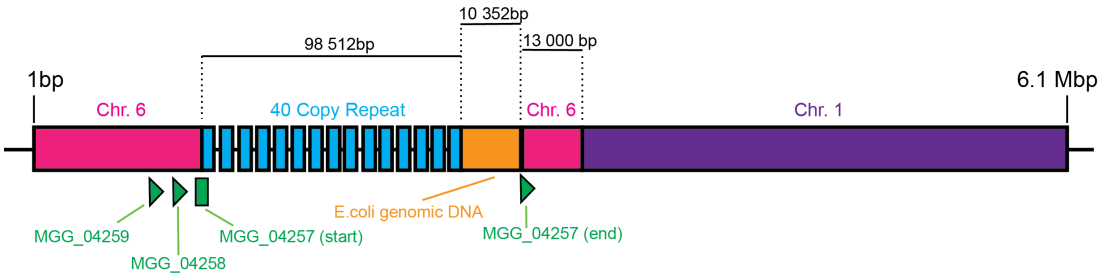


**Figure 5-18 The PS-2 tandem insertion is located in a region of structural variation.** Blue represents BLAST hit matches to the donor DNA (vector backbone and *AvrSr50* expression cassette). Pink regions represent blast hit matches to chromosome 6 of the 70-15 rice blast reference genome. Green annotations are genes surrounding the insertion site that have confirmed signal peptides. The orange region represents the ~10,000 bp stretch of *E.coli* chromosomal DNA. The purple region represents sequences are contiguous with chromosome 1 of the rice blast reference assembly.

### 5.4.10 RNA-seq data analysis suggests no read through from the MGG_04257 promoter

As mentioned in the previous section, the 40-copy tandem insertion was found disrupting gene MGG_04257. To determine the possibility of transcription read through from the native MGG_04257 promoter, I analysed the first insertion in more detail. This disruption occurred 242 bp downstream the start of the MGG_04257 coding sequence (**Figure 5-19**). The start of the tandem insertion consisted of the last 91 bp of the PWT3 promoter, followed by the rest of the pPWT3:PWT3SP:AvrSr50 expression vector. I searched possible open reading frames in this region. One possible reading frame uses the start codon from MGG_04257, however, this transcript is predicted to be terminated near the insertion site as the pPWT3 promoter sequence introduces a stop codon (**Figure 5-19**). Furthermore, aligning RNA-seq reads from 3 DPI (section **5.4.6)** to this region suggests *AvrSr50* expression is not driven by the MGG_04257 promoter. There is a drop off in aligned reads at the predicted stop codon introduced by the first pPWT3 sequence indicated by a star in (**Figure 5-19**). There is a possibility a fusion event could be missed due to reads mapping to other copies of the tandem insertion. To test this, RNA-seq reads were aligned to the first insertion region (shown in Figure 5-19) without the other tandem copies. No fusion transcripts were identified from this analysis. Further, RNA-seq reads were *de novo* assembled using Trinity v2.11.0 (Grabherr *et al.*, 2011). None of the transcripts containing the *AvrSr50* coding sequence contained a 5' UTR originating from MGG_04257. Therefore, I conclude the pPWT3 promoter is likely the only promoter driving *AvrSr50* transcription in the PS-2 transformant at 3 DPI. Any positional effects this locus may have on *AvrSr50* transcription is not due to the MGG_04257 promoter.

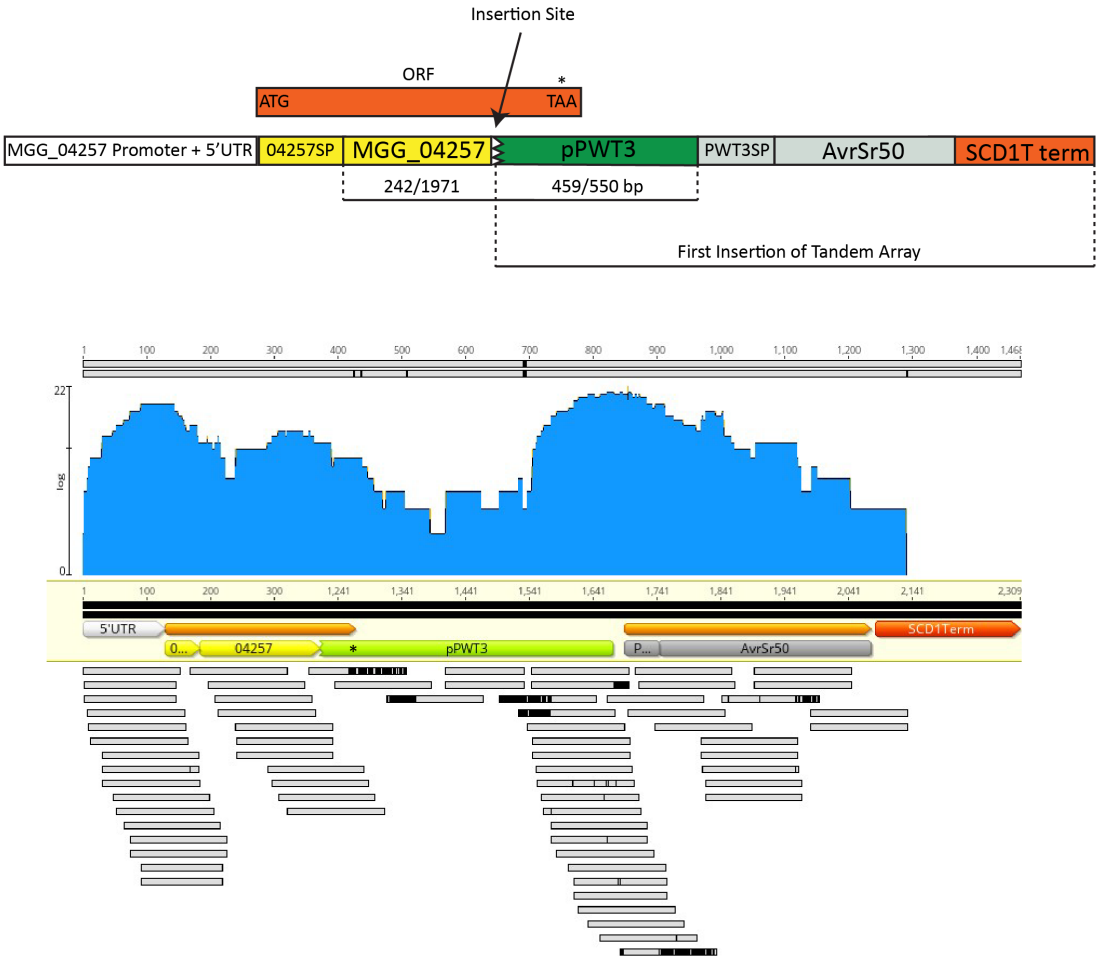


**Figure 5-19 The PS-2 transformant does not express *AvrSr50* via the MGG_04257 promoter at 3 DPI.** RNA-seq reads obtained from Gabo (*Sr50-*) leaves infected with PS-2 at 3DPI were aligned to the first tandem insertion. The top panel is a schematic of the first insertion which is disrupting MGG_04257. The MGG_04257 ORF is shown with the predicted premature stop codon (asterisk) introduced by the p*PWT3* sequence. The bottom panel shows the raw RNA-seq reads aligned to this region, with a drop off of reads spanning the introduced stop codon.

### 5.4.11 CRISPR/CAS9 targeted insertion of *AvrSr50* to select places in the *Magnaporthe* genome

The evidence provided thus far suggests both copy number and insertion location may be important for the expression of *AvrSr50*. Curiously, transformant PWLS-8 (expression construct pPWL2:PWT3SP:AvrSr50) has 21 copies of *AvrSr50* yet does not show *R* dependent HR (**Table 5-1**). This suggests that either 21 copies still do not reach the threshold for the induction of HR or the particular insertion location of these copies is not conducive to high transcription during infection, potentially due to chromatin states. To answer the question if insertion location is important for transformants to induce *Sr50* dependant HR, I decided to use Crispr/Cas9 targeted insertion of *AvrSr50* to selected regions in the *M. oryzae* genome.

#### 5.4.11.1 Other known effectors that are expressed at 3DPI are chosen for targeted insertion

Along with the original site of the tandem insertion, MGG_04257, I decided to choose other effector genes present in PY06047 that are expressed during infection on wheat for targeted insertion. First, I obtained sequences from previously described *M. oryzae* effectors described in Yoshida *et al*. (2016). Then, I performed a BLAST search on the PY06047 Nanopore reference to find presence/absence polymorphisms for these avirulence genes. For avirulence genes present in the genome, I obtained TPM expression values from the RNA-seq analysis from section **5.4.6.** Genes with non-zero levels of expression are shown in **Figure 5-20**. Next, I targeted *AvrSr50* to these locations and selected transformants. I was able to obtain positive transformants with *AvrSr50* targeted to MGG_04257, *AvrRmg8*, and *AvrPib*. The following sections will characterise these transformants in more detail.

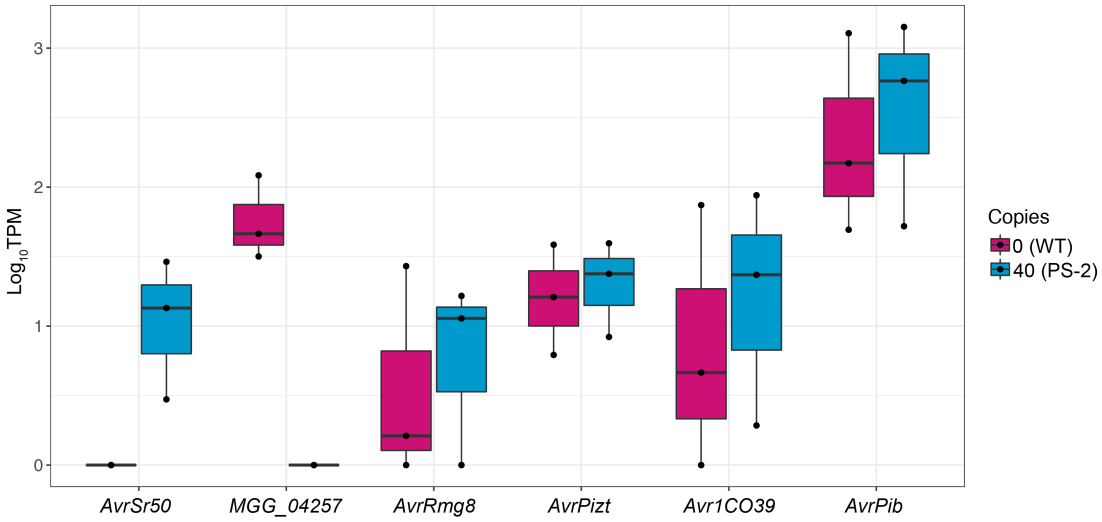


**Figure 5-20 Expression of known effectors in the PY06047 strain.** Expression is shown as the $log_{10}$TPM (transcript per million) value calculated from the Kallisto software. RNA-seq reads were obtained from Gabo (*Sr50*-) leaves infected with WT and PS-2 conidia. Three biological replicates were collected at 3DPI. TPM values for each biological replicate are shown as individual data points.

#### 5.4.11.2 Transformants with *AvrSr50* targeted to the *AvrPib* genomic locus do not elicit *R* dependent HR

One of the most highly expressed known *AVR* genes in the PY06047 genome is *AvrPib* (**Figure 5-20**). I targeted the pPWT3:PWT3SP:AvrSr50 expression construct to a region in the *AvrPib* coding sequence that had the highest predicted CRISPR site activity as calculated by Doench *et al*. (2014). The donor DNA was cloned to have 5' and 3' homology to either side of the predicted cut site, which is usually 3-4 bp upstream of the PAM (NGG) sequence, indicated by a star in **Figure 5-21A.** To check if the transformants obtained incorporated the donor DNA, I amplified genomic DNA from each transformant with primers in the 5' and 3' homology regions of the donor DNA, as indicated by F1 and R1 primers in **Figure 5-21**A. Using this primer pair, I determined 32/35 transformants had the insertion (**Figure 21B).** To determine if the vector inserted into the *AvrPib* locus, I used a forward primer just upstream of the 5' homology region cloned into the donor vector and a reverse primer located in the *AvrSr50* coding sequence (denoted as F2 and R2 in **Figure 5-21**A). The majority of transformants had the insert at the *AvrPib* genomic locus (**Figure 5-21**C). The efficiency of CRISPR/Cas9 targeted insertion can therefore be very efficient in *M. oryzae*. Five separate transformants were randomly chosen to screen on plants for cell death. None of the transformants were able to elicit *R* dependent HR (**Figure 5-22** A,B). Therefore, although this particular genomic locus carries a highly expressed effector during early time points of infection (*AvrPib)*, it may not be suitable for the heterologous expression of *AvrSr50*.

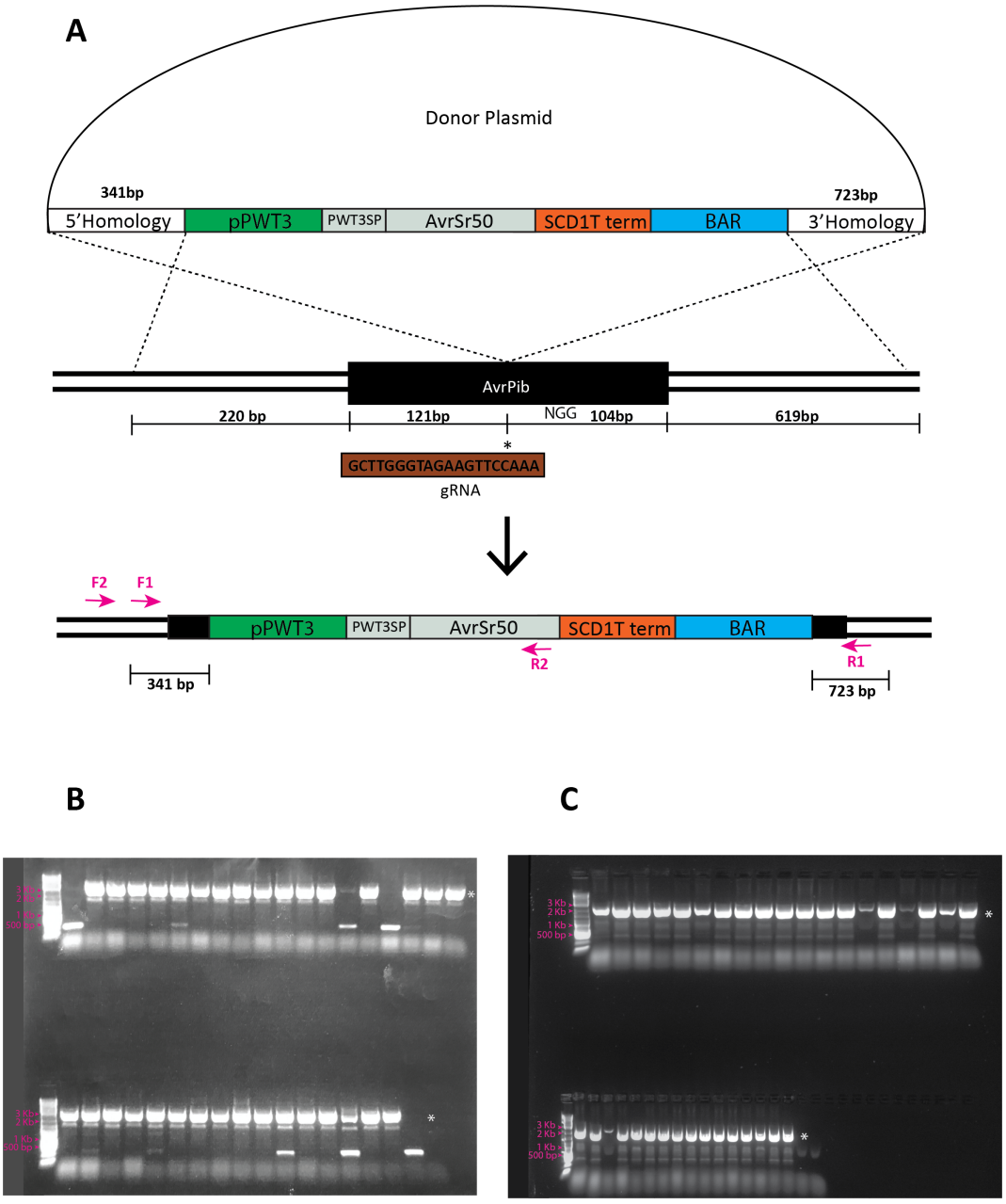


**Figure 5-21 *AvrSr50* is successfully targeted to the *AvrPib* locus using CRISPR/Cas9 technology.** A) The donor plasmid was cloned to contain the pPWT3:PWT3SP:AvrSr50 expression construct with 5'and 3' regions homologous to the insertion region. The gRNA (brown) was designed to target the region upstream of a PAM (NGG) sequence. The asterisk denotes the predicted cut site (~3bp upstream the PAM). After homologous recombination with the donor DNA, the expression construct is integrated at the *AvrPib* locus. B) Using primers F1 and R1 (designed in pink in figure A), most transformants show integration of the donor DNA via PCR. The correct predicted amplicon size, 2362 bp, is indicatede by the star. C) Using primers F2 and R2 (designed in pink in figure A), most transformants show integration of the donor DNA in the correct place via PCR. The predicted amplicon size, 1685 bp, is indicated by the star. The ladders shown in B and C is 1 Kb plus (NEB).

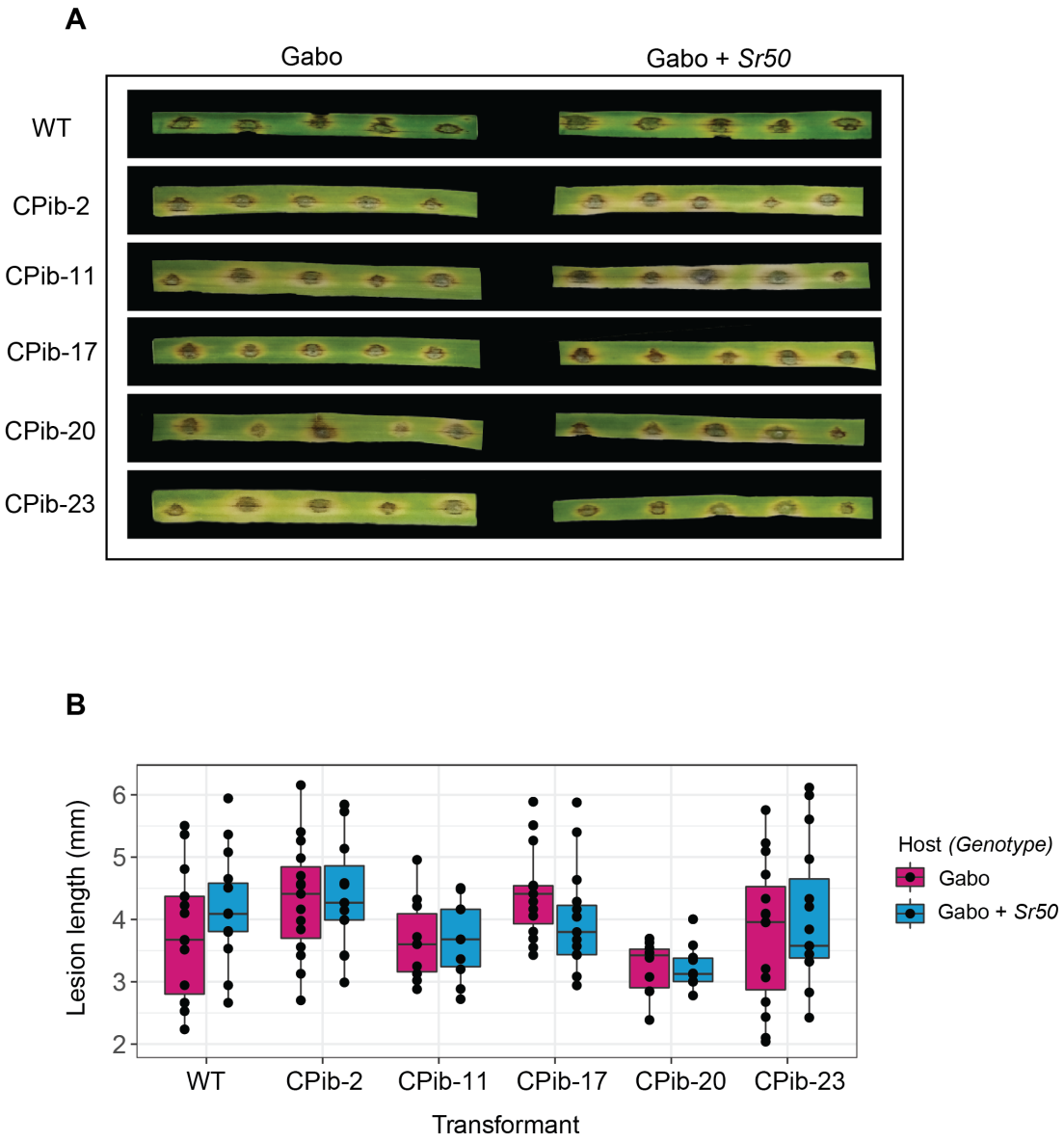


**Figure 5-22 Transformants with *AvrSr50* targeted to the *AvrPib* locus do not show R dependent HR.** Five separate transformants with *AvrSr50* targeted to the *AvrPib* locus were chosen to infect plants. The second leaf of 14-day old wheat seedling were infected using the spot inoculation method. Photos were taken 4 DPI. A representative of three biological replicates are shown. B) Lesion lengths from 2-3 separate leaves of each host genotype were measured at 4 DPI.

#### 5.4.11.3 Transformants with *AvrSr50* targeted to the *AvrRmg8* genomic locus in a different highly virulent strain do not display *R* dependent HR

In addition to assessing the importance of the genomic locus, the expression of *AvrSr50* may vary in different wheat blast strains used for transformations. To explore both of these possibilities, I chose a highly virulent strain obtained from the recent Bangladesh outbreak (BTJP4-1), all of which are known to carry the avirulent allele of *AvrRmg8*. Using a strategy similar to the previous section, the pPWT3:PWT3SP:AvrSr50 expression construct was targeted to the *AvrRmg8* locus of BTJP4-1 (**Figure 5-23**A). Using primers F1 and R1 (indicated in **Figure 5-23**A) I determined four transformants contained the donor DNA (**Figure 5-23**B). Using primers F2 and R2, I determined two transformants (8 and 11) contained the donor DNA in the right 5' position in the intended *AvrRmg8* locus (**Figure 5-23**). Neither of these two transformants were able to elicit *R* dependent HR (**Figure 5-24A, B).** Similar to the previous section, although the *AvrRmg8* locus is highly expressed during early time points of infection in Bangladeshi isolates, it may not be suitable for the heterologous expression of *AvrSr50*.

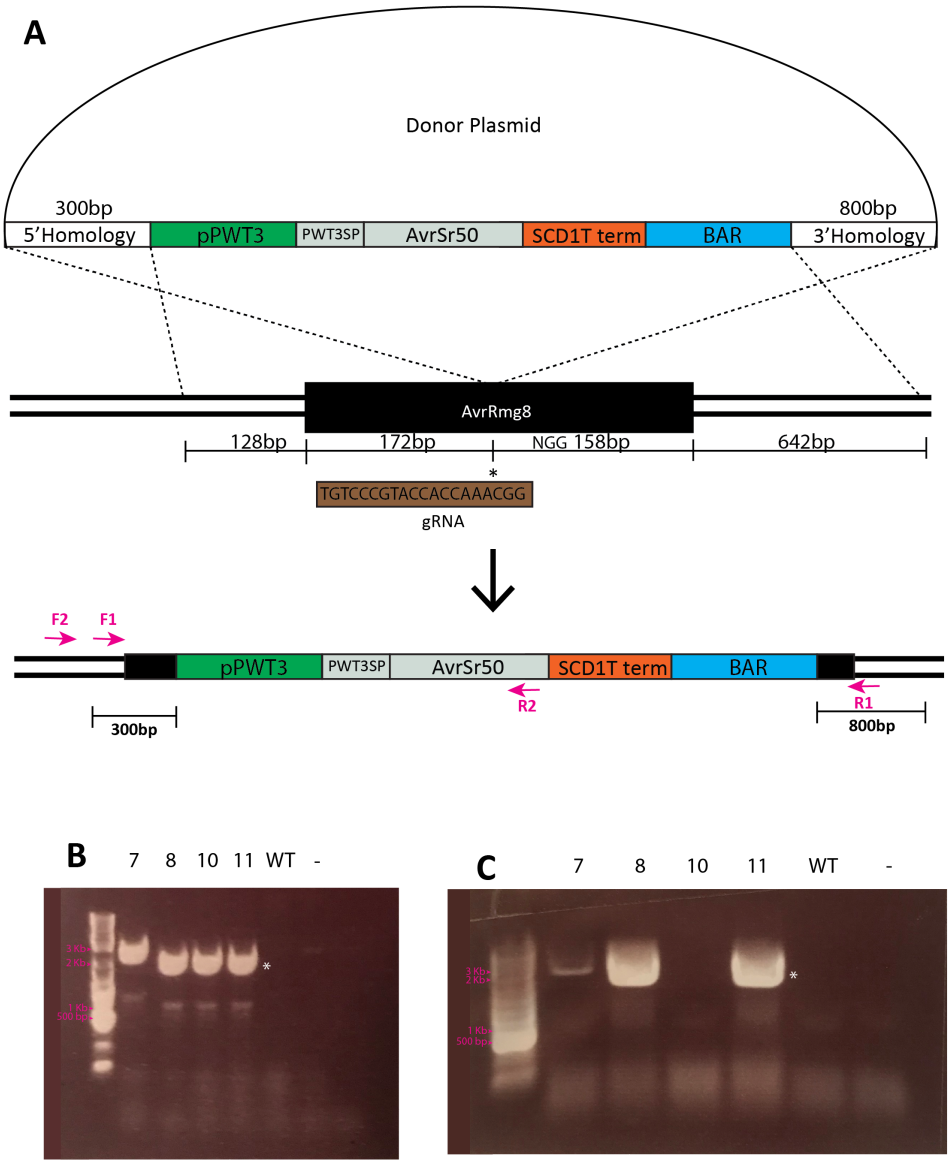


**Figure 5-23 *AvrSr50* is successfully targeted to the *AvrRmg8* locus using CRISPR/Cas9 technology.** A) The donor plasmid was cloned to contain the pPWT3:PWT3SP:AvrSr50 expression construct with 5'and 3' regions homologous to the insertion region. The gRNA (brown) was designed to target the region upstream of a PAM (NGG) sequence. The asterisk denotes the predicted cut site (~3bp upstream the PAM). After homologous recombination with the donor DNA, the expression construct is integrated at the *AvrRmg8* locus. B) Using primers F1 and R1 (designed in pink in figure A), four transformants show integration of the donor DNA via PCR. The correct predicted amplicon size, 1839 bp, is indicated by the star. C) Using primers F2 and R2 (designated in pink in figure A), two transformants show integration of the donor DNA in the correct place via PCR. The correct predicted amplicon size, 2325 bp, is indicated by the star. The ladders shown in B and C is 1 Kb plus (NEB).

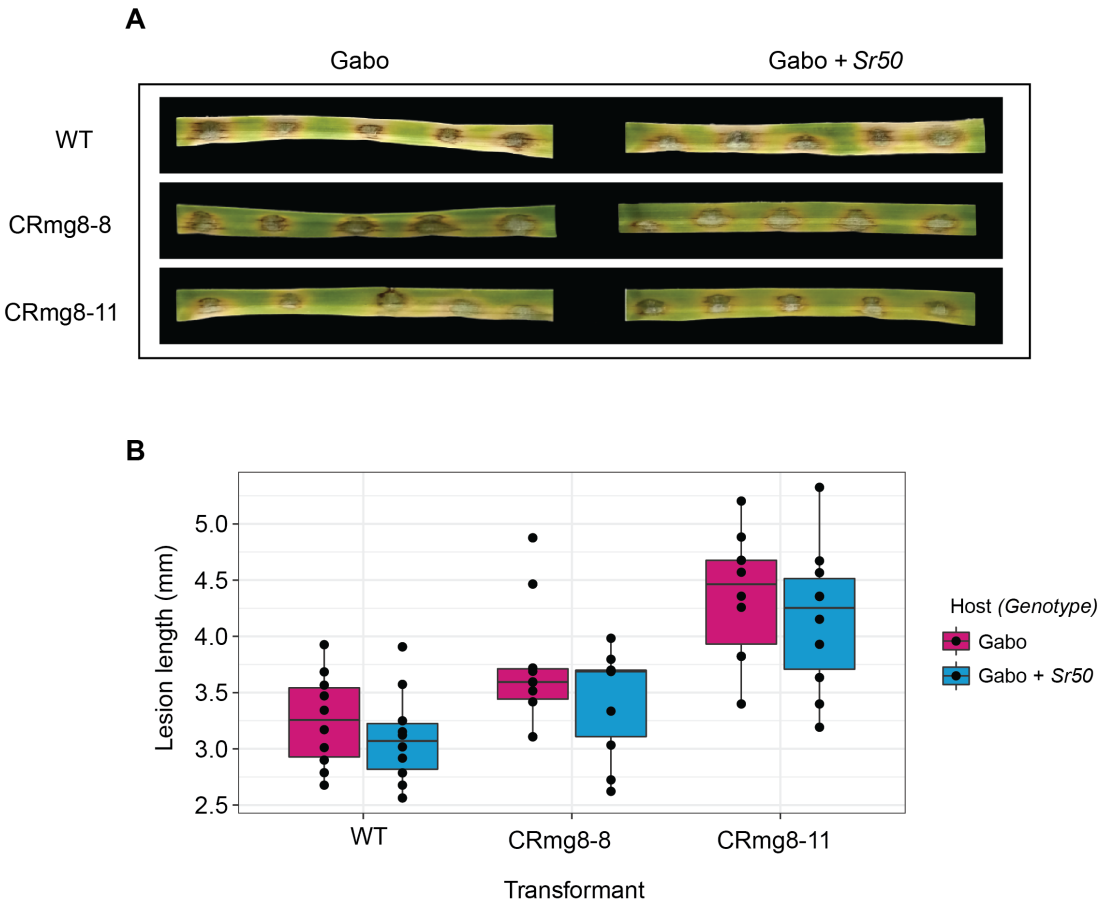


**Figure 5-24 Transformants with *AvrSr50* targeted to the *AvrRmg8* locus do not show *Sr50* dependent HR.** Two separate transformants with *AvrSr50* targeted to the *AvrRmg8* locus were inoculated on plants. The second leaf of 14-day old wheat seedling were infected using the spot inoculation method. Photos were taken 4 DPI. A representative of three biological replicates are shown. B) Lesion lengths from 2-3 separate leaves of each host genotype were measured at 4 DPI.

#### 5.4.11.4 Targeting *AvrSr50* to the original MGG_04257 genomic locus gives variable infection results

Using the same strategy as the two previous sections, I was able to target *AvrSr50* to the original MGG_04257 location where the 40-copy tandem insertion was found (**Figure 5-25**A). Three transformants (1,2 and 4) contained the donor DNA as confirmed using PCR primers denoted as F1and R1 (**Figure 5-25**A,B). These three transformants were also inserted into the right 5' locus as determined via PCR using primers denoted as F2 and R2 (**Figure 5-25**A,C). Two transformants, C04257-1 and C042574 were unable to elicit R dependent HR (**Figure 5-26A,B**). Transformant C04257-2, however, displayed an avirulence phenotype on *Sr50*+ leaves that was subtle, yet statistically significant (**Figure 5-26A,B**). Due to the subtlety of this phenotype, I repeated the infection assay multiple times (**Figure 5-27**). As a positive control, I included the PS-2 transformant in these assays. Out of four infection assays, C04257-2 displayed significant avirulence phenotypes half of the time (Fi**gure 27A,B).** Further, these avirulence phenotypes were much more subtle than those caused by PS-2. The lesion lengths were more variable and on average larger than those caused by PS-2 on *Sr50*+ wheat (Fi**gure 27A,B).**

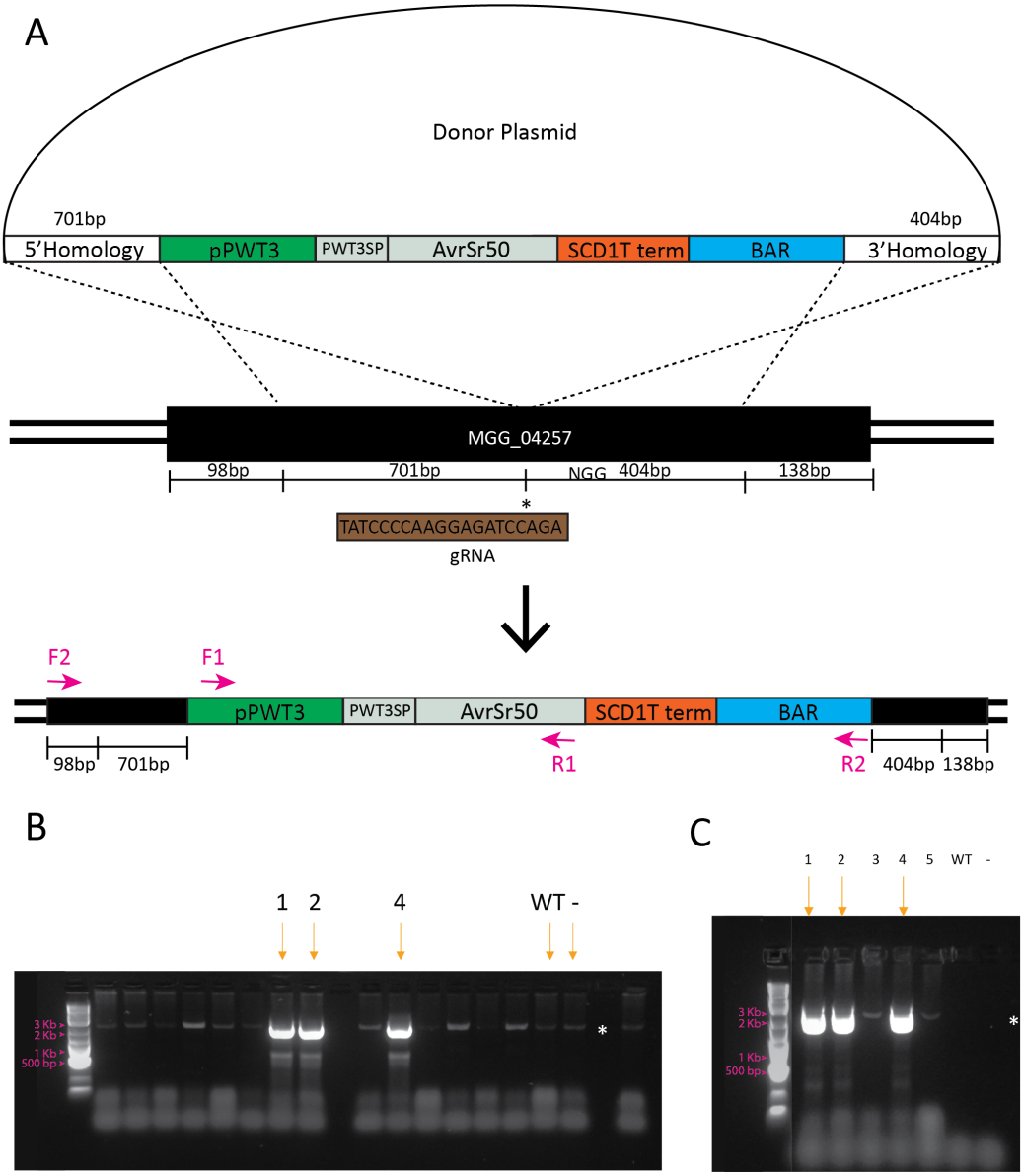


**Figure 5-25 *AvrSr50* is successfully targeted to the MGG_04257 locus using CRISPR/Cas9 technology.** A) The donor plasmid was cloned to contain the pPWT3:PWT3SP:AvrSr50 expression construct with 5'and 3' regions homologous to the insertion region. The gRNA (brown) was designed to target the region upstream of a PAM (NGG) sequence. The asterisk denotes the predicted cut site (~3bp upstream the PAM). After homologous recombination with the donor DNA, the expression construct is integrated at the MGG_04257 locus. B) Using primers F1 and R1 (designed in pink in figure A), three transformants show integration of the donor DNA via PCR. The correct predicted amplicon size, 1839 bp, is indicated by the star. C) Using primers F2 and R2 (designated in pink in figure A), three transformants show integration of the donor DNA in the correct place via PCR. The correct predicted amplicon size, 1849 bp, is indicated by the star. The ladders shown in B and C is 1Kb plus (NEB).

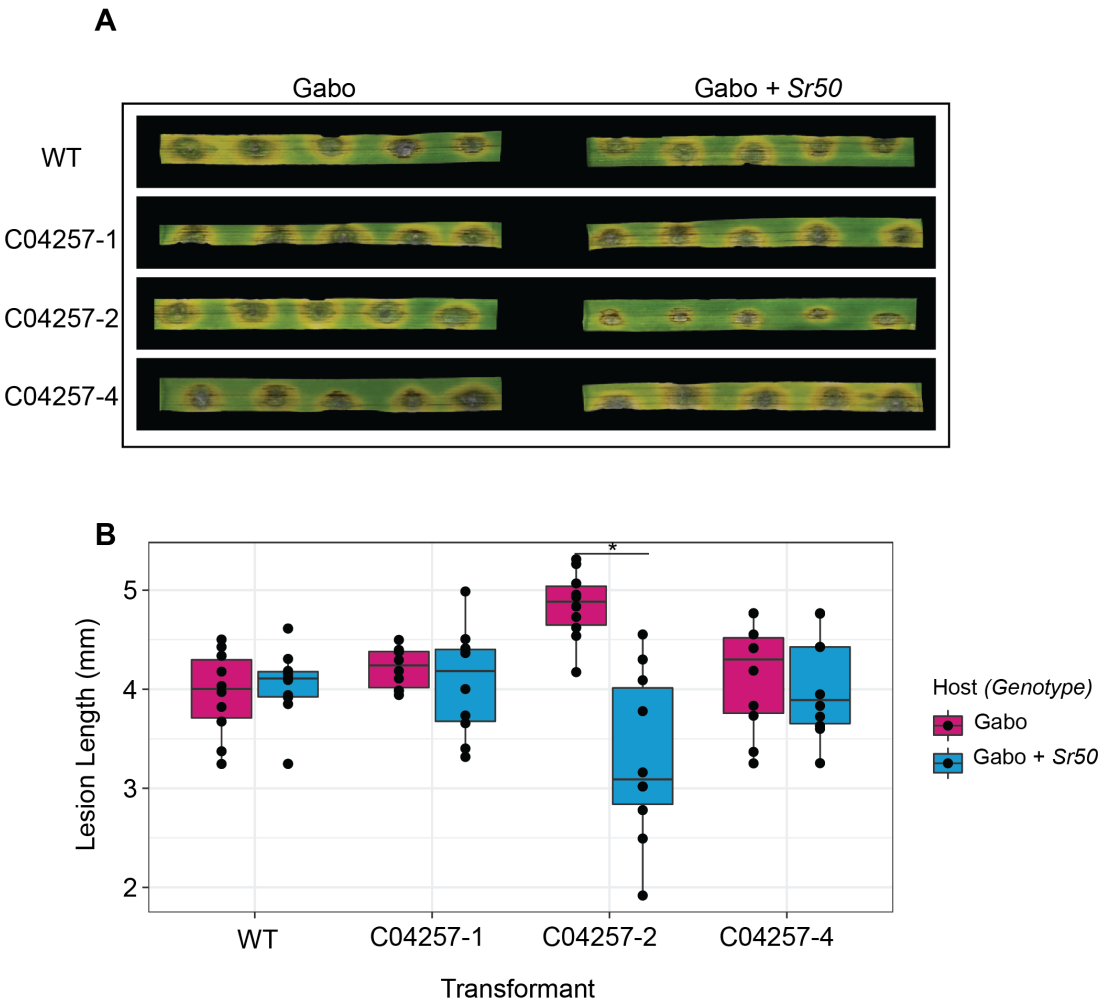


**Figure 5-26 A single transformant with *AvrSr50* targeted to the MGG_04257 locus shows *R* dependent HR.** Three separate transformants with *AvrSr50* targeted to the MGG_04257 locus were inoculated on plants. The second leaf of 14-day old wheat seedling were infected using the spot inoculation method. Photos were taken 4 DPI. A representative of three biological replicates are shown. B) Lesion lengths from 2-3 separate leaves of each host genotype were measured at 4 DPI. Asterisks denote statistically significant differences (***: $p < 0.001$, **: $p < 0.01$, *: $p < 0.05$; 2-tailed t-test).

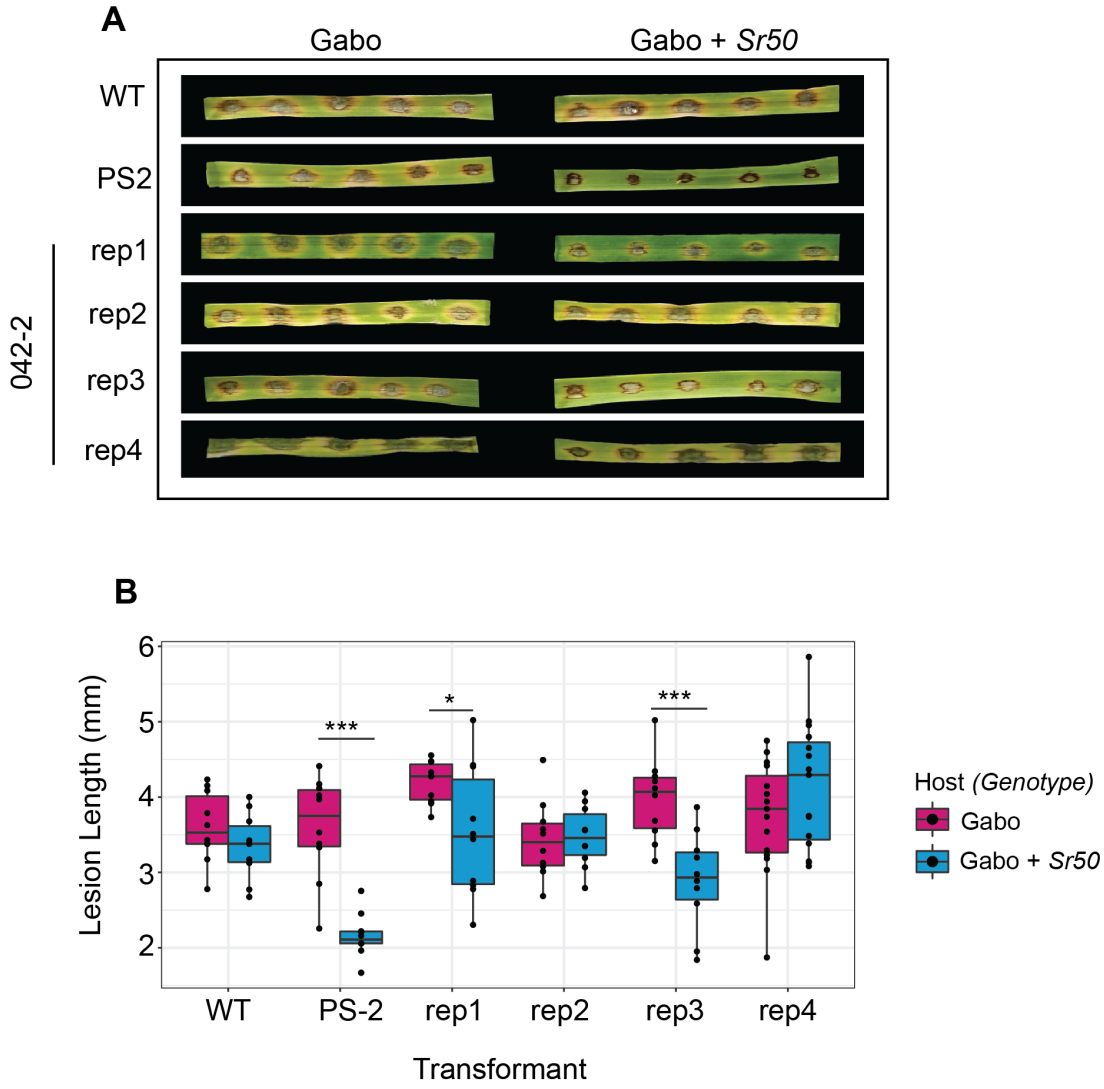


**Figure 5-27 Transformant C04257-2 inconsistently shows *R* dependent HR.** Infections on wheat seedings were repeated with transformant C04257-2. The second leaf of 14-day old wheat seedling were infected using the spot inoculation method. Photos were taken 4 DPI. A representative of three biological replicates are shown. B) Lesion lengths from 2-3 separate leaves of each host genotype were measured at 4 DPI. Asterisks denote statistically significant differences (***: $p < 0.001$, **: $p < 0.01$, *: $p < 0.05$; 2-tailed t-test).

#### 5.4.11.5 Transformant 042-2 is a single copy transformant with the entire donor vector insert at the 3′ end

It is possible the C04257-2 tranformant has multiple copies, with *AvrSr50* mRNA levels approaching those found in PS-2. To determine if the HR induced by 042-2 could be due to multiple insertions similar to PS-2, I first PCR amplified the 3' end of the insertion in transformants 1-5 (1,2,4 were previously confirmed to have the insert at the right 5' position). The reverse primer was designed to prime downstream of the homology region in the donor vector (primers are indicated as the pink arrows in **Figure 5-28**). Only transformants 1 and 4 displayed a band, suggesting transformant C04257-2 contains multiple copies or a 3' rearrangement. I decided to analyse all CRISPR transformants for copy number variation (**Table 5-4**). Interestingly, transformant C04257-2 had a single copy of the transgene. To understand what had occurred at the 3' end of the insertion in transformant C04257-2, I sequenced the genome using Nanopore technology, as described in section **5.3.12**. Using a BLAST search, I was able to find the insert, which was at the correct 5' location. However, instead of homologous recombination occurring at the 3' end of the vector with *M. oryzae* genomic DNA, the whole vector had inserted at the 3' end.

In summary, although the phenotype produced from C04257-2 was subtle, it is promising a single copy of *AvrSr50* may be able to elicit *R* dependent HR in the *M. oryzae* expression system. These data suggest not only copy number is important, however insertion location may also be important for expressing avirulence effectors. In particular, the chromatin folding status of the insertion location may be important, as the only thing in common between the C04257-2 and PS-2 transformant is a long DNA insertion disrupting the MGG-04257 locus caused by vector DNA.

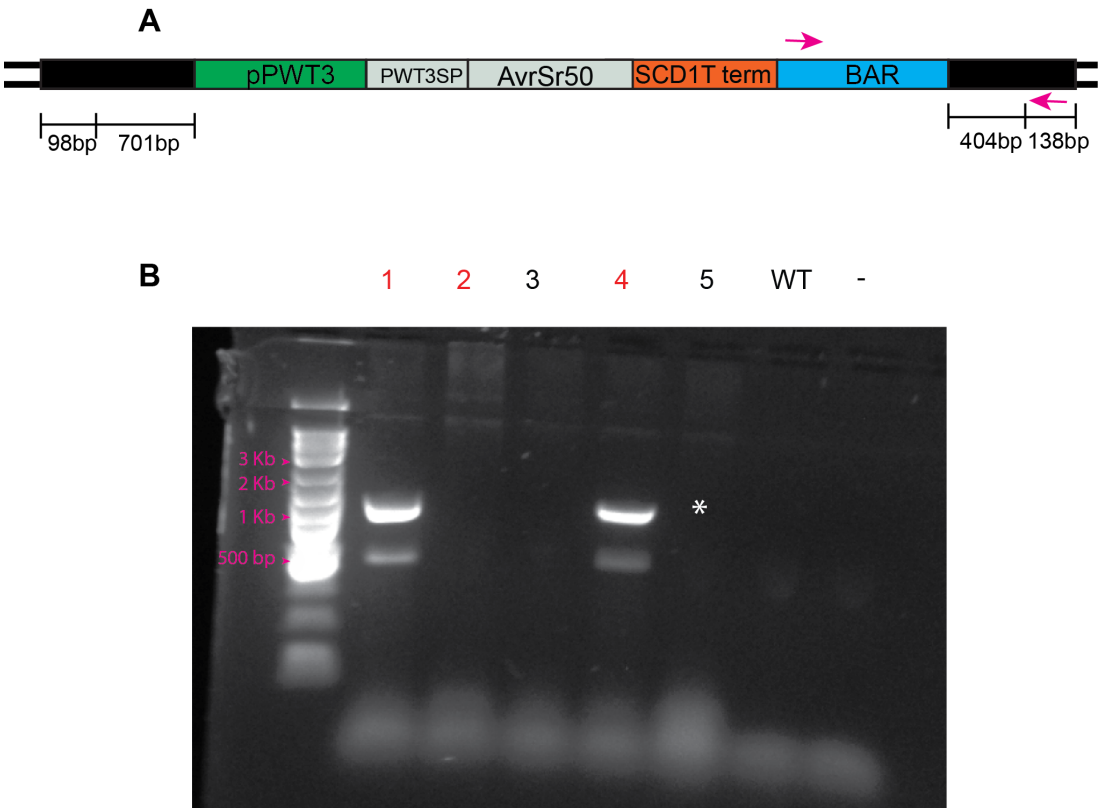


**Figure 5-28 Transformant C04257-2 shows an unexpected lack of amplification at the 3′ end of the construct.** A) Primers denoted in pink were designed to amplify DNA downstream of the 3' homology arm and part of the *BAR* gene. B) PCR with primers shown in 'A' suggest an unexpected sequence conformation at the 3' end of the insertion. The correct predicted amplicon size, 926 bp, is indicated by the star. The ladder shown is 1 Kb plus (NEB).

**Table 5-4** Transgene copy number of the CRISPR/Cas9 transformants.

| Construct Name/Insertion location | Background WT strain | Transformant Name | HR | Copy Number[1] |
|---|---|---|---|---|
| pPWT3:PWT3SP:AvrSr50/ AvrPib | PY06047 | CPib-2 | N | 2 |
| | | CPib-5 | N | 12 |
| | | CPib-11 | N | 25 |
| | | CPib-15 | N | 1 |
| | | CPib-17 | N | 12 |
| | | CPib-20 | N | 4 |
| | | CPib-23 | N | 1 |
| | | CPib-25 | N | 2 |
| | | CPib-30 | N | 1 |
| | | CPib-33 | N | 3 |
| pPWT3:PWT3SP:AvrSr50/ AvrRmg8 | BTJP4-1 | CRmg8-7 | N | 2 |
| | | CRmg8-8 | N | 1 |
| | | CRmg8-10 | N | 1 |
| | | CRmg8-11 | N | 1 |
| pPWT3:PWT3SP:AvrSr50 / MGG_04257 | PY06047 | C04257-1 | N | 1 |
| | | C04257-2 | variable | 1 |
| | | C04257-4 | N | 1 |

[1]Copy number analysis was performed by IDNA genetics (Norwich, UK).

### 5.4.12 The *Magnaporthe* expression system is unable to elicit R dependent HR when expressing a different fungal effector

All experiments conducted thus far use *AvrSr50* from stem rust as a positive control for detecting avirulence phenotypes in wheat. It is possible other *AVR/R* pairs require less AVR protein expression for the elicitation of cell death (Saur *et al.* 2019; Morel and Dangl, 1997). To test this possibility I chose a different effector from a biotrophic fungal pathogen of wheat; $AvrPm3^{a2/f2}$ from *Blumeria graminis* (Bourras *et al.*, 2015). First, the $AvrPm3^{a2/f2}$ coding sequence was cloned into the same expression vector as the PS-2 transformant, swapping out *AvrSr50* (**Figure 5-29A**). Of the four independent transformants that were obtained, none were able to elicit HR on leaves containing the associated *R* gene, *Pm3a* (**Figure 5-29A**). Disease lesions on *Pm3a*+ plants were not significantly different than those on *Pm3a*- plants, confirming no *R* dependent HR phenotypes from these transformants (**Figure 5-29B**). In summary, $AvrPm3^{a2/f2}$ expression may also require fine tuning in the *M. oryzae* system to elicit *R* dependent HR.

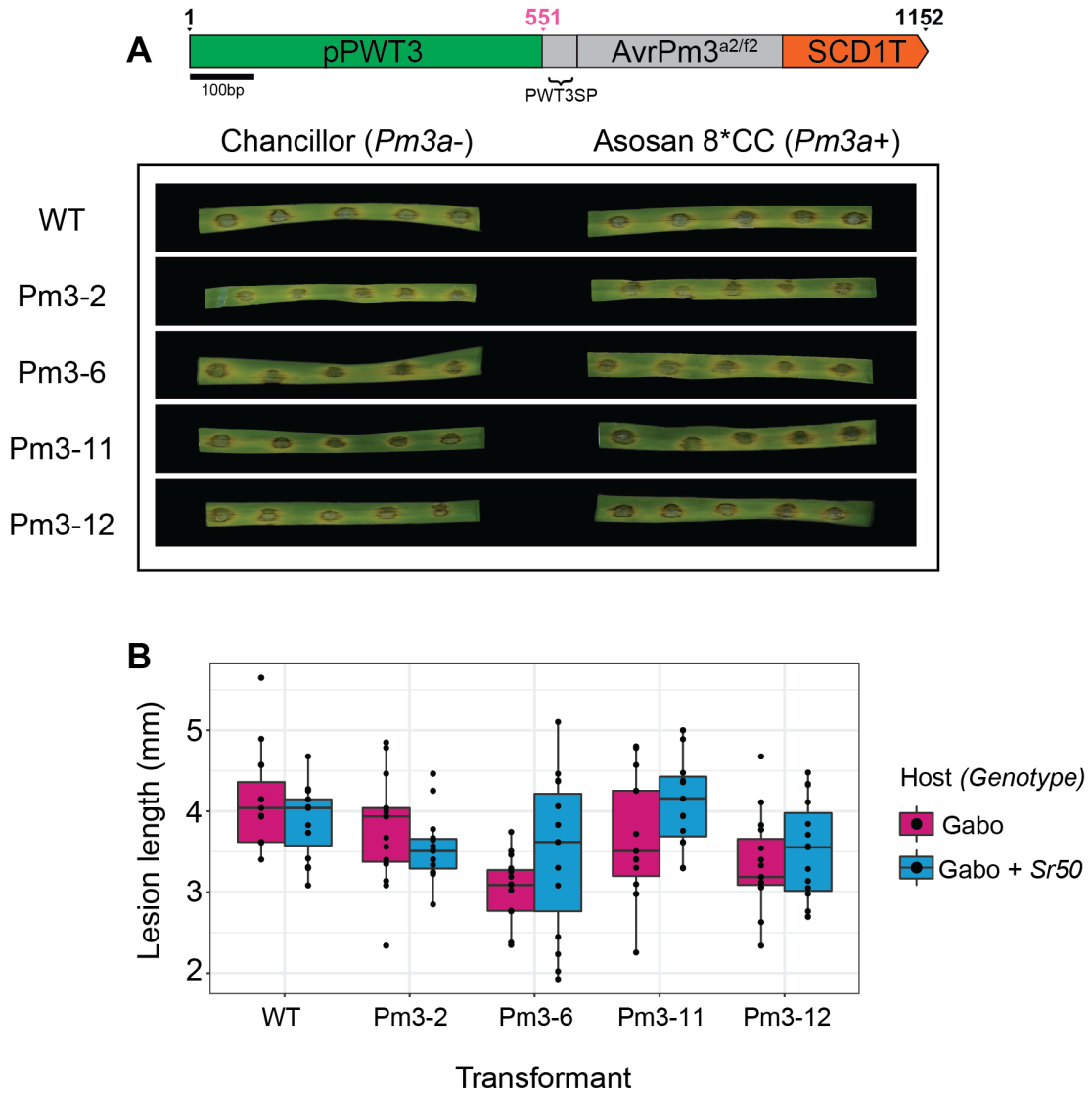


**Figure 5-29 Transformants expressing a different effector, *AvrPm3$^{a2/f2}$*, do not elicit *R* dependent HR. A)** Top panel: schematic of the construct used to express *AvrPm3$^{a2/f2}$*. Black arrows above the transgene model indicate the start and end of the construct. The start of the coding sequence is denoted by a pink arrow. The scale shows 100 bp. The *PWT3* signal peptide was cloned into the construct to replace the native *AvrPm3$^{a2/f2}$* signal peptide. Bottom panel: four separate transformants were infected on the second leaf of 14-day old wheat plants differential for *Pm3a*. Photos were taken 4 DPI. A representative of three biological replicates are shown. B) Lesion lengths from 2-3 separate leaves of each host genotype were measured at 4 DPI.

### 5.4.13 Fluorescently tagged *AvrSr50* is undetectable using confocal microscopy using a *Magnaporthe* expression system

It is possible that transformants with fewer than 40 copies of *AvrSr50* may express enough transcript for localisation studies. To test this, I transformed isolate PY06047 with the same construct as PS-2, but with an mcherryNLS tagged onto the 3' end of *AvrSr50*. Positive transformants were further transformed with another vector: BAS4GFP. BAS4 is an apoplastic effector that has previously been shown to line the invasive hyphae when tagged with a fluorescent protein (Khang *et al.*, 2010). In the same study, cytoplasmic effectors tagged with a fluorescent protein and NLS were shown to accumulate in the BIC and subsequently in the plant host nucleus (Khang *et al.*, 2010). Five separate transformants with both constructs (pPWT3:PWT3SP:AvrSr50mcherryNLS and BAS4:GFP) were screened for fluorescence signals. First, transformants were inoculated into wheat leaf sheaths. Starting at 24 HPI, leaf sheath sections were analysed under the confocal microscope. A GFP signal could be seen outlining the invasive hyphae of transformants (**Figure 5-30A**), suggesting transformations were successful. However, no mCherry signal could be seen in the BIC or wheat nuclei. Single transformants with pPWT3:PWT3SP:AvrSr50mcherryNLS were also obtained. Of six separate transformants, none displayed a fluorescence signal in the BIC or wheat nucleus (**Figure 5-30B**). It is likely not enough *AvrSr0* protein is produced for a signal to be detected by microscopy. Similar levels of protein required to induce *R* dependent HR may also be required to detect fluorescence signals using microscopy.

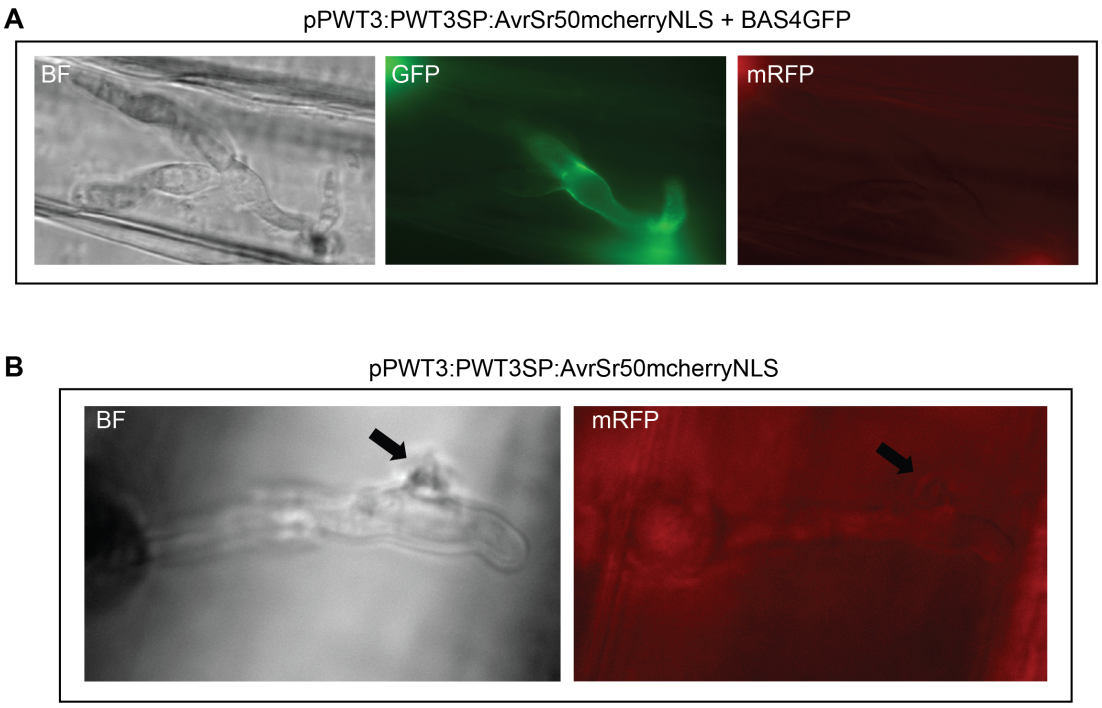


**Figure 5-30. Transformants containing *AvrSr50* with an mcherry:NLS tag do not show fluorescence signals in the BIC or host nucleus.** A) Representative confocal image of transformants with both expression constructs indicated. BAS4:GFP (green) is seen outlining the invasive hyphae. AvrSr50:mcherryNLS (red) was not seen in the BIC or host nucleus. B) Representative confocal images of transformants with the single expression construct indicated. AvrSr50:mcherryNLS (red) was not seen in the BIC or host nucleus. Black arrows indicate a BIC. BF, Bright Field. Images taken from infected tissue at 24 HPI.

## 5.5 Discussion

The results provided in this chapter provide foundational data for a novel *M. oryzae* heterologous expression system for detecting avirulence phenotypes of rust effectors in wheat. Initially I was able to express a homologous protein, *AvrRmg8*, in *M. oryzae* using an expression vector that contained the *PWL2* promoter (**Figure 5-8**). Two separate transformants were obtained that could elicit *R* dependent HR on wheat leaves. Although the expression levels of these transformants were not checked in this chapter, it is known homologous recombinant proteins are often expressed 10-1000 fold higher than heterologous proteins (Nevalainen *et al.,* Bergquist 2005). Therefore, it is not surprising achieving high expression of a rust effector, *AvrSr50*, would require modifications in gene expression. A single transformant, PS-2, successfully hit this high transcription threshold presumably through multiple copy insertion of the transgene (**Figure 5-18**). The following section will explore alternative ways to replicate this phenotype and the many confounding factors that may supress or enhance heterologous protein production in *M. oryzae*.

### 5.5.1 Copy number: lessons from industry

Filamentous fungi are often used to heterologously express industrially important compounds including enzymes for food processing. Species used for industrial heterologous expression include *Aspergillus* spp., *Trichoderma reesei*, *and Neurospora* crassa (Su *et al.*, 2012). Copy number variants of integrated plasmids are often seen with transformation of these filamentous fungi (Jeenes *et al.*, 1991; Ruiz-Diez, 2002). Multiple vector integration has been reported to occur at one or several positions in the genome, with tandem insertions at a single location also common. Tandem insertions can occur either as the vector concatenates before integration, or a single vector integrates via non-homologous recombination, providing a template for further homologous recombination events (**Figure 5-31**).

Multiple copy insertions in *Magnaporthe* have been anecdotally reported, however, records of a tandem insertion of similar magnitude to the PS-2 transformant generated in this thesis are currently unknown. It is also not specified in the literature how often tandem insertions occur. Out of the many transformants produced in this thesis, a 40 copy tandem insertion occurred once. Therefore, reproduction of this phenotype using the same method is likely to be rare and inefficient. Re-creating high copy number transformants are in theory possible, however, the methods would be labour intensive and low-throughput. For example, van den Hondel *et al.* (1991) were able to produce an *Aspergillus niger* transformant with 160 copies by engineering a donor cosmid vector with 10 copies of the transgene. This resulted in five to

ten-fold increase in protein production. Producing a donor DNA with 10 tandem copies of a gene is possible using current Golden Gate technology. However, 10 copies is the upper limit as homologous recombination can occur within the vector during *E. coli* propagation, resulting in the loss of multiple copies (Mark Youles, TSL, personal communication).

In these situations, multiple copies of the transgene only sometimes produce higher levels of heterologous protein. Indeed, the increase in protein production is often not completely linear to copy number increase. The PS-2 transformant for instance does not show 40 times more transcription than a single copy transformant (**Figure 5-14**). Rather, this transformant shows a 5-10-fold increase in transcription, which of course may not even produce 5-10 times more protein product, depending on translation dynamics. These observations suggest confounding factors other than copy number are at work. Other factors to consider include transcription factor titration of multiple copies, transgene silencing, and "positional effects" in which a transgene can insert into a transcriptionally active part of the genome resulting in higher levels of gene expression.

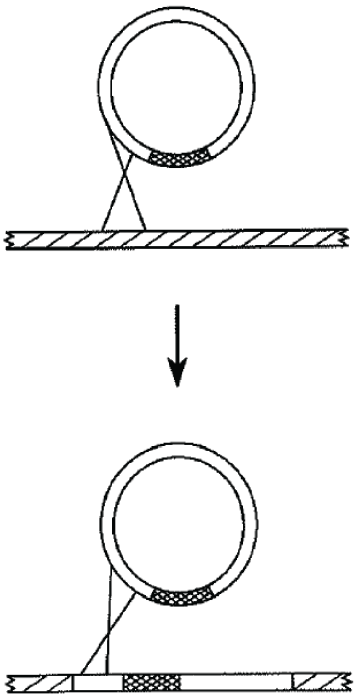

**Figure 5-31. A model of integrative transformation leading to a tandem insertion.** A single crossover event occurs at a non-homologous region. This first insertion acts as a template for homologous recombination, leading to tandem multi-copy insertions. This image was first published in Jeenes *et al*. (1991) and is reused with permission from copyright holders.

### 5.5.2 Issues with multiple copies: transgene silencing and transcription factor titration

All 40 copies of the PS-2 transformant may not lead to a 40-fold increase in mRNA due to a transcription factor (TF) titration phenomenon. The copy number of a gene can surpass the amount of TF's available for particular promoters required to express these genes. This may be ameliorated by engineering promoter regions to contain binding sites from different TFs (Nevalainen *et al.,* 2005). Additionally, the same transgene can be expressed under multiple different promoters that do not share the same regulatory factors (Nevalainen and Peterson, 2014).

Further, it is possible that not all copies of *AvrSr50* in PS-2 are contributing to increased mRNA levels due to transgene silencing. Transgene silencing is a phenomenon that has been described in many species, including filamentous fungi (Cogoni and Macino, 2000). In *Neurospora crassa*, post transcriptional gene silencing during the asexual phase is known as quelling, a process which involves RNAi (Romano and Macino, 1992). Transgenes, particularly those present in tandem array, can produce aberrant mRNAs that are recruited by RNA-dependent RNA polymerases (RdRPs) which are then converted to dsRNA (Dang *et al*., 2011). Strong constitutive promoters can also cause the production of abnormal mRNAs, including those with an absence of a poly(A) tail (Baeg *et al*., 2017). Once an aberrant mRNA is recruited by an RdRP and dsRNA is produced, it enters the RNAi pathway (**Figure 5-32**). Transgene silencing in *M. oryzae* is thought to occur through a similar process, as MoRdRP2 and MoAgo3 are homologous to the QDE1 and QDE2 genes of *N. crassa* which are involved in transgene silencing (Lee *et al*., 2010; Raman *et al*., 2017). Further experiments are needed to confirm if transgene silencing is partially occurring with the 40-copy tandem insertion.

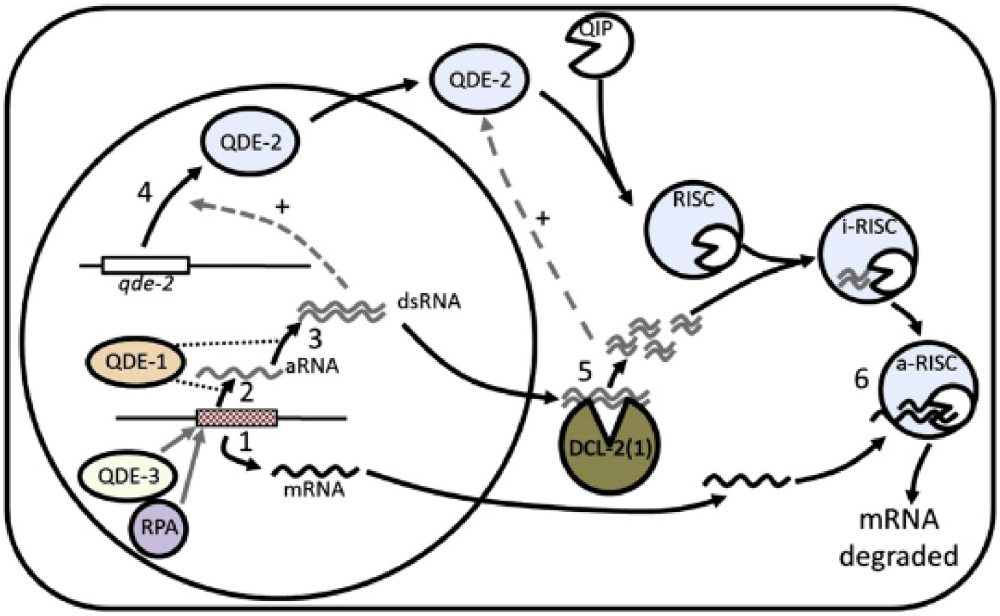


**Figure 5-32 Model of transgene silencing via quelling in *Neurospora crassa*.** 1) Host RNA polymerase generates either a normal transcript (mRNA) or 2) the DNA dependent RNA polymerase QDE-1 generates an aRNA from the transgene. 3) QDE-1 generates dsRNA. 4) The dsRNA induces transcription of the qde-2 gene. 5) Dicer like proteins DCL-2 and DCL-1 cleave the dsRNA into siRNA. The siRNA are loaded onto a RISC molecule. 6) The RISC complex is guided to the complementary mRNA transcript which is then degraded. This image was first published in Su *et al.* (2012).

### 5.5.3 Resisting transgene silencing: the role of introns and the 3′UTR

In plants, the presence of introns in transgenes has shown reduction of silencing. The hypothesis is that aberrant mRNAs are stabilised by spliceosome machinery and are unavailable for the recruitment of RDR6 (functionally similar to QDE-1 of *Neurospora*) into the RNAi pathway. In tobacco, a transgene with an endogene intron was less prone to post transcriptional gene silencing (Dadami *et al.*, 2013). Similarly, Christie *et al.* (2011) found the introduction of an intron into a transgene reduced silencing by four-fold, further suggesting competitive inhibition of RDR6 by spliceosome machinery. Therefore, one possible option for the reduction of potential transgene silencing in the *M. oryzae* delivery system would be inserting an intron into the *AvrSr50* coding sequence.

Another option for reducing transgene silencing is optimizing the choice of transcription terminator. The transcription terminator has previously thought to have a minimal role in transgene expression. Recent work from de Felippes *et al.* (2020) showed the terminator sequence has a significant effect on transgene silencing mediated by sRNA accumulation. Aberrant mRNAs conferred by improper poly(A) tails can be abrogated by a strong terminator with a well-defined poly(A) processing site. In this chapter, the terminator from the *SCD1* melanin biosynthesis gene from *Colletotrichum lagenarium* was used for all constructs.

Although this terminator has been successfully used in *M. oryzae,* it is unknown whether a different terminator with a stronger poly(A) signal would enhance *AvrSr50* transgene expression.

### 5.5.4 Positional effects: chromosomal location matters

Another explanation for the lack of strict correlation between copy number and protein yield is that certain places in the fungal genome are more transcriptionally active than others (Jeenes *et al*. 1991). Indeed, previous studies have shown integration of heterologous gene products in the *Aspergillus niger* glaA (glucoamylase) gene and *T. reesi chb1* (cellulase) gene, both known to be expressed at prodigious levels, have increased heterologous protein production levels (van Hartingsveldt *et al*., 1991; Uusitalo *et al*., 1991). In filamentous fungi, effector gene transcription is tightly regulated and coordinated (Soyer *et al*., 2014). Little expression occurs in culture, whereas high expression occurs during infection. Experiments involving the plant pathogen *Leptosphaeria maculans* suggest this tight regulation is location specific and mediated through epigenetic modification (Soyer *et al*., 2014). Therefore, I hypothesized that targeting *AvrSr50* to select regions in the genome that follow the transcriptional activity of effectors would increase *AvrSr50* mRNA (**5.4.11**).

To achieve targeted insertion, I utilised a CRISPR/Cas9 method recently optimised for *M. oryzae* (Foster *et al*. 2018). The main pathway for repairing double stranded breaks in filamentous fungi, including *M. oryzae*, is the NHEJ pathway. Thus, the efficiency of homologous recombination remains low. However, CRISPR/Cas9 technology allows double stranded breaks to occur at select places in the genome. Providing a donor DNA with homologous flanking regions increases the efficiency of HR. In this thesis, I used CRISPR/Cas9 technology to target *AvrSr50* to different *M. oryzae AVR* loci (presumed transcriptionally active regions). I targeted the PS-2 expression construct (pPWT3:PWT3SP:AvrSr50) to the *AvrPib*, *AvrRmg8*, and MGG_04257 regions. Targeting *AvrSr50* to the *AvrPib* or *AvrRmg8* locus did not result in transformants that can elicit R dependent HR (**Figure 5-22**, **Figure 5-24**). However, a single transformant targeted to MGG_04257 (C04257-2) showed inconsistent signs of HR on *Sr50*+ wheat leaves (**Figure 5-27**). It would be interesting to perform RNA-seq or RT-qPCR on this transformant to see if it has elevated levels of *AvrSr50* mRNA. This transformant has the whole vector inserted into the MGG_04257 region. It is possible large fragments of DNA in this region caused a disruption in chromatin folding dynamics, allowing the transgene to be transcriptionally active. It is possible the inconsistency in the phenotype is because the disruption is not as

large-scale as the 40-copy insertion, however, more detailed experiments are needed to assess this.

Further evidence suggesting positional effects are important for expression is that transformant CPib-11 has 25 copies of pPWT3:PWT3SP:AvrSr50 at the *AvrPib* locus but does not elicit HR on *Sr50*+ wheat (**Table 5-4**). Either these copies are being silenced, or they have been integrated into a chromosomal region that is not very transcriptionally active. It would be interesting to see where exactly the other insertions have occurred in transformants that were not able to elicit *R* dependent HR. Comparing the transcriptional dynamics of these areas during early time points of infection may provide information on the importance of positional effects in *M. oryzae* transgene expression.

### 5.5.5 Codon optimization

Codon usage bias, which exists across both prokaryotic and eukaryotic genomes, also exists in filamentous fungi (Su *et al.*, 2012). Different codons (between one and six) can code for the same amino acid, however, preference for different synonymous codons exists between different species (Gustafsson *et al.*, 2004). Inefficient translation of mRNA into protein product can be the result of "rare codons." Further, in studies involving *Neurospora*, transcriptional silencing occurs in genes containing nonoptimal codons (Zhou *et al.*, 2016). Therefore, codon optimisation plays a role in both transcription and translation. In *N. crassa*, the introduction of rare codons into the glutamate dehydrogenase gene decreased protein production by just over one third that of wild type levels (Fincham *et al.*, 1985). Inversely, when rare codons are optimised, protein production can increase. For example, Gooch *et al.* (2008) codon optimised the luciferase gene from *Photinus pyralis* (firefly) for expression in *Neurospora crassa*. This led to a 4 log order increase of light signal in comparison to a non-codon optimised gene (Gooch *et al.*, 2008) .

Codon optimization can be obtained by either site directed mutagenesis of the donor vector, or if multiple codons are to be changed, synthesizing an optimised version of the gene of interest. In terms of the *M. oryzae* expression system described in this chapter, codon optimisation would not be suitable for screening multiple AVR candidates due to time and monetary constraints. However, it would be a promising choice for characterising or confirming a few candidates of high priority. Future experiments will involve codon optimising rust avirulence genes such as *AvrSr50* for an *M. oryzae* expression system. Indeed, *AvrSr50* has 14 rare codons (fraction, or abundance of the codon relative to all other

synonymous codons, <0.07) whereas a native *M. oryzae* gene, *AvrRmg8*, only contains three (**Figure 5-33**).

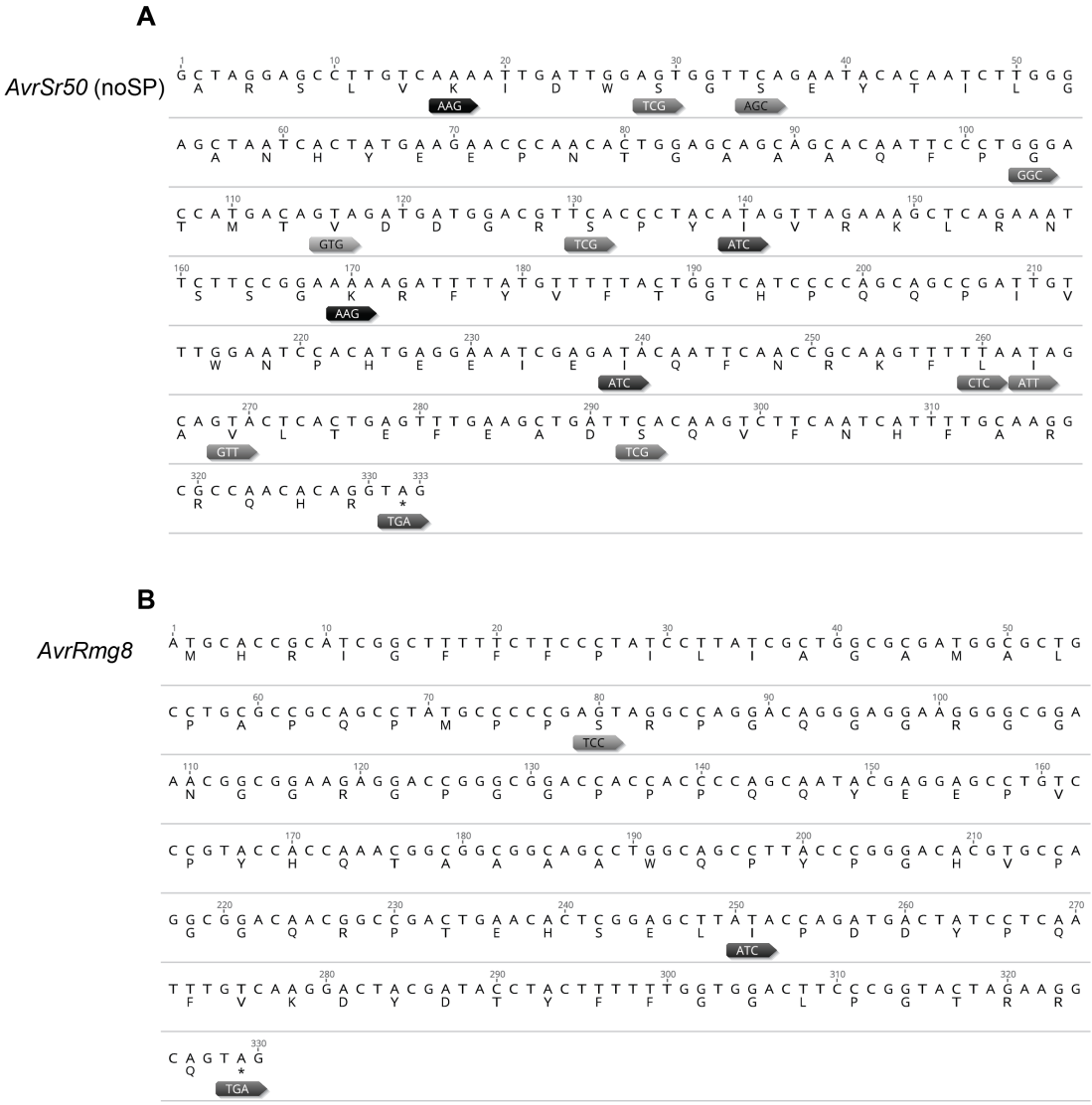


**Figure 5-33 The *AvrSr50* coding sequence contains many rare codons**. Using the codon usage table of *M. oryzae*, the coding sequence from A) *AvrSr50* shows 14 rare codons and the coding sequence from B) *AvrRmg8* shows three rare codons. Suggested alternate, non-rare codons are annotated below the rare codons. Rare codons are defined as those with a fraction or abundance relative to all other synonymous codons <0.07.

### 5.5.6 Promoter and signal peptide

The promoter and signal peptide combination, in addition to levels of transcription, also seems pertinent for proper targeting of cytoplasmic effectors to the BIC and host cytoplasm. Khang *et al*. (2010) observed fluorescent proteins can accumulate at the BIC when a cytoplasmic effector promoter and signal peptide are used. When a constitutive promoter and apoplastic effector signal peptide are used, fluorescent proteins are found outlining the invasive hyphae. Thus, the authors conclude important sequences for translocation of proteins into the host reside in the promoter and/or signal peptide region. Similarly, Rodriguez Herrero (2020) determined an apoplastic effector gene under the control of a cytoplasmic effector promoter and signal peptide re-directs the effector to the BIC and subsequently inside host plant cells. The inverse was found when a cytoplasmic effector was expressed under the control of an apoplastic effector promoter and signal peptide. It is now clear that distinct secretion systems exist for targeting cytoplasmic and apoplastic effectors to their correct locations. It is likely signals in the promoter and/or signal peptide region of an effector are responsible for targeting proteins to the correct secretion system. Khang *et al*. (2010) suggest BIC accumulation, therefore, may be a result of enhanced expression of cytoplasmic effectors in BIC associated cells. Alternatively, the authors posit 5' mRNA sequences may target mRNA to BIC associated cells before translation, an exciting prospect that to date has not been further explored. In other systems, mRNA trafficking to specific cellular locations before translation is dependent upon microtubule movement along the cytoskeleton (Vollmeister *et al*., 2012). Further, microtubule dependent mRNA transport can be determinded by 'RNA zipcodes' – localisation elements that are often located in the 5' or 3' UTR of the transcript (Vollmeister *et al*., 2012). For example, in the fungus *Ustilago maydis*, trafficking of mRNA along microtubules is essential for determining polarity during hyphal growth (Becht *et al*., 2006). If an analogous system is required for proper secretion of *M. oryzae* cytoplasmic effectors, discovery of RNA zipcodes for this process will be essential for targeting heterologous rust effectors to their proper domain.

The data provided in this chapter corresponds with previous findings that an *M. oryzae* cytoplasmic effector signal peptide and promoter can direct proteins to the cytoplasm of the host. I discovered a single transformant expressing *AvrSr50* under the control of a *PWT3* promoter and a *PWT3* signal peptide is able to elicit *R* dependent HR (**Figure 5-12**). Other transformants with a constitutive fungal promoter or native rust signal peptide were unable to elicit *R* dependent HR. I am unable to conclude if these transformants were unable to elicit *R*

dependent HR due to inappropriate promoter and signal peptide combinations, or if low copy number has prevented sufficient mRNA accumulation.

A native rust signal peptide may be functional in *M. oryzae* if rusts utilise the same secretion pathways for cytoplasmic and apoplastic effectors as *M. oryzae*. Indeed, all haustoria and invasive hyphae producing fungi might utilise similar secretion systems for partitioning effectors to their proper domains. For example, in *M. oryzae*, apoplastic effectors are secreted via the conventional ER-Golgi pathway, and cytoplasmic effectors are secreted via a Golgi independent pathway (Giraldo *et al*., 2013). *Phytophthora infestans*, an oomycete that produces haustoria, also targets cytoplasmic effectors via a Golgi independent pathway (Wang *et al*., 2017). It remains unknown if convergent evolution has occurred at the sequence level and if the signal peptides are functionally interchangeable between these diverse species. Further experiments are needed to ascertain the functionality of these signal peptides across species, and whether or not a rust signal peptide could be used in an *M. oryzae* expression system.

Currently, it remains unclear whether constitutive promoters, in combination with a cytoplasmic signal peptide, can be used to target cytoplasmic effectors to the correct domain. This has not thoroughly been investigated in *M. oryzae* to date. If 5' mRNA sequences are important for proper protein localisation, these signals may not be conferred by a constitutive promoter. Further experiments are needed to discover the exact signals required for targeting cytoplasmic effectors to their proper location. Such information will be critical for the further development of an *M. oryzae* system for the heterologous expression of rust proteins in wheat.

The use of a constitutive promoter may also be problematic for two reasons. For one, intensity of transcription conferred by constitutive promoters can also induce transgene silencing, as described above (Que *et al*., 1997). Constitutive promoters may also induce stress on the cell due to over-expression (Nevalainen & Peterson, 2014). Excessive amounts of protein targeted to the ER can overload the folding and secretion machinery (Ward, 2012). Therefore, expression must be fine-tuned. Finding the right promoter for a transcriptional sweet spot in *M. oryzae* will likely involve more trial and error experiments.

### 5.5.7 So many options, so little time

Evidently, there are many options to explore for fine tuning an *M. oryzae* heterologous expression system for cytoplasmic rust effectors. Although different *R/AVR* combinations will require different thresholds to induce cell death (only two were explored in this chapter), it is

possible to discover conditions that will be suitable for the heterologous expression of many *AVR*s. Such conditions may include what is known as a genomic "landing pad" or "safe haven". These regions within the genome not only successfully express all genes tested, but they also do not interfere with fungal growth or virulence (Schuster and Kahmann, 2019).

Further pursuing a fungal expression system for delivering AVRs in wheat is a fruitful cause. If successful, this would allow, for the first time ever, the characterisation of a rust effector in the native wheat host. Conceivably, this would allow localisation studies and protein-protein interaction studies such as an *in planta* (wheat) co-immunoprecipitation (Co-IP) to find host interactors. This is an incredibly exciting prospect, as *AvrSr50* is known to supress cell death caused by auto active coiled-coiled NLR domains (Chen *et al.*, 2017). Further studies in wheat would therefore uncover the role of *AvrSr50* in virulence and the suppression of host defence responses.

HR may sometimes reduce pathogen virulence in the absence of macroscopic cell death phenotypes. One advantage of a fungal assay is that both scenarios for HR would be detectable. Although a bacterial delivery system would be beneficial for high-throughput screens, HR that does not cause macroscopic cell death may be missed. Overall, a *M. oryzae* delivery system would be useful to confirm and complement the results obtained from other assays. In conclusion, the data provided in this chapter provides critical information for the development of another tool in the currently very limited toolbox for characterising biotrophic fungal effectors in wheat.

# Chapter 6 General Discussion

## 6.1 Identifying and characterising effectors from the wheat yellow rust pathogen

Demand for wheat in human diets remains consistently high. As a result, wheat is widely cultivated and is the leading source of plant derived protein in the human diet (Curtis *et al.*, 2002). Since the green revolution, agro-ecosystems have transformed into monocultures of elite high yielding cultivars (Van De Wouw *et al.*, 2010). The lack of genetic diversity in these crops favours the evolution of rapidly evolving pathogens that are highly virulent (McDonald and Stukenbrock, 2016). Wheat rust pathogens in particular cause losses of approximately 4 billion pounds in the UK alone (Figueroa *et al.*, 2018). Identifying novel sources of resistance to these fungal pathogens is therefore crucial to abrogate pathogen outbreak. Effectoromics, an approach for identifying the effector repertoire of a pathogen, is a major asset to modern breeding for resistance (Prasad *et al.*, 2019). The cloning of avirulence effectors, for one, can expedite discovery of resistance in wheat or other hosts with a cognate *R* gene (Prasad *et al.*, 2019). Further, monitoring allelic diversity of effectors in a current pathogen population can inform deployment of *R* genes in the subsequent growing season (Vleeshouwers and Oliver, 2014). Despite the importance of effectors on identifying resistance to the wheat rusts, few effectors have been functionally characterised. To date, zero avirulence effectors have been confirmed for the yellow rust pathogen *Pst*. In this thesis I aimed to address this issue by using comparative genomics and heterologous expression systems to identify and functionally characterise effectors of *Pst*.

## 6.2 Comparative genomic studies for finding cereal rust effectors

Comparative genomics is used to reveal differences between the genomes of individuals with variances in a phenotype of interest (Plissonneau *et al.*, 2017). These genomic differences are identified as candidates for contributing to the phenotype in question. This has been done with pathogenic fungi, whereby the genomes of isolates with differing virulence profiles are compared. For example, the avirulence effector Ave1 from the fungal phytopathogen *Verticillium dahliae* was identified through comparative genomics between races that differed in pathogenicity to tomato plants with and without the cognate receptor (De Jonge *et al.*, 2012). Using a similar method, Schmidt *et al.* (2016) compared the genomes of pathogenic and non-pathogenic strains of the melon wilt fungal pathogen *Fusarium oxysporum f.sp. melonis* to find AvrFom2.

### 6.2.1 Limitations

Clearly, comparative genomics is an incredibly powerful method for identifying effectors of fungal phytopathogens. Like all methods, comparative genomics is limited by the resources put into it. For example, comparing the genomes of isolates with multiple differences in their virulence profiles provides effector candidates that may not be associated with a single *R* gene. For example, Upadhyaya *et al.* (2015) compared the genomes between the *Pgt* isolate 21-0 and clonal derivatives 34M1 and 34M2 that gained virulence for resistance genes *Sr5, Sr11, Sr27*, and *SrSatu*. Novel mutations found in 34M1 and 34M2 may explain virulence towards the four *Sr* genes 21-0 is avirulent to. However, further analyses will require association between these variants and individual *Sr* genes. Further, the 21-0 isolate was sampled in the 1950s, whereas the gain of virulence field isolates derived from 21-0 were sampled in 1980. Over time, somatic mutations may have occurred that are not associated with phenotypic changes at all.

In this thesis I used isolates with minimal variation due to phylogenetic divergence. This was achieved by comparing wild type isolates containing *AvrYr2* with spontaneous gain of virulence mutants that were sampled over 1-2 growing seasons (chapter 2). This decreased the amount of time for stepwise mutations to occur that may not be associated with virulence. Further, I was able to compare isolates that only differed in their virulence to a single *R* gene, *YR2*. These exact same conditions were required for the cloning of the *Pgt* avirulence effector *AvrSr50* (Chen *et al.*, 2017).

### 6.2.2 Gain of virulence mutants combined with second and third generation sequencing: the future of *AVR* discovery?

As previously mentioned, recent spontaneous gain of virulence mutants are ideal for comparative genomics studies as phylogenetic divergence between the isolates is limited, and there is only one change in the virulence profile between the two isolates. Gain of virulence mutants can be obtained spontaneously, or through induced mutagenesis using agents such as EMS. Spontaneous gain of virulence mutants can be obtained for *Pst* in as little as two growing seasons (Sørensen *et al.*, 2013). Obtaining spontaneous gain of virulence mutants for the cloning of avirulence alleles in the cereal rusts is become more and more common, as evidenced in the cloning of *AvrSr50* from *Pgt* (Chen *et al.*, 2017). Similarly, chemically induced gain of virulence mutants are becoming very useful and common in identifying avirulence alleles of the cereal rusts (Salcedo *et al.*, 2017). Clearly, both methods are now established for use in the cereal rusts and will likely play a major role in identifying further *AVR* genes.

In combination with gain of virulence mutants, identification of *AVR* genes seems to be dependent on a highly contiguous reference genome or pan-genome produced with both second and third generation sequencing (Chen *et al.*, 2017; Salcedo *et al.*, 2017) . As these methods are becoming more accessible, I predict producing such references will become part of a gold standard in future effector discovery pipelines.

The next step in the *AvrYr2* analysis described in this thesis, therefore, will be generating a new *de novo* assembly of the *AvrYr2* wild type isolates, which has multi-fold advantages. Firstly, the generation of these new references will likely aid in the discovery of *AvrYr2*. Secondly, sequences found in these isolates that are absent in the currently available phased references can be used towards producing a pan-genome. Further, these genomes will aid in the study of large structural variations between *Pst* isolates, and how this may contribute to virulence evolution.

## 6.3 Challenges, limitations, and future directions in functional characterisation of wheat rust effectors

Functional characterisation of wheat rust effectors is mainly hampered by the lack of genetic transformation methods. Particle bombardment of urediniospores of *Pgt* has been previously successful (Schillberg *et al.,* 2000) however frequency events are low and rarely replicated (Bakkeren and Szabo, 2020). With developments in molecular biology, waiting for the right conditions for stable transformants is just a matter of time. Until then, functional characterisation of cereal rust effectors in the native host will heavily rely on heterologous expression systems. Like all heterologous expression systems, those designed for the delivery of rust effectors in wheat have their limitations.

### 6.3.1 Heterologous expression systems are limited by the knowledge of the surrogate organism

#### 6.3.1.1 The bacterial T3SS

In chapter 4, I investigated the utility of the T3SS from three bacteria for the delivery of rust effectors in wheat. Although I could not confirm avirulence of two previously described fungal effectors in these systems, further optimisation of a bacterial delivery system would be useful due to the high-throughput nature of this protein delivery method. These further experiments would benefit from more knowledge of the basic biology of the T3SS. Currently it is unclear whether or not the N-terminal secretion signal is within the mRNA or the amino acid sequence (Habyarimana and Ahmer, 2013). Some studies show frameshift mutations in the

N-terminal region of a T3SS effector do not affect secretion or protein function, suggesting the amino acid sequence of the signal is not important (Sorg *et al.,* 2005). Further, some 5' UTRs from effectors of *Salmonella* can translocate the Cya protein into eukaryotic host cells (Niemann *et al*., 2013). It is likely different effectors may require different kinds of secretory signals and may have evolved several methods for targeting to the same location. Understanding these aspects of T3SS secretion in better detail would aid in developing a heterologous expression system using T3SS components.

Another element to consider is that cereal rust proteins are eukaryotic and very divergent from those produced in native bacterial cells. There may be nuances in bacterial transcription and translation regulation that are efficient with bacterial sequences and not eukaryotic sequences. Testing codon optimisation in bacteria may be helpful for this reason. However, divergent oomycete and flax rust effector sequences have successfully been delivered by the T3SS of *Pfo* EtHAn into *Arabidopsis* and *N. tabacum* (Sohn *et al*., 2007; Upadhyaya *et al*., 2014). This suggests a wheat specific incompatibility with the *Pfo* EtHAn system for unknown reasons. These reasons may be determined as more information is revealed about the basic biology of the T3SS.

Currently, it is incredibly difficult to study the translocation of effectors across the T3SS, as fluorescent tags often clog the narrow pilus (Galán, 2009). Some success of protein translocation has been shown by tagging a calmodulin-dependent adenylate cyclase (Cya) domain to the effector being studied (Young and Palmer, 2017). This domain, only active in eukaryotes, will bind to calmodulin to produce cAMP, which is easily detected in an ELISA (enzyme-linked immunosorbent assay). However, the Cya domain itself, although naturally secreted by *Bordetella pertussis* through the T3SS, has the potential to clog the pilus as a chimeric protein. In *Arabidopsis*, stable transgenic lines have recently been made to express $GFP_{1-10}$ which contains ten out of the eleven strands of the GFP barrel (Henry *et al*., 2017). Effectors delivered via the T3SS are tagged with only the $11^{th}$ strand of GFP, and thus localisation is detected upon reconstitution of all 11 GFP strands in the plant. Creating wheat transgenic lines expressing $GFP_{1-10}$ would be incredibly useful for detecting the translocation of effectors via the T3SS. It is currently unknown how much heterologous rust protein the Pfo EtHAn system described in chapter 4 is being delivered into wheat, if at all. A reliable system for detecting translocation would mitigate this issue, and further aid in the optimisation of T3SS mediated delivery in wheat.

#### 6.3.1.2 *Magnaporthe oryzae* mediated protein secretion

Similar to the bacterial T3SS, the exact requirements for secretion to the host cytoplasm is not fully known for *Magnaporthe*. Although cytoplasmic effector signal peptides are required for proper localisation to the host cytoplasm, the involvement of other components such as the 5' UTR within the promoter region is not known (Khang *et al.*, 2010). Further, *Magnaporthe* is an ascomycete, whereas the cereal rusts are basidiomycetes. Similar to the bacterial system, there may be differences between the regulation of transcription and translation that differ between these two groups of fungi. When *M. oryzae* expresses non-codon optimised mRFP under a cytoplasmic effector signal peptide, clear localisation can be seen in rice cells (Khang *et al.*, 2010). This suggests the *M. oryzae* heterologous expression system is capable of translocating divergent proteins into the host. However, specific levels of protein may be required for the elicitation of a hypersensitive response. Therefore, more knowledge on the targeting and transcriptional regulation of native *Magnaporthe* cytoplasmic effectors will be beneficial for optimising a heterologous expression system.

### 6.3.2 Advances in *M. oryzae* molecular genetics: optimisation of a heterologous secretion system in MoT is likely near

The optimisation of the *M. oryzae* heterologous secretion system is likely near due to recent advances in molecular genetics of this system. In 2018, a CRISPR/Cas9 system was described for editing the *M. oryzae* genome (Foster *et al.*, 2018). In chapter 5 I confirmed this protocol efficiently produces mutants in selected regions of the *M. oryzae* genome. Therefore, further investigations requiring targeted insertions of rust effectors to specific locations in the *M. oryzae* genome will be easy to do. Further optimisation of the *M. oryzae* heterologous secretion system may also require additional sequencing with next generation technologies. For example, it may be useful to understand chromatin accessibility of the *Magnaporthe* genome during early stages of infection to determine candidate regions for inserting rust effectors. It would also be beneficial to confirm if silencing is occurring in transformants that are not expressing the *AvrSr50* transgene described in chapter 5. These questions can easily be answered with technologies that require next generation sequencing such as Assay for Transposase-Accessible Chromatin with high-throughput sequencing (ATAC-seq) (Yan *et al.*, 2020) . This method identifies open regions of chromatin by probing with Tn5 transposase that can insert sequence adapters only to open regions of the genome (Buenrostro *et al.*, 2013). In chapter 5 I describe the sequencing of the *M. oryzae* genome with Nanopore technology - a relatively straightforward and quick process. Due to the amenability of this fungus to molecular manipulation, it is likely other methods such as ATAC-seq will work well *M.*

*oryzae*. Therefore, it is only a matter of time until this method is optimised for the functional characterisation of rust effectors in wheat.

### 6.3.3 Towards a more holistic view of functional characterisation

The toolbox for functional characterisation of effectors in wheat continues to grow. All of these methods will have their own pros and cons, summarized in **Table 6-1**. No one system will be perfect and applicable in all cases. Therefore, it is useful to consider all of these methods side by side as the results from multiple systems may complement one another. In chapter 4, I tested delivery systems involving the bacterial T3SS. In chapter 5, I explored a novel MoT mediated delivery system. In both chapters, only two fungal *AVRs* of wheat pathogens were tested. Due to the nature of these heterologous expression systems, it is entirely possible other *R/AVR* pairs could be identified using these systems in their current state. Both systems require the production of chimeric proteins, as a signal peptide is required for targeting effectors to both the T3SS of bacteria and to the BIC of MoT. The stability and functionality of chimeric proteins are sometimes unpredictable and will vary between proteins being delivered.

Only three systems listed in **Table 6-1** are capable of detecting both virulence and avirulence phenotypes of candidate effectors in wheat. These include the T3SS delivery system, the viral overexpression system, and the MoT delivery system. As mentioned in chapter 4, the T3SS delivery system is already routinely used to describe virulence properties of effectors (Prasad *et al.*, 2019). However, to date, its functionality in describing avirulence properties is not known. The viral overexpression system has successfully been used to describe avirulence properties of effectors by the subsequent decrease in viral propagation in incompatible wheat cultivars (Chen *et al.*, 2017). However, its utility in describing virulence is currently not known. Conceptually, fluorescent tags could be used for localisation studies using viral systems compatible with larger constructs such as FoMV (Bouton *et al.*, 2018). However, this has not yet been shown. In chapter 5, I have shown that the MoT system can be used to confirm avirulence of wheat rust effectors via an HR response in wheat containing the cognate *R* gene. Further studies are required to optimise this system to allow the replication of these results. Once this is achieved, localisation and Co-IP experiments could be easily achieved with tags, as these experiments are already done with native *Magnaporthe* effectors. However, depending on the strain being used, the native MoT effectors may unintentionally interact with the rust *AVR* being studied. Therefore, it is important to utilise multiple methods concurrently to functionally characterise wheat rust effectors.

**Table 6-1** Pros and cons of different heterologous systems for studying cereal rust effectors in the native wheat host

| Method | Pros | Cons |
|---|---|---|
| **T3SS delivery** | - High-throughput<br>- If successful, can detect avirulence via cell death<br>- Used routinely to study virulence (suppression of cell death or PTI in wheat leaves) (Prasad *et al.*, 2019) | - No successful case yet for detecting cereal rust *AVR*s in wheat<br>- Fluorescent tags often clog the T3SS, localisation of effectors is limited (Galán, 2009)<br>- The presence of native bacterial effectors may confound analysis (depending on which bacterial isolate is being used) |
| **Viral overexpression** | - Can detect avirulence via decrease in viral reproduction (Chen *et al.*, 2017)<br>- Viruses that can stably express larger fragments could be used for localisation (ex. FoMV, however this has not yet been demonstrated) (Bouton *et al.*, 2018) | - Stable expression is size limited in some viruses including BSMV (Bouton *et al.*, 2018). Larger *AVRs* are excluded and localisation with a large fluorescent tag cannot be done<br>- Limited to wheat varieties the chosen virus can replicate in |
| **Protoplast assays** | - Can confirm avirulence via decrease in reporter signal in wheat protoplasts (Saur *et al.*, 2019)<br>- If the associated *R* gene is cloned, the *AVR* and *R* gene can be co-delivered, allowing fine tuning for expression required for avirulence (Saur *et al.*, 2019) | - Cannot be used to study virulence beyond localisation<br>- Natural *R* gene expression varies between different wheat varieties. Some varieties may show signs of avirulence, while others may not |
| **Particle Bombardment** | - Can confirm avirulence via decrease in reporter signal in wheat leaves (Jia *et al.*, 2000) | - Difficult to use for studying virulence |
| **HIGS** | - Can be used to detect virulence of non-redundant effectors: silencing results in reduced *Pst* virulence (Zhao *et al.*, 2018) | - Effectors with redundant roles in virulence will not be detected<br>- utility for detecting avirulence not known (conceptually possible via gain of virulence if the avirulence gene is silenced) |
| **Immuno-cytochemical localisation** | - Could be used to show localisation of effectors in wheat | - Can only be used for localisation studies<br>- Incredibly labour intensive; only done with bean rust effector RTP1p (Kemen *et al.*, 2005) |
| **Magnaporthe delivery system** | - Can be used to detect avirulence via HR or reduced pathogenesis (this thesis)<br>- Could be used for localisation with a fluorescent tag<br>- Could potentially be used for *in planta* Co-IP experiments to find plant interactors | - Presence of effectors in the WT *MoT* isolate being used may affect interpretation of results |

## 6.4 Chasing effectors: Why bother?

This entire thesis has focussed on identifying and characterising wheat rust effectors in the native host. The following section describes the importance of this search, and the practical implications of effector discovery.

### 6.4.1 Using effectors to clone new *R* genes

One major utility of effectors in the context of resistance breeding is accelerating the cloning of new *R* genes (Prasad *et al.*, 2019). For example, cloning *AvrYr2* could in turn be used to clone the cognate resistance gene *YR2*. Currently *YR2* is not cloned, however, the closest SSR marker determined is 5.6 cM from the *YR2* locus (Lin *et al.*, 2005). If the recognition of *AvrYR2* by *YR2* is direct or not dependent on wheat specific proteins, NLR proteins within this locus could be transiently co-expressed in *N. benthamiana* with *AvrYr2* to identify *YR2*.

Further, cloned *Pst* effectors could be used to screen the wheat germplasm for novel sources of resistance. A relatively untapped source of resistance also lies within wild relatives and other closely related species of wheat (Wulff and Moscou, 2014). Cloned *Pst* effectors could be used to screen for novel recognition in these sources of resistance. The wheat blast delivery system described in this thesis would aid in this discovery, as MoT can infect multiple different hosts including grasses, barley, and rye (Ceresini *et al.*, 2018).

### 6.4.2 Testing *R* gene stacking

Although deploying new resistance genes into the wheat germplasm is a popular method of managing disease caused by pathogens, *R* gene-mediated resistance is often hindered by the rapid evolution of pathogen effectors (Zhang and Coaker, 2017). Currently, breeding programs are working to mitigate this issue by integrating multiple *R* genes within a single cultivar, a process known as stacking or pyramiding (Dong and Ronald, 2019; Mundt, 2018). This method is predicted to increase the durability of resistance to pathogen strains as overcoming multiple *R* genes simultaneously is less likely to happen. Although evaluating durability is extremely difficult, pyramiding by delaying resistance breakdown remains a promising strategy to control pathogen outbreaks (Mundt, 2018).

However, it is unknown if all *R* genes in a stack will be expressed, or if there will be negative interactions between them. Each corresponding *AVR* from the pathogen therefore must be individually tested on these stacked wheat cultivars. For example, resistance conferred by

stacked *R* genes in the potato cultivar 'Sarpo Mira' were disentangled by individual *Phytophthora infestans* effectors instead of differential pathogen sets (Rietman *et al.*, 2012). Currently, there are more cloned *R* genes for resistance to *Pst* than there are cloned *AVR* genes. Therefore, finding new *AVR* genes for *Pst* is essential for verifying the validity of stacking *R* genes. In other pathosystems, transient expression of these effectors (ex. via agroinfiltration) has provided confirmation that all components of the *R* gene stack are functional (Vleeshouwers and Oliver, 2014). The development of the *M. oryzae* expression system described in this thesis would potentially aid in the assessment of *R* gene stacks by delivering *Pst AVR* genes individually, as opposed to challenge with differential *Pst* isolates.

### 6.4.3 Engineering new *R* genes

Another strategy for broadening the resistance of a wheat cultivar is to engineer a single resistance gene to recognize multiple *AVR* alleles at the same time (Rodriguez-Moreno *et al.*, 2017). Better yet, resistance genes that can detect multiple alleles of a "core effector", proteins that are essential to pathogen fitness, are predicted to provide durable resistance (Vleeshouwers and Oliver, 2014). In order to engineer these resistance proteins, however, more information is needed from the effectors themselves. As previously mentioned, no *AVR* proteins have been identified for *Pst.* This would be essential for determining the 3D structure of these effectors, information required for engineering resistance.

For example, De La Concepcion *et al.* (2019) used structural information of a rice NLR bound to its cognate *AVR* protein to expand recognition specificity of the NLR. Using this technique, the rice NLR protein Pikp was engineered to recognize additional alleles to the effector AVR-Pik from *M. oryzae*. A particular mutation in the binding interface between the NLR and effector was responsible for the recognition of additional alleles previously not recognized by Pikp.

As more effectors are cloned from *Pst*, this technique would be possible for the *Pst*-wheat pathosystem. It would be particularly interesting to find matching effectors associated with *R* genes that have been widely overcome, such as *YR2* (Wellings, 2011). For example, if AvrYr2 interacts with its cognate R protein directly, there may be an allelic series similar to Avr-Pik that differ in amino acids at the binding interface. Therefore, YR2 could theoretically be engineered to recognize multiple alleles already in the population.

### 6.4.4 Baits for finding new *S* genes

Plant susceptibility genes (*S* genes) are critical for facilitating compatible interactions with phytopathogenic fungi and often function as negative regulators of defence (Pavan *et al.*, 2010). Therefore, deploying loss of *S* genes is another strategy for breeding resistance in wheat.

Perhaps one of the best characterised *S* genes is barley *Mlo* (mildew locus O) which functions as a negative regulator of immunity. Resistance can be conferred to powdery mildew pathogens by causing loss of function mutations in the *Mlo* locus (Büschges *et al.*, 1997). In terms of wheat, the *TaNAC1* gene has been functionally validated as a susceptibility factor towards *Pst*. When silenced via BSMV-VIGS, this gene confers enhanced resistance to yellow rust (Wang *et al.*, 2015).

Effectors can be used as baits for finding *S* genes, as effector proteins often bind directly to *S* gene products (Hogenhout *et al.*, 2009). For example, a study in *Arabidopsis* identified plant proteins that were targets of multiple effectors from diverse pathogens (Weßling *et al.*, 2014). Plant mutants for one of these genes, *CSN5A*, displayed enhanced resistance towards hemibiotrophic and biotrophic pathogens.

For *Pst*, not many *S* genes in wheat have been identified. Therefore, it is pertinent to identify and characterise more *Pst* effectors that could be used as baits for discovering *S* genes. Until *Pst* can be transformed, using effectors as molecular probes to find *S* genes in the wheat germplasm will have to be via heterologous expression. It would be interesting to see if an *M. oryzae* delivery system could be optimised for the delivery of *AVR* proteins in wheat for the identification of *S* genes. If enough protein can be delivered, an *in-planta* Co-IP in wheat could identify susceptibility proteins.

### 6.4.5 Effectors as markers for monitoring allelic diversity

Cloned effectors can also be used as markers to track the changes in virulence across pathogen populations (Bakkeren and Szabo, 2020). Phenotyping and genotyping multiple isolates over time can reveal changes in frequency of virulent isolates and changes in sequence diversity of the associated avirulence allele. Knowledge of effector allelic diversity in current pathogen populations can help inform breeders which *R* genes to deploy in the subsequent growing season (Vleeshouwers and Oliver, 2014). For example, *Pst* isolates that are heterozygous for an avirulent allele pose a high risk of mutating to evade recognition of the cognate R protein. Unfortunately, since no *AVR* genes are cloned for *Pst*, genotyping field isolates will only

provide race information of the current population (Bakkeren and Szabo, 2020). Therefore, identifying and cloning effectors are crucial for breeding strategies informed by the allelic diversity of current *Pst* populations. As pathogen diagnostics are becoming more sophisticated, genotypic analysis of field isolates can happen in real-time (Figueroa *et al*., 2020). For example, the Mobile And Real-time PLant disEase (MARPLE) diagnostic system utilises portable sequencing technology to sequence and identify pathogen isolate races in real time (Radhakrishnan *et al*., 2019). In the future, as *AVR* alleles are discovered, these sequences can be incorporated into pathogen surveillance systems such as MARPLE to better inform *R* gene deployment.

## 6.5 Concluding statement

The cereal rust fungi are incredibly beautiful and complex organisms in their own right. Their complexity ranges from their complicated life styles to their incredibly large genomes (Duplessis *et al.,* 2014). Many aspects of the cereal rust fungi, including the infection process on compatible hosts, remains elusive. This is largely due to the intractability of these organisms to molecular biology. Despite this, recent advances in heterologous expression systems and genome sequencing have progressed the field. For example, in chapter 2, I utilised comparative genomics to identify candidate *AvrYr2* effectors. Further, in chapters 4 and 5 I utilised advances in molecular biology to investigate heterologous systems for studying rust effector biology. It is an exciting time to study cereal rust biology as there is still so much to explore and discover. With molecular biological techniques and genome sequencing constantly improving, the unknowns of the cereal rusts are slowly starting to be deciphered.

# References


Agrios G. N. (2005). *Plant Pathology.* Burlington, MA: Elsevier Academic Press.

Aime, M. Catherine, Alistair R. McTaggart, Stephen J. Mondo, and Sébastien Duplessis. 2017. "Phylogenetics and Phylogenomics of Rust Fungi." *Advances in Genetics* 100: 267–307. https://doi.org/10.1016/bs.adgen.2017.09.011.

Akeda, Yukihiro, and Jorge E. Galán. 2005. "Chaperone Release and Unfolding of Substrates in Type III Secretion." *Nature* 437 (7060): 911–15. https://doi.org/10.1038/nature03992.

Ali, Sajid, Pierre Gladieux, Marc Leconte, Angélique Gautier, Annemarie F. Justesen, Mogens S. Hovmøller, Jérôme Enjalbert, and Claude de Vallavieille-Pope. 2014. "Origin, Migration Routes and Worldwide Population Genetic Structure of the Wheat Yellow Rust Pathogen *Puccinia striiformis f.* sp. *tritici*." *PLoS Pathogens* 10 (1). https://doi.org/10.1371/journal.ppat.1003903.

Anders, Simon, Paul Theodor Pyl, and Wolfgang Huber. 2015. "HTSeq-A Python Framework to Work with High-Throughput Sequencing Data." *Bioinformatics* 31 (2): 166–69. https://doi.org/10.1093/bioinformatics/btu638.

Anderson, Jeffrey C., Ying Wan, Young Mo Kim, Ljiljana Pasa-Tolic, Thomas O. Metz, and Scott C. Peck. 2014. "Decreased Abundance of Type III Secretion System Inducing Signals in *Arabidopsis* Mkp1 Enhances Resistance against *Pseudomonas syringae*." *Proceedings of the National Academy of Sciences of the United States of America* 111 (18): 6846–51. https://doi.org/10.1073/pnas.1403248111.

Andrews, S. (2010). FastQC: A Quality Control Tool for High Throughput Sequence Data [Online]. Available online at: http://www.bioinformatics.babraham.ac.uk/projects/fastqc/

Anh, Vu Lan, Yoshihiro Inoue, Soichiro Asuke, Trinh Thi Phuong Vy, Nguyen Tuan Anh, Shizhen Wang, Izumi Chuma, and Yukio Tosa. 2018. "*Rmg8* and *Rmg7*, Wheat Genes for Resistance to the Wheat Blast Fungus, Recognize the Same Avirulence Gene *AVR-Rmg8*." *Molecular Plant Pathology* 19 (5): 1252–56. https://doi.org/10.1111/mpp.12609.

Antipov, Dmitry, Anton Korobeynikov, Jeffrey S. McLean, and Pavel A. Pevzner. 2016. "HybridSPAdes: An Algorithm for Hybrid Assembly of Short and Long Reads." *Bioinformatics* 32 (7): 1009–15. https://doi.org/10.1093/bioinformatics/btv688.

Arnold, Roland, Stefan Brandmaier, Frederick Kleine, Patrick Tischler, Eva Heinz, Sebastian

Behrens, Antti Niinikoski, Hans Werner Mewes, Matthias Horn, and Thomas Rattei. 2009. "Sequence-Based Prediction of Type III Secreted Proteins." *PLoS Pathogens* 5 (4). https://doi.org/10.1371/journal.ppat.1000376.

Arora, Sanu, Burkhard Steuernagel, Kumar Gaurav, Sutha Chandramohan, Yunming Long, Oadi Matny, Ryan Johnson, et al. 2019. "Resistance Gene Cloning from a Wild Crop Relative by Sequence Capture and Association Genetics." *Nature Biotechnology* 37 (2): 139–43. https://doi.org/10.1038/s41587-018-0007-9.

Avgeri, Sophia G., Dimitrios K. Matthaiou, George Dimopoulos, Alexandros P. Grammatikos, and Matthew E. Falagas. 2009. "Therapeutic Options for *Burkholderia cepacia* Infections beyond Co-Trimoxazole: A Systematic Review of the Clinical Evidence." *International Journal of Antimicrobial Agents* 33 (5): 394–404. https://doi.org/10.1016/j.ijantimicag.2008.09.010.

Baeg, Kyungmin, Hiro Oki Iwakawa, and Yukihide Tomari. 2017. "The Poly(A) Tail Blocks RDR6 from Converting Self mRNAs into Substrates for Gene Silencing." *Nature Plants* 3 (March). https://doi.org/10.1038/nplants.2017.36.

Bakkeren, Guus, and Les J. Szabo. 2020. "Progress on Molecular Genetics and Manipulation of Rust Fungi." *Phytopathology* 110 (3): 532–43. https://doi.org/10.1094/PHYTO-07-19-0228-IA.

Bao, Jiandong, Meilian Chen, Zhenhui Zhong, Wei Tang, Lianyu Lin, Xingtan Zhang, Haolang Jiang, et al. 2017. "PacBio Sequencing Reveals Transposable Elements as a Key Contributor to Genomic Plasticity and Virulence Variation in *Magnaporthe oryzae*." *Molecular Plant* 10 (11): 1465–68. https://doi.org/10.1016/j.molp.2017.08.008.

Bayer, Philipp E., Agnieszka A. Golicz, Armin Scheben, Jacqueline Batley, and David Edwards. 2020. "Plant Pan-Genomes Are the New Reference." *Nature Plants* 6 (8): 914–20. https://doi.org/10.1038/s41477-020-0733-0.

Becht, P., König, J., & Feldbrügge, M. (2006). The RNA-binding protein Rrm4 is essential for polarity in *Ustilago maydis* and shuttles along microtubules. *Journal of Cell Science*, *119*(23), 4964–4973. https://doi.org/10.1242/jcs.03287

Beddow, Jason M., Philip G. Pardey, Yuan Chai, Terrance M. Hurley, Darren J. Kriticos, Hans Joachim Braun, Robert F. Park, William S. Cuddy, and Tania Yonow. 2015. "Research Investment Implications of Shifts in the Global Geography of Wheat Stripe Rust." *Nature Plants* 1 (October): 1–5. https://doi.org/10.1038/nplants.2015.132.

Blumke, A., C. Falter, C. Herrfurth, B. Sode, R. Bode, W. Schafer, I. Feussner, and C. A.

Voigt. 2014. "Secreted Fungal Effector Lipase Releases Free Fatty Acids to Inhibit Innate Immunity-Related Callose Formation during Wheat Head Infection." *Plant Physiology* 165 (1): 346–58. https://doi.org/10.1104/pp.114.236737.

Bolger, Anthony M., Marc Lohse, and Bjoern Usadel. 2014. "Trimmomatic: A Flexible Trimmer for Illumina Sequence Data." Bioinformatics 30 (15): 2114–20. https://doi.org/10.1093/bioinformatics/btu170.

Bourras, Salim, Kaitlin Elyse McNally, Roi Ben-David, Francis Parlange, Stefan Roffler, Coraline Rosalie Praz, Simone Oberhaensli, et al. 2015. "Multiple Avirulence Loci and Allele-Specific Effector Recognition Control the *Pm3* Race-Specific Resistance of Wheat to Powdery Mildew." *Plant Cell* 27 (10): 2991–3012. https://doi.org/10.1105/tpc.15.00171.

Bouton, Clément, Robert C. King, Hongxin Chen, Kasi Azhakanandam, Stéphane Bieri, Kim E. Hammond-Kosack, and Kostya Kanyuka. 2018. "Foxtail Mosaic Virus: A Viral Vector for Protein Expression in Cereals." *Plant Physiology* 4 (177): 1352-1367. https://doi.org/10.1104/pp.17.01679.

Bray, Nicolas L., Harold Pimentel, Páll Melsted, and Lior Pachter. 2016. "Near-Optimal Probabilistic RNA-Seq Quantification." *Nature Biotechnology* 34 (5): 525–27. https://doi.org/10.1038/nbt.3519.

Brethour, C, and a Weersink. 2001. "An Economic Evaluation of the Environmental Benefits from Pesticide Reduction." *Agricultural Economics* 25: 219–26. https://doi.org/DOI: 10.1016/S0169-5150(01)00079-2.

Bueno-Sancho, V., Clare M. Lewis, Diane G. O. Saunders. 2020. Advances in Understanding the Biology and Epidemiology of Rust Diseases of Cereals. In *Achieving durable disease resistance in cereals.*

Buenrostro, Jason D., Paul G. Giresi, Lisa C. Zaba, Howard Y. Chang, and William J. Greenleaf. 2013. "Transposition of Native Chromatin for Fast and Sensitive Epigenomic Profiling of Open Chromatin, DNA-Binding Proteins and Nucleosome Position." *Nature Methods* 10 (12): 1213–18. https://doi.org/10.1038/nmeth.2688.

Burg, Harrold A. Van den, Nienke Westerink, Kees Jan Francoijs, Ronelle Roth, Esmeralda Woestenenk, Sjef Boeren, Pierre J.G.M. De Wit, Matthieu H.A.J. Joosten, and Jacques Vervoort. 2003. "Natural Disulfide Bond-Disrupted Mutants of AVR4 of the Tomato Pathogen *Clados*p*orium fulvum* Are Sensitive to Proteolysis, Circumvent Cf-4-Mediated Resistance, but Retain Their Chitin Binding Ability." *Journal of Biological Chemistry* 278 (30): 27340–46. https://doi.org/10.1074/jbc.M212196200.

Büschges, Rainer, Karin Hollricher, Ralph Panstruga, Guus Simons, Marietta Wolter, Adrie

Frijters, Raymond Van Daelen, et al. 1997. "The Barley *Mlo* Gene: A Novel Control Element of Plant Pathogen Resistance." *Cell* 88 (5): 695–705. https://doi.org/10.1016/S0092-8674(00)81912-1.

Büttner, Daniela, and Sheng Yang He. 2009. "Type III Protein Secretion in Plant Pathogenic Bacteria." *Plant Physiology* 150 (4): 1656–64. https://doi.org/10.1104/pp.109.139089.

Calonnec, A., R. Johnson, and C. De Vallavieille-Pope. 1997. "Identification and Expression of the Gene *Yr2* for Resistance to *Puccinia striiformis* in the Wheat Differential Cultivars Heines Kolben, Heines Peko and Heines VII." *Plant Pathology* 46 (3): 387–96. https://doi.org/10.1046/j.1365-3059.1997.d01-22.x.

Cantu, D, V Segovia, D MacLean, R Bayles, X Chen, S Kamoun, J Dubcovsky, D G Saunders, and C Uauy. 2013. "Genome Analyses of the Wheat Yellow (Stripe) Rust Pathogen *Puccinia striiformis f.* sp. *tritici* Reveal Polymorphic and Haustorial Expressed Secreted Proteins as Candidate Effectors." *BMC Genomics* 14: 270. https://doi.org/10.1186/1471-2164-14-270\n1471-2164-14-270 [pii].

Cantu, Dario, Manjula Govindarajulu, Alex Kozik, Meinan Wang, Xianming Chen, Kenji K. Kojima, Jerzy Jurka, Richard W. Michelmore, and Jorge Dubcovsky. 2011. "Next Generation Sequencing Provides Rapid Access to the Genome of *Puccinia striiformis f.* sp. *tritici*, the Causal Agent of Wheat Stripe Rust." *PLoS ONE* 6 (8): 4–11. https://doi.org/10.1371/journal.pone.0024230.

Carroll, Anne M., James A. Sweigard, and Barbara Valent. 1994. "Improved Vectors for Selecting Resistance to Hygromycin." *Fungal Genetics Reports* 41 (1): 22. https://doi.org/10.4148/1941-4765.1367.

Casper-Lindley, Catharina, Douglas Dahlbeck, Eszter T. Clark, and Brian J. Staskawicz. 2002. "Direct Biochemical Evidence for Type III Secretion-Dependent Translocation of the AvrBs2 Effector Protein into Plant Cells." *Proceedings of the National Academy of Sciences of the United States of America* 99 (12): 8336–41. https://doi.org/10.1073/pnas.122220299.

Cassandri, Matteo, Artem Smirnov, Flavia Novelli, Consuelo Pitolli, Massimiliano Agostini, Michal Malewicz, Gerry Melino, and Giuseppe Raschellà. 2017. "Zinc-Finger Proteins in Health and Disease." *Cell Death Discovery* 3 (1). https://doi.org/10.1038/cddiscovery.2017.71.

Catanzariti, A.-M., Peter N. Dodds, G. J. Lawrence, M. A. Ayliffe, and J. G. Ellis. 2006. "Haustorially Expressed Secreted Proteins from Flax Rust Are Highly Enriched for Avirulence Elicitors." *The Plant Cell* 18 (1): 243–56. https://doi.org/10.1105/tpc.105.035980.

Catanzariti, Ann-Maree, Peter N Dodds, Thomas Ve, Bostjan Kobe, Jeffrey G Ellis, and Brian J Staskawicz. 2010. "The AvrM Effector from Flax Rust Has a Structured C-Terminal Domain and Interacts Directly with the M Resistance Protein." *Molecular Plant-Microbe Interactions* 23 (1): 49–57. https://doi.org/10.1094/MPMI-23-1-0049.

Ceresini, Paulo Cezar, Vanina Lilián Castroagudín, Fabrício Ávila Rodrigues, Jonas Alberto Rios, Carlos Eduardo Aucique-Pérez, Silvino Intra Moreira, Eduardo Alves, Daniel Croll, and João Leodato Nunes Maciel. 2018. "Wheat Blast: Past, Present, and Future." *Annual Review of Phytopathology* 56:427–56. https://doi.org/10.1146/annurev-phyto-080417-050036.

Chang, Jeff H., Darrell Desveaux, and Allison L. Creason. 2014. "The ABCs and 123s of Bacterial Secretion Systems in Plant Pathogenesis." *Annual Review of Phytopathology* 52 (1): 317–45. https://doi.org/10.1146/annurev-phyto-011014-015624.

Chang, C. C., Chow, C. C., Tellier, L. C. A. M., Vattikuti, S., Purcell, S. M., & Lee, J. J. (2015). "Second-generation PLINK: Rising to the challenge of larger and richer datasets" *GigaScience*, 4(1), 1–16. https://doi.org/10.1186/s13742-015-0047-8

Chen, Jiapeng. 2017. "Genomics Studies of Two Cereal Rust Fungi with a Focus on Avirulence Gene Searches." PhD dissertation. The University of Sydney, 201.

Chen, Jiapeng, Narayana M. Upadhyaya, Diana Ortiz, Jana Sperschneider, Feng Li, Clement Bouton, Susan Breen, et al. 2017. "Loss of *AvrSr50* by Somatic Exchange in Stem Rust Leads to Virulence for *Sr50* Resistance in Wheat." *Science* 358 (6370): 1607–10. https://doi.org/10.1126/science.aao4810.

Chen, Shisheng, Wenjun Zhang, Stephen Bolus, Matthew N. Rouse, and Jorge Dubcovsky. 2018. "Identification and Characterization of Wheat Stem Rust Resistance Gene *Sr21* Effective against the Ug99 Race Group at High Temperature." *PLoS Genetics* 14 (4): 1–21. https://doi.org/10.1371/journal.pgen.1007287.

Chen, Songbiao, Lizen Tao, Lirong Zeng, Miguel E. Vega-Sanchez, Kenji Umemura, and Guo Liang Wang. 2006. "A Highly Efficient Transient Protoplast System for Analyzing Defence Gene Expression and Protein-Protein Interactions in Rice." *Molecular Plant Pathology* 7 (5): 417–27. https://doi.org/10.1111/j.1364-3703.2006.00346.x.

Chen, Wanquan, Colin Wellings, Xianming Chen, Zhengsheng Kang, and Taiguo Liu. 2014. "Wheat Stripe (Yellow) Rust Caused by *Puccinia striiformis* f. sp. *tritici*." *Molecular Plant Pathology* 15 (5): 433–46. https://doi.org/10.1111/mpp.12116.

Chen, Xianming, and Zhensheng Kang. 2017. Stripe Rust.

Cheng, Yulin, Kuan Wu, Juanni Yao, Shumin Li, Xiaojie Wang, Lili Huang, and Zhensheng

Kang. 2017. "PSTha5a23 , a Candidate Effector from the Obligate Biotrophic Pathogen *Puccinia striiformis* f . sp . *tritici* , Is Involved in Plant Defence Suppression and Rust Pathogenicity" 19: 1717–29. https://doi.org/10.1111/1462-2920.13610.

Cho, Seung Woo, Jihyun Lee, Dana Carroll, Jin Soo Kim, and Junho Lee. 2013. "Heritable Gene Knockout in *Caenorhabditis elegans* by Direct Injection of Cas9-sgRNA Ribonucleoproteins." *Genetics* 195 (3): 1177–80. https://doi.org/10.1534/genetics.113.155853.

Choi, Kyoung-Hee, Ayush Kumar, and Herbert P. Schweizer. 2006. "A 10-min method for preparation of highly electrocompetent Pseudomonas aeruginosa cells: Application for DNA fragment transfer between chromosomes and plasmid transformation." *Journal of Microbiological Methods* 64 (3): 391-397. https://doi.org/10.1016/j.mimet.2005.06.001.

Christie, Michael, Larry J. Croft, and Bernard J. Carroll. 2011. "Intron Splicing Suppresses RNA Silencing in *Arabidopsis*." *Plant Journal* 68 (1): 159–67. https://doi.org/10.1111/j.1365-313X.2011.04676.x.

Chuma, Izumi, Chihiro Isobe, Yuma Hotta, Kana Ibaragi, Natsuru Futamata, Motoaki Kusaba, Kentaro Yoshida, et al. 2011. "Multiple Translocation of the *Avr-Pita* Effector Gene among Chromosomes of the Rice Blast Fungus *Magnaporthe oryzae* and Related Species." *PLoS Pathogens* 7 (7). https://doi.org/10.1371/journal.ppat.1002147.

Cingolani, Pablo, Adrian Platts, Le Lily Wang, Melissa Coon, Tung Nguyen, Luan Wang, Susan J. Land, Xiangyi Lu, and Douglas M. Ruden. 2012. "A Program for Annotating and Predicting the Effects of Single Nucleotide Polymorphisms, SnpEff." *Fly* 6 (2): 80–92. https://doi.org/10.4161/fly.19695.

Cloutier, Sylvie, Brent D. McCallum, Caroline Loutre, Travis W. Banks, Thomas Wicker, Catherine Feuillet, Beat Keller, and Mark C. Jordan. 2007. "Leaf Rust Resistance Gene *Lr1*, Isolated from Bread Wheat (*Triticum aestivum* L.) Is a Member of the Large *Psr567* Gene Family." *Plant Molecular Biology* 65 (1–2): 93–106. https://doi.org/10.1007/s11103-007-9201-8.

Cogoni, Carlo, and Giuseppe Macino. 2000. "Post-Transcriptional Gene Silencing across Kingdoms." *Current Opinion in Genetics and Development* 10 (6): 638–43. https://doi.org/10.1016/S0959-437X(00)00134-9.

Cooper, David N. 2010. "Functional Intronic Polymorphisms: Buried Treasure Awaiting Discovery within Our Genes." *Human Genomics* 4 (5): 284–88. https://doi.org/10.1186/1479-7364-4-5-284.

Cruz, Christian D., and Barbara Valent. 2017. "Wheat Blast Disease: Danger on the Move." *Tropical Plant Pathology* 42 (3): 210–22. https://doi.org/10.1007/s40858-017-0159-z.

Cuomo, Christina A., Guus Bakkeren, Hala Badr Khalil, Vinay Panwar, David Joly, Rob Linning, Sharadha Sakthikumar, et al. 2017. "Comparative Analysis Highlights Variable Genome Content of Wheat Rusts and Divergence of the Mating Loci." *G3: Genes, Genomes, Genetics* 7 (2): 361–76. https://doi.org/10.1534/g3.116.032797

Curtis, B.C., Rajaram, S. and Gomez Macpherson, H. (2002) Bread Wheat; Improvement and Production. FAO Plant Production and Protection Series No. 30. FAO, Rome

Dadami, Elena, Mirko Moser, Michele Zwiebel, Gabi Krczal, Michael Wassenegger, and Athanasios Dalakouras. 2013. "An Endogene-Resembling Transgene Delays the Onset of Silencing and Limits siRNA Accumulation." *FEBS Letters* 587 (6): 706–10. https://doi.org/10.1016/j.febslet.2013.01.045.

Dagvadorj, Bayantes, Ahmet Caglar Ozketen, Ayse Andac, Cian Duggan, Tolga Osman Bozkurt, and Mahinur S. Akkaya. 2017. "A *Puccinia striiformis* f. sp. *tritici* Secreted Protein Activates Plant Immunity at the Cell Surface." *Scientific Reports* 7 (1): 1–10. https://doi.org/10.1038/s41598-017-01100-z.

Dang, Yunkun, Qiuying Yang, Zhihong Xue, and Yi Liu. 2011. "RNA Interference in Fungi: Pathways, Functions, and Applications." *Eukaryotic Cell* 10 (9): 1148–55. https://doi.org/10.1128/EC.05109-11.

Dangl, Jeffery L, Diana M Horvath, and Brian J Staskawicz. 2013. "Pivoting the Plant Immune System from Dissection to Deployment." *Science* 341 (6147): 746–51. https://doi.org/10.1126/science.1236011.

Dawson, Jennifer E., Jolita Šečkute, Soumya De, Samuel A. Schueler, Aaron B. Oswald, and Linda K. Nicholson. 2009. "Elucidation of a PH-Folding Switch in the *Pseudomonas syringae* Effector Protein AvrPto." *Proceedings of the National Academy of Sciences of the United States of America* 106 (21): 8543–48. https://doi.org/10.1073/pnas.0809138106.

Dean, Ralph A., N.J. Talbot, D J Ebbole, ML Farman, T. K. Mitchell, M. J. Orbach, M Thon, and R Kulkarni. 2005. "The Genome Sequence of the Rice Blast Fungus *Magnaporthe grisea*." *Nature* 434 (7036): 980–86. https://doi.org/10.1038/nature03449.

Dicarlo, James E., Julie E. Norville, Prashant Mali, Xavier Rios, John Aach, and George M. Church. 2013. "Genome Engineering in *Saccharomyces cerevisiae* Using CRISPR-Cas Systems." *Nucleic Acids Research* 41 (7): 4336–43. https://doi.org/10.1093/nar/gkt135.

Ding, Pingtao, Toshiyuki Sakai, Ram K Shrestha, Nicolas M Perez, Wenbin Guo, B.P.M. Ngou, Shengbo He, et al. 2019. Chromatin Accessibility Landscapes Activated by Cell Surface and Intracellular Immune Receptors. *BioRxiv*. https://doi.org/10.1017/CBO9781107415324.004.

Ding, Yuduan, Hong Li, Ling Ling Chen, and Kabin Xie. 2016. "Recent Advances in Genome Editing Using CRISPR/Cas9." *Frontiers in Plant Science* 7: 1–12. https://doi.org/10.3389/fpls.2016.00703.

Djamei, Armin, Kerstin Schipper, Franziska Rabe, Anupama Ghosh, Volker Vincon, Jörg Kahnt, Sonia Osorio, et al. 2011. "Metabolic Priming by a Secreted Fungal Effector." *Nature* 478 (7369): 395–98. https://doi.org/10.1038/nature10454.

Dodds, P. N., G. J. Lawrence, A.-M. Catanzariti, M. A. Ayliffe, and J. G. Ellis. 2004. "The *Melampsora lini AvrL567* Avirulence Genes Are Expressed in Haustoria and Their Products Are Recognized inside Plant Cells." *The Plant Cell Online* 16 (3): 755–68. https://doi.org/10.1105/tpc.020040.

Dodds, P. N., G. J. Lawrence, A.-M. Catanzariti, T. Teh, C.-I. A. Wang, M. A. Ayliffe, B. Kobe, and J. G. Ellis. 2006. "Direct Protein Interaction Underlies Gene-for-Gene Specificity and Coevolution of the Flax Resistance Genes and Flax Rust Avirulence Genes." *Proceedings of the National Academy of Sciences* 103 (23): 8888–93. https://doi.org/10.1073/pnas.0602577103.

Dodds, Peter N., and John P. Rathjen. 2010. "Plant Immunity: Towards an Integrated View of Plant–Pathogen Interactions." *Nature Reviews Genetics* 11 (8): 539–48. https://doi.org/10.1038/nrg2812.

Doench, John G., Ella Hartenian, Daniel B. Graham, Zuzana Tothova, Mudra Hegde, Ian Smith, Meagan Sullender, Benjamin L. Ebert, Ramnik J. Xavier, and David E. Root. 2014. "Rational Design of Highly Active sgRNAs for CRISPR-Cas9-Mediated Gene Inactivation." *Nature Biotechnology* 32 (12): 1262–67. https://doi.org/10.1038/nbt.3026.

Dong, Oliver Xiaoou, and Pamela C. Ronald. 2019. "Genetic Engineering for Disease Resistance in Plants: Recent Progress and Future Perspectives." *Plant Physiology* 180 (1): 26–38. https://doi.org/10.1104/pp.18.01224.

Dong, Suomeng, Sylvain Raffaele, and Sophien Kamoun. 2015. "The Two-Speed Genomes of Filamentous Pathogens: Waltz with Plants." *Current Opinion in Genetics and Development* 35: 57–65. https://doi.org/10.1016/j.gde.2015.09.001.

Duplessis, Sébastien, Guus Bakkeren, and Richard Hamelin. 2014. Advancing Knowledge on

Biology of Rust Fungi through Genomics. *Advances in Botanical Research*. 1st ed. Vol. 70. Elsevier Ltd. https://doi.org/10.1016/B978-0-12-397940-7.00006-9.

Duplessis, Sébastien, Christina A. Cuomo, Yao Cheng Lin, Andrea Aerts, Emilie Tisserant, Claire Veneault-Fourrey, David L. Joly, et al. 2011. "Obligate Biotrophy Features Unraveled by the Genomic Analysis of Rust Fungi." *Proceedings of the National Academy of Sciences of the United States of America* 108 (22): 9166–71. https://doi.org/10.1073/pnas.1019315108.

Duplessis, Sébastien, David L Joly, and Peter N. Dodds. 2012. "Rust Effectors." In Effectors in Plant-Microbe Interactions, 155–93. https://doi.org/10.1002/9781119949138.

Ebbole, Daniel J. 2007. "*Magnaporthe* as a Model for Understanding Host-Pathogen Interactions." *Annual Review of Phytopathology* 45 (1): 437–56. https://doi.org/10.1146/annurev.phyto.45.062806.094346.

Eckardt, Nancy A. 2010. "Evolution of Domesticated Bread Wheat." *Plant Cell* 22 (4): 993. https://doi.org/10.1105/tpc.110.220410.

Elert, Emily. 2014. "Rice: A Good Grain." *Nature* 514: s50–51.

Ellis, Jeffrey G., Evans S. Lagudah, Wolfgang Spielmeyer, and Peter N. Dodds. 2014. "The Past, Present and Future of Breeding Rust Resistant Wheat." *Frontiers in Plant Science* 5 (November): 1–13. https://doi.org/10.3389/fpls.2014.00641.

Eriksson, J. & Henning, E. 1896. Die Getreideroste. Ihre Geschichte und Natur sowie Massregein gegen dieselben, p. 463. Stockholm, P.A. Norstedt and Soner.

Eschenbrenner, C. J., Alice Feurtey, and Eva H. Stukenbrock. 2020. "Population Genomics of Fungal Plant Pathogens and the Analyses of Rapidly Evolving Genome Compartments." In Statistical Population Genomics, Methods in Molecular Biology, edited by Julien Y. Dutheil, 2090:337–55.

FAO 2017. Online statistical database: Food balance. FAOSTAT

FAO. 2019. FAO Cereal Supply and Demand Brief. 2019. http://www.fao.org/worldfoodsituation/csdb/en/.

F. de Felippes, Felipe, Marcus McHale, Rachel L. Doran, Sally Roden, Andrew L. Eamens, E. Jean Finnegan, and Peter M. Waterhouse. 2020. "The Key Role of Terminators on the Expression and Post-Transcriptional Gene Silencing of Transgenes." *Plant Journal*. https://doi.org/10.1111/tpj.14907.

Faino, Luigi, Michael F. Seidl, Xiaoqian Shi-Kunne, Marc Pauper, Grardy C M Van Den Berg, Alexander H J Wittenberg, and Bart P H J Thomma. 2016. "Transposons Passively and Actively Contribute to Evolution of the Two-Speed Genome of a Fungal Pathogen." *Genome Research*. https://doi.org/10.1101/gr.204974.116.

Feldman, Mario F., and Guy R. Cornelis. 2003. "The Multitalented Type III Chaperones: All You Can Do with 15 KDa." *FEMS Microbiology Letters* 219 (2): 151–58. https://doi.org/10.1016/S0378-1097(03)00042-9.

Feldman, Mario F., Simone Müller, Esther Wüest, and Guy R. Cornelis. 2002. "SycE Allows Secretion of YopE-DHFR Hybrids by the *Yersinia enterocolitica* Type III Ysc System." *Molecular Microbiology* 46 (4): 1183–97. https://doi.org/10.1046/j.1365-2958.2002.03241.x.

Fernandez, Jessie, and Kim Orth. 2018. "Rise of a Cereal Killer: The Biology of *Magnaporthe oryzae* Biotrophic Growth." *Trends in Microbiology* 26 (7): 582–97. https://doi.org/10.1016/j.tim.2017.12.007.

Feuillet, Catherine, Silvia Travella, Nils Stein, Laurence Albar, Aurélie Nublat, and Beat Keller. 2003. "Map-Based Isolation of the Leaf Rust Disease Resistance Gene *Lr10* from the Hexaploid Wheat (*Triticum aestivum* L.) Genome." *Proceedings of the National Academy of Sciences of the United States of America* 100 (25): 15253–58. https://doi.org/10.1073/pnas.2435133100.

Fincham, J.R.S., J. H. Kinnaird, & P. A. Burns. (1985). "The *am* (NADPH-Specific Glutamate Dehydrogenase) Gene of *Neurospora crassa*. In *Molecular* Genetics *of Filamentous Fungi* (Timberlake W. E. ed.): 117-125.

Figueroa, Melania, Peter N Dodds, and Eva C Henningsen. 2020. "Evolution of Virulence in Rust Fungi — Multiple Solutions to One Problem." *Current Opinion in Plant Biology* 56: 20–27. https://doi.org/10.1016/j.pbi.2020.02.007.

Figueroa, Melania, Kim E. Hammond-Kosack, and Peter S. Solomon. 2018. "A Review of Wheat Diseases—a Field Perspective." *Molecular Plant Pathology* 19 (6): 1523–36. https://doi.org/10.1111/mpp.12618.

Flor, H H. 1971. "Current Status of the Gene-For-Gene Concept." *Annual Review of Phytopathology* 9: 275-296

Foster, Andrew J., Magdalena Martin-Urdiroz, Xia Yan, Harriet Sabrina Wright, Darren M. Soanes, and Nicholas J. Talbot. 2018. "CRISPR-Cas9 Ribonucleoprotein-Mediated Co-Editing and Counterselection in the Rice Blast Fungus." *Scientific Reports* 8 (1): 1–12. https://doi.org/10.1038/s41598-018-32702-w.

Frantzeskakis, Lamprinos, Stefan Kusch, and Ralph Panstruga. 2019. "The Need for Speed: Compartmentalized Genome Evolution in Filamentous Phytopathogens." *Molecular Plant Pathology* 20 (1): 3–7. https://doi.org/10.1111/mpp.12738.

Galán, Jorge E. 2009. "Common Themes in the Design and Function of Bacterial Effectors." *Cell Host and Microbe* 5 (6): 571–79. https://doi.org/10.1016/j.chom.2009.04.008.

Gan, Pamela H.P., Maryam Rafiqi, Adrienne R. Hardham, and Peter N. Dodds. 2010. "Effectors of Biotrophic Fungal Plant Pathogens." *Functional Plant Biology* 37 (10): 913–18. https://doi.org/10.1071/FP10072.

Garnica, Diana P., Adnane Nemri, Narayana M. Upadhyaya, John P. Rathjen, and Peter N. Dodds. 2014. "The Ins and Outs of Rust Haustoria." *PLoS Pathogens* 10 (9): 10–13. https://doi.org/10.1371/journal.ppat.1004329.

Garnica, Diana P., Narayana M. Upadhyaya, Peter N. Dodds, and John P. Rathjen. 2013. "Strategies for Wheat Stripe Rust Pathogenicity Identified by Transcriptome Sequencing." *PLoS ONE* 8 (6). https://doi.org/10.1371/journal.pone.0067150.

Gijzen, Mark, Chelsea Ishmael, and Sirjana D. Shrestha. 2014. "Epigenetic Control of Effectors in Plant Pathogens." *Frontiers in Plant Science* 5 (November): 1–4. https://doi.org/10.3389/fpls.2014.00638.

Giraldo, Martha C., Yasin F. Dagdas, Yogesh K. Gupta, Thomas A. Mentlak, Mihwa Yi, Ana Lilia Martinez-Rocha, Hiromasa Saitoh, Ryohei Terauchi, Nicholas J. Talbot, and Barbara Valent. 2013. "Two Distinct Secretion Systems Facilitate Tissue Invasion by the Rice Blast Fungus *Magnaporthe oryzae*." *Nature Communications* 4: 1–12. https://doi.org/10.1038/ncomms2996.

Giraldo, Martha C., and Barbara Valent. 2013. "Filamentous Plant Pathogen Effectors in Action." *Nature Reviews Microbiology* 11 (11): 800–814. https://doi.org/10.1038/nrmicro3119.

Gooch, Van D., Arun Mehra, Luis F. Larrondo, Julie Fox, Melissa Touroutoutoudis, Jennifer J. Loros, and Jay C. Dunlap. 2008. "Fully Codon-Optimized Luciferase Uncovers Novel Temperature Characteristics of the *Neurospora* Clock." *Eukaryotic Cell* 7 (1): 28–37. https://doi.org/10.1128/EC.00257-07.

Goritschnig, Sandra, Ksenia V. Krasileva, Douglas Dahlbeck, and Brian J. Staskawicz. 2012. "Computational Prediction and Molecular Characterization of an Oomycete Effector and the Cognate *Arabidopsis* Resistance Gene." *PLoS Genetics* 8 (2). https://doi.org/10.1371/journal.pgen.1002502.

Gou, Jin-Ying, Kun Li, Kati Wu, Xiaodong Wang, Huiqiong Lin, Dario Cantu, Cristobal Uauy, et al. 2015. "Wheat Stripe Rust Resistance Protein WKS1 Reduces the Ability of the Thylakoid-Associated Ascorbate Peroxidase to Detoxify Reactive Oxygen Species." *The Plant Cell* 27 (6): 1755–70. https://doi.org/10.1105/tpc.114.134296.

Grabherr, Manfred G., Brian J. Haas, Moran Yassour, Joshua Z. Levin, Dawn A. Thompson,

Ido Amit, Xian Adiconis, et al. 2011. "Full-Length Transcriptome Assembly from RNA-Seq Data without a Reference Genome." *Nature Biotechnology* 29 (7): 644–52. https://doi.org/10.1038/nbt.1883.

Grant, Sarah R., Emily J. Fisher, Jeff H. Chang, Beth M. Mole, and Jeffery L. Dangl. 2006. "Subterfuge and Manipulation: Type III Effector Proteins of Phytopathogenic Bacteria." Annual Review of Microbiology 60 (1): 425–49. https://doi.org/10.1146/annurev.micro.60.080805.142251.

Gustafsson, Claes, Sridhar Govindarajan, and Jeremy Minshull. 2004. "Codon Bias and Heterologous Protein Expression." *Trends in Biotechnology* 22 (7): 346–53. https://doi.org/10.1016/j.tibtech.2004.04.006.

Guttman, D. S., and J. T. Greenberg. 2001. "Functional Analysis of the Type III Effectors *AvrRpt2* and *AvrRpm1* of *Pseudomonas syringae* with the Use of a Single-Copy Genomic Integration System." *Molecular Plant-Microbe Interactions* 14 (2): 145–55. https://doi.org/10.1094/MPMI.2001.14.2.145.

Habyarimana, Fabien, and Brian M.M. Ahmer. 2013. "More Evidence for Secretion Signals within the mRNA of Type 3 Secreted Effectors." *Journal of Bacteriology* 195 (10): 2117–18. https://doi.org/10.1128/JB.00303-13.

Hein, Ingo, Maria Barciszewska-Pacak, Katarina Hrubikova, Sandie Williamson, Malene Dinesen, Ida E. Soenderby, Suresh Sundar, Artur Jarmolowski, Ken Shirasu, and Christophe Lacomme. 2005. "Virus-Induced Gene Silencing-Based Functional Characterization of Genes Associated with Powdery Mildew Resistance in Barley." *Plant Physiology* 138 (4): 2155–64. https://doi.org/10.1104/pp.105.062810.

Hemetsberger, Christoph, Christian Herrberger, Bernd Zechmann, Morten Hillmer, and Gunther Doehlemann. 2012. "*The Ustilago maydis* Effector Pep1 Suppresses Plant Immunity by Inhibition of Host Peroxidase Activity." *PLoS Pathogens* 8 (5). https://doi.org/10.1371/journal.ppat.1002684.

Henry, Elizabeth, Tania Y. Toruño, Alain Jauneau, Laurent Deslandes, and Gitta Coaker. 2017. "Direct and Indirect Visualization of Bacterial Effector Delivery into Diverse Plant Cell Types during Infection." *Plant Cell* 29 (7): 1555–70. https://doi.org/10.1105/tpc.17.00027.

Hogenhout, Saskia A., Renier A. L. Van der Hoorn, Ryohei Terauchi, and Sophien Kamoun. 2009. "Emerging Concepts in Effector Biology of Plant-Associated Organisms." *Molecular Plant-Microbe Interactions* 22 (2): 115–22. https://doi.org/10.1094/MPMI-22-2-0115.

Hooven, H. W. Van den, H. A. Van den Burg, P. Vossen, S. Boeren, P. J.G.M. De Wit, and

J. Vervoort. 2001. "Disulfide Bond Structure of the AVR9 Elicitor of the Fungal Tomato Pathogen *Cladosporium fulvum*: Evidence for a Cystine Knot." Biochemistry 40 (12): 3458–66. https://doi.org/10.1021/bi0023089.

Horner, David Stephen, Giulio Pavesi, Tiziana Castrignano', Paolo D.Onorio de Meo, Sabino Liuni, Michael Sammeth, Ernesto Picardi, and Graziano Pesole. 2009. "Bioinformatics Approaches for Genomics and Post Genomics Applications of Next-Generation Sequencing." *Briefings in Bioinformatics* 11 (2): 181–97. https://doi.org/10.1093/bib/bbp046.

Hovmøller, M. S., S. Walter, R. A. Bayles, A. Hubbard, K. Flath, N. Sommerfeldt, M. Leconte, et al. 2016. "Replacement of the European Wheat Yellow Rust Population by New Races from the Centre of Diversity in the Near-Himalayan Region." *Plant Pathology* 65 (3): 402–11. https://doi.org/10.1111/ppa.12433.

Hovmøller, Mogens S., and Annemarie F. Justesen. 2007. "Appearance of Atypical *Puccinia striiformis* f. sp. *tritici* Phenotypes in North-Western Europe." *Australian Journal of Agricultural Research* 58 (6): 518–24. https://doi.org/10.1071/AR06146.

Hovmøller, Mogens S., Chris K. Sørensen, Stephanie Walter, and Annemarie F. Justesen. 2011. "Diversity of *Puccinia striiformis* on Cereals and Grasses." *Annual Review of Phytopathology* 49 (1): 197–217. https://doi.org/10.1146/annurev-phyto-072910-095230.

Huang, Li, Steven A Brooks, Wanlong Li, John P Fellers, Harold N Trick, and Bikram S Gill. 2003. "Map-Based Cloning of Leaf Rust Resistance Gene." *Genetics* 164: 655–64.

Hubbard, Amelia, Clare M Lewis, Kentaro Yoshida, Ricardo H Ramirez-Gonzalez, Claude de Vallavieille-Pope, Jane Thomas, Sophien Kamoun, Rosemary Bayles, Cristobal Uauy, and Diane G O Saunders. 2015. "Field Pathogenomics Reveals the Emergence of a Diverse Wheat Yellow Rust Population." *Genome Biology* 16 (1): 23. https://doi.org/10.1186/s13059-015-0590-8.

Huynh, Thanh V., Dahlbeck, D., Staskawicz, B. J. 1989. "Bacterial Blight of Soybean : Regulation of a Pathogen Gene Determining Host Cultivar Specificity." *Science* 245: 1374–77.

Inoue, Authors Yoshihiro, Trinh T P Vy, Kentaro Yoshida, and Hokuto Asano. 2017. "Evolution of the Wheat Blast Fungus through Functional Losses in a Host Specificity Determinant" 583: 80-83 . https://doi.org/10.1126/science.aam9654.

Islam, M Tofazzal, Daniel Croll, Pierre Gladieux, Darren M Soanes, Antoine Persoons,

Pallab Bhattacharjee, Shaid Hossain, et al. 2016. "Emergence of Wheat Blast in Bangladesh Was Caused by a South American Lineage of *Magnaporthe oryzae*." *BMC Biology,* 1–11. https://doi.org/10.1186/s12915-016-0309-7.

Islam, M Tofazzal, Dipali Rani Gupta, Akbar Hossain, Krishna K Roy, Xinyao He, Muhammad R Kabir, Pawan K Singh, Arifur Rahman Khan, Mahfuzur Rahman, and Guo-liang Wang. 2020. "Wheat Blast : A New Threat to Food Security." *Phytopathology Research* 2 (28): 1- 13. https://doi.org/10.1186/s42483-020-00067-6

Jeenes, D. J., D. A. Mackenzie, I. N. Roberts, and D. B. Archer. 1991. "Heterologous Protein Production by Filamentous Fungi." *Biotechnology and Genetic Engineering Reviews* 9 (1): 327–68. https://doi.org/10.1080/02648725.1991.10647884.

Jia, Yulin, Sean A Mcadams, Gregory T Bryan, Howard P Hershey, and Barbara Valent. 2000. "Direct Interaction of Resistance Gene and Avirulence Gene Products Confers Rice Blast Resistance" *The EMBO Journal* 19 (15):4004-4014.

Jones, Jonathan D G, and Jeffery L. Dangl. 2006. "The Plant Immune System." *Nature* 444 (7117): 323–29. https://doi.org/10.1038/nature05286.

Jones, Kiersun, Jie Zhu, Cory B Jenkinson, Dong Won Kim, and Chang Hyun Khang. 2017. Disruption of the Interfacial Membrane Leads to *Magnaporthe oryzae* Effector Re-Location and Lifestyle Switch during Rice Blast Disease. *BioRxiv* https://doi.org/10.1101/177147

Jong, Joke C. De, Barbara J. McCormack, Nicholas Smirnoff, and Nicholas J. Talbot. 1997. "Glycerol Generates Turgor in Rice Blast." *Nature* 389 (6648): 244–45. https://doi.org/10.1038/38418.

Jonge, Ronnie De, H. Peter Van Esse, Karunakaran Maruthachalam, Melvin D. Bolton, Parthasarathy Santhanam, Mojtaba Keykha Saber, Zhao Zhang, et al. 2012. "Tomato Immune Receptor Ve1 Recognizes Effector of Multiple Fungal Pathogens Uncovered by Genome and RNA Sequencing." *Proceedings of the National Academy of Sciences of the United States of America* 109 (13): 5110–15. https://doi.org/10.1073/pnas.1119623109.

Jonge, Ronnie De, H Peter Van Esse, Anja Kombrink, Tomonori Shinya, Yoshitake Desaki, Ralph Bours, Sander Van Der Krol, Naoto Shibuya, Matthieu H A J Joosten, and Bart P H J Thomma. 2010. "Conserved Fungal LysM Effector Ecp6 Prevents Chitin-Triggered Immunity in Plants" *Science* 329: 953–55.

Kale, Shiv D., Biao Gu, Daniel G S Capelluto, Daolong Dou, Emily Feldman, Amanda

Rumore, Felipe D. Arredondo, et al. 2010. "External Lipid PI3P Mediates Entry of Eukaryotic Pathogen Effectors into Plant and Animal Host Cells." *Cell* 142 (2): 284–95. https://doi.org/10.1016/j.cell.2010.06.008.

Kanja, Claire, and Kim E. Hammond-Kosack. 2020. "Proteinaceous Effector Discovery and Characterization in Filamentous Plant Pathogens." *Molecular Plant Pathology* 1353–76. https://doi.org/10.1111/mpp.12980.

Kankanala, Prasanna, Kirk Czymmek, and Barbara Valent. 2007. "Roles for Rice Membrane Dynamics and Plasmodesmata during Biotrophic Invasion by the Blast Fungus" *The Plant Cell* 19: 706–24. https://doi.org/10.1105/tpc.106.046300.

Kawahara, Yoshihiro, Youko Oono, Hiroyuki Kanamori, Takashi Matsumoto, Takeshi Itoh, and Eiichi Minami. 2012. "Simultaneous RNA-Seq Analysis of a Mixed Transcriptome of Rice and Blast Fungus Interaction." *PloS One* 7 (11): 1–15. https://doi.org/10.1371/journal.pone.0049423.

Kemen, Eric, Ariane C. Kemen, Maryam Rafiqi, Uta Hempel, Kurt Mendgen, Matthias Hahn, and Ralf T. Voegele. 2005. "Identification of a Protein from Rust Fungi Transferred from Haustoria into Infected Plant Cells." *Molecular Plant-Microbe Interactions* 18 (11): 1130–39. https://doi.org/10.1094/MPMI-18-1130.

Khang, Chang Hyun, Romain Berruyer, Martha C. Giraldo, Prasanna Kankanala, Sook-Young Park, Kirk Czymmek, Seogchan Kang, and Barbara Valent. 2010. "Translocation of *Magnaporthe oryzae* Effectors into Rice Cells and Their Subsequent Cell-to-Cell Movement." *The Plant Cell* 22 (4): 1388–1403. https://doi.org/10.1105/tpc.109.069666.

Kiran, Kanti, Hukam C. Rawal, Himanshu Dubey, R. Jaswal, Subhash C. Bhardwaj, P. Prasad, Dharam Pal, B. N. Devanna, and Tilak R. Sharma. 2017. "Dissection of Genomic Features and Variations of Three Pathotypes of *Puccinia striiformis* through Whole Genome Sequencing." *Scientific Reports* 7 (January): 1–16. https://doi.org/10.1038/srep42419.

Klymiuk, Valentina, Elitsur Yaniv, Lin Huang, Dina Raats, Andrii Fatiukha, Shisheng Chen, Lihua Feng, et al. 2018. "Cloning of the Wheat *Yr15* Resistance Gene Sheds Light on the Plant Tandem Kinase-Pseudokinase Family." *Nature Communications* 9 (1). https://doi.org/10.1038/s41467-018-06138-9.

Kohli, M.M., Y.R. Mehta, E. Guzman, L. De Viedma, and L.E. Cubilla. 2011. "*Pyricularia* Blast - a Threat to Wheat Cultivation." *Czech Journal of Genetics and Plant Breeding* 47: S130–34. https://doi.org/10.17221/3267-cjgpb.

Koren, S., B.P. Walenz, K Berlin, J. R. Miller, N. H. Bergman, and A. M. Philippy. 2017.

"Canu: Scalable and Accurate Long-Read Assembly via Adaptive k-Mer Weighting and Repeat Separation." *Genome Research* 27: 1–15. https://doi.org/10.1101/gr.215087.116.

Krappmann, Sven. 2007. "Gene Targeting in Filamentous Fungi: The Benefits of Impaired Repair." *Fungal Biology Reviews* 21 (1): 25–29. https://doi.org/10.1016/j.fbr.2007.02.004.

Krusche, Peter, Len Trigg, Paul C. Boutros, Christopher E. Mason, Francisco M. De La Vega, Benjamin L. Moore, Mar Gonzalez-Porta, et al. 2019. "Best Practices for Benchmarking Germline Small-Variant Calls in Human Genomes." *Nature* Biotechnology 37 (5): 555–60. https://doi.org/10.1038/s41587-019-0054-x.

Kurtz, Stefan, Adam Phillippy, Arthur L. Delcher, Michael Smoot, Martin Shumway, Corina Antonescu, and Steven L. Salzberg. 2004. "Versatile and Open Software for Comparing Large Genomes." *Genome Biology* 5 (2). https://doi.org/10.1186/gb-2004-5-2-r12.

La Concepcion, Juan Carlos De, Marina Franceschetti, Dan Maclean, Ryohei Terauchi, Sophien Kamoun, and Mark J. Banfield. 2019. "Protein Engineering Expands the Effector Recognition Profile of a Rice NLR Immune Receptor." *ELife* 8: 1–19. https://doi.org/10.7554/eLife.47713.

Lawrence, Gregory J., Peter N. Dodds, and Jeffrey G. Ellis. 2010. "Transformation of the Flax Rust Fungus, *Melampsora lini*: Selection via Silencing of an Avirulence Gene." *Plant Journal* 61 (2): 364–69. https://doi.org/10.1111/j.1365-313X.2009.04052.x.

Lee, Heng-Chi, Liande Li, Weifeng Gu, Zhihong Xue, S.K. Crosthwaite, A. Pertsemlidis, Z.A. Lewis, et al. 2010. "Diverse Pathways Generate MicroRNA-like RNAs and Dicer-Independent Small Interfering RNAs in Fungi." *Mol Cell* 38 (6): 803–14. https://doi.org/10.1161/CIRCULATIONAHA.110.956839.

Lee, Vincent T., and Olaf Schneewind. 2002. "Yop Fusions to Tightly Folded Protein Domains and Their Effects on *Yersinia enterocolitica* Type III Secretion." *Journal of Bacteriology* 184 (13): 3740–45. https://doi.org/10.1128/JB.184.13.3740-3745.2002.

Lee, Wing Sham, Kim E. Hammond-Kosack, and Kostya Kanyuka. 2012. "Barley Stripe Mosaic Virus-Mediated Tools for Investigating Gene Function in Cereal Plants and Their Pathogens: Virus-Induced Gene Silencing, Host-Mediated Gene Silencing, and Virus-Mediated Overexpression of Heterologous Protein." Plant Physiology 160 (2): 582–90. https://doi.org/10.1104/pp.112.203489.

Li, Feng, Narayana M. Upadhyaya, Jana Sperschneider, Oadi Matny, Hoa Nguyen-Phuc,

Rohit Mago, Castle Raley, et al. 2019. "Emergence of the Ug99 Lineage of the Wheat Stem Rust Pathogen through Somatic Hybridisation." *Nature Communications* 10 (1): 5068. https://doi.org/10.1038/s41467-019-12927-7.

Li, Heng, and Richard Durbin. 2009. "Fast and Accurate Short Read Alignment with Burrows-Wheeler Transform." *Bioinformatics* 25 (14): 1754–60. https://doi.org/10.1093/bioinformatics/btp324.

Li, H., Handsaker, B., Wysoker, A., Fennell, T., Ruan, J., Homer, N., Marth, G., Abecasis, G., & Durbin, R. 2009. "The Sequence Alignment/Map format and SAMtools." *Bioinformatics 25* (16): 2078–2079. https://doi.org/10.1093/bioinformatics/btp352

Li, Heng. 2018. "Minimap2: Pairwise alignment for nucleotide sequences." *Bioinformatics 34* (18): 3094–3100. https://doi.org/10.1093/bioinformatics/bty191

Li, Yuxiang, Meinan Wang, Deven R. See, and Xianming Chen. 2019. "Ethyl-Methanesulfonate Mutagenesis Generated Diverse Isolates of *Puccinia striiformis* f. sp. *tritici*, the Wheat Stripe Rust Pathogen." *World Journal of Microbiology and Biotechnology* 35 (2): 0. https://doi.org/10.1007/s11274-019-2600-6.

Li, Yuxiang, Chongjing Xia, Meinan Wang, Chuntao Yin, and Xianming Chen. 2019. "Genome Sequence Resource of a *Puccinia striiformis* Isolate Infecting Wheatgrass" 109 (9): 1509–12. https://doi.org/10.1094/PHYTO-02-19-0054-A.

Liu, Changhai, Carsten Pedersen, Torsten Schultz-larsen, Geziel B Aguilar, Kenneth Madriz-Orde, and Hans Thordal-Christensen. 2016. "The Stripe Rust Fungal Effector PEC6 Suppresses Pattern-Triggered Immunity in a Host Species-Independent Manner and Interacts with Adenosine Kinases." *New Phytologist* https://doi.org/10.1111/nph.14034

Liu, Wei, Michele Frick, Rene Huel, Cory L. Nykiforuk, Xiaomin Wang, Denis A. Gaudet, François Eudes, et al. 2014. "The Stripe Rust Resistance Gene *Yr10* Encodes an Evolutionary-Conserved and Unique CC-NBS-LRR Sequence in Wheat." *Molecular Plant* 7 (12): 1740–55. https://doi.org/10.1093/mp/ssu112.

Liu, Zhaohui, Timothy L. Friesen, Hua Ling, Steven W. Meinhardt, Richard P. Oliver, Jack B. Rasmussen, and Justin D. Faris. 2006. "The Tsn1-ToxA Interaction in the Wheat-*Stagonospora nodorum* Pathosystem Parallels That of the Wheat-Tan Spot System." *Genome* 49 (10): 1265–73. https://doi.org/10.1139/G06-088.

Lohou, David, Fabien Lonjon, Stéphane Genin, and Fabienne Vailleau. 2013. "Type III Chaperones & Co in Bacterial Plant Pathogens: A Set of Specialized Bodyguards Mediating Effector Delivery." *Frontiers in Plant Science* 4: 1–8. https://doi.org/10.3389/fpls.2013.00435.

Lorrain, Cécile, Karen Cristine Gonçalves dos Santos, Hugo Germain, Arnaud Hecker, and Sébastien Duplessis. 2019. "Advances in Understanding Obligate Biotrophy in Rust Fungi." *New Phytologist*. https://doi.org/10.1111/nph.15641.

Losada, Liliana C., and Steven W. Hutcheson. 2005. "Type III Secretion Chaperones of *Pseudomonas syringae* Protect Effectors from Lon-Associated Degradation." *Molecular Microbiology* 55 (3): 941–53. https://doi.org/10.1111/j.1365-2958.2004.04438.x.

Lu, Xunli, Barbara Kracher, Isabel M L Saur, Saskia Bauer, Simon R Ellwood, Roger Wise, and Takashi Yaeno. 2016. "Allelic Barley MLA Immune Receptors Recognize Sequence-Unrelated Avirulence Effectors of the Powdery Mildew Pathogen." *Proceedings of the National Academy of Sciences* 113(42): E6486-E6495 https://doi.org/10.1073/pnas.1612947113.

Ma, Li-Jun, H. Charlotte van der Does, Katherine A. Borkovich, Jeffrey J. Coleman, Marie-Josée Daboussi, Antonio Di Pietro, Marie Dufresne, et al. 2010. "Comparative Genomics Reveals Mobile Pathogenicity Chromosomes in *Fusarium*." *Nature* 464 (7287): 367–73. https://doi.org/10.1038/nature08850.

Mago, Rohit, Peng Zhang, Sonia Vautrin, Hana Šimková, Urmil Bansal, Ming Cheng Luo, Matthew Rouse, et al. 2015. "The Wheat *Sr50* Gene Reveals Rich Diversity at a Cereal Disease Resistance Locus." *Nature Plants* 1: 6–8. https://doi.org/10.1038/nplants.2015.186.

Manning, Viola A., Ashley L. Chu, Steven R. Scofield, and Lynda M. Ciuffetti. 2010. "Intracellular Expression of a Host-Selective Toxin, *ToxA*, in Diverse Plants Phenocopies Silencing of a ToxA-Interacting Protein, ToxABP1." *New Phytologist* 187 (4): 1034–47. https://doi.org/10.1111/j.1469-8137.2010.03363.x.

Manning, Viola A., Sara M. Hamilton, P. Andrew Karplus, and Lynda M. Ciuffetti. 2008. "The Arg-Gly-Asp-Containing, Solvent-Exposed Loop of Ptr ToxA Is Required for Internalization." *Molecular Plant-Microbe Interactions* 21 (3): 315–25. https://doi.org/10.1094/MPMI-21-3-0315.

Marchal, Clemence, Jianping Zhang, Peng Zhang, Paul Fenwick, Burkhard Steuernagel, Nikolai M. Adamski, Lesley Boyd, et al. 2018. "BED-Domain-Containing Immune Receptors Confer Diverse Resistance Spectra to Yellow Rust." *Nature Plants* 4 (9): 662–68. https://doi.org/10.1038/s41477-018-0236-4.

Mares, D. J. 1979. "Microscopic Study of the Development of Yellow Rust (*Puccinia striiformis*) in a Wheat Cultivar Showing Adult Plant Resistance." *Physiological Plant Pathology* 15 (3): 289–96. https://doi.org/10.1016/0048-4059(79)90080-8.

Mary Gearing. 2016. “CRISPR 101: A Desktop Resource” 2016.

McDonald, Bruce A., and Eva H. Stukenbrock. 2016. “Rapid Emergence of Pathogens in Agro-Ecosystems: Global Threats to Agricultural Sustainability and Food Security.” *Philosophical Transactions of the Royal Society B: Biological Sciences* 371 (1709). https://doi.org/10.1098/rstb.2016.0026.

McIntosh, RA, CR Wellings, and RF Park. 1995. “Wheat Rusts: An Atlas of Resistance Genes.” *Plant Breeding*, 205. https://doi.org/10.1007/978-94-011-0083-0.

Mehmood, Sajid, Marina Sajid, Jie Zhao, Lili Huang, and Zhensheng Kang. 2020. “Alternate Hosts of *Puccinia striiformis* f. sp. *tritici* and Their Role.” *Pathogens* 9 (6): 1–21. https://doi.org/10.3390/pathogens9060434.

Miller, Marisa E, Ying Zhang, Vahid Omidvar, Jana Sperschneider, Benjamin Schwessinger, Castle Raley, Jonathan M Palmer, et al. 2018. “De Novo Assembly and Phasing of Dikaryotic Genomes from Two Isolates of *Puccinia coronata* f. sp. *avenae*, the Causal Agent of Oat Crown Rust” *American Society for Microbiology* 9 (1): 1–21.

Milne, Ricky J., Katherine E. Dibley, Wendelin Schnippenkoetter, Martin Mascher, Andy C.W. Lui, Lanxiang Wang, Clive Lo, Anthony R. Ashton, Peter R. Ryan, and Evans S. Lagudah. 2019. “The Wheat *LR67* Gene from the Sugar Transport Protein 13 Family Confers Multi pathogen Resistance in Barley.” *Plant Physiology* 179 (4): 1285–97. https://doi.org/10.1104/pp.18.00945.

Mitchell, Alex L., Teresa K. Attwood, Patricia C. Babbitt, Matthias Blum, Peer Bork, Alan Bridge, Shoshana D. Brown, et al. 2019. “InterPro in 2019: Improving Coverage, Classification and Access to Protein Sequence Annotations.” *Nucleic Acids Research* 47 (D1): D351–60. https://doi.org/10.1093/nar/gky1100.

Moldenhauer, J., B. M. Moerschbacher, and A. J. Van Der Westhuizen. 2006. “Histological Investigation of Stripe Rust (*Puccinia striiformis* f.sp. *tritici*) Development in Resistant and Susceptible Wheat Cultivars.” *Plant Pathology* 55 (4): 469–74. https://doi.org/10.1111/j.1365-3059.2006.01385.x.

Möller, Mareike, and Eva H. Stukenbrock. 2017. “Evolution and Genome Architecture in Fungal Plant Pathogens.” *Nature Reviews Microbiology* 15 (12): 756–71. https://doi.org/10.1038/nrmicro.2017.76.

Morel, Jean Benoit, and Jeffery L. Dangl. 1997. “The Hypersensitive Response and the Induction of Cell Death in Plants.” *Cell Death and Differentiation* 4 (8): 671–83. https://doi.org/10.1038/sj.cdd.4400309.

Mosquera, G., M. C. Giraldo, C. H. Khang, S. Coughlan, and B. Valent. 2009. “Interaction

Transcriptome Analysis Identifies *Magnaporthe oryzae* BAS1-4 as Biotrophy-Associated Secreted Proteins in Rice Blast Disease." *The Plant Cell* Online 21 (4): 1273–90. https://doi.org/10.1105/tpc.107.055228.

Mudgett, Mary Beth, and Brian J. Staskawicz. 1999. "Characterization of the *Pseudomonas syringae* p.v. *tomato* AvrRpt2 Protein: Demonstration of Secretion and Processing during Bacterial Pathogenesis." *Molecular Microbiology* 32 (5): 927–41. https://doi.org/10.1046/j.1365-2958.1999.01403.x.

Mundt, Christopher C. 2018. "Pyramiding for Resistance Durability: Theory and Practice." *Phytopathology* 108 (7): 792–802. https://doi.org/10.1094/PHYTO-12-17-0426-RVW.

Na, Ren, Dan Yu, B. Patrick Chapman, Yun Zhang, Kuflom Kuflu, Ryan Austin, Dinah Qutob, Jun Zhao, Yuanchao Wang, and Mark Gijzen. 2014. "Genome Re-Sequencing and Functional Analysis Places the *Phytophthora sojae* Avirulence Genes *Avr1c* and *Avr1a* in a Tandem Repeat at a Single Locus." *PLoS ONE* 9 (2): 1–11. https://doi.org/10.1371/journal.pone.0089738.

Nevalainen, Helena, and Robyn Peterson. 2014. "Making Recombinant Proteins in Filamentous Fungi- Are We Expecting Too Much?" *Frontiers in Microbiology* 5: 1–10. https://doi.org/10.3389/fmicb.2014.00075.

Nevalainen, K. M.Helena, Valentino S.J. Te'o, and Peter L. Bergquist. 2005. "Heterologous Protein Expression in Filamentous Fungi." *Trends in Biotechnology* 23 (9): 468–74. https://doi.org/10.1016/j.tibtech.2005.06.002.

Ngou, B.P.M., Hee-kyung Ahn, Pingtao Ding, Amey Redkar, Hannah Brown, Mark Youles, and Laurence Tomlinson. 2020. "Estradiol-Inducible *AvrRps4* Expression Reveals Distinct Properties of TIR-NLR-Mediated Effector-Triggered Immunity." *Journal of Experimental Botany* 71 (6): 2186-2197

Niemann, George S., Roslyn N. Brown, Ivy T. Mushamiri, Nhu T. Nguyen, Rukayat Taiwo, Afke Stufkens, Richard D. Smith, Joshua N. Adkins, Jason E. McDermott, and Fred Heffron. 2013. "RNA Type III Secretion Signals That Require Hfq." *Journal of Bacteriology* 195 (10): 2119–25. https://doi.org/10.1128/JB.00024-13.

Nimchuk, Zachary, Eric Marois, Susanne Kjemtrup, R. Todd Leister, Fumiaki Katagiri, and Jeffery L. Dangl. 2000. "Eukaryotic Fatty Acylation Drives Plasma Membrane Targeting and Enhances Function of Several Type III Effector Proteins from *Pseudomonas syringae*." *Cell* 101 (4): 353–63. https://doi.org/10.1016/S0092-8674(00)80846-6.

Oerke, E. C., and H. W. Dehne. 2004. "Safeguarding Production - Losses in Major Crops

and the Role of Crop Protection." *Crop Protection* 23 (4): 275–85. https://doi.org/10.1016/j.cropro.2003.10.001.

Oliver, Richard P. 2014. "A Reassessment of the Risk of Rust Fungi Developing Resistance to Fungicides." *Pest Management Science* 70 (11): 1641–45. https://doi.org/10.1002/ps.3767.

O'Neill, E. M., Mucyn, T. S., Patteson, J. B., Finkel, O. M., Chung, E. H., Baccile, J. A., Massolo, E., Schroeder, F. C., Dangl, J. L., & Li, B. (2018). "Phevamine A, a small molecule that suppresses plant immune responses." *Proceedings of the National Academy of Sciences of the United States of America 115*(41): E9514–E9522. https://doi.org/10.1073/pnas.1803779115

Pais, Marina, Kentaro Yoshida, Artemis Giannakopoulou, Mathieu A. Pel, Liliana M. Cano, Ricardo F. Oliva, Kamil Witek, Hannele Lindqvist-Kreuze, Vivianne G.A.A. Vleeshouwers, and Sophien Kamoun. 2018. "Gene Expression Polymorphism Underpins Evasion of Host Immunity in an Asexual Lineage of the Irish Potato Famine Pathogen." *BMC Evolutionary Biology* 18 (1): 1–11. https://doi.org/10.1186/s12862-018-1201-6.

Paradis, E., J. & Claude, K. Strimmer. (2004). "APE: Analyses of phylogenetics and evolution in R language. *Bioinformatics* 20 (2): 289-290. https://doi.org/10.1093/bioinformatics/btg412

Patron, Nicola, and et al. 2015. "Standards for Plant Synthetic Biology: A Common Syntax for Exchange of DNA Parts." *New Phytologist* 208:13–19.

Pavan, Stefano, Evert Jacobsen, Richard G.F. Visser, and Yuling Bai. 2010. "Loss of Susceptibility as a Novel Breeding Strategy for Durable and Broad-Spectrum Resistance." *Molecular Breeding* 25 (1): 1–12. https://doi.org/10.1007/s11032-009-9323-6.

Peng, Zhao, Ely Oliveira-Garcia, Guifang Lin, Ying Hu, Melinda Dalby, Pierre Migeon, Haibao Tang, et al. 2019. "Effector Gene Reshuffling Involves Dispensable Mini-Chromosomes in the Wheat Blast Fungus." *PLoS Genetics* 15 (9): 1–23. https://doi.org/10.1371/journal.pgen.1008272.

Pennington, Helen G; Youles, Mark; Kamoun, Sophien (2017): Golden-Gate compatible *Magnaporthe oryzae* protoplast transformation vectors. *figshare*. Dataset. https://doi.org/10.6084/m9.figshare.5375428.v1

Pennisi, E. 2010. "Armed and Dangerous." *Science* 327: 804–5.

Periyannan, Sambasivam, John Moore, Michael Ayliffe, Urmil Bansal, Xiaojing Wang, Li

Huang, Karin Deal, et al. 2013. "The Gene *Sr33,* an Ortholog of Barley *Mla* Genes, Encodes Resistance to Wheat Stem Rust Race Ug99." *Science* 341 (6147): 786–88. https://doi.org/10.1126/science.1239028.

Petersen, Thomas Nordahl, Søren Brunak, Gunnar Von Heijne, and Henrik Nielsen. 2011. "SignalP 4.0: Discriminating Signal Peptides from Transmembrane Regions." *Nature Methods* 8 (10): 785–86. https://doi.org/10.1038/nmeth.1701.

Petre, Benjamin, David L. Joly, and Sebastien Duplessis. 2014. "Effector Proteins of Rust Fungi." *Frontiers in Plant Science* 5: 1–7. https://doi.org/10.3389/fpls.2014.00416.

Petre, Benjamin, and Sophien Kamoun. 2014. "How Do Filamentous Pathogens Deliver Effector Proteins into Plant Cells?" *PLoS Biology* 12 (2). https://doi.org/10.1371/journal.pbio.1001801.

Petre, Benjamin, Diane G. O. Saunders, Jan Sklenar, Cécile Lorrain, Ksenia V. Krasileva, Joe Win, Sébastien Duplessis, and Sophien Kamoun. 2016. "Heterologous Expression Screens in *Nicotiana benthamiana* Identify a Candidate Effector of the Wheat Yellow Rust Pathogen That Associates with Processing Bodies." *Plos One* 11 (2): e0149035. https://doi.org/10.1371/journal.pone.0149035.

Pfeifer, S. P. 2017. "From Next-Generation Resequencing Reads to a High-Quality Variant Data Set." *Heredity* 118 (2): 111–24. https://doi.org/10.1038/hdy.2016.102.

Plissonneau, Clémence, Juliana Benevenuto, and Norfarhan Mohd-assaad. 2017. "Using Population and Comparative Genomics to Understand the Genetic Basis of Effector-Driven Fungal Pathogen Evolution" 8: 1–15. https://doi.org/10.3389/fpls.2017.00119.

Plissonneau, Clémence, Juliana Benevenuto, Norfarhan Mohd-Assaad, Simone Fouché, Fanny E. Hartmann, and Daniel Croll. 2017. "Using Population and Comparative Genomics to Understand the Genetic Basis of Effector-Driven Fungal Pathogen Evolution." *Frontiers in Plant Science* 8: 1–15. https://doi.org/10.3389/fpls.2017.00119.

Poplin, Ryan, Valentin Ruano-Rubio, Mark A. DePristo, Tim J. Fennell, Mauricio O. Carneiro, Geraldine A. Van der Auwera, David E. Kling, et al. 2017. "Scaling Accurate Genetic Variant Discovery to Tens of Thousands of Samples." *BioRxiv*, 1–22. https://doi.org/10.1101/201178.

Popp, József, and Krisztina Hantos. 2013. "The Impact of Crop Protection on Agricultural Production." *Studies in Agricultural Economics* 113 (1): 47–66. https://doi.org/10.7896/j.1003.

Prasad, Pramod, Siddanna Savadi, S C Bhardwaj O P Gangwar, and Subodh Kumar. 2019.

"Rust Pathogen Effectors : Perspectives in Resistance Breeding." *Planta*, no. 0123456789. https://doi.org/10.1007/s00425-019-03167-6.

Puhar, Andrea, and Philippe J. Sansonetti. 2014. "Type III Secretion System." *Current Biology* 24 (17): R784–91. https://doi.org/10.1016/j.cub.2014.07.016.

Que, Qiudeng, Huai Yu Wang, James J. English, and Richard A. Jorgensen. 1997. "The Frequency and Degree of Cosuppression by Sense Chalcone Synthase Transgenes Are Dependent on Transgene Promoter Strength and Are Reduced by Premature Nonsense Codons in the Transgene Coding Sequence." *Plant Cell* 9 (8): 1357–68. https://doi.org/10.1105/tpc.9.8.1357.

Radhakrishnan, Guru V., Nicola M. Cook, Vanessa Bueno-Sancho, Clare M. Lewis, Antoine Persoons, Abel Debebe Mitiku, Matthew Heaton, et al. 2019. "MARPLE, a Point-of-Care, Strain-Level Disease Diagnostics and Surveillance Tool for Complex Fungal Pathogens." *BMC Biology* 17 (1): 1–17. https://doi.org/10.1186/s12915-019-0684-y.

Raffaele, Sylvain, and Sophien Kamoun. 2012. "Genome Evolution in Filamentous Plant Pathogens: Why Bigger Can Be Better." *Nature Reviews Microbiology* 10(6): 417–430. https://doi.org/10.1038/nrmicro2790.

Raffaele, Sylvain, Joe Win, Liliana M Cano, and Sophien Kamoun. 2010. "Analyses of Genome Architecture and Gene Expression Reveal Novel Candidate Virulence Factors in the Secretome of *Phytophthora infestans*." *BMC Genomics* 11 (1): 637. https://doi.org/10.1186/1471-2164-11-637.

Rafiqi, Maryam, Jeffrey G. Ellis, Victoria A. Ludowici, Adrienne R. Hardham, and Peter N. Dodds. 2012. "Challenges and Progress towards Understanding the Role of Effectors in Plant-Fungal Interactions." *Current Opinion in Plant Biology* 15 (4): 477–82. https://doi.org/10.1016/j.pbi.2012.05.003.

Rafiqi, Maryam, Pamela H.P. Gan, Michael Ravensdale, Gregory J. Lawrence, Jeffrey G. Ellis, David A. Jones, Adrienne R. Hardham, and Peter N. Dodds. 2010. "Internalization of Flax Rust Avirulence Proteins into Flax and Tobacco Cells Can Occur in the Absence of the Pathogen." *The Plant Cell* 22 (6): 2017–32. https://doi.org/10.1105/tpc.109.072983.

Rahme, L. G., M. N. Mindrinos, and N. J. Panopoulos. 1992. "Plant and Environmental Sensory Signals Control the Expression of Hrp Genes in *Pseudomonas syringae pv. phaseolicola*." *Journal of Bacteriology* 174 (11): 3499–3507. https://doi.org/10.1128/jb.174.11.3499-3507.1992.

Ramachandran, Sowmya R, Chuntao Yin, Joanna Kud, Kiwamu Tanaka, Aaron K Mahoney,

Fangming Xiao, and Scot H Hulbert. 2017. "Effectors from Wheat Rust Fungi Suppress Multiple Plant Defence Responses" *Phytopathology* 107 (1): 75–83.

Raman, Vidhyavathi, Stacey A. Simon, Feray Demirci, Mayumi Nakano, Blake C. Meyers, and Nicole M. Donofrio. 2017. "Small RNA Functions Are Required for Growth and Development of *Magnaporthe oryzae*." *Molecular Plant-Microbe Interactions* 30 (7): 517–30. https://doi.org/10.1094/MPMI-11-16-0236-R.

Rentel, Maike C., Lauriebeth Leonelli, Douglas Dahlbeck, Bingyu Zhao, and Brian J. Staskawicz. 2008. "Recognition of the Hyaloperonospora Parasitica Effector ATR13 Triggers Resistance against Oomycete, Bacterial, and Viral Pathogens." *Proceedings of the National Academy of Sciences of the United States of America* 105 (3): 1091–96. https://doi.org/10.1073/pnas.0711215105.

Ribot, Cécile, Stella Césari, Imène Abidi, Véronique Chalvon, Caroline Bournaud, Julie Vallet, Marc Henri Lebrun, Jean Benoit Morel, and Thomas Kroj. 2013. "The *Magnaporthe oryzae* Effector AVR1-CO39 Is Translocated into Rice Cells Independently of a Fungal-Derived Machinery." *Plant Journal* 74 (1): 1–12. https://doi.org/10.1111/tpj.12099.

Rietman, Hendrik, Gerard Bijsterbosch, Liliana M. Cano, Heung Ryul Lee, Jack H. Vossen, Evert Jacobsen, Richard G.F. Visser, Sophien Kamoun, and Vivianne G.A.A. Vleeshouwers. 2012. "Qualitative and Quantitative Late Blight Resistance in the Potato Cultivar Sarpo Mira Is Determined by the Perception of Five Distinct RXLR Effectors." *Molecular Plant-Microbe Interactions* 25 (7): 910–19. https://doi.org/10.1094/MPMI-01-12-0010-R.

Robinson, James T., Helga Thorvaldsdóttir, Wendy Winckler, Mitchell Guttman, Eric S. Lander, Gad Getz, and Jill P. Mesirov. 2011. "Integrative Genomics Viewer." *Nature Biotechnology* 29 (1): 24–26. https://doi.org/10.1038/nbt.1754.

Rodriguez-Algaba, Julian, Stephanie Walter, Chris K. Sørensen, Mogens S. Hovmøller, and Annemarie F. Justesen. 2014. "Sexual Structures and Recombination of the Wheat Rust Fungus *Puccinia striiformis* on *Berberis Vulgaris*." *Fungal Genetics and Biology* 70: 77–85. https://doi.org/10.1016/j.fgb.2014.07.005.

Rodriguez-Herraro, C. 2020. "Investigating The Delivery And Secretion Of Effectors In The Rice Blast Fungus *Magnaporthe oryzae*." A PhD dissertation submitted to the University of Exeter.

Rodriguez-Moreno, Luis, Yin Song, and Bart PHJ Thomma. 2017. "Transfer and

Engineering of Immune Receptors to Improve Recognition Capacities in Crops." Current Opinion in Plant Biology 38: 42–49. https://doi.org/10.1016/j.pbi.2017.04.010.

Romano, Nicoletta, and Giuseppe Macino. 1992. "Quelling: Transient Inactivation of Gene Expression in *Neurospora crassa* by Transformation with Homologous Sequences." *Molecular Microbiology* 6 (22): 3343–53. https://doi.org/10.1111/j.1365-2958.1992.tb02202.x.

Rouxel, Thierry, Jonathan Grandaubert, James K. Hane, Claire Hoede, Angela P. Van De Wouw, Arnaud Couloux, Victoria Dominguez, et al. 2011. "Effector Diversification within Compartments of the Leptosphaeria Maculans Genome Affected by Repeat-Induced Point Mutations." *Nature Communications* 2 (1). https://doi.org/10.1038/ncomms1189.

Ruiz-Diez, B. 2002. "Strategies for the Transformation of Filamentous Fungi." *Journal of Applied Microbiology*, 189–95.

Saintenac, Cyrille, Wenjun Zhang, Andres Salcedo, Matthew N. Rouse, Harold N. Trick, Eduard Akhunov, and Jorge Dubcovsky. 2013. "Identification of Wheat Gene *Sr35* That Confers Resistance to Ug99 Stem Rust Race Group." *Science* 341 (6147): 783–86. https://doi.org/10.1126/science.1239022.

Saitoh, Hiromasa, Shizuko Fujisawa, Chikako Mitsuoka, Akiko Ito, Akiko Hirabuchi, Kyoko Ikeda, Hiroki Irieda, et al. 2012. "Large-Scale Gene Disruption in *Magnaporthe oryzae* Identifies MC69, a Secreted Protein Required for Infection by Monocot and Dicot Fungal Pathogens." *PLoS Pathogens* 8 (5). https://doi.org/10.1371/journal.ppat.1002711.

Saitoh, Hiromasa, and R. Terauchi. 2013. *Burkholderia glumae* Competent Cells Preparation and Transformation. *Bio-protocol* 3(23): e985. DOI: 10.21769/BioProtoc.985.

Salcedo, Andres, William Rutter, Shichen Wang, Alina Akhunova, Stephen Bolus, Shiaoman Chao, Nickolas Anderson, Monica Fernandez De Soto, et al. 2017. "Variation in the *AvrSr35* Gene Determines *Sr35* Resistance against Wheat Stem Rust Race Ug99." *Science* 358 (6370): 1604–6. https://doi.org/10.1126/science.aao7294.

Samudrala, Ram, Fred Heffron, and Jason E. McDermott. 2009. "Accurate Prediction of Secreted Substrates and Identification of a Conserved Putative Secretion Signal for Type III Secretion Systems." *PLoS Pathogens* 5 (4). https://doi.org/10.1371/journal.ppat.1000375.

Saunders, Diane G O, Joe Win, Liliana M. Cano, Les J. Szabo, Sophien Kamoun, and Sylvain

Raffaele. 2012. "Using Hierarchical Clustering of Secreted Protein Families to Classify and Rank Candidate Effectors of Rust Fungi." *PLoS ONE* 7 (1). https://doi.org/10.1371/journal.pone.0029847.

Saur, Isabel M.L., Saskia Bauer, Barbara Kracher, Xunli Lu, Lamprinos Franzeskakis, Marion C. Müller, Björn Sabelleck, et al. 2019. "Multiple Pairs of Allelic MLA Immune Receptor-Powdery Mildew AVRa Effectors Argue for a Direct Recognition Mechanism." *ELife* 8: 1–31. https://doi.org/10.7554/eLife.44471.

Saur, Isabel M.L., Saskia Bauer, Xunli Lu, and Paul Schulze-Lefert. 2019. "A Cell Death Assay in Barley and Wheat Protoplasts for Identification and Validation of Matching Pathogen AVR Effector and Plant NLR Immune Receptors." *Plant Methods* 15 (1): 1–17. https://doi.org/10.1186/s13007-019-0502-0.

Savary, Serge, Laetitia Willocquet, Sarah Jane Pethybridge, Paul Esker, Neil McRoberts, and Andy Nelson. 2019. "The Global Burden of Pathogens and Pests on Major Food Crops." *Nature Ecology and Evolution* 3 (3): 430–39. https://doi.org/10.1038/s41559-018-0793-y.

Schillberg, S., R. Tiburzy, and R. Fischer. 2000. "Transient Transformation of the Rust Fungus *Puccinia graminis* f. sp. *tritici*." *Molecular and General Genetics* 262 (6): 911–15. https://doi.org/10.1007/PL00008658.

Schmidt, Sarah Maria, Joanna Lukasiewicz, Rhys Farrer, Peter van Dam, Chiara Bertoldo, and Martijn Rep. 2016. "Comparative Genomics of *Fusarium oxysporum* f. sp. *melonis* Reveals the Secreted Protein Recognized by the Fom-2 Resistance Gene in Melon." *New Phytologist* 209 (1): 307–18. https://doi.org/10.1111/nph.13584.

Schmittgen, Thomas D., and Kenneth J. Livak. 2008. "Analyzing Real-Time PCR Data by the Comparative CT Method." *Nature Protocols* 3 (6): 1101–8. https://doi.org/10.1038/nprot.2008.73.

Schuster, Mariana, and Regine Kahmann. 2019. "CRISPR-Cas9 Genome Editing Approaches in Filamentous Fungi and Oomycetes." *Fungal Genetics and Biology* 130: 43–53. https://doi.org/10.1016/j.fgb.2019.04.016.

Schwessinger, Benjamin. 2016. "Fundamental Wheat Stripe Rust Research in the 21st Century." *New Phytologist*, 1–7. https://doi.org/10.1111/nph.14159.

Schwessinger, Benjamin, Yan Jun Chen, Richard Tien, Josef Korbinian Vogt, Jana Sperschneider, Ramawatar Nagar, Mark McMullan, et al. 2020. "Distinct Life Histories Impact Dikaryotic Genome Evolution in the Rust Fungus *Puccinia striiformis* Causing Stripe Rust in Wheat." *Genome Biology and Evolution* 12 (5): 597–617. https://doi.org/10.1093/gbe/evaa071.

Schwessinger, Benjamin, Jana Sperschneider, William Cuddy, Marisa Miller, Diana Garnica, Jen Taylor, Peter Dodds, Melania Figueroa, Park Robert, and John Rathjen. 2017. "A near Complete Haplotype-Phased Genome of the Dikaryotic Wheat Stripe Rust Fungus *Puccinia striiformis* f. sp. *tritici* Reveals High Inter-Haplotye Diversity." Doi.Org, 192435. https://doi.org/10.1101/192435.

Schwessinger, Benjamin, Jana Sperschneider, William S Cuddy, Diana P Garnica, Marisa E Miller, Jennifer M Taylor, Peter N Dodds, Melania Figueroa, Robert F Park, and John P. Rathjen. 2018. "A Near-Complete Haplotype-Phased Genome of the Dikaryotic Wheat Stripe Rust Fungus *Puccinia striiformis* f. sp. *tritici* Reveals High Interhaplotype Diversity." *American Society for Microbiology* 9 (1): 1–24.

Sedlazeck, Fritz J, Hayan Lee, and Charlotte A Darby. 2018. "Piercing the Dark Matter: Bioinformatics of Long-Range Sequencing and Mapping." *Nature Reviews Genetics* 19: 329-346. http://dx.doi.org/10.1038/s41576-018-0003-4.

Seidl, Michael F., and Bart P.H.J. Thomma. 2014. "Sex or No Sex: Evolutionary Adaptation Occurs Regardless." *BioEssays* 36 (4): 335–45. https://doi.org/10.1002/bies.201300155.

Shan, Weixing, Minh Cao, Dan Leung, and Brett M. Tyler. 2004. "The Avr1b Locus of *Phytophthora sojae* Encodes an Elicitor and a Regulator Required for Avirulence on Soybean Plants Carrying Resistance Gene *Rps1b*." *Molecular Plant-Microbe Interactions* 17 (4): 394–403. https://doi.org/10.1094/MPMI.2004.17.4.394.

Sharma, Shailendra, Shiveta Sharma, Akiko Hirabuchi, Kentaro Yoshida, Koki Fujisaki, Akiko Ito, Aiko Uemura, et al. 2013. "Deployment of the *Burkholderia glumae* Type III Secretion System as an Efficient Tool for Translocating Pathogen Effectors to Monocot Cells." *Plant Journal* 74 (4): 701–12. https://doi.org/10.1111/tpj.12148.

Shewry, Peter R., and Sandra J. Hey. 2015. "The Contribution of Wheat to Human Diet and Health." *Food and Energy Security* 4 (3): 178–202. https://doi.org/10.1002/FES3.64.

Shipman, Emma N., Kiersun Jones, Cory B. Jenkinson, Dong Won Kim, Jie Zhu, and Chang Hyun Khang. 2017. "Nuclear and Structural Dynamics during the Establishment of a Specialized Effector-Secreting Cell by *Magnaporthe oryzae* in Living Rice Cells." *BMC Cell Biology* 18 (1): 1–10. https://doi.org/10.1186/s12860-017-0126-z.

Simpson, Jared T., Kim Wong, Shaun D. Jackman, Jacqueline E. Schein, Steven J.M. Jones, and Inanç Birol. 2009. "ABySS: A Parallel Assembler for Short Read Sequence Data." *Genome Research* 19 (6): 1117–23. https://doi.org/10.1101/gr.089532.108.

Sohn, K. H., R. K. Hughes, S. J. Piquerez, J. D. G. Jones, and M. J. Banfield. 2012. "Distinct

Regions of the *Pseudomonas syringae* Coiled-Coil Effector AvrRps4 Are Required for Activation of Immunity." *Proceedings of the National Academy of Sciences* 109 (40): 16371–76. https://doi.org/10.1073/pnas.1212332109.

Sohn, K. H., R. Lei, A. Nemri, and J. D.G. Jones. 2007. "The Downy Mildew Effector Proteins ATR1 and ATR13 Promote Disease Susceptibility in *Arabidopsis thaliana*." *The Plant Cell* Online 19 (12): 4077–90. https://doi.org/10.1105/tpc.107.054262.

Sohn, Kee Hoon, Yan Zhang, and Jonathan D.G. Jones. 2009. "The *Pseudomonas syringae* Effector Protein, AvrRPS4, Requires in Planta Processing and the KRVY Domain to Function." *Plant Journal* 57 (6): 1079–91. https://doi.org/10.1111/j.1365-313X.2008.03751.x.

Sonah, Humira, Rupesh K. Deshmukh, and Richard R. Bélanger. 2016. "Computational Prediction of Effector Proteins in Fungi: Opportunities and Challenges." *Frontiers in Plant Science* 7: 1–14. https://doi.org/10.3389/fpls.2016.00126.

Sørensen, C. K., A. F. Justesen, and M. S. Hovmøller. 2013. "Spontaneous Loss of Yr2 Avirulence in Two Lineages of *Puccinia striiformis* Did Not Affect Pathogen Fitness." *Plant Pathology* 62 (S1): 19–27. https://doi.org/10.1111/ppa.12147.

Sørensen, Chris K., Mogens S. Hovmøller, Marc Leconte, Françoise Dedryver, and Claude de Vallavieille-Pope. 2014. "New Races of *Puccinia striiformis* Found in Europe Reveal Race Specificity of Long-Term Effective Adult Plant Resistance in Wheat." *Phytopathology* 104 (10): 1042–51. https://doi.org/10.1094/PHYTO-12-13-0337-R.

Sorg, Joseph A., Nathan C. Miller, and Olaf Schneewind. 2005. "Substrate Recognition of Type III Secretion Machines - Testing the RNA Signal Hypothesis." *Cellular Microbiology* 7 (9): 1217–25. https://doi.org/10.1111/j.1462-5822.2005.00563.x.

Soyer, Jessica L., Mennat El Ghalid, Nicolas Glaser, Bénédicte Ollivier, Juliette Linglin, Jonathan Grandaubert, Marie Hélène Balesdent, et al. 2014. "Epigenetic Control of Effector Gene Expression in the Plant Pathogenic Fungus *Leptosphaeria maculans*." *PLoS Genetics* 10 (3). https://doi.org/10.1371/journal.pgen.1004227.

Stauber, Jennifer L., Ekaterina Loginicheva, and Lisa M. Schechter. 2012. "Carbon Source and Cell Density-Dependent Regulation of Type III Secretion System Gene Expression in *Pseudomonas syringae* pv. *tomato* DC3000." *Research in Microbiology* 163 (8): 531–39. https://doi.org/10.1016/j.resmic.2012.08.005.

Steele, K. A., E. Humphreys, C. R. Wellings, and M. J. Dickinson. 2001. "Support for a Stepwise Mutation Model for Pathogen Evolution in Australasian *Puccinia striiformis* f. sp. *tritici* by Use of Molecular Markers." *Plant Pathology* 50 (2): 174–80. https://doi.org/10.1046/j.1365-3059.2001.00558.x.

Stergiopoulos, Ioannis, and Pierre J.G.M. de Wit. 2009. "Fungal Effector Proteins." *Annual Review of Phytopathology* 47 (1): 233–63. https://doi.org/10.1146/annurev.phyto.112408.132637.

Sternberg, Samuel H., Sy Redding, Martin Jinek, Eric C. Greene, and Jennifer A. Doudna. 2014. "DNA Interrogation by the CRISPR RNA-Guided Endonuclease Cas9." *Nature* 507 (7490): 62–67. https://doi.org/10.1038/nature13011.

Steuernagel, Burkhard, Sambasivam K Periyannan, Inmaculada Hernández-Pinzón, Kamil Witek, Matthew N Rouse, Guotai Yu, Asyraf Hatta, et al. 2016. "Rapid Cloning of Disease-Resistance Genes in Plants Using Mutagenesis and Sequence Capture." *Nature Biotechnology* 34 (August 2015). https://doi.org/10.1038/nbt.3543.

Su, Xiaoyun, George Schmitz, Meiling Zhang, Roderick I. Mackie, and Isaac K.O. Cann. 2012. Heterologous Gene Expression in Filamentous Fungi. *Advances in Applied Microbiology*. Vol. 81. Elsevier. https://doi.org/10.1016/B978-0-12-394382-8.00001-0.

Sweigard, James A, Anne M Carroll, Seogchan Kang, Leonard Farrall, Forrest G Chumley, and Barbara Valent. 1995. "Identification, Cloning, and Characterization of *PWL2*, a Gene for Host Species Specificity in the Rice Blast Fungus." *The Plant Cell* 7 : 1221–33.

Talbot, N. J. 2003. "On the Trail of a Cereal Killer: Exploring the Biology of *Magnaporthe grisea.*" *Annual Review of Microbiology* 57 (1): 177–202. https://doi.org/10.1146/annurev.micro.57.030502.090957.

Talbot, N J, D J Ebbole, and J E Hamer. 1993. "Identification and Characterization of *MPG1*, a Gene Involved in Pathogenicity from the Rice Blast Fungus *Magnaporthe grisea*." *The Plant Cell* 5 (11): 1575–90. https://doi.org/10.1105/tpc.5.11.1575.

Tang, Xiaoyan, Yanmei Xiao, and Jian Min Zhou. 2006. "Regulation of the Type III Secretion System in Phytopathogenic Bacteria." *Molecular Plant-Microbe Interactions* 19 (11): 1159–66. https://doi.org/10.1094/MPMI-19-1159.

Tembo, Batiseba, Rabson M. Mulenga, Suwilanji Sichilima, Kenneth K. M'siska, Moses Mwale, Patrick C. Chikoti, Pawan K. Singh, et al. 2020. "Detection and Characterization of Fungus (*Magnaporthe oryzae* Pathotype *Triticum*) Causing Wheat Blast Disease on Rain-Fed Grown Wheat (*Triticum aestivum* L.) in Zambia." *PLoS One* 15: 1–10. https://doi.org/10.1371/journal.pone.0238724.

Thind, Anupriya Kaur, Thomas Wicker, Hana Šimková, Dario Fossati, Odile Moullet, Cécile

Brabant, Jan Vrána, Jaroslav Doležel, and Simon G. Krattinger. 2017. "Rapid Cloning of Genes in Hexaploid Wheat Using Cultivar-Specific Long-Range Chromosome Assembly." *Nature Biotechnology* 35 (8): 793–96. https://doi.org/10.1038/nbt.3877.

Thomas, William J., Caitlin A. Thireault, Jeffrey A. Kimbrel, and Jeff H. Chang. 2009. "Recombineering and Stable Integration of the *Pseudomonas syringae* pv. *syringae* 61 Hrp/Hrc Cluster into the Genome of the Soil Bacterium *Pseudomonas fluorescens* Pf0-1." *Plant Journal* 60 (5): 919–28. https://doi.org/10.1111/j.1365-313X.2009.03998.x.

Thomma, Bart P.H.J., Thorsten Nürnberger, and Matthieu H.A.J. Joosten. 2011. "Of PAMPs and Effectors: The Blurred PTI-ETI Dichotomy." *The Plant Cell* 23 (1): 4–15. https://doi.org/10.1105/tpc.110.082602.

Tian, Shulan, Huihuang Yan, Eric W. Klee, Michael Kalmbach, and Susan L. Slager. 2018. "Comparative Analysis of de Novo Assemblers for Variation Discovery in Personal Genomes." *Briefings in Bioinformatics* 19 (5): 893–904. https://doi.org/10.1093/bib/bbx037.

Udvardi, Michael K., Tomasz Czechowski, and Wolf Rüdiger Scheible. 2008. "Eleven Golden Rules of Quantitative RT-PCR." *Plant Cell* 20 (7): 1736–37. https://doi.org/10.1105/tpc.108.061143.

Uhse, Simon, and Armin Djamei. 2018. "Effectors of Plant-Colonizing Fungi and Beyond." *PLOS Pathogens* 14 (6): e1006992. https://doi.org/10.1371/journal.ppat.1006992.

Upadhyaya, Narayana M., Diana P. Garnica, Haydar Karaoglu, Jana Sperschneider, Adnane Nemri, Bo Xu, Rohit Mago, et al. 2015. "Comparative Genomics of Australian Isolates of the Wheat Stem Rust Pathogen *Puccinia graminis* f. sp. *tritici* Reveals Extensive Polymorphism in Candidate Effector Genes." *Frontiers in Plant Science* 5: 1–13. https://doi.org/10.3389/fpls.2014.00759.

Upadhyaya, Narayana M, Rohit Mago, Brian J Staskawicz, Michael a Ayliffe, Jeffrey G Ellis, and Peter N Dodds. 2014. "A Bacterial Type III Secretion Assay for Delivery of Fungal Effector Proteins into Wheat." *Molecular Plant Microbe Interactions* 27 (3): 255–64. https://doi.org/10.1094/MPMI-07-13-0187-FI.

Urashima, A.S., and H. Kato. 1993. "Host Range, Mating Type, and Fertility of *Pyricularia grisea* from Wheat in Brazil." *Plant Disease* 77 (12): 1211–16.

Uusitalo, Jaana M., K. M. Helena Nevalainen, Anu M. Harkki, Jonathan K.C. Knowles, and Merja E. Penttilä. 1991. "Enzyme Production by Recombinant *Trichoderma reesei* Strains." *Journal of Biotechnology* 17 (1): 35–49. https://doi.org/10.1016/0168-1656(91)90025-Q.

Valent, B., L. Farrall, and F. G. Chumley. 1991. "*Magnaporthe grisea* Genes for

Pathogenicity and Virulence Identified through a Series of Backcrosses." *Genetics* 127 (1): 87–101.

Valent, B, and C.H. Khang. 2010. "Recent Advances in Rice Blast Effector Research." *Current Opinion in Plant Biology* 13 (4): 434–41. https://doi.org/10.1016/j.pbi.2010.04.012.

Vasquez-Gross, Hans, Sukhwinder Kaur, Lynn Epstein, and Jorge Dubcovsky. 2020. A Haplotype-Phased Genome of Wheat Stripe Rust Pathogen *Puccinia striiformis* f. sp. *tritici*, Race PST-130 from the Western USA. *BioRxiv*. https://doi.org/https://doi.org/10.1101/2020.08.21.260687.

Ve, T., S. J. Williams, A.-M. Catanzariti, M. Rafiqi, M. Rahman, J. G. Ellis, A. R. Hardham, et al. 2013. "Structures of the Flax-Rust Effector AvrM Reveal Insights into the Molecular Basis of Plant-Cell Entry and Effector-Triggered Immunity." *Proceedings of the National Academy of Sciences* 110 (43): 17594–99. https://doi.org/10.1073/pnas.1307614110.

Villalba, François, Jérôme Collemare, Patricia Landraud, Karine Lambou, Viviane Brozek, Bénédicte Cirer, Damien Morin, Christophe Bruel, Roland Beffa, and Marc Henri Lebrun. 2008. "Improved Gene Targeting in *Magnaporthe grisea* by Inactivation of MgKU80 Required for Non-Homologous End Joining." *Fungal Genetics and Biology* 45 (1): 68–75. https://doi.org/10.1016/j.fgb.2007.06.006.

Vleeshouwers, Vivianne G.A.A., and Richard P. Oliver. 2014. "Effectors as Tools in Disease Resistance Breeding against Biotrophic, Hemibiotrophic, and Necrotrophic Plant Pathogens." *Molecular Plant-Microbe Interactions* 27 (3): 196–206. https://doi.org/10.1094/MPMI-10-13-0313-IA.

Voegele, Ralf T., Matthias Hahn, and Kurt Mendgen. 2009. "The Uredinales: Cytology, Biochemistry, and Molecular Biology." *The Mycota*, 69–98. https://doi.org/10.1007/978-3-540-87407-2_4.

Voegele, Ralf T., and Kurt W. Mendgen. 2011. "Nutrient Uptake in Rust Fungi: How Sweet Is Parasitic Life?" *Euphytica* 179 (1): 41–55. https://doi.org/10.1007/s10681-011-0358-5.

Vollmeister, E., Schipper, K., & Feldbrügge, M. (2012). "Microtubule-dependent mRNA transport in the model microorganism *Ustilago maydis*." *RNA Biology* *9* (3). 261–268. https://doi.org/10.4161/rna.19432

Wagner, Samuel, Iwan Grin, Silke Malmsheimer, Nidhi Singh, Claudia E. Torres-Vargas,

and Sibel Westerhausen. 2018. "Bacterial Type III Secretion Systems: A Complex Device for the Delivery of Bacterial Effector Proteins into Eukaryotic Host Cells." *FEMS Microbiology Letters* 365 (19): 1–13. https://doi.org/10.1093/femsle/fny201.

Wang, C.-I A., G. Guncar, J. K. Forwood, T. Teh, A.-M. Catanzariti, G. J. Lawrence, F. E. Loughlin, et al. 2007. "Crystal Structures of Flax Rust Avirulence Proteins AvrL567-A and -D Reveal Details of the Structural Basis for Flax Disease Resistance Specificity." *The Plant Cell* Online 19 (9): 2898–2912. https://doi.org/10.1105/tpc.107.053611.

Wang, Fengtao, Ruiming Lin, Jing Feng, Wanquan Chen, Dewen Qiu, and Shichang Xu. 2015. "TaNAC1 Acts as a Negative Regulator of Stripe Rust Resistance in Wheat, Enhances Susceptibility to *Pseudomonas syringae*, and Promotes Lateral Root Development in Transgenic *Arabidopsis thaliana*." *Frontiers in Plant Science* 6: 1–17. https://doi.org/10.3389/fpls.2015.00108.

Wang, Jizong, Meijuan Hu, Jia Wang, Jinfeng Qi, Zhifu Han, Guoxun Wang, Yijun Qi, Hong Wei Wang, Jian Min Zhou, and Jijie Chai. 2019. "Reconstitution and Structure of a Plant NLR Resistosome Conferring Immunity." *Science* 364 (6435). https://doi.org/10.1126/science.aav5870.

Wang, Shizhen, Soichiro Asuke, Trinh Thi Phuong Vy, Yoshihiro Inoue, Izumi Chuma, Joe Win, Kenji Kato, and Yukio Tosa. 2018. "A New Resistance Gene in Combination with *Rmg8* Confers Strong Resistance Against *Triticum* Isolates of *Pyricularia oryzae* in a Common Wheat Landrace." *Phytopathology* 108 (11): 1299–1306. https://doi.org/10.1094/phyto-12-17-0400-r.

Wang, Shumei, Petra C. Boevink, Lydia Welsh, Ruofang Zhang, Stephen C. Whisson, and Paul R.J. Birch. 2017. "Delivery of Cytoplasmic and Apoplastic Effectors from *Phytophthora infestans* Haustoria by Distinct Secretion Pathways." *New Phytologist*, 205–15. https://doi.org/10.1111/nph.14696.

Ward, Owen P. 2012. "Production of Recombinant Proteins by Filamentous Fungi." *Biotechnology Advances* 30 (5): 1119–39. https://doi.org/10.1016/j.biotechadv.2011.09.012.

Weber, Ernst, Carola Engler, Ramona Gruetzner, Stefan Werner, and Sylvestre Marillonnet. 2011. "A Modular Cloning System for Standardized Assembly of Multigene Constructs." *PLoS ONE* 6 (2). https://doi.org/10.1371/journal.pone.0016765.

Wellings, C. R. 2007. "*Puccinia striiformis* in Australia: A Review of the Incursion, Evolution, and Adaptation of Stripe Rust in the Period 1979-2006." *Australian Journal of Agricultural Research* 58 (6): 567–75. https://doi.org/10.1071/AR07130.

Wellings, Colin R. 2011. "Global Status of Stripe Rust: A Review of Historical and Current Threats." *Euphytica* 179 (1): 129–41. https://doi.org/10.1007/s10681-011-0360-y.

Weßling, Ralf, Petra Epple, Stefan Altmann, Yijian He, Li Yang, Stefan R. Henz, Nathan McDonald, et al. 2014. "Convergent Targeting of a Common Host Protein-Network by Pathogen Effectors from Three Kingdoms of Life." *Cell Host and Microbe* 16 (3): 364–75. https://doi.org/10.1016/j.chom.2014.08.004.

Wickham H (2016). *ggplot2: Elegant Graphics for Data Analysis*. Springer-Verlag New York. ISBN 978-3-319-24277-4, https://ggplot2.tidyverse.org.

Wilkinson, Paul A., Mark O. Winfield, Gary L.A. Barker, Alexandra M. Allen, Amanda Burridge, Jane A. Coghill, and Keith J. Edwards. 2012. "CerealsDB 2.0: An Integrated Resource for Plant Breeders and Scientists." *BMC Bioinformatics* 13 (1). https://doi.org/10.1186/1471-2105-13-219.

Wilson, Richard A., and Nicholas J. Talbot. 2009. "Under Pressure: Investigating the Biology of Plant Infection by *Magnaporthe oryzae*." *Nature Reviews Microbiology* 7 (3): 185–95. https://doi.org/10.1038/nrmicro2032.

Win, J., A C Haparro Arcia, K B Elhaj, D G O S Aunders, K Y Oshida, S D Ong, S S Chornack, et al. 2012. "Effector Biology of Plant-Associated Organisms : Concepts and Perspectives." Cold Spring Harbor Symposia on Quantitative Biology LXXVII: 235–47.

Win, J., A. Chaparro-Garcia, K. Belhaj, D. G.O. Saunders, K. Yoshida, S. Dong, S. Schornack, et al. 2012. "Effector Biology of Plant-Associated Organisms: Concepts and Perspectives." *Cold Spring Harbor Symposia on Quantitative Biology* 77: 235–47. https://doi.org/10.1101/sqb.2012.77.015933.

Win, J., E. Chanclud, C. Sarai Reyes-Avila, T. Langner, T. Islam, and S. Kamoun. 2019. "Nanopore Sequencing of Genomic DNA from Magnaporthe oryzae Isolates from Different Hosts." Zenodo. doi:/10.5281/zenodo.2564950.

Wirthmueller, Lennart, Yan Zhang, Jonathan D G Jones, and Jane E. Parker. 2007. "Nuclear Accumulation of the *Arabidopsis* Immune Receptor RPS4 Is Necessary for Triggering EDS1-Dependent Defense." *Current Biology* 17 (23): 2023–29. https://doi.org/10.1016/j.cub.2007.10.042.

Wouw, Mark Van De, Chris Kik, Theo Van Hintum, Rob Van Treuren, and Bert Visser. 2010. "Genetic Erosion in Crops: Concept, Research Results and Challenges." *Plant Genetic Resources*: Characterisation and Utilisation 8 (1): 1–15. https://doi.org/10.1017/S1479262109990062.

Wu, Jun, Yanjun Kou, Jiandong Bao, Ya Li, Mingzhi Tang, Xiaoli Zhu, Ariane Ponaya, et

al. 2015. "Comparative Genomics Identifies the *Magnaporthe oryzae* Avirulence Effector *AvrPi9* That Triggers *Pi9*-Mediated Blast Resistance in Rice." *New Phytologist* 206 (4): 1463–75. https://doi.org/10.1111/nph.13310.

Wulff, Brande B. H., and Matthew J. Moscou. 2014. "Strategies for Transferring Resistance into Wheat: From Wide Crosses to GM Cassettes." *Frontiers in Plant Science* 5: 1–11. https://doi.org/10.3389/fpls.2014.00692.

Xia, Chongjing, Meinan Wang, Chuntao Yin, Omar E. Cornejo, Scot H. Hulbert, and Xianming Chen. 2018. "Genomic Insights into Host Adaptation between the Wheat Stripe Rust Pathogen (*Puccinia striiformis* f. sp. *tritici*) and the Barley Stripe Rust Pathogen (*Puccinia striiformis* f. sp. *hordei*)." *BMC Genomics* 19 (1): 1–21. https://doi.org/10.1186/s12864-018-5041-y.

Xu, Qiang, Chunlei Tang, Xiaodong Wang, Shutian Sun, Jinren Zhao, Zhensheng Kang, and Xiaojie Wang. 2019. "An Effector Protein of the Wheat Stripe Rust Fungus Targets Chloroplasts and Suppresses Chloroplast Function." *Nature Communications* 10 (1): 5571. https://doi.org/10.1038/s41467-019-13487-6.

Xue, Minfeng, Jun Yang, Zhigang Li, Songnian Hu, Nan Yao, Ralph A. Dean, Wensheng Zhao, et al. 2012. "Comparative Analysis of the Genomes of Two Field Isolates of the Rice Blast Fungus *Magnaporthe oryzae*." *PLoS Genetics* 8 (8). https://doi.org/10.1371/journal.pgen.1002869.

Yan, Feng, David R. Powell, David J. Curtis, and Nicholas C. Wong. 2020. "From Reads to Insight: A Hitchhiker's Guide to ATAC-Seq Data Analysis." *Genome Biology* 21 (1): 1–16. https://doi.org/10.1186/s13059-020-1929-3.

Yan, Xia, and Nicholas J. Talbot. 2016. "Investigating the Cell Biology of Plant Infection by the Rice Blast Fungus *Magnaporthe oryzae*." *Current Opinion in Microbiology* 34: 147–53. https://doi.org/10.1016/j.mib.2016.10.001.

Yin, Chuntao, and Scot Hulbert. 2011. "Prospects for Functional Analysis of Effectors from Cereal Rust Fungi," 57–67. https://doi.org/10.1007/s10681-010-0285-x.

Yoshida, Kentaro, Diane G. O. Saunders, Chikako Mitsuoka, Satoshi Natsume, Shunichi Kosugi, Hiromasa Saitoh, Yoshihiro Inoue, et al. 2016. "Host Specialization of the Blast Fungus *Magnaporthe oryzae* Is Associated with Dynamic Gain and Loss of Genes Linked to Transposable Elements." *BMC Genomics* 17 (1): 370. https://doi.org/10.1186/s12864-016-2690-6.

Young, Alexandra M., and Amy E. Palmer. 2017. "Methods to Illuminate the Role of *Salmonella* Effector Proteins during Infection: A Review." *Frontiers in Cellular and Infection Microbiology* 7(363): 1-12. https://doi.org/10.3389/fcimb.2017.00363.

Yuan, Congying, Meinan Wang, Danniel Z. Skinner, Deven R. See, Chongjing Xia, Xinhong Guo, and Xianming Chen. 2018. "Inheritance of Virulence, Construction of a Linkage Map, and Mapping Dominant Virulence Genes in *Puccinia striiformis* f. sp. *tritici* through Characterization of a Sexual Population with Genotyping-by-Sequencing." Phytopathology 108 (1): 133–41. https://doi.org/10.1094/PHYTO-04-17-0139-R.

Zhang, Chaozhong, Lin Huang, Huifei Zhang, Qunqun Hao, Bo Lyu, Meinan Wang, Lynn Epstein, et al. 2019. "An Ancestral NB-LRR with Duplicated 3′UTRs Confers Stripe Rust Resistance in Wheat and Barley." *Nature Communications* 10 (1). https://doi.org/10.1038/s41467-019-11872-9.

Zhang, Haifeng, Xiaobo Zheng, and Zhengguang Zhang. 2016. "The *Magnaporthe grisea* Species Complex and Plant Pathogenesis." *Molecular Plant Pathology* 17 (6): 796–804. https://doi.org/10.1111/mpp.12342.

Zhang, Jianping, Peng Zhang, Peter Dodds, and Evans Lagudah. 2020. "How Target-Sequence Enrichment and Sequencing (TEnSeq) Pipelines Have Catalyzed Resistance Gene Cloning in the Wheat-Rust Pathosystem." *Frontiers in Plant Science* 11: 1–13. https://doi.org/10.3389/fpls.2020.00678.

Zhang, Meixiang, and Gitta Coaker. 2017. "Harnessing Effector-Triggered Immunity for Durable Disease Resistance." *Phytopathology* 107 (8): 912–19. https://doi.org/10.1094/PHYTO-03-17-0086-RVW.

Zhang, Wenjun, Shisheng Chen, Zewdie Abate, Jayaveeramuthu Nirmala, Matthew N. Rouse, and Jorge Dubcovsky. 2017. "Identification and Characterization of *Sr13*, a Tetraploid Wheat Gene That Confers Resistance to the Ug99 Stem Rust Race Group." *Proceedings of the National Academy of Sciences of the United States of America* 114 (45): E9483–92. https://doi.org/10.1073/pnas.1706277114.

Zhang, Xiaoxiao, Nadya Farah, Laura Rolston, Daniel J. Ericsson, Ann Maree Catanzariti, Maud Bernoux, Thomas Ve, et al. 2018. "Crystal Structure of the *Melampsora lini* Effector AvrP Reveals Insights into a Possible Nuclear Function and Recognition by the Flax Disease Resistance Protein P." *Molecular Plant Pathology* 19 (5): 1196–1209. https://doi.org/10.1111/mpp.12597.

Zhao, Jie, Long Wang, Zhiyan Wang, Xianming Chen, Hongchang Zhang, Juanni Yao, Gangming Zhan, Wen Chen, Lili Huang, and Zhensheng Kang. 2013. "Identification of Eighteen *Berberis* Species as Alternate Hosts of *Puccinia striiformis* f. sp. *tritici* and Virulence Variation in the Pathogen Isolates from Natural Infection

of Barberry Plants in China." *Phytopathology* 103 (9): 927–34. https://doi.org/10.1094/PHYTO-09-12-0249-R.

Zhao, Mengxin, Jianfeng Wang, Sen Ji, Zengju Chen, Jinghua Xu, Chunlei Tang, Shuntao Chen, Zhensheng Kang, and Xiaojie Wang. 2018. "Candidate Effector Pst_8713 Impairs the Plant Immunity and Contributes to Virulence of *Puccinia striiformis* f. sp. *tritici*." *Frontiers in Plant Science* 9: 1294. https://doi.org/10.3389/fpls.2018.01294.

Zheng, Wenming, Lili Huang, Jinqun Huang, Xiaojie Wang, Xianming Chen, Jie Zhao, Jun Guo, et al. 2013. "High Genome Heterozygosity and Endemic Genetic Recombination in the Wheat Stripe Rust Fungus." *Nature Communications* 4: 1–10. https://doi.org/10.1038/ncomms3673.

Zhou, Zhipeng, Yunkun Danga, Mian Zhou, Lin Li, Chien Hung Yu, Jingjing Fu, She Chen, and Yi Liu. 2016. "Codon Usage Is an Important Determinant of Gene Expression Levels Largely through Its Effects on Transcription." *Proceedings of the National Academy of Sciences of the United States of America* 113 (41): E6117–25. https://doi.org/10.1073/pnas.1606724113.

# Appendices

**Appendix 1** Working concentration of antibiotics used for cloning

| Antibiotic | Working concentration | Solvent |
|---|---|---|
| Gentamycin | 50 μg/mL | $H_2O$ |
| Chloramphenicol | 25 μg/mL | EtOH |
| Kanamycin | 50 μg/mL | $H_2O$ |
| Carbenicillin | 100 μg/mL | $H_2O$ |
| Spectinomycin | 50 μg/mL | $H_2O$ |
| Trimethoprim | 10 μg/mL | DMSO |
| Tetracycline | 10 μg/mL | EtOH |

**Appendix 2** - List of bacterial strains used in chapter 4

| Pathogen | Strain | Source |
|---|---|---|
| *Burkholderia glumae* | 106619 | (Sharma *et al.*, 2013) |
| | 301682 | |
| | 302544 | |
| | 302744 | |
| | 302925 | |
| | 302928 | |
| *Burkholderia cepacia* | ATCC 24516 | American Type Culture Collection (Manassas, Virginia) |
| *Pseudomonas syringae pv. lapsa* | ATCC10859 | American Type Culture Collection (Manassas, Virginia) |
| *Pseudomonas fluorescens* | EtHAn | (Upadhyaya *et al.*, 2014) |
| *Escherichia coli* | Pkr2013 | LGC standards (Teddington, UK) |

**Appendix 3** - Primers used for cloning T3SS vectors

| Primer name | Sequence (5' – 3') |
|---|---|
| AvrSr50-TOPOF | CAC CAT GGC TAG GAG CCT TGT |
| avrSr50-TOPOF | CAC CAT GGC TAG GAG CCT TAT |
| Sr50-TOPOR | CTA CCT GTG TTG GCG CCT TGC |
| dhfr-BsrDI-F | GCAATGTTGTTGACAATTAATCATCGGC |
| dhfr-BsrDI-R | GCAATGCGGGTCACTGATGCCTCCGTGT |
| AvrRmg8-TopoF | CACCATGCTGCCTGCGCCGCAGCCTA |
| AvrRmg8-R | CTA CTG CCT TCT AGT ACC GGG AAG T |

**Appendix 4** – Vectors used in chapter 4

| Vector name | Description | Antibiotic resistance | Source |
|---|---|---|---|
| **pNR526-G2AC3A** | Effector detector vector with the N-terminal *AvrRpm1* secretion signal. Contains site mutations abolishing the myristoylation and palmitoylation motifs. Gateway compatible. | Gentamycin, chloramphenicol | (Upadhyaya *et al.*, 2014) |
| **Puc57- AvrSr50** | Synthesized avirulent *AvrSr50* allele for subcloning in the Puc57 vector | carbenicillin | This thesis |
| **Puc57-avrSr50** | Synthesized virulent *avrSr50* allele for subcloning in the Puc57 vector | carbenicillin | This thesis |
| **pNR526-G2AC3A-AvrSr50** | *AvrSr50* in the effector detector vector (pEDV) | Gentamycin | This thesis |
| **pNR526-G2AC3A-avrSr50** | *avrSr50* in the effector detector vector (pEDV) | Gentamycin | This thesis |
| **pTKDP-dhfr** | Vector with trimethoprim resistance for subcloning | Carbenicillin, trimethoprim | Addgene |
| **pNR526-G2AC3A-Tpr** | Effector detector vector with trimethoprim resistance (TpR pEDV) | Trimethoprim, chloramphenicol | This thesis |
| **pNR526-G2AC3A-Tpr-AvrSr50** | *AvrSr50* in the TpR pEDV | Trimethoprim | This thesis |
| **pNR526-G2AC3A-Tpr-AvrRmg8** | *AvrRmg*8 in the TpR pEDV | Trimethoprim | This thesis |

**Appendix 5** - Vector constructs made in chapter 5

| Construct Name | Promoter | Signal Peptide | Vector backbone |
|---|---|---|---|
| pPWL2:AvrRmg8 | *PWL2* (rice blast) | Native AvrRmg8 (wheat blast) | pcB-pPWL2-mcherry-stop (Saitoh *et al.*, 2012) |
| pPWL2:AvrSr50 | *PWL2* (rice blast) | Native AvrSr50 (stem rust) | pcB-pPWL2-mcherry-stop (Saitoh *et al.*, 2012) |
| pPWT3:AvrSr50 | *PWT3* (wheat blast) | Native AvrSr50 (stem rust) | pPWL2:AvrSr50 (this thesis) |
| pRP27:AvrSr50 | *RP27* (constitutive fungal) | Native AvrSr50 (stem rust) | pPWL2:AvrSr50 (This thesis) |
| pTrpc:AvrSr50 | *Trpc* (constitutive fungal) | Native AvrSr50 (stem rust) | pPWL2:AvrSr50 (This thesis) |
| pPWL2:PWT3SP:AvrSr50 | *PWL2* (rice blast) | PWT3 (wheat blast) | pPWL2:AvrSr50 (This thesis) |
| pPWT3:PWT3SP:AvrSr50 | *PWT3* (wheat blast) | PWT3 (wheat blast) | pPWT3:AvrSr50 (This thesis) |
| pRP27:PWT3SP:AvrSr50 | *RP27* (constitutive fungal) | PWT3 (wheat blast) | pRp27:AvrSr50 (This thesis) |
| pTrpc:PWT3SP:AvrSr50 | *Trpc* (constitutive fungal) | PWT3 (wheat blast) | pTrpc:AvrSr50 (This thesis) |
| pPWT3:PWT3SP:AvrPm3$^{a2/f2}$ | *PWT3* (wheat blast) | PWT3 (wheat blast) | pCB1532B-RFP (Pennington *et al.*, 2017) |
| pPWT3:PWT3SP:AvrSr50:mcherryNLS | *PWT3* (wheat blast) | PWT3 (wheat blast) | pCB1532S-RFP (Pennington *et al.*, 2017) |

**Appendix 6** - List *of Magnaporthe* strains and transformants made in chapter 5

| Expression Construct Name | Transformant Name | Description [background strain; plasmid used; other] |
|---|---|---|
| pPWL2:AvrSr50 | PWL-1<br>PWL-2<br>PWL-5<br>PWL-8<br>PWL-13 | Wheat blast expressing *AvrSr50* under the rice blast effector *PWL2* promoter. [PY06047, Ppwl2:AvrSr50] |
| pPWT3:AvrSr50 | P-17<br>P-29<br>P-30<br>P-32 | Wheat blast expressing *AvrSr50* under the wheat blast effector *PWT3* promoter. [PY06047, Ppwt3:AvrSr50] |
| pRP27:AvrSr50 | R-1<br>R-3 | Wheat blast expressing *AvrSr50* under the constitutive fungal promoter *RP27* [PY06047, Prp27:AvrSr50] |
| pTrpc:AvrSr50 | T-2<br>T-7 | Wheat blast expressing *AvrSr50* under the constitutive fungal promoter *Trpc*. [PY06047, Ptrpc:AvrSr50] |
| pPWT3:PWT3SP:AvrSr50 | PS-2<br>PS-7<br>PS-10<br>PS-22<br>PS-35<br>PS-41<br>PS-42<br>PS-43<br>PS-44 | Wheat blast expressing *AvrSr50* (without its native signal peptide) under the wheat blast *PWT3* promoter and signal peptide. [PY06047, Ppwt3:PWT3SP:AvrSr50] |
| pRP27:PWT3SP:AvrSr50 | RS-2<br>RS-6 | Wheat blast expressing *AvrSr50* (without its native signal peptide) under the constitutive fungal promoter *Rp27*, and wheat blast PWT3 signal peptide. [PY06047, Prp27:PWT3SP:AvrSr50] |
| pTrpc:PWT3SP:AvrSr50 | TS-7<br>TS-11 | Wheat blast expressing *AvrSr50* (without its native signal peptide) under the constitutive fungal promoter Trpc, and wheat blast PWT3 signal peptide. [PY06047, Ptrpc:PWT3SP:AvrSr50] |
| pPWT3:PWT3SP:AvrPm3$^{a2/f2}$ | Pm3-2<br>Pm3-6<br>Pm3-11<br>Pm3-12 | Wheat blast expressing *AvrPm3* $^{a2/f2}$ (without its native signal peptide) under the PWT3 promoter and PWT3 signal peptide. [PY06047, pPWT3:PWT3SP:AvrPm3$^{a2/f2}$] |
| pPWT3:PWT3SP:AvrSr50 | CPib-2<br>CPib-5<br>CPib-11<br>CPib-15<br>CPib-17 | Wheat blast expressing *AvrSr50* (without its native signal peptide) under the wheat blast *PWT3* promoter and signal peptide. [PY06047, |

| | | |
|---|---|---|
| | CPib-20<br>CPib-23<br>CPib-25<br>CPib-30<br>CPib-33 | 5'Pib:pPWT3:PWT3SP:AvrSr50:3'Pib, targeted to the *AvrPib* genomic locus] |
| pPWT3:PWT3SP:AvrSr50 | CRmg8-7<br>CRmg8-8<br>CRmg8-10<br>CRmg8-11 | Wheat blast expressing *AvrSr50* (without its native signal peptide) under the wheat blast PWT3 promoter and signal peptide. [BTJP4-1, 5'Rmg8:pPWT3:PWT3SP:AvrSr50:3'Rmg8, targeted to the *AvrRmg8* genomic locus] |
| pPWT3:PWT3SP:AvrSr50 | C04257-1<br>C04257-2<br>C04257-4 | Wheat blast expressing *AvrSr50* (without its native signal peptide) under the wheat blast PWT3 promoter and signal peptide. [PY06047, 5'04257:pPWT3:PWT3SP:AvrSr50:3'04257, targeted to the MGG_04257 genomic locus] |

**Appendix 7** - Primers used for genotyping and cloning in chapter 5

| Primer Name | Sequence |
|---|---|
| AvrRmg8F | ATGCACCGCATCGGCTTTTTCTTCC |
| AvrRmg8R | CTACTGCCTTCTAGTACCGGGAAGT |
| AvrRmg8_BamH1F | AAGGATCCATGCACCGCATCGGCTTTTTCTTCC |
| AvrRmg8_EcoRV_R | AAGATATCCTACTGCCTTCTAGTACCGGGAAGT |
| sr50-BamHIF | AAGGATCCATGATGCATTCAATTATCT |
| sr50-EcoRV-R | AAGATATCCTACCTGTGTTGGCGCCTT |
| pRP27-Not1F | AAGCGGCCGCATAAATGTAGGTATTACCTGTAC |
| pRP27-Xba1R | AATCTAGATTTGAAGATTGGGTTCCTAC |
| pPWT3-Not1F | AAGCGGCCGCGCTTTGCCGACTTTGGTAATAG |
| pPWT3-Xba1R | AATCTAGAAATGTTATATGTGCAAATATATATG |
| pTrpc-Not1F | AAGCGGCCGCAACTGATATTGAAGGAGCAT |
| pTrpc-Xba1R | AATCTAGATTGGATGCTTGGGTAGAATA |
| PWT3SP-BAMHI-F | AAGGATCCATGAACCTCAGACTTATTACTTTTTTA |
| PWT3SP-OverlapAvr-R | GACAAGGCTCCTAGCAGCCACCGCGCCG |
| AvrSr50-OverlapPWT3SP-F | GCCGGCGCGGTGGCTGCTAGGAGCCTTGTCAAAAT |
| AvrSr50-HindIII-R | AAAAGCTTCTACCTGTGTTGGCGCCTTG |
| pPWT3_GGF | AAGAAGACAACTCAGGAGGCTTTGCCGACTTTGGTA |
| pPWT3_GGR | AAGAAGACAACTCGCATTAATGTTATATGTGCAAATATA TATGAG |
| PWT3SP_GGF | AAGAAGACAACTCAAATGAACCTCAGACTTATTACTTTT TTAATG |
| PWT3SP_GGR | AAGAAGACAACTCGTGCCACCGCGCCGGCCA |
| AvrPm3a_GGF | AAGAAGACAACTCAGGCAGGCCCTGTCGCTAACGCT |
| AvrPm3a_GGR | AAGAAGACAACTCGAAGCCTAGTGCAGAATTATGTTTAA TTGAGG |
| 3SCD1T_GGF | AAGAAGACAACTCAGCTTAGCGGCGTGCTCTGCACA |
| 3SCD1T_GGR | AAGAAGACAACTCGAGCGCCGGGAGGCTGAATCGGA |
| AvrSr50_GGF | AAGAAGACAACTCAGGCAGCTAGGAGCCTTGTCAAA |
| AvrSr50_GGR | AAGAAGACAACTCGCGAACCCCTGTGTTGGCGCCTTGC |
| AvrSR50_Q5_F | ATTCACAAGTgTTCAATCATTTTG |
| AvrSr50_Q5_R | CAGCTTCAAACTCAGTGAG |
| 5'Pib_GGF | AAGAAGACAACTCAGGAGCGTCTTTGTTTGACAATTTC |
| 5'Pib_GGR | AAGAAGACAACTCGGTCATTGGAACTTCTACCCAAGCA |
| 3'Pib_GGF | AAGAAGACAACTCATCCCAGGGGGAATCCAGAGAATTT |
| 3'Pib_GGR | AAGAAGACAACTCGAGCGGGGAGGACCTTGGAATTCAC |
| 5'04257_GGF | AAGAAGACAACTCAGGAGCGCCATCGCCACCGAGAACT |
| 5'04257_GGR | AAGAAGACAACTCGGTCAGGATCTCCTTGGGGATAAGC |
| 3'04257_GGF | AAGAAGACAACTCATCCCAGAGGGCCGGCCCGAACG |
| 3'04257_GGR | AAGAAGACAACTCGAGCGGGCCTGGGGCACAGACAG |
| 5'AvrRmg8_GGF | AAGAAGACAACTCAGGAGACTTTCTTTTGTACTTTGCTT C |
| 5'AvrRmg8_GGR | AAGAAGACAACTCGGTCAGGTGGTACGGGACAGGCT |
| 3'AvrRmg8_GGF | AAGAAGACAACTCATCCCAAACGGCGGCGGCAGCCT |
| 3'AvrRmg8_GGR | AAGAAGACAACTCGAGCGGCACTACCATTTGCACCATTT ATCGCC |
| pPWT3_TGAC_GGF | AAGAAGACAACTCATGACGCTTTGCCGACTTTGGTA |
| SCD1T_TACT_GGR | AAGAAGACAACTCGAGTACCGGGAGGCTGAATCGGA |
| Mcherry_GGF | AAGAAGACAACTCATTCGATGGTGAGCAAGGGCGAG |
| NLStop_GGR | AAGAAGACAACTCGAAGCCTTAAGCTCCATAATCTACC |

**Appendix 8** - RT-PCR primers used in Chapter 5

| Primer Name | Sequence (5' – 3') | Description |
|---|---|---|
| MGactinF | TCGACGTCCGAAAGGATCTGT | Forward primer for M. oryzae Actin |
| MGactinR | ACTCCTGCTTCGAGATCCACATC | Reverse primer for M. oryzae Actin |
| PWT3SP_LONGF | ATGAACCTCAGACTTATTACTTTTTTAATGACCTCCGTGG | Forward primer for PWT3SP:AvrSr50 |
| AvrSr50_RTPCR_RLONG | CTACCTGTGTTGGCGCCTTGCAAAATGA | Reverse primer for PWT3SP:AvrSr50 |

**Appendix 9** -RT-qPCR primers used in Chapter 5

| Primer Name | Sequence (5' – 3') | Description |
|---|---|---|
| Mgactin_qpcrF | ACAATGGTTCGGGTATGTGC | Forward primer for M. oryzae Actin |
| Mgactin_qpcrR | CGACAATGGACGGGAAGAC | Reverse primer for M. oryzae Actin |
| AvrSr50_741F | ATGATGGACGTTCACCCTACATAG | Forward primer for *AvrSr50* |
| AvrSr50_851R | CCTCATGTGGATTCCAAACAATCG | Reverse primer for *AvrSr50* |

**Appendix 10** - Donor DNA constructs used for Crispr/Cas9 mediated targeted insertion of *AvrSr50*

| Construct Name | Vector backbone |
|---|---|
| 5'Pib:pPWT3:PWT3SP:AvrSr50:3'Pib | Pcb1532B-RFP (Pennington *et al.*, 2017) |
| 5'04257:pPWT3:PWT3SP:AvrSr50:3'04257 | pICH47732 (Weber *et al.* 2011) |
| 5'Rmg8:pPWT3:PWT3SP:AvrSr50:3'Rmg8 | pICH47732 (Weber *et al.* 2011) |

**Appendix 11** - sgRNA sequences used for Crispr/Cas9 mediated targeted insertion of *AvrSr50*

| sgRNA gene target | sgRNA sequence |
|---|---|
| MGG_04257 | TATCCCCAAGGAGATCCAGA |
| *AvrRmg8* | TGTCCCGTACCACCAAACGG |
| *AvrPib* | GCTTGGGTAGAAGTTCCAAA |